ACID/BASE CATALYTIC CONVERSION OF POLYSACCHARIDE-RICH FOOD WASTE

SI CHEN

PhD

The Hong Kong Polytechnic University

2019

Temporary Binding for Examination Purposes

The Hong Kong Polytechnic University

Department of Civil and Environmental Engineering

Acid/Base Catalytic Conversion of Polysaccharide-rich Food Waste

Si CHEN

A thesis submitted in partial fulfilment of the
requirements for the degree of Doctor of Philosophy

September 2018

CERTIFICATE OF ORIGINALITY

I hereby declare that this thesis is my own work and that, to the best of my knowledge and belief, it reproduces no material previously published or written, nor material that has been accepted for the award of any other degree or diploma, except where due acknowledgement has been made in the text.

Si CHEN

Abstract

Food waste has been a monumental issue in many metropolitan cities. Approximately 1.3 billion tonnes food waste is generated worldwide annually. In Hong Kong, over 3,600 tonnes food waste is produced daily and ends up in landfills, which accounts for one-third of the municipal solid waste. The pressing situation demands new technologies and outlets for food waste recycling. Rice, noodles, and bread are common food from our diet which are rich in starch, a polysaccharide consisting of glucose. Vegetable is rich in cellulose, another polysaccharide which is also consisting of glucose. The carbohydrate in polysaccharide-rich food waste will be a potential source for value-added chemical production to substitute petrochemicals.

This study has demonstrated vegetable food waste can be converted to levulinic acid (LA, 17 C mol% yield) in aqueous environment with the aid of microwave-assisted heating and Amberlyst 36 at 150 ºC in 5 min. Addition of dimethyl sulfoxide (DMSO) in the reaction media resulted in 17 C mol% of hydroxymethylfurfural (HMF) at 150 ºC in 5 min. Dilute sulphuric acid has been compared with Amberlyst 36, and the swelling structure of cellulose in the presence of dilute acid was considered to enhance cellulose dissolution and beneficial to LA production. The established reaction system is therefore validated for vegetable waste conversion.

Bread waste has been selectively converted to glucose (> 70 C mol%) at moderate temperatures (120 - 135 ºC) by Brønsted acid catalyst. Further conversion to HMF or LA was hindered by glucose isomerization to fructose, which was the rate-limiting step in the reaction. Elevating the reaction temperature resulted in loss of products due to humin formation in acid catalysis. Therefore, glucose isomerization has been investigated via base catalysis to enhance overall conversion and carbon efficiency.

Brønsted base solid catalyst derived from melamine and spent coffee grounds has presented the capacity of glucose isomerization, where 12% glucose and high selectivity of fructose (84%) was converted in 20 min at 120 ºC. Co-solvent of acetone in the system promoted fructose yield to 19% due to the increase of overall basicity in the media.

Investigation on catalyst nature and chemical environment in glucose isomerization via base catalysis revealed that in addition to the basicity in the solution, intramolecular hydrogen bonding in the catalyst, or the intermolecular hydrogen bonding between catalyst-solvent-substrate system also has great impact on glucose activity. The type of amines, availability of the basic sites, and the stereochemistry of amines may also affect the catalytic performance by displacement of equilibrium between glucose isomerization to fructose and the competing side reactions.

Publications Arising from PhD Study

First Author Journal Papers of Food Waste/ Biomass Valorization:

1. **Chen, S.S.,** Maneerung, T., Tsang, D.C.W.*, Ok, Y.S., Wang, C.H.*, 2017. Valorization of biomass to hydroxymethylfurfural, levulinic acid, and fatty acid methyl ester by heterogeneous catalysts. Chem. Eng. J. 328, 246-273. **[Impact Factor: 6.159; Grade A (Chemical Engineering)]**
2. **Chen, S.S.,** Yu, I.K.M., Tsang, D.C.W.*, Yip, A.C.K., Khan, E., Wang, L., Ok, Y.S., Poon, C.S., 2017. Valorization of cellulosic food waste into levulinic acid catalyzed by heterogeneous Brønsted acids: Temperature and solvent effects. Chem. Eng. J. 327, 328-335. **[Impact Factor: 6.159; Grade A (Chemical Engineering)]**
3. **Chen, S.S.,** Wang, L., Yu, I.K.M., Tsang, D.C.W.*, Hunt, A.J., Francois, J., Ok, Y.S., Poon, C.S., 2017. Valorization of lignocellulosic fibres of paper towel waste into levulinic acid over solid and aqueous Brønsted acid. Bioresour. Technol. 247, 387-394. **[Impact Factor: 6.102; Grade A (Agricultural Engineering)]**
4. **Chen, S.S.,** Yu, I.K.M., Cho, D.W., Song, H., Tsang, D.C.W.*, Tessonnier, J.-P., Ok, Y.S., Poon, C.S. Selective glucose isomerization to fructose via nitrogen-doped solid base catalyst derived from spent coffee grounds. ACS Sustainable Chemical Engineering *in press*. **[Impact Factor: 6.079; Grade A (Green & Sustainable Science & Technology)]**
5. **Chen, S.S.,** Tsang, D.C.W.*, Tessonnier, J.-P.* Roles of catalyst nature and chemical environment in glucose isomerization to fructose via Brønsted bases. Journal of Catalysis Under review. **[Impact Factor: 6.921; Grade A (Catalysis & Chemical Engineering)]**
6. **Chen, S.S.,** Tsang, D.C.W.*, Tessonnier, J.-P.* Effect of the local chemical environment on carbocatalyst performance: on the reactivity of grafted amines for the base-catalyzed isomerization of glucose to fructose. ACS Sustainable Chemical Engineering. Under review. **[Impact Factor: 6.921; Grade A (Catalysis & Chemical Engineering)]**

Other Journal Papers of Food Waste/ Biomass Valorization:

1. Cao, L., Yu, I.K.M., **Chen, S.S.,** Tsang, D.C.W.*, Wang, L., Xiong, X., Zhang, S., Ok, Y.S., Kwon, E.E., Song, H., Poon, C.S. Production of 5-hydroxymethylfurfural from starch-rich food waste catalyzed by sulfonated biochar. Bioresource Technology 252, 76-82.
2. Xiong, X., Yu, I.K.M., **Chen, S.S.,** Tsang, D.C.W.*, Cao, L., Song, H., Kwon, E.E., Ok, Y.S., Zhang, S., Poon, C.S. 2018. Sulfonated biochar as acid catalyst for sugar hydrolysis and dehydration. Catalysis Today 314, 52-61.
3. Yu, I.K.M., Tsang, D.C.W., **Chen, S.S.,** Wang, L., Hunt, A.J., Sherwood, J., De Oliveira Vigier, K., Jérôme, F., Ok, Y.S., Poon, C.S., 2017a. Polar aprotic solvent-water mixture as the medium for catalytic production of hydroxymethylfurfural (HMF) from bread waste. Bioresource Technology 245, 456-462.
4. Yu, I.K.M., Ong, K.L., Tsang, D.C.W.*, Haque, M.A., Kwan, T.H., **Chen, S.S.,** Uisan, K., Kulkarni, S., Lin, C.S.K., 2018. Chemical transformation of food and

beverage waste-derived fructose to hydroxymethylfurfural as a value-added product. Catalysis Today 314, 70-77.

5. Yu, I.K.M., Tsang, D.C.W.*, Yip, A.C.K., **Chen, S.S.,** Ok, Y.S., Poon, C.S., 2017b. Valorization of starchy, cellulosic, and sugary food waste into hydroxymethylfurfural by one-pot catalysis. Chemosphere 184, 1099-1107. **[Impact Factor: 4.506; Grade A (Environmental Sciences)]**
6. Yu, I.K.M., Tsang, D.C.W.*, Yip, A.C.K., **Chen, S.S.,** Ok, Y.S., Poon, C.S., 2016. Valorization of food waste into hydroxymethylfurfural: Dual role of metal ions in successive conversion steps. Bioresource Technology 219, 338-347.
7. Yu, I.K.M., Tsang, D.C.W., Yip, A.C.K., **Chen, S.S.,** Wang, L., Ok, Y.S., Poon, C.S., 2017c. Catalytic valorization of starch-rich food waste into hydroxymethylfurfural (HMF): Controlling relative kinetics for high productivity. Bioresource Technology 237, 222-230. **[Impact Factor: 6.102; Grade A (Agricultural Engineering)]**

Other Journal Papers of Environmental Engineering:

1. **Chen, S.S.,** Sun, Y., Tsang, D.C.W.*, Graham, N.J.D., Ok, Y.S., Feng, Y., Li, X.D., 2017b. Insights into the subsurface transport of As(V) and Se(VI) in produced water from hydraulic fracturing using soil samples from Qingshankou Formation, Songliao Basin, China. Environmental Pollution 223, 449-456.
2. **Chen, S.S.,** Sun, Y., Tsang, D.C.W.*, Graham, N.J.D., Ok, Y.S., Feng, Y., Li, X.D., 2017c. Potential impact of flowback water from hydraulic fracturing on agricultural soil quality: Metal/metalloid bioaccessibility, Microtox bioassay, and enzyme activities. Science of the Total Environment 579, 1419-1426.
3. **Chen, S.S.,** Taylor, J.S., Baek, K., Khan, E., Tsang, D.C.W.*, Ok, Y.S., 2017d. Sustainability likelihood of remediation options for metal-contaminated soil/sediment. Chemosphere 174, 421-427.
4. Sun, Y., **Chen, S.S.,** Tsang, D.C.W.*, Graham, N.J.D., Ok, Y.S., Feng, Y., Li, X.D., 2017a. Zero-valent iron for the abatement of arsenate and selenate from flowback water of hydraulic fracturing. Chemosphere 167, 163-170.
5. Rajapaksha, A.U., **Chen, S.S.,** Tsang, D.C.W.*, Zhang, M., Vithanage, M., Mandal, S., Gao, B., Bolan, N.S., Ok, Y.S., 2016. Engineered/designer biochar for contaminant removal/immobilization from soil and water: Potential and implication of biochar modification. Chemosphere 148, 276-291.
6. Wang, L., **Chen, S.S.,** Tsang, D.C.W.*, Poon, C.S., Dai, J.G., 2017a. CO_2 curing and fibre reinforcement for green recycling of contaminated wood into high-performance cement-bonded particleboards. Journal of CO2 Utilization 18, 107-116.
7. Wang, L., **Chen, S.S.,** Tsang, D.C.W.*, Poon, C.S., Ok, Y.S., 2017b. Enhancing anti-microbial properties of wood-plastic composites produced from timber and

plastic wastes. Environmental Science and Pollution Research 24, 12227-12237.

8. Wang, L., **Chen, S.S.,** Tsang, D.C.W.[*], Poon, C.S., Shih, K., 2016a. Recycling contaminated wood into eco-friendly particleboard using green cement and carbon dioxide curing. Journal of Cleaner Production 137, 861-870.
9. Wang, L., **Chen, S.S.,** Tsang, D.C.W.[*], Poon, C.S., Shih, K., 2016b. Value-added recycling of construction waste wood into noise and thermal insulating cement-bonded particleboards. Construction and Building Materials 125, 316-325.
10. You, S., Ok, Y.S., **Chen, S.S.,** Tsang, D.C.W.[*], Kwon, E.E., Lee, J., Wang, C.H., 2017. A critical review on sustainable biochar system through gasification: Energy and environmental applications. Bioresource Technology 246, 242-253.
11. Sun, Y., Lei, C., Khan, E., **Chen, S.S.,** Tsang, D.C.W.[*], Ok, Y.S., Lin, D., Feng, Y., Li, X.D., 2017b. Nanoscale zero-valent iron for metal/metalloid removal from model hydraulic fracturing wastewater. Chemosphere 176, 315-323.
12. Sun, Y., Lei, C., Khan, E., **Chen, S.S.,** Tsang, D.C.W.[*], Ok, Y.S., Lin, D., Feng, Y., Li, X.D., 2018. Aging effects on chemical transformation and metal(loid) removal by entrapped nanoscale zero-valent iron for hydraulic fracturing wastewater treatment. Science of the Total Environment 615, 498-507.
13. Lei, C., Sun, Y., Khan, E., **Chen, S.S.,** Tsang, D.C.W.[*], Graham, N.J.D., Ok, Y.S., Yang, X., Lin, D., Feng, Y., Li, X.D., 2018. Removal of chlorinated organic solvents from hydraulic fracturing wastewater by bare and entrapped nanoscale zero-valent iron. Chemosphere 196, 9-17.
14. Zhu, X., Beiyuan, J., Lau, A.Y.T., **Chen, S.S.,** Tsang, D.C.W.[*], Graham, N.J.D., Lin, D., Sun, J., Pan, Y., Yang, X., Li, X.D., 2018. Sorption, mobility, and bioavailability of PBDEs in the agricultural soils: Roles of co-existing metals, dissolved organic matter, and fertilizers. Science of the Total Environment 619-620, 1153-1162.
15. Zhang, Y., Leng, Z., Zou, F., Wang, L., **Chen, S.S.,** Tsang, D.C.W.[*], 2018. Synthesis of zeolite A using sewage sludge ash for application in warm mix asphalt. Journal of Cleaner Production 172, 686-695.

Conference Proceedings/Abstracts of Food Waste Valorization:

1. **Chen, S.S.,** Yu, I.K.M., Tsang, D.C.W. Catalytic conversion of towel paper to levulinic acid. The 2nd International Conference on Biological Waste as Resource 2017 (BWR2017), 25-28 May, Hong Kong, China, 2017.

2. **Chen, S.S.,** Yu, I.K.M., Tsang, D.C.W.; Yip, A.C.K. Valorisation of cellulosic food waste to value-added chemicals by heterogeneous Brønsted catalysts: A kinetic study. 4th International Symposium on Green Chemistry, 16-19 May, La Rochelle, France, 2017.

3. Yu, I.K.M., **Chen, S.S.,** Tsang, D.C.W. Food waste management in Hong Kong: Centralized or decentralized? Anaerobic digestion, composting, or landfill disposal? 3rd International Conference on Solid Waste, 20-23 May, Hong Kong, China, 2015.
4. Yu, I.K.M., **Chen, S.S.,** Tsang, D.C.W. Solvent effect on catalytic conversion of starch-rich food waste to hydroxymethylfurfural. The 2nd International Conference on Biological Waste as Resource 2017 (BWR2017), 25-28 May, Hong Kong, China, 2017.
5. Lam, C.M., Medel-Jimenez, F.J., Hsu, S.C., Yu, I.K.M., **Chen, S.S.,** Tsang, D.C.W. Integrated life-cycle assessment and cost-benefit analysis of food waste treatment scenarios at airport: A Hong Kong case study. 9th Asia-Pacific Landfill Symposium, 9-11 November, Hong Kong, China, 2016.

Acknowledgements

I would like to express my heartfelt gratitude to Dr. Daniel Tsang, my research advisor, and my mentor, who lightened my passion for research with his enthusiasm, taught me perseverance in the face of challenges, and inspired me to have vision with his devotion in education. I would also like to extend my sincere gratitude to Prof. Chi Sun Poon, who has always been my role model in academia, and supported and encouraged me in many ways.

My thanks must also go to our kind and helpful lab technicians in the Water and Waste Laboratory, who maintain a safe working environment to all the graduates, and provide professional and continuous help to me from experimental setup, troubleshooting to analytical work. Special thanks are to Mr. W.S. Lam, who is knowledgeable, trustworthy and does everything for the best benefit of the students and the advance of science. My previous and current group mates, I am not naming them all here, but in my heart. I must thank them for the things we experienced together, the happiness and the depression, the cheers and the support. Their companies brought so much strengths and joyful moments to my doctoral work.

Special appreciation and deep thanks are to Dr. Jean-Philippe Tessonnier at Iowa State University, for his devotion of a great deal of time and resources, and his generous sharing and support in terms of career during my ten-month visiting. My thanks of course extend to my dearest friends in Dr. Tessonnier's groups and all my friends at BRL second floor, for all the time we spent together and the intellectual talks we provoked. Also, I am grateful to have the support and company of my friends to get over many ups and downs in these years, especially for Zhiqi Yao, Peijie Chen, Qing

Ye, and Wilson Ko. Thanks to the opportunities given by Hong Kong PhD Fellowship Scheme and Fulbright Programme, which made every wonderful peace of my doctoral journey possible.

Above all, I owe my profound appreciation and respect to my parents, who may know little about my research, but know all about me. They are my superheroes. Mom’s tremendous love to me and to this family always make me feel peaceful when I am tired from work, and her patience and kindness motivate me to be a better person just like her. I admire Dad’s calmness, optimism and integrity, which guides me and reminds me in every aspect of my life. I am more than lucky to be their daughter, to be in this family full of love and laughter.

Table of Contents

Chapter 1 - Introduction

1.1 Background

Food waste crisis is an urgent global issue. According to the Food and Agriculture Organization, about one-third of the produced food (*i.e.,* 1.3 billion tonnes per year) covering from agriculture, industrial processing, to consumption ends up as food waste (Lin et al., 2013; Mirabella et al., 2013). There is approximately 3,600 tonnes food waste generated in Hong Kong daily, accounting for 35% municipal solid waste (HK EPD, 2016). Tradition disposal of food waste to landfills not only results in rapid depletion of precious land space, but also produces greenhouse gases and wastewater that exerts severe environmental burden. The Hong Kong government has planned to develop the Organic Resources Recovery Centre in phase, which adopt biological technologies (*i.e.,* composting and anaerobic digestion) to recover potential resources such as compost and biogas from the organic waste. In view of the capacities of the planned facilities, there will still be about 1,500 tonnes remaining food waste per day, which demonstrate a pressing need to explore alternatives of food waste/ biomass valorization to facilitate local recycling capacity.

Food waste, harbouring a variety of compounds, is a valuable yet less exploited resource for the conversion into value-added chemicals (Tabasso et al., 2015). Vegetable waste is primarily composed of cellulose (Nawirska et al., 2005), which is the most abundant biopolymer on Earth (Roy et al., 2009). Cellulose is first hydrolyzed to its monosaccharide, glucose, which is usually followed by isomerization to fructose, a key intermediate for the production of platform chemicals such as hydroxymethylfurfural (HMF), levulinic acid (LA), alkyl fructosides, and 5-

ethoxymethylfurfural. Starch is another polysaccharide consisting of glucose units which is also commonly found in food such as rice, noodles and bread.

Utilization of biomass to replace petroleum-based chemistry has been the new trend in recent decades, and the exploration of the wasted biomass, food waste, for the production of valuable chemicals, will render an alternative to contribute towards green chemistry and sustainable development. A previous study has demonstrated a maximum 4.3% HMF yield from catering waste and underlined the economic benefits (Parshetti et al., 20015), showcasing the potential and necessity of food waste valorization technology advancement. Therefore, this work articulated selective conversion of cellulosic-rich food waste by understanding the reaction kinetics, influence of substrate compositions, and morphological changes etc. from engineering perspectivess, and pinpointed the fundamental roles of local chemical environment on the rate-limiting step (*i.e.,* glucose isomerization).

1.2 Scopes and objectives

Vegetable and bread waste was recycled from the local market for selective and efficient conversion to platform chemicals such as HMF and LA catalyzed by heterogeneous Brønsted acids (*i.e.,* cation-exchange resins) under microwave heating. The reaction kinetics, solvent effects, and catalytic performance between homogeneous and heterogeneous acids were investigated in batch experiments. Glucose isomerization was identified as the rate-limiting step during bread food waste valorization, and selective isomerization of glucose to fructose was carried out via base catalysis. Chemical analysis was performed by using high performance liquid chromatography (HPLC) and ^{1}H nuclear magnetic resonance (NMR) spectroscopy.

Physico-chemical properties of important solid catalysts and residues were also characterized to elucidate the reaction mechanism.

The objectives of the thesis are listed below:

- Showcase selective conversion of cellulosic and starchy food waste;
- Reveal reaction kinetics in the catalytic pathway;
- Investigate roles of key factors in effective conversion;
- Facilitate the rate-limiting step in the course of conversion (*i.e.*, glucose isomerization) via base catalysis;
- Validate the feasibility of solid base catalyst in glucose isomerization to fructose;
- Unravel local chemical environment on glucose activity.

1.3 Thesis overview

This thesis contains eight chapters in total (**Figure 1.1**). Following **Chapter 1** as the introduction, **Chapter 2** is the literature review focusing on recent advances in the heterogeneous catalysts for the conversion of platform chemicals such as HMF and LA from food waste and other biomass waste (e.g., wood and agricultural products). It features the performance and roles of various types of solid catalysts in the catalytic pathways, and highlights the perspective and challenges during the conversion of actual biomass. As such, the research gaps are highlighted, which lay the cornerstone of this thesis.

Chapter 3 describes the methodologies and materials used in this study, from the collection and characterization of the substrate, synthesis of catalysts, conditions of the catalytic experiments, to product/ material characterization and analysis, which were designed on the basis of the corresponding research questions.

Chapter 4 – 7 investigate the roles of key factors in the catalytic system (*i.e.,* temperature, solvent and catalyst) and local chemical environment (*i.e.,* interaction between catalyst-solvent-substrate), in determining the efficiency and selectivity of cellulosic food waste to HMF and LA. The first step is to validate selective and effective conversion of vegetable waste, and reveal the associated reaction kinetics in the selected catalytic systems (**Chapter 4**), followed by investigating physico-chemical properties of the catalysts and substrates on the catalytic performance (**Chapter 5**). Similar catalytic system is applied for starchy food waste valorization, where glucose isomerization to fructose has been identified as the rate-limiting step. Therefore, **Chapter 6** focuses on enhancing glucose isomerization by solid base catalyst. To elucidate the fundamental roles of local chemical environment on glucose activity, various types and structures of homogeneous and heterogeneous base catalysts are examined (**Chapter 7**).

Chapter 8 concludes the key findings in this thesis and suggests the next-stage research to enhance fundamental understanding of the mechanisms associated with selective food waste conversion, and achieve effective and sustainable valorization of food waste/biomass waste in the future.

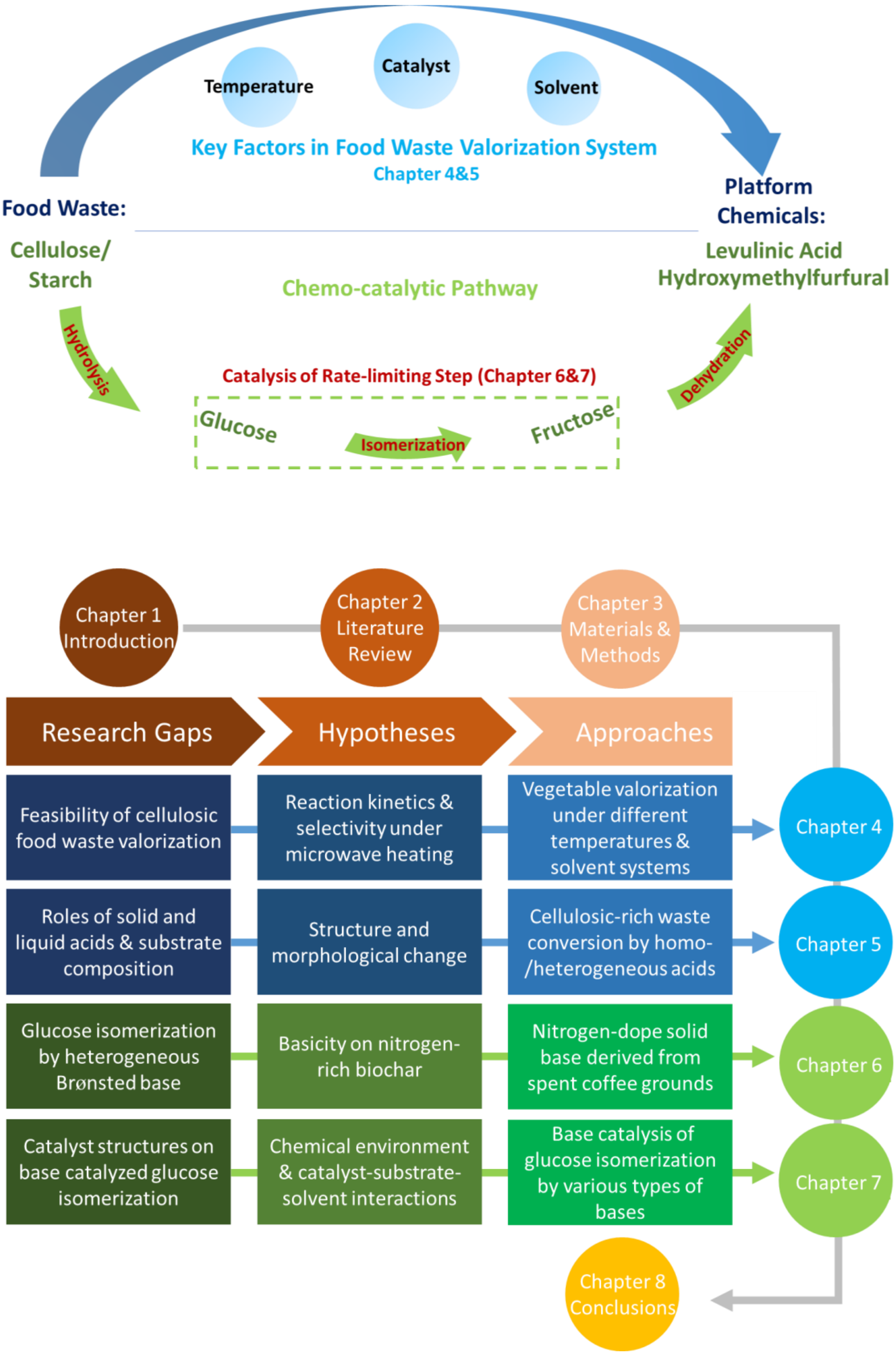

Figure 1.1 Thesis overview.

Chapter 2 - Literature Review

Abstract

Biomass conversion to value-added chemicals and fuels over heterogeneous catalysts is one of the top issues in green chemistry. This review focuses on recent advances in the application of solid catalysts for producing two prominent bio-based chemicals, hydroxymethylfurfural (HMF) and levulinic acid (LA) from biomass materials, respectively. Our work highlights the perspectives and challenges during the conversion of actual biomass, including the impact of complex constituents and impurities of biomass on the solid catalysts, mass transfer limitation in the reactions, and the stability and deactivation of the solid catalysts. Transformation of solid catalysts from research to industrialization necessitates more future work on identification of interactions between the catalysts and actual biomass, and comprehensive evaluation of the suitability of the catalysts in the reaction systems.

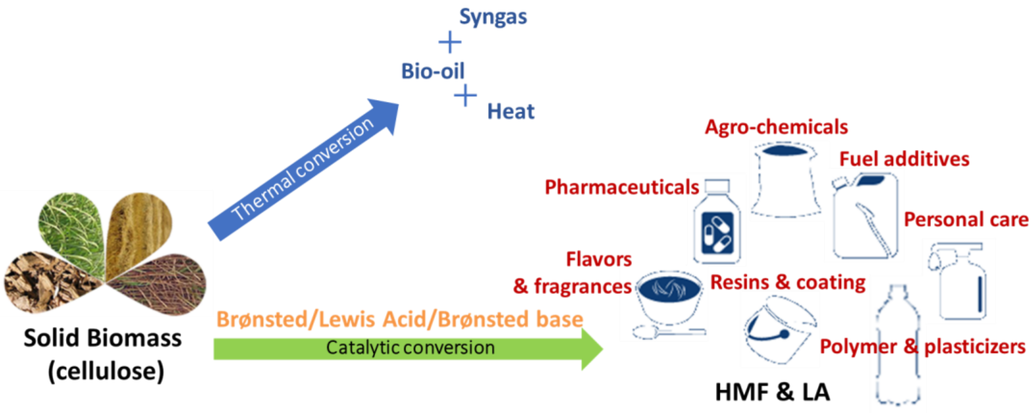

Figure 2.1. Graphical abstract of **Chapter 2.**

2.1 Introduction

Global energy demand is anticipated to increase by 2% per annum, with a predicted consumption to be twice of 2001 by 2050 (Li et al., 2016a). The gradual decrease in fossil fuel has urged a shift to biomass valorization as an alternative to secure the energy and chemical supplies. Utilization of biomass as a substitute for fossil feedstocks and generation of chemicals and products outstands in view of its carbon neutral circular framework (Zhang et al., 2016b). Besides, the emerging concept of “zero waste economy” encourages utilization of waste biomass as raw materials in productions and applications (Mirabella et al., 2014). Driven by environmental and economic needs, a considerable number of studies on biomass conversion into fuels and chemicals have been carried out from various approaches including thermal, biological, and chemo-catalytic processes (Zhang et al., 2016b).

Thermal conversion can produce heat and syngas via gasification, liquid hydrocarbon fuels via fast pyrolysis, and high energy density bio-oils via liquefaction (Bridgwater, 2003; Elliott et al., 2015). Biological transformations range from microbial or yeast-based fermentation processes to biocatalytic processes (Qureshi et al., 2010; Abdel-Rahman et al., 2013; Nanda et al., 2014). Chemo-catalytic conversion can be categorized into homogeneous and heterogeneous reactions. Mineral acids such as H_2SO_4, HNO_3 and $HClO_4$ are widely used in homogeneous catalytic reactions and exhibit favorable yields with reasonable cost. However, the practical applications raise concerns on reactor corrosion, waste generation, and limited recyclability (Zhou et al., 2013; He et al., 2014; Pang et al., 2014). Therefore, heterogeneous catalysis has attracted increasing attention in the applications for biomass conversion in view of its recyclability and easy separation from a reaction mixture (Lee et al., 2014; De et al., 2016; Zhang et al., 2016b).

Extensive research studies have investigated the production of various chemicals and biofuels such as 5-hydromethylfurfural (HMF), levulinic acid (LA), levulinic esters, and furfural over heterogeneous catalysts (Teong et al., 2014; Lee et al., 2014; Ennaert et al., 2016). The use of model compounds such as microcrystalline cellulose, glucose, and fructose (Ordomsky et al., 2012; Otomo et al., 2014; Hu et al., 2015) in the majority of the studies necessitates a comprehensive understanding of the catalytic systems and underlying mechanisms for biomass valorization (Yu and Tsang, 2017). Meanwhile, the technological barriers and engineering concerns of using actual biomass over the heterogeneous catalysis deserve closer investigation, which determine the success in industrial applications yet are often overlooked.

Therefore, instead of documenting all the published work in the relevant field in this review, we focus on the promising solid catalysts on the actual biomass conversion, and address the issues regarding the biomass categories and the interactions between biomass and catalysts (**Figure 2.2**). Based on our previous studies (Maneerung et al., 2016; Yu et al., 2017a; Yu et al., 2017b), the production of three valuable chemicals, namely HMF and LA are targeted in this review.

2.2 Production of HMF and LA from lignocellulosic biomass

Utilization of edible biomass towards bioethanol and first-generation biodiesel production has impacted food supply and aroused debates on its ethical issues (Zhang et al., 2016b). Lignocellulosic biomass is one of the most abundant renewable and inedible resources on earth, which provides an economical alternative to produce bioderived chemicals (Rackemann and Doherty, 2011; Zhou and Zhang, 2016). On the course of lignocellulosic biomass conversion, hemicellulose and cellulose can be hydrolyzed into pentoses and hexoses, which will further dehydrate into furfural and 5-hydroxymethylfurfural (HMF), respectively (Pileidis and Titirici, 2016). HMF is one of the top ten value-added bio-based chemicals listed by the US Department of Energy (Zhou and Zhang, 2016), and an important precursor for a variety of commodity chemicals and liquid fuels (**Figure 2.2**). For instance, it can be oxidized to 2,5-furandicarboxylic acid (FDCA) can replace petrochemical-derived terephthalic acid, or it can undergo hydrogenation or etherification to 2,5-dimethylfuran and 5-ethoxymethylfurfural, respectively, as promising liquid fuels.

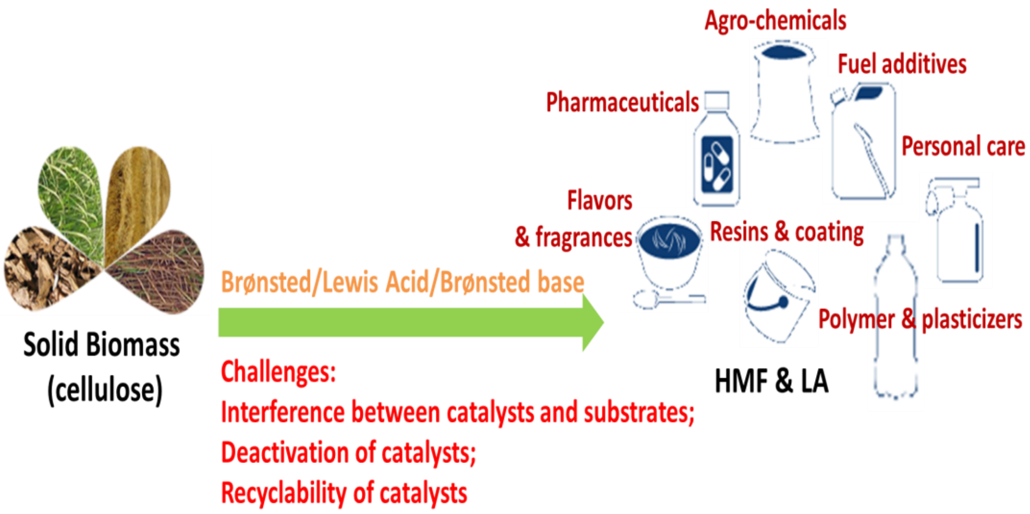

Figure 2.2. Illustrative conversion of biomass into hydroxymethylfurfural (HMF) and levulinic acid (LA)

Levulinic acid (LA) is produced via rehydration of HMF under acidic conditions, which is endowed with wide functionality and reactivity due to the presence of the ketone and carboxylic groups. It has also been identified as one of top twelve platform chemicals by the US Department of Energy, which can be used for the production of pharmaceuticals, solvents, fuel and oil additives, and plasticizers (Serrano-Ruiz and Dumesic, 2011; Gürbüz et al., 2011). Moreover, it can be transformed into levulinate esters through esterification in the presence of an alcohol, which can be applied in the flavoring and fragrance industries and as additives for production of liquid hydrocarbon fuels (Climent et al., 2014; Bond et al., 2014; Wettstein et al., 2012; Delidovich et al., 2014). Besides, it can be converted to succinic acid, diphenolic acid and GVL via oxidation, condensation and hydrogenation, respectively (Pileidis and Titirici, 2016). Alternatively, LA can be produced from hemicellulose through furfural and then furfuryl alcohol in three steps.

2.2.1 Hydrolysis

Hydrolysis is the starting point to convert polysaccharides in biomass into more active and accessible compounds, thus this section will focus on the hydrolysis of actual lignocellulosic biomass over solid acid catalysts, such as corn starch, sawdust, woods, paper, pulp, bagasse, rice hulls, corn stalks sorghum grains, cotton stems, wheat and rice straw. **Table 2.1** summarizes the valorization conditions and product yields of various biomass over solid catalysts, and the corresponding conversion principle is shown in **Fig 2.3**.

2.2.1.2 Brønsted acid catalysts

2.2.1.2.1 Sulfonated solids

Ion-exchange resins are insoluble polymeric materials that are capable of exchanging certain ions inside their structure with others in the reaction mixture. Sulfonated ion-exchange resins are typically co-polymers of styrene, divinylbenzene, and the active acid sites (*i.e.,* -SO_3H groups). Amberlyst, Nafion, and Dowen have been widely applied for acid hydrolysis of commercial polysaccharides into glucose (Onda et al., 2008; Ishida et al., 2014), or further dehydration to HMF (Oh et al., 2015). The comparably strong acidity of these sulfonated resins and their macroporous characteristics (~25 nm) make them suitable materials to cleave the large chains in the biomass (Rinaldi et al., 2008; Siril et al., 2008). For wood hydrolysis to sugars, Rinaldi et al. (2008) demonstrated that aluminosilicate zeolite such as zeolite Y and ZSM-5 barely had catalytic effect on depolymerization of cellulose because the pores of these solids were too narrow (0.7-1.2 nm) to be accessed by cellulose molecules. Although the sulfonated resins are capable of breaking down the β-1,4-glycosidic bonds on the cellulose chain, the rate of hydrolysis is retarded at the beginning, which is known as the induction time, due to the mass transfer limitation between the solid biomass and the catalyst (Rinaldi et al., 2008; Guo et al., 2013). Even though mass transfer can be facilitated by increasing the reaction temperature, the ion-exchange resins usually suffer from poor thermal stability (~ 150 °C) (Siril et al., 2008). To address this issue, silica-based and carbonaceous materials have been explored for the preparation of sulfonated catalysts.

Silica-based materials with mesoporous structure are selected because of high surface area and large pore volume that facilitate acid functionalization and saccharification (**Table 2.2**), which allow facile diffusion of the biomass into the catalytic centres enabling effective conversion in a short reaction time (Mondal et al., 2015). The silica matrix also presents the virtue of mechanical and thermal stability (Van de Vyver et al., 2010). The sulfonation is usually carried out in concentrated sulfonic acid with heating or by the use of organic sulfonating agents (Lai et al., 2011; Li et al., 2012). After sulfonation, both the pore volume and surface area of the catalysts decrease, and the thermal stability ranging from 160 to 270 °C is improved with the introduction of SO_3H groups depending on the specific sulfonation method (Ordomsky et al., 2012; Mondal et al., 2015; Hu et al., 2016). Sulfonated SBA-15 was demonstrated to convert rice straw into up to 38% monosaccharide at 180 °C within 1 h in water (Li et al., 2012). It was proposed that the protons of the $-SO_3H$ groups attacked the hemicellulose and cellulose in the rice straw that led to production of water-soluble oligosaccharides, which were further broken down into monosaccharides and by-products.

Table 2.1 Valorization of actual biomass into sugars, HMF and LA over solid catalysts.

Lignocellulose to Sugars

Biomass	**Catalyst**	**Solvent**	**Reaction Temperature (°C)**	**Reaction Time**	**Product Yield (wt%)**	**Heating**	**Feedstock Loading**	**Reference**
Spruce wood: 5 g	Amberlyst15: 1 g	[BMIM][Cl]: 100 g	100	5 h	TRS: 21%	Conventional	5%	Rinaldi et al., 2008
Rice straw: 3 g	Mesoporous silica-based solid acid: SBA-15: 0.5 g	Distilled water: 30 g	180	1 h	Monosaccharide: 38%	Conventional	10%	Li et al., 2012
Rice straw: 1 g	Mesoporous carbon-based catalyst: 0.5 g	Distilled water: 30 g	150	1 h	Monosaccharide: 43.4%	Conventional	3.33%	Qian et al., 2015
Corn cob 0.2 g	Corn cob hydrolyzed residue-derived carbonaceous solid acid: 0.2 g	Water: 2 mL	130	40 min	Glucose: 34.6%	Microwave	10.00%	Jiang et al., 2012
Corn cob: 1.5g	Fe_3O_4-SBA-SO_3H: 1.5 g	Water: 15 mL	150	3 h	TRS: 45%	Conventional	10%	Lai et al., 2011
Crop stalks (maize, wheat bean and rice): 0.5 g	Sulfonated magnetic carbon nanotube arrays: 0.5 g	DI water: 50 g	150	2 h	Glucose: 28.1-31.0%	Conventional	1%	Liu et al., 2014
Oil palm frond: 0.1 g	Fe/HY: 0.1 g	[BMIM]Br: 2 g and water: 0.1 g	120	3 h	TRS: 27.4%	Conventional	4.76%	Ramli and Amin, 2014

Empty fruit bunch: 0.1 g	Fe/HY: 0.1 g	[BMIM]Br: 2 g and water: 0.1 g	120	3 h	TRS: 24.8%	Conventional	4.76%	Ramli and Amin, 2014
Cellulose to Sugars								
Biomass	**Catalyst**	**Solvent**	**Reaction Temperature (°C)**	**Reaction Time**	**Product Yield (wt%)**	**Heating**	**Feedstock Loading**	**Reference**
Cellulose: 0.5 g	0.1 g	Water: 50 ml	180	9 h	TRS: 51%	Conventional	1.00%	Guo et al., 2013
Cellulose: 50 mg (Predissolved in [BMIM][Cl])	Cellulose-derived superparamagnetic carbonaceous solid acid: 30 mg	[BMIM][Cl]: 1g (and 0.01g water)	130	3 h	TRS: 68.9%	Conventional	4.95%	Guo et al., 2013
Rice straw: 50 mg (Predissolved in [BMIM][Cl])	Cellulose-derived superparamagnetic carbonaceous solid acid: 30 mg	[BMIM][Cl]: 1g (and 0.01g water)	150	2 h	TRS: 35.5%	Conventional	4.95%	Guo et al., 2013
Birch kraft pulp: 0.64 g	H-MCM-48: 0.30 g	Water: 150 mL	185	24 h	Glucose: 14%;	Conventional	0.42%	Käldström et al., 2012
Red macroalgae (*G. amansill.*): 50 mg	SBA-IL–HPW (SBA-15 supported ionic liquid phase with $H_2PW_{12}O_{40}$): 60 mg	Water: 5 mL	120	12 h	TRS: 58% (based on total sugar contents in	Conventional	1%	Malihan et al., 2016

					the biomass)			
Cotton cellulose: 4g	Sulphonated metal oxide: SO_4^{2-}/SnO_2 0.2g	Water: 50 mL	190	3.5 h	Glucose: 26.8%	Conventional	8.00%	Yang et al., 2015
Rice straw-derived cellulose: 50 mg	Chlorine-doped magnetic carbonaceous solid acid: 30 mg	[BMIM]Cl: 1g (and 0.01 g water)	130	4 h	TRS: 73.2%	Hydrothermal	4.95%	Hu et al., 2016
Lignocellulose/Cellulose to HMF or LA								
Biomass	**Catalyst**	**Solvent**	**Reaction Temperature (°C)**	**Reaction Time**	**Product Yield (wt%)**	**Heating**	**Feedstock Loading**	**Reference**
Cassava waste: 1 g	Sulfonated carbon-based catalyst: 0.05 g	acetone/DMSO (70:30 w/w) to water (10:90 w/w): 50 g	250	1 min	HMF: 12.5%; Furfural: 2.1%	Conventional	2.00%	Daengprasert et al., 2011
Corn stalk: 50 mg	Corn stalk-derived carbonaceous solid acid: 50 mg	[BMIM][Cl]: 1g	150	30 min	HMF: 44.1 mol%	Conventional	5%	Yan et al., 2014
Sugarcane bagasse: 25 mg	Sulfonated polytriphenylamine (SPTPA): 5 mg	DMSO: 2 mL	140	1 min	HMF: 18.8%	Microwave	1%	Mondal et al., 2015
Corn stalk: 0.4 g	Sulfonated carbon catalyst: 0.3 g	GVL: 20 mL	210	1 h	HMF: 2.24% ^{a}; Furfural: 60% ^{a}	Conventional	2.00%	Zhang et al., 2016

Corn cob: 25 mg	SPTPA: 30 mg	GVL: 2 mL	175	30 min	HMF: 33% ^{a}; Furfural: 73% ^{a}	Conventional	1.25%	Zhang et al., 2017
Corncob: 40 mg	SPTPA: 12 mg	GVL: 2 mL	175	45 min	HMF: 27.1% ^{a}; Furfural: 62.4% ^{a};	Conventional		Zhang et al., 2017
Corn stalk: 0.4 g	PTSA-POM: 0.2 g	GVL: 15 mL & Water: 1.5 mL	190	100 min	HMF: 19.5% ^{a}; Furfural: 83.5% ^{a}	Conventional	2.67%	Xu et al., 2015
Foxtail weed: 25 mg	HPA-SiO_2: 5 mg	DMA-LiCl: 0.5 g	120	2 min	HMF: 32%	Microwave		Alam et al., 2012
Mixture of corn stover, pinewood or husk of xanthoceras: 0.1 g	$ChH_2PW_{12}O_{40}$: 0.11 mmol	MIBK:water 5 mL: 0.5mL	140	8 h	HMF: 13.1-27.6%	Conventional		Zhang et al., 2016c
Birch kraft pulp: 0.64 g	H-MCM-48: 0.30 g	Water: 150 mL	185	24 h	HMF: 8%	Conventional	0.42%	Käldström et al., 2012
Cotton cellulose: 4g	Sulphonated metal oxide: SO_4^{2-}/SnO_2 0.2g	Water: 50 mL	190	3.5 h	HMF: 11.0%;	Conventional	8.00%	Yang et al., 2015
Microalgae: 0.3 g	H-ZSM-5: 0.2 g	substrate solution: 30 mL	200	2 h	HMF: 38.6%	Conventional	1%	Wang et al., 2015
Corn strover: 0.18 g	Amberlyst70: 0.2 g	GVL: 2.7 ml; water: 0.3 mL	160	16 h	LA: 54%	Conventional	6.00%	Alonso et al., 2013
Cotton Straw: 1 g	SBA-SO_3H: 1 g	Water: 20 mL	180	6 h	LA: 18 mol%	Conventional	5%	Lai et al., 2011
Rice straw: 0.5 g	Ga@HPMo; GaHPMo: 0.1 g	Not reported	175	6 h	LA: 56% (from	Conventional	Not reported	Kumar et al.,

					hydrolysate)			2016
Empty fruit bunch	$CrCl_3$-HY hybrid catalyst: 0.1 g	Water	145.2	2.445 h	LA: 53.2% [a]	Conventional	1.00%	Ya'aini et al., 2012
Kenaf	$CrCl_3$-HY hybrid catalyst: 0.1 g	Water	145.2	2.445 h	LA: 66.1% [a]	Conventional		Ya'aini et al., 2012
Sugars to HMF or LA								
Biomass	**Catalyst**	**Solvent**	**Reaction Temperature (°C)**	**Reaction Time**	**Product Yield (wt%)**	**Heating**	**Feedstock Loading**	**Reference**
Fructose corn syrup: 14.3 g (50 mmol fructose)	Amberlyst 15: 10 g (47 mmol SO_3H)	1,4-dioxane: 100 mL	100	3 h	HMF: 80%	Conventional	10.73%	Jeong et al., 2013
Fructose corn syrup: 14.3 g (50 mmol fructose)	Wood powder-derived carbon catalyst: 12 mol%	dimethoxyethane: 3 mL	120	4 h	HMF: 75%	Conventional	357%	Kim et al., 2014
Hydrolyse of rice Straw	WO_3/ZrO_2	Water	130	6 h	HMF: ~10%	Conventional	Not reported	Giang et al., 2014
Jerusalem artichoke juice	$Nb_2O_5 \cdot H_2O$: 0.1 g	Water: 2-butanol: 20:30 mL	160	40 min	HMF: 22%	Conventional	6%	Yang et al., 2011b
Mannose: 25 mg	TiO_2-H: 10 mg	DMA-LiCl (10wt% LiCl): 0.5 g	140	5 min	HMF: 35%	Microwave	Not reported	De et al., 2012

Table 2.2 Selected properties of sulfonated catalysts.

Conversion Pathway	**Yield (wt%)**	**Catalyst**	**Surface area (m^2 g^{-1})**	**Pore volume (cm^3 g^{-1})**	**Acid amount (mmol g^{-1})**	**Reference**
Lignocellulose to sugars	Monosaccharides: 38%	Mesoporous Silica (SBA-15) -based Solid Acid	680	0.58	2.2	Li et al., 2012
	Glucose: 34.6%	Corn cob hydrolyzed residue-derived carbonaceous solid acid	1	/	1.42	Jiang et al., 2012
	Monosaccharides: 43.4%	Mesoporous carbon-based catalyst	169	0.86	1.8	Qian et al., 2015
Cellulose to sugars	TRS: 68.9% (in ionic liquid); 51% (in water)	Cellulose-derived superparamagnetic carbonaceous solid acid	/	/	0.64 (-SO_3H group)	Guo et al., 2013
	TRS: 73.2%	Chlorine-doped magnetic carbonaceous solid acid	63.65	0.0536	1.82	Hu et al., 2016
Lignocellulose to HMF	HMF: 2.24%	Sulfonated carbon catalyst	654.8	0.9	1.14	Zhang et al., 2016
	HMF: 18.8%	Sulfonated polytriphenylamine	737	0.338	4.30	Mondal et al., 2015
	HMF: 33%	Sulfonated polytriphenylamine	344.3	0.134	1.8	Zhang et al., 2017
Cellulose to HMF	HMF: 12.5%	Sulfonated carbon-based catalyst	1.1	0.07	1.46 (-SO_3H group)	Daengprasert et al., 2011

TRS: total reducing sugar

2.2.1.2.2 Carbonaceous materials

Similarly, carbon-based materials are favourable for generating porous structure via incomplete carbonization (usually below 500 °C) followed by sulfonation for the hydrolysis of polysaccharides (Shopsowitz et al., 2011; Chen et al., 2015). Lignocellulosic biomass such as wood, corn stalk, and cotton is a suitable and naturally abundant precursor for porous carbonaceous material (Yan et al., 2014; Liu et al., 2014). The CH-π interactions between the carbohydrates and the hydrophobic carbon surface are vital to the adsorption process, where van der Waals forces are dominant in the interactions (Chinn et al., 1999; Yabushita et al., 2014). The sulfonated carbon catalysts also present weak acidic functional groups such as carboxylic (–COOH) and hydroxyl (–OH) groups. These hydrophilic surfaces are considered as the active sites for the hydrolysis of carbohydrates by the sorption of cellulose molecules or glucan chains via hydrogen bonds, although they are less significant compared to the sorption onto hydrophobic surface (Yamaguchi et al., 2009; Chung et al., 2014; Foo et al., 2015; Wang et al., 2016). It is suggested that the sorption of glucan chains onto the weak acid sites, which are present at the edges or the defect sites of the carbon surface, may induce a conformational change that enables the attack of glycosidic bonds (Loerbroks et al., 2013; Foo et al., 2015).

As reported by Qian et al. (2015), the monosaccharide produced from rice straw was up to 43.4% by using sucrose-derived catalyst on a mesoporous silica template at 150 °C for an hour in water. The functional groups and total acidity of the sulfonated carbonaceous catalysts are more important than surface area and pore size in terms of the catalytic performance (Table 2) (Geng et al., 2011; Hu et al., 2016;

Zhang et al., 2016). A chlorine-doped magnetic carbonaceous solid generated 73.2% monosaccharide from rice straw in an ionic liquid at 130 °C for 4 hours (Hu et al., 2016). The presence of –Cl in the sulfonated catalysts showed synergistic effect together with $–SO_3H$, as the former can act as strong electron donor to enhance the acidity of $–SO_3H$ **(**Pang et al., 2014**)**. At the same time, –Cl promoted adsorption of cellulose due to its stronger electronegativity than weak acids such as –COOH and –OH (Hu et al., 2014).

In general, increasing the total acidity of the catalysts, especially the portion of $–SO_3H$, will increase the hydrolysis rate of the cellulosic structure in biomass (Foo et al., 2015). However, at the higher dosage of catalysts, the yield of target products will first increase and then decrease due to the excess of $–SO_3H$ catalyzed sugars and quick decomposition of HMF (Li et al., 2012; Yan et al., 2014; Xu et al., 2015). This suggests that the optimal production is controlled by the equilibrium between biomass hydrolysis and sugar conversion/decomposition. The reported sulfonated catalysts could maintain the catalytic performance in four to five cycles owing to the thermal stability of $–SO_3H$ under the reaction temperature (< 220 °C). Besides, more fused rings in the catalysts allow dispersion of conjugated π binding that contributes to hydrothermal stability (Hara, 2010; Wang et al., 2016).

2.2.1.2.3 Magnetic Brønsted catalysts

Magnetite (Fe_3O_4) was introduced to a sulfonated mesoporous silica base via a surfactant-templated sol-gel method (Lai et al., 2011), after which the catalyst could be easily separated from the reaction mixtures by an external magnet and reused for three runs without obvious loss of catalytic activity. Magnetic solid catalysts were also developed on carbonaceous materials derived from glucose and cellulose, where –SO_3H groups serve as the active sites for biomass hydrolysis (Zhang et al., 2012; Guo et al., 2013; Hu et al., 2016). The porous structure of carbonaceous materials allows the introduction of Fe_3O_4 without reducing the amount of –SO_3H groups.

Nanoparticles such as $CoFe_2O_4$ (Takagaki et al., 2011) and Fe-graphene oxide (Verma et al., 2013) were also embedded in the solid catalysts for the hydrolysis of cellulose to glucose. Besides, hydrotalcite nanoparticles were activated with $Ca(OH)_2$ and hydrolysed cellulose into glucose at 150 °C (Fang et al., 2011). By using the functionalized nanostructure of graphene oxide (Fe-GO-SO_3H), a 42% yield of monosaccharides (39% xylose and 3% glucose) was reached from the conversion of sugarcane bagasse in water at 75 °C for 44 h (Verma et al., 2013). The excellent catalytic activity was attributed to the synergistic effect of adsorption of cellulose onto –OH groups of graphene surface and hydrolysis of cellulose by soluble –COOH groups.

2.2.1.2.4 Heteropoly acids

Heteropoly acids (HPAs) are protonic acids displaying Brønsted acidity and good stability in the presence of early transition metal-oxygen anion clusters (Hill, 2007; Kozhevnikov, 2009; Macht et al., 2007). The Keggin type ($[XY_xM_{(12-x)}O_{40}]^{n-}$ (X is the heteroatom; M and Y are addendum atoms)) is most widely used, while it will release proton in polar solvents. The stronger Brønsted acidity of the HPA, the more favourable for the cleavage of β-1,4-glycosidic bonds of cellulose in aqueous solution (Shimizu et al., 2009). The strong hydrogen-bond accepting ability of HPA resulting from the external metal-oxygen clusters from the anions leads to the decreased crystallinity of cellulose, which accounts for high catalytic performance of HPA.

The introduction of cations such as Cs^+, Ag^+, Hf^{4+}, Sn^{4+} and Ga^{3+} to replace protons could not only make the catalyst insoluble in polar environment, but also increase the basicity of the heteropolyanion, therefore endowing an acid-base bifunctional characteristic to the catalyst (Okuhara et al., 1992). Among the salts of $H_3PW_{12}O_{40}$, the hydrolysis of cellulose increased along with increasing Lewis acidity of cations, while the selectivity to reducing sugars was the highest with the presence of moderate Lewis acidity such as Sn^{4+} and Ru^{3+} (Shimizu et al., 2009). For instance, Kumar et al. (2016) synthesized Ga salt of polyoxometallate (GaHPMo) and encapsulated HPMo in Ga spheres (Ga@HPMo) via sonochemical irradiation, where the Keggin structure of heteropoly acid retained. The catalysts were used for conversion of starch, cellulose and rice straw derived glucose into levulinic acid, and exhibited 100% conversion of glucose and up to 56% yield of LA at 175 °C for 6 h.

The heteropoly acids can be immobilized in the supported materials as solid catalysts. Malihan et al. (2016) used the photungstic acid ($H_3PW_{12}O_{40}$)-based acidic ionic liquid anchored on mesoporous SBA-15 to hydrolyse a red macroalgae, *Gelidium amansill.,* at 120 °C and yielded 55% total reducing sugar. The catalyst was prepared by attaching the chloride-containing ionic liquid on SBA-15 via covalent bonds, followed by anion exchange between chloride and $H_3PW_{12}O_{40}$ to create acid sites. Most of the supported heteropoly acids were employed in acidic ionic liquids in order to assist the decomposition or hydrolysis of cellulose (Alam et al., 2012; Zhang et al., 2016c). However, expensive cost and high viscosity of ionic liquid limits its upscale commercialization. Therefore, it is important to develop suitable catalysts that can work on the crystalline structure of cellulose (Hu et al., 2016). Recently, Zhang et al. (2016c) prepared a series of $Ch_xH_{3-x}PW_{12}O_{40}$ with choline chloride and $H_3PW_{12}O_4$, which entitled the catalysts with hydrophobic tail (Ch^+) and hydrophilic head ($H_2PW_{12}O_{40}^-$). The use of $Ch_xH_{3-x}PW_{12}O_{40}$ in a MIBK/H_2O biphasic system achieved a HMF yield of 13.1-27.6% from a mixed lignocellulosic biomass of corn stover, pinewood, and husk of xanthoceras at 140 °C. It is concluded that the hydrophilic head of the catalyst concentrates cellulose for catalytic conversion while the hydrophobic tail inhibits further hydration of HMF to LA, which highlights the synergistic effects between the components in the tailored catalysts.

2.2.1.2.5 Zeolites

Highly polarized hydroxyl groups in zeolites act as Brønsted acids, while the coordinatively unsaturated cations act as Lewis acids (Kuster, 1990). For example, the substitution of Si atoms in the zeolite framework by Ti (Mal and Ramaswamy, 1997; Mal et al., 1994), Sn (Moliner, 2014; Yang et al., 2013), Zr (Lewis et al., 2014;), Hf (Dzwigaj et al., 2010), V (Chien et al., 1997), Nb (Corma et al., 2009), and Ta (Corma et al., 2009) can generate Lewis acidity. Some extra-framework species such as Ga, Al, and Zn also demonstrate Lewis acidity. The Brønsted acid sites in the zeolite are found to assist in the hydrolysis of cellulose into soluble cello-oligomers, suggesting the existence of solid-solid interactions between the acid sites and the cellulose polymers (Ennaert et al., 2015).

Due to mass transfer limitation between substrates and zeolites , the hydrolysis of cellulosic materials via zeolite alone usually generates low yield of glucose or HMF. A series of zeolite catalysts with various Si-to-Al ratio were synthesized for the transformation of birch kraft pulp to glucose and HMF in water, and the yield was lower than 15% and 10%, respectively (Käldström et al., 2012). Ya'aini et al. (2012) synthesized hybrid catalyst with $CrCl_3$ and HY zeolite in order to generate higher porosity and stronger Lewis acidity of the catalyst. The catalytic conditions of empty fruit bunch and kenaf conversion to LA were optimized based on response surface methodology and central composite design. In addition, the shape selectivity effect of HY zeolite controlled the formation of LA. The HMF molecule (0.82 nm) would not be released from the pore of HY zeolite (0.75 nm) until it was rehydrated into levulinic acid. The yield of LA was 53.2% and 66.1% from empty fruit bunch and kenaf at 145.2 °C for 2.5 hour in water, respectively, based on the maximum theoretical yield.

In order to enhance the catalyst acidity and retain the mesoporous structure, while avoiding the use of hazardous materials such as $CrCl_3$, Ramli and Amin (2014) implemented wet impregnation of Fe on the HY zeolite. The synthesized catalyst was used to hydrolyse oil palm biomass in ionic liquid to reducing sugar (25-27% under optimal conditions), and the hydrolysate was further used to produce LA. As shown in **Table 2.1**, the hydrolysis temperature in the presence of ionic liquid (100-150 °C) is much lower than those in aqueous solutions (120-250°C). The use of ionic liquid in the catalytic hydrolysis of cellulose can enhance the solubility of the substrate (Ramli and Amin, 2014). However, separation of sugars from ionic liquid is a challenge for the catalytic process. To avoid the use of ionic liquids, hierarchical zeolites consisting of a secondary level of mesoporous structure can increase the number of accessible active sites and facilitate diffusion of biomass-derived substrates (Jacobs et al., 2014; Kubička et al., 2015b).

2.2.1.3 Supported metal catalysts

The supported metal catalysts are widely used for oxidation and hydrogenation reactions in the conversion of biomass to chemicals (Alonso et al., 2012; Singh and Xu, 2013; Besson et al., 2014), yet they are less common for the hydrolysis of cellulose into glucose. A range of carbon materials, including mesoporous carbon materials (CMK-3), activation carbon, fullerene, and carbon black could be used to support Ru catalyst for hydrolysing cellulose to sugars (Hu et al., 2015). The selectivity of glucose increased with the Ru content on CMK-3, while the yield of total reducing sugar was little affected. It was suggested that Ru plays an important role in converting oligosaccharides into glucose after the conversion of cellulose into oligosaccaharides by CMK-3 (Kobayashi et al., 2010). It was also proposed that Ru species could act as a Brønsted acid by heterolysis of water molecules on Ru as well as a Lewis acid by desorption of hydrated water of $RuO_2 \cdot H_2O$ (Komanoya et al., 2011; Huang and Fu, 2013).

2.2.2 Engineering aspects & summary

2.2.2.1 Pretreatment of biomass

The utilization of lignocellulosic biomass in place of sugars, starch, and vegetable oils eliminates the ethical concern of competing with food supply for feedstocks (Alonso et al., 2010). Lignocellulosic biomass from agricultural residues (including corn stover and sugarcane bagasse) as well as energy crops and forestry residues (including sawmill and paper mill discards) is composed of cellulose (40-50%), hemicellulose (25-35%) and lignin (15-20%) (Rackemann and Doherty, 2011; Filiciotto et al., 2017). The decomposition of hemicellulose is much easier than that of cellulose due to the branched structure of hemicellulose. It was shown that pentoses accounted for 50% of the solubilized oligomers where hexoses were less than 2% resulting from poplar wood chips at 170 °C for 2 h (Gürbüz et al., 2013) **Table 2.1** also exihited that glucose rather than HMF or LA was the major product from cellulosic biomass valorization, indicating the rate-limiting step of glucose isomerization to fructose hampered further conversion.

The presence of impurity in the biomass could interfere with the catalytic reactions. In addition, the lignin-cellulose-hemicellulose network in the lignocellulosic biomass makes its hydrolysis more challenging than that of cellulose (Zhang et al., 2016). It was reported that residual xylose in rice straw fibre could adversely affect the synthesis of LA due to the formation of humins via polymerization of furfurals with saccharides (Runge and Zhang, 2012; Elumalai et al., 2016). Besides, inorganic salts in the raw biomass could poison the Brønsted acidic sites in sulfonated catalysts and zeolites, resulting in a significant drop of product yield (Ennaert et al., 2016). Therefore, pretreatment of biomass is a critical process to the success of biorefinery, especially for enzymatic hydrolysis, where cellulase can be irreversibly adsorbed into lignin (Ravindran and Jaiswal, 2016). However, the pretreatment process could be overlooked due to the use of model compounds in many research studies (Ennaert et al., 2015a).

Depending on the pretreatment techniques, it can be classified into physical, chemical, physio-chemical, and biological methods, which are extensively reviewed by Ravindran and Jaiswal (2016) particularly for subsequent enzymatic hydrolysis. The commonly used pretreatment methods include: (i) mechanical disruption by grinding and milling, which can not only reduce the particle size and increase the surface area, but also break hydrogen bonds and facilitate access to the solid acid catalysts (Tabasso et al., 2015); (ii) explosive depressurisation by steam or CO_2 to swell the feedstocks (Zheng et al., 1998; Ramos, 2003); and (iii) immersion in diluted acids or ionic liquids to decrease the crystallinity (Kim et al., 2010). After the pretreatment, the XRD patterns of biomass (rice straw, poplar, and switchgrass) showed consistent increase in cellulose crystallinity, which is the collective results of enhanced removal of soluble hemicellulose and lignin as well as amorphous cellulose, leaving highly ordered cellulose intact in the solid fibres (He et al., 2008; Foston and Ragauskas, 2010; Pu et al., 2013; Elumalai et al., 2016). There were some drawbacks such as generation of lignin-like polymeric products when treating rice hulls and straw, corn stalks, and saw dust with HCl at 160-190 °C (Rackemann and Dohertyand, 2011; Galletti et al., 2013). A cost-effective pretreatment for biomass valorisation should produce a high yield of sugars while low yield of by-products at mild conditions.

2.2.2.2 Microwave-assisted hydrolysis

The more sophisticated and recalcitrant structures in the biomass materials may require higher temperature for conversion than model compounds, which indicates a possibility of more side products and less selectivity (Ramli and Amin, 2014; Zhang et al., 2016). Tabasso et al. (2015) conducted comprehensive review on the use of microwave-assisted catalysis for bio-waste valorisation in mineral acids, ionic liquids, metal chlorides, and solid acid catalysts, where the higher reaction rate was attributed to the effectiveness of structure disruption and release of cell constituents from the bio-waste. Li et al. (2012) catalyzed cellulose hydrolysis by concentrated $H_3PW_{12}O_{14}$, and the yields of glucose reached 27.8-43.3% when using bagasse, corncob, and corn stover as feedstock at a low temperature of 90 °C. Fan et al. (2013a) investigated depolymerisation of cellulose under microwave heating, and found that the yield of glucose was almost 50 times higher than conventional heating under similar conditions. Conversion of tomato plant into LA reached a yield of 63% under microwave heating at 225 °C in 2 min, compared to 5% yield from conventional heating for 2 h (Tabasso et al., 2014).

These studies clearly demonstrated that intensified process via microwave irradiation can assist biomass hydrolysis. Nevertheless, unconventional heating method might generate different product profiles compared to conventional heating (Tian et al., 2010; Fan et al., 2013b). For instance, formation of levoglucosan was only observed under microwave treatment according to Fan et al. (2013b), which suggested a different active centre between microwave and conventional hydrolysing media. A recent kinetic study on the LA production from starch showed that the activation energy of glucose dehydration to HMF was 91–101 kJ mol^{-1}, which was significantly lower than that under oil bath heating of 228-246 kJ mol^{-1} (Mukherjee and Dumont, 2016). These activation energy values account for different product formation between microwave and conventional heating conversion.

2.2.2.3 Preparation & deactivation of catalysts

Cost effectiveness is a crucial element for the success of scale-up biomass valorisation, which highlights the consideration of the synthesis cost and life-time of the catalysts. Sadaba et al. (2015) developed a decision flowchart to evaluate the suitability of a solid catalyst in terms of stability and recyclability. Sulfonated catalysts have been extensively applied for their surface acidity and demonstrated promising results in valorization of hemicellulosic/cellulosic materials. One of the raw materials to synthesize this sulfonated catalyst was chloromethyl polystyrene (CP), which is a petroleum-based material, thus the economic cost could hamper its commercial application. In addition, leaching of SO_4^{2-} was commonly reported during the reaction and resulted in decreasing catalytic activities (Wang et al., 2016). Besides, ionic liquid, humins, and other by-products were found to block the active sites in the zeolitic materials and accounted for the loss of catalytic activity (O'Neill et al., 2009; Taarning et al., 2009; Ramli and Amin, 2014). While thermal calcination was the most commonly used to remove deposited products due to catalyst fouling or poisoning, leaching and deterioration of the active sites may require resource- and time-consuming regeneration of the catalyst (Yang et al., 2015). Changing the polarity of the medium may mitigate leaching (Sadaba et al., 2015). Therefore, specific consideration for regeneration and recycling of the catalysts may be needed when using the raw biomass in an industrial scale.

Product and catalyst recovery is of vital importance in the reaction processes, yet challenges remain in the literature. For instance, Girisuta (2007) found that LA could be heavily adsorbed onto the surface of the catalyst, which could hinder industrialization due to low product recovery. During the conversion of lignocellulosic biomass, the formation of solid residues was inevitable due to inactivity of lignin, formation of humins, and incomplete conversion of cellulose, which created difficulty in recycling the solid catalysts from the system (Lai et al., 2011).

2.2.2.4 Summary

In the course of hydrolysis of lignocellulosic biomass, mass transfer limitation should be overcome, which can be assisted by a variety of pretreatment methods and microwave heating. In terms of catalytic performance of the catalyst, the embedded functional groups and the Brønsted acidity may play a more important role than its surface area. Apart from the product yields, it is of significance to evaluate the recovery and reusability of the catalysts, as the impurities of the actual biomass may bring about uncertain effects and lead to catalyst deactivation. **Figure 2.3** shows an overview of heterogeneous catalysis from lignocellulosic biomass

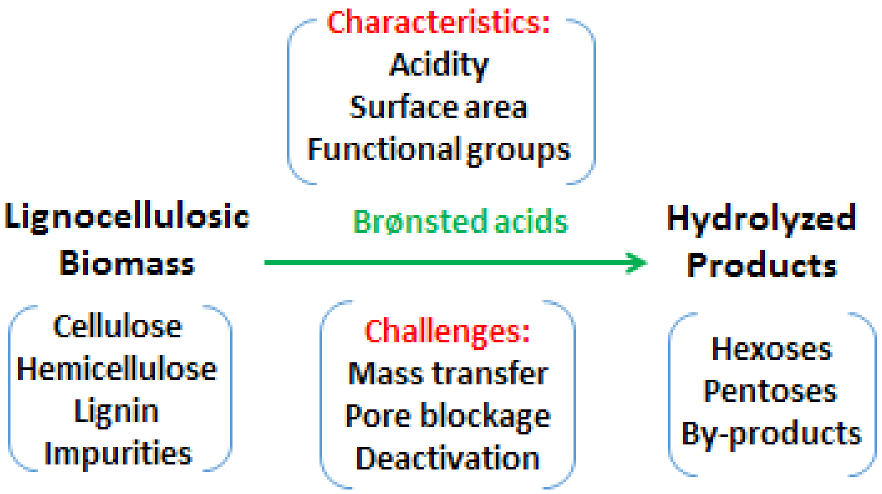

Figure 2.3 Overview of heterogeneous catalysis from lignocellulosic biomass.

2.3 Production of HMF and LA from sugary biomass

Upon the hydrolysis of polysaccharide biomass, the production of sugars is ready for further conversion to HMF and LA. Apart from cellulosic- and hemicellulosic-derived sugars, sugary biomass can also be obtained from waste streams or derived from algal biomass. High fructose corn syrup, as an industrial available sweetener, has been used to produce HMF and gave a remarkable yield of 80% by using Amberlyst 15 in 1,4-dioxane (Jeong et al., 2013). In recent years, rich carbohydrate content in food waste also makes it a promising feedstock for value-added chemicals production (Tabasso et al., 2015; Pleissner et al., 2016; Yu and Tsang, 2017). The mixed food waste generated a 4.3% yield of HMF as first reported (Parshetti et al., 2015). Fruit waste and vegetable waste from food waste streams are also favourable substrates in view of their high levels of free fructose and glucose. Wang et al. (2015) produced 14.7 wt% LA from kiwifruit waste in water in 15 min at 190 °C by using 20% Nb/Al oxide, and Chen et al. (2017) reported a fast yield of 17 C mol% LA from vegetable waste in 5 min at 150 °C by Amberlyst 36. Besides, owing to the rapid growth rate, marine algal biomass is also attractive for catalytic valorisation into HMF and LA by using commercial catalysts (Oh et al., 2015; Wang et al., 2015). The algal biomass contains various monosaccharides such as glucose, galactose, fructose, and xylose, which depend on the species (Goo et al., 2013).

It is widely recognized that HMF is converted from C6 sugars including dehydration of fructose and isomerization of glucose to fructose prior to dehydration, whereas LA is the rehydration product from HMF, which is companied by the formation of the same mole amount of formic acid. However, recent studies have found excess fraction of formic acid to levulinic acid, revealing the possible pathways of formic acid formation from direct hexose transformations and hexose-derived intermediates, such as furfuryl alcohol, furfural formation, pyruvaldehyde, and D-drythrose (Flannelly et al., 2016). In addition, C5 sugars such as xylose and arabinose provide an alternative for LA production through dehydration to furfural, hydrogenation to furfuryl alcohol followed by acid-catalyzed hydrolysis. This pathway represents a high atom economy due to the preservation of all carbon atoms (Ennaert et al., 2016). However, it is still limited by the excessive formation of by-products in the reaction medium (Antonnetti et al., 2016).

2.3.1 Isomerization by Brønsted base/Lewis acid catalysts

Although conversion of fructose to HMF or LA is convenient, glucose is a more abundant and cheaper substrate of cellulosic- and starchy-derived monosaccharide that may facilitate upscale production (Yan et al., 2009; Saravanamurugan et al., 2013). Starting with glucose, an aldose (glucose)-to-ketose (fructose) isomerization is necessary, which can be catalyzed by Lewis acid or Brønsted base catalysts. The catalytic mechanism via Lewis acid involves an intramolecular 1,2-hydride shift from the C2 to C1 position of the acyclic glucose (by forming a six membered cyclic intermediate), which is analogous to metalloenzyme catalysis (Román-Leshkov et al., 2010; Bermejo-Deval et al., 2012). Previous ^{13}C and ^{1}H NMR spectroscopic investigations confirmed the mechanistic similarities of glucose isomerization to fructose between homogeneous ($CrCl_3$ and $AlCl_3$) and heterogeneous (Sn-beta) Lewis acids in aqueous medium (Choudhary et al., 2013a). It is also noteworthy that not all Lewis acid sites are active or effective for glucose isomerization but they simultaneously catalyze side reactions of soluble polymers and insoluble humins (Choudhary et al., 2013b). Brønsted base activates the isomerization via promoting the formation of the 1,2-enediol intermediate and proton transfer from C2 to C1 (Liu et al., 2014).

2.3.1.1 Brønsted base catalysts

Strong inorganic bases were reported to achieve high glucose conversion but low selectivity to fructose due to the production of undesired by-products involving aldolization/retro-aldolization, 2,2-enediol anion, β-elimination and benzylic rearrangements (de Brujin et al., 1986; Liu et al., 2014). The typical yields of fructose from strong inorganic bases were below 10% (Román-Leshkov and Davis, 2011). Therefore, Liu et al. (2014) investigated the glucose isomerization by different types of amines because their broader range of pK_a values than inorganic bases could enable optimization to higher fructose selectivity. The fructose selectivity (54%) and yield (31%) by trimethylamine in 10 wt% glucose solution were similar to that by Sn-beta (Moliner et al., 2010). In spite of the formation of by-products, activated carbon showed selective removal of undesired compounds without affecting fructose concentration in the solution. It was suggested that organic amines may also reduce the number of water molecules in the vicinity of fructose to limit the side reactions. Amino acids containing amine groups and carboxylic acids were also investigated for glucose isomerization as nontoxic process, where arginine generated similar yield of fructose (31%) but higher selectivity (76%) than amines (Yang et al., 2016).

Strong basic anion-exchange resins such as Amberlite IRA-400 and Dowex #1 and #2 were also employed for glucose isomerization with about 30% of fructose yield (Langlois and Larson, 1956). Modified aluminate-bound resins could achieve high yield of fructose (up to 72%), where aluminate was a complexing agent for fructose and isomerization was attributed to hydroxide ions (Delidovich and Palkovits, 2016). Despite high yield, the resins suffered from low thermal stability and difficulty in removing the adsorbed substrate, which limited the reuse of catalysts in multiple cycles (Li et al., 2017).

Hydrotalcites (HTs) contain anionic species in their inter-lamellar spaces and have the general chemical formula of $[M^{2+}_{1-x}M^{3+}_{x}(OH)_2]^{x+}[A^{n-}]_{x/n}.yH_2O$, where M^{2+} is a metallic divalent cation (e.g., Co, Zn, Mg or Fe) and M^{3+} is a metallic trivalent cation. The basicity is controlled by the structure of the layered HTs and it can be modified in the course of calcination and rehydration (Li et al., 2017), where A^{n-} represents an interlayer anion and acts as an active centre for isomerization (Cavani et al., 1991). In the investigation of HO^- and CO_3^{2-} form of HTs, the former exhibited superior catalytic activity than the latter due to higher basicity of HO^- than CO_3^{2-} (Delidovich and Palkovits, 2016). By varying the synthesis conditions, Delidovich and Palkovits (2015) prepared Mg-Al HTs with different structural parameters and varied the catalyst basicity (0.01-0.41 mmol g^{-1}). These studies concluded that glucose conversion on the weak basic sites of carbonate anions was highly correlated to the basicity of HTs. However, the yield of fructose might not be solely attributed to the total basicity, as rehydrated Mg-Al HT prepared by Yu et al. (2012) containing abundant weak basic sites resulted in comparable fructose yield to that with strong basic sites (Lima et al., 2008). It was inferred that the rehydration process resulted in smaller crystallite size due to exfoliation and vertical breaking of HT layers (Yu et al., 2012).

2.3.1.2 Lewis acid catalysts

2.3.1.2.1 Metal oxides

Metal oxides from Group IV and V are generally active for glucose isomerisation due to unsaturated coordination of metal species as water-tolerant Lewis acid sites (Nakajima et al., 2011; Jimenez-Morales et al., 2014a). Early transition metal oxides with a high density of Lewis acid sites share similar catalytic mechanism with zeolite and enzyme catalysts for glucose isomerization (Brand et al., 2016; Dijkmans et al., 2016). Mesoporous metal oxides can be prepared to increase surface area of the catalysts and facilitate accessibility of substrates via a variety of templates such as block copolymers, surfactants, and amines (Chandra et al., 2008; Parida et al., 2010; Jagtap et al., 2011). A layered zirconosilicate catalyst prepared from mesoporous molecular sieves was observed to possess insufficient stability, where the yield of fructose decreased from 27% to 19% after the third run (Yue et al., 2013). Spectroscopic evidence confirmed that isomerization of glucose was catalyzed by the basic sites generated from the metal oxides TiO_2 and ZrO_2 (Watanabe et al., 2005). Recent studies found that higher basicity of the catalysts increased the selectivity toward fructose (Kitajima et al., 2016). In addition to tunable properties, Li et al. (2016) revealed that the introduction of transition metals such as Zr^{4+}, Ti^{4+}, Nb^{5+} and Ta^{5+} on tungstite ($WO_3 \cdot H_2O$) facilitated stabilization of the deprotonated form of glucose and thus lowered the energy barrier for isomerization on the basis of density functional theory study.

2.3.1.2.2 Zeolites

The Lewis acid catalyzed reactions are often carried out in apolar and aprotic solvents, as otherwise the electron-rich oxygen atoms in protic solvents coordinate with the Lewis acid sites that hinder the substrate coordination or lead to solvation effect (Ennaert et al., 2016). The Sn-beta form is one of the most active Lewis-acid-containing zeolites for glucose isomerization to fructose because of its open Sn site (Bermejo-Deval et al., 2014). Its hydrophobic structure can reduce the number of surrounding water molecules. The relatively large pore diameter of beta type zeolite (BEA, 0.77 nm (Baerlocher et al., 2010)) makes it suitable for sugar conversion (Ennaert et al., 2016). A 29 wt% of fructose yield was obtained from 45 wt% glucose solution, and the Sn-beta catalyst was stable for four consecutive reactions (Moliner et al., 2010).

However, the stability of Sn-beta in an aqueous medium was inconsistent among studies. A continuous flow of glucose isomerization in an aqueous medium showed a permanent loss of over 90% activity of Sn-beta (Padovan et al., 2016), and a kinetic study conducted by Rajabbeigi et al. (2014) suggested that the deactivation of Sn-beta was not only related to the formation of by-products, but also due to the reaction between water and catalysts. Alternative solvents may be required for Sn-beta. Nevertheless, thermal stability at high temperatures and tolerance in acidic environment make Sn-beta feasible for coupling isomerization with hydrolysis and hydration/dehydration in a one-pot reaction (Davis, 2015; Orazov and Davis, 2015; Luo et al., 2016).

In addition to Sn-beta, MFI-type zeolites have attracted investigation for sugar isomerization owing to its shorter synthesis time compared to Sn-beta (2 days vs 22-40 days) and avoidance of fluoride media (Lew et al., 2012; Dapsens et al., 2014). The employment of Sn-MFI showed superior catalytic performance for the conversion of sugars such as xylose, lactose, and dihydroxyacetone in water or methanol (Lew et al., 2012; Cho et al., 2014; Dapsens et al, 2014). However, the largest pore dimension of MFI is 0.56 nm, which is narrower than the kinetic diameter of glucose (0.86 nm) (Baerlocher et al., 2007; Jae et al., 2011), thus limiting the reactivity to external surface of the catalysts. Due to limited access and diffusion limitation to the active sites, fructose yield was only 4% from glucose isomerization by Sn-MFI (Lew et al., 2012). Synthesis of hierarchical Sn-MFI via stannation of silicate-1 improved the fructose yield to 27% in 2 h (Dapsens et al., 2014), which was attributed to both alleviation of diffusion constrains and higher utilisation of Sn at the external surface of zeolite. By tailoring the physicochemical properties, a single-unit-cell Sn-MFI zeolite with uniformly distributed Sn at the framework has exhibited a high yield of 65% fructose from glucose via a two-step protocol with an intermediate of ethyl fructoside (Ren et al., 2015).

Since the yield of fructose was often below 40% using auxiliary metal-containing zeolites, Saravanamurugan et al. (2013) proposed the use of commercially available zeolites in methanol via a one-pot, two-step approach. In the first step, glucose was converted to fructose, and a part of fructose undertook etherification to methyl fructoside. Then, the addition of water into the system hydrolyzed methyl fructoside back to fructose. Zeolite Y was the most active catalyst, which generated 55% fructose at 120 °C for 1 h.

2.3.2 Dehydration and rehydration by bifunctional catalysts

Compared to glucose isomerization, fructose dehydration to HMF requires higher temperatures (Jimenez-Morales et al., 2014a; 2014b). Lewis and Brønsted acid catalysts can be combined to catalyze sequential reactions of isomerization and dehydration/rehydration and thus produce HMF and LA in a single reactor. A combination of $CrCl_3$ and HCl reached a yield of 59% HMF in a biphasic system and 46% LA in a single phase (Choudhary et al., 2013a). Hydrolysis of Lewis acids such as metal chlorides can also result in the production of Brønsted acidic proton to catalyze the dehydration of fructose or rehydration of HMF. A recent study on the acid types of various Niobium oxides revealed that glucose conversion to HMF was most effective and selective by Lewis acid, while it was also possible by strong Brønsted acid but negligible by weak Brønsted acid (Kreissl et al., 2016). In contrast, fructose dehydration to HMF was more selective by weak than strong Brønsted acid. It was also reported that Lewis acidity would promote side reactions of fructose conversion more than HMF formation (Choudhary et al., 2013b).

2.3.2.1 Metal oxides

Water-tolerant Lewis acids have attracted extensive interest in the development of solid catalysts for aqueous-phase transformation of waste-derived sugar streams to HMF or LA (Reche et al., 2016). Acidic hydroxyl groups of metal oxides are responsible for the Brønsted acid sites, while exposed oxygen-deficient cations act as Lewis acid sites (Takagaki et al., 2010; Nakajima et al., 2011; Zhao et al., 2012). Metal oxides (such as $Nb_2O_5 \cdot H_2O$, $Ta_2O_5 \cdot H_2O$) treated with sulphuric acid or phosphoric acid improved fructose dehydration to HMF, which was attributed to the synergy between a Brønsted and Lewis acids (Yang et al., 2011a). In addition to higher acidity, zirconium and tin phosphates also showed larger surface area compared to their crystalline analogues, presenting more active and selective functionality for isomerization and dehydration reactions (Lee et al., 2016). However, surface areas were less important under sub-critical water conditions (513K) as illustrated by Asghari and Yoshida (2006) with zirconium phosphates of varying surface areas. To increase Lewis acidity of the catalyst surface, Nb was introduced into tungstite ($WO_3 \cdot H_2O$) to facilitate glucose isomerization for conversion to HMF, (Yue et al., 2016). These results suggest the importance to tailor the Brønsted to Lewis acid ratios for the catalytic reactions.

However, production of HMF from glucose over aqueous medium was often less than 15% yield of HMF by bare metal oxides including TiO_2, ZrO_2, ZrO2/TiO2, γ-Al_2O_3, SiO_2/Al_2O_3 (Noma et al., 2015; Marianou et al., 2016). Niobic acid ($Nb_2O_5 \cdot nH_2O$) attracted attention among metal oxides due to its low toxicity and cost as well as promising yield of HMF (Yang et al., 2011b; Ngee et al., 2014). It exhibited a yield of 23% HMF with glucose conversion of 91% at 160 °C in 40 min over aqueous medium because of strong Lewis acid sites (Noma et al., 2015). Unlike other metal oxides, anatase TiO_2 and phosphate/TiO_2 did not follow widely recognized aldose-ketose isomerization and subsequent dehydration of fructose for HMF production, but involved stepwise dehydration as revealed by Noma et al. (2015) in an isotope-labelled and ^{13}C NMR study.

Along with the change of acidity by metal doping and acid treatment, the structure of the catalysts has a significant effect on the catalytic performance (Osatiashtiani et al., 2014; Osatiashtiani et al., 2015; Zhang et al., 2015). Nakajima et al. (2011) reported that Brønsted acid sites of H_3PO_4-treated $Nb_2O_5{\cdot}nH_2O$ were covered with phosphate ions, yet the side reactions during glucose conversion were significantly suppressed and the HMF yield increased from 12.1% to 47.9% compared to that of pristine niobic acid catalyst. It was suggested that the phosphate might be adsorbed on the hydroxyl groups on niobic acid and thus reduced undesirable products. Besides, the acid type and strength are also related to the structure of the catalysts. For instance, the strength of Lewis sites in niobium oxides is positively correlated to the distortion of octahedral NbO_6 structure, whereas strong and weak Brønsted acid sites are associated with bridging hydroxyl groups of edge- or face-sharing octahedra and terminal hydroxyl groups, respectively (Kreissl et al., 2016). Therefore, understanding the structure of the catalysts can inform the design of tailored catalysts.

2.3.2.2 Zeolites

Compared to mesoporous catalysts (sulfonated zirconia supported over SBA-15), microporous zeolitic materials (H-BEA, H-MOR) exhibited higher selectivity to HMF or LA due to the shape-selectivity effects, which limit secondary reactions such as polymerization and fragmentation (Zeng et al., 2010; Jae et al., 2011; Kruger and Vlachos, 2012; Lanzafame et al., 2012). An appropriate reaction system would accomplish an efficient production of HMF in a combination of hydrolysis and dehydration. A high yield of 48% HMF was generated at mild temperature (120 °C) in an ionic liquid system in the presence of zeolite Y (CBV 400) and $CrCl_2$ (Tan et al., 2011). However, the use of ionic liquid is expensive and toxic while $CrCl_2$ is hazardous to the environment (Li et al., 2016).

In view of the promising outcomes of glucose isomerization by Sn-beta (Moliner et al., 2010), many studies have examined the combination of Sn-beta and various types of Brønsted acid catalysts such as HCl and Amberlyst resins in the reaction systems (Nikolla et al., 2011; Gallo et al., 2013). A biphasic system to extract HMF into the organic phase is desirable for protecting this relatively unstable intermediate from side reactions under single or co-catalysts (Li et al., 2016). Bifunctional zeolites may show the advantage of catalytic cascades in a single catalyst, while the balance of Brønsted-to-Lewis acid sites is critical for catalyst design or modification. For zeolite BEA, Otomo et al. (2014) found that calcination and steam treatment increased Lewis acid sites due to the loss of tetrahedral Al species as Brønsted acid sites. The high pressure of H_2O vapor at high temperature largely promoted the hydrolysis of Si-O-Al bonds in the framework, which was manifested as severe dealumination of zeolite BEA under steam treatment.

The formation of HMF over zeolite BEA at a Brønsted-to-Lewis acid ratio (B/L) of 0.6 showed a high conversion from glucose (78%) and satisfying selectivity (55%) in the reaction media of H2O-DMSO/THF at 180 °C for 3 h (Otomo et al., 2014). Bimodal-HZ-5 (B/L = 0.817) synthesized from H-ZSM-5 (B/L = 0.641) via desilication also demonstrated higher activity in HMF formation than the pristine zeolite (Nandiwale et al., 2014). Impregnating appropriate amount of FeCl3 on HY zeolite (Fe/HY zeolite) can increase the total acid sites and enlarge mesopore size to produce larger amount of LA in aqueous medium than the parent HY zeolite (Ramli and Amin, 2015). These results showed the enhancement of catalytic performance by tuning material properties using post-modification approaches (Li et al., 2016; Zhang et al., 2016b). However, as mentioned in the previous section, the yield of HMF over zeolites in aqueous medium was still low (< 10%) (Otomo et al., 2014; Nandiwale et al., 2014) unless high temperatures (180-200 °C) were applied, where LA was the main product (Ramli and Amin, 2015; Ramli and Amin, 2016).

Tandem/one-pot reaction also requires comprehensive understanding of the kinetics of the reaction network (Lacerda et al., 2015; Ennaert et al., 2016; Yu and Tsang, 2017). Swift et al. (2016) revealed that the tandem reactions of glucose isomerization and subsequent dehydration to HMF exhibited multiple kinetic regimes over a bifunctional zeolite (H-BEA-25) with varying B/L ratio but fixed amount of total acid sites. The relative rates of glucose isomerization and fructose dehydration were altered in accordance with B/L ratio of the zeolite. The rate of glucose isomerization first increased along with Lewis acid sites until insufficient Brønsted acid sites limited fructose dehydration and led to fructose accumulation, which eventually became the rate-determining step (Swift et al., 2016). An investigation of the kinetics of the reaction network can inform and optimize the production process (Yu et al., 2017a). For instance, the kinetic study over Fe/HY zeolite demonstrated advantages on glucose conversion with lower activation energies compared to the reported homogeneous acid catalysts, which highlighted the feasibility of LA production at a temperature of 120-200 °C (Ramli and Amin, 2016).

2.3.2.3 Acid-base catalysts

In a physical mixture of solid acid and solid base catalysts (Amberlyst 15 and hydrotalcite), Ohara et al. (2010) produced HMF from glucose in polar aprotic solvents through a two-step in one-pot system at mild temperatures. However, HMF was not found in the medium of water probably due to the inactivation of Amberlyst-15 in the presence of hydrotalcite, which was a strong base catalyst. Therefore, bifunctional catalysts may be more desirable in view of their self-compatibility. Acid–base bifunctional heteropolyacid (HPA) nanospheres (C6H15O2N2)3-xHxPW12O40 (lysine functionalized HPAs) were evaluated for the production of HMF and LA from glucose in choline chloride (ChCl), giving 52.6% yield of LA at 130 °C in 30 min (Zhao et al., 2014). The first acid/base bifunctional HPAs were designed by Helms et al. (2005) with amine and phosphotungstic acid groups for one-pot tandem reactions.

Although glucose isomerization is mainly catalyzed by Lewis acid or Brønsted base sites, the total amount of acid/base site does not account for the maximum conversion of glucose. It was suggested that Brønsted acid could catalyze direct dehydration of glucose through alternative pathway. Yang et al. (2015) revealed that dehydration of protonated glucose was the rate-limiting step of Brønsted acid-catalyzed conversion.

2.3.3 Engineering aspects & summary

Figure 2.4 illustrates an overview of heterogeneous catalysis from sugary biomass. In order to facilitate industrialization, a high loading of substrate is desirable in the production process, which is not achieved in current literature. **Table 2.1** shows that the feedstock loading of using real biomass is still about 10 wt%, which needs to be improved for industrial scale up. The solubility of the substrates and products in the solvent should be considered. For instance, THF with low boiling point was adopted in the production of HMF, yet a part of the concentrated fructose corn syrup (contained 67.5% fructose) was crystallized during conversion due to its low solubility (Jeong et al., 2013). The resulting yield of HMF was significantly lower (25%) than that from 1,4-dioxane (80%). High substrate loadings also increase the difficulty for mechanical mixing and possibly lead to high amount of by-product formation (Ohara et al., 2010; Weingarten et al., 2012). Microporous and mesoporous zeolites with shape selectivity and tunable acidity may limit secondary reactions and enhance the product production (Kruger and Vlachos, 2012; Lanzafame et al., 2012; Filiciotto et al., 2017), however mass transfer limitation is less severe for conversion of sugars than that of hemicellulosic and cellulosic biomass.

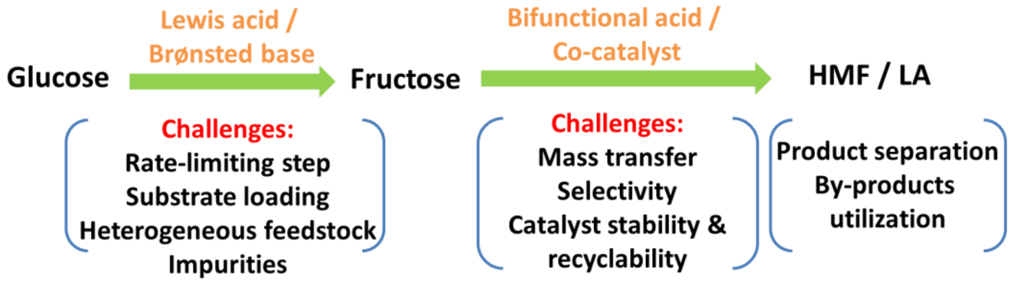

Figure 2.4 Overview of heterogeneous catalysis from sugary biomass.

One-pot reactions are widely examined for the production of HMF or LA, which requires compatibility between the catalysts and the reaction media. Although basic and enzymatic catalysis can be adopted in industrial applications for glucose isomerization (Fenn and Ringe, 2004), it is not feasible to combine with subsequent acid-catalyzed dehydration reaction. In order to enhance the production of HMF, addition of inorganic salts such as NaCl into the aqueous phase was confirmed to increase HMF partitioning into organic phase by salting-out effect (Román-Leshkov and Dumesic, 2009). However, the presence of salts can be detrimental to the solid catalysts. Gardner et al. (2015) demonstrated that even less than 1% of NaCl in the catalytic system significantly hampered the hydrothermal stability of zeolites and induced significant leaching of Al and Si from ZSM-5 via hydrolysis of Si-O-Al bridges. It should be noted that dry biomass may contain up to 1.5 wt% inorganic salts (Brown and Brown, 2014), which highlights the consideration of pretreatment and/or fractionation before biomass valorization.

2.4 Future outlook

Utilization of waste biomass as the raw material has provided an appealing alternative for production of value-added chemicals and biofuels. Although there are extensive studies on the catalytic conversion from model compounds, the use of actual biomass raises particular concerns in the production process. The complex composition of biomass and the presence of impurities such as inorganic salts could hinder the production process, which may require additional pretreatment or fractionation of biomass, yet this operational challenge is often overlooked in the existing literature. It should be noted that the sustainability of biomass from waste stream may vary with changes in regulations and technological developments. However, valorization of waste biomass as raw materials should not be hijacked to justify an increase in waste generation (Bennett et al., 2016).

The interactions between biomass materials and solid catalysts may pose additional challenges to the catalytic process. For instance, the mass transfer limitation between solid biomass and solid catalysts should be overcome, while the solid catalysts should be compatible with the compositions of the biomass and the reaction media to minimize catalyst deactivation and allow catalyst recycling. Although the use of solid catalysts facilitates downstream separation process, the synthesis and production of such catalyst should not create severe environmental pollution of safety concern. Besides, the cost of catalysts is one of the most significant expenses in the valorization process of waste biomass in spite of its small amount needed in the reaction (Brown et al., 2012). Therefore, the environmental and economic implication of solid catalysts should be carefully examined in addition to the catalytic efficiency. Although water is a preferred option as an environmentally-friendly solvent for moisture-containing biomass, promising product yields are often obtained in organic solvents and ionic liquids. Besides, minimization of by-product formation remains a hurdle in aqueous medium. Future research on biomass valorization by heterogeneous catalysts should strive to address the above issues for the goal of upscaling the process for industrial applications.

2.5 Research gaps and hypotheses

This thesis aims to address the engineering and scientific questions associated with actual biomass waste conversion highlighted in this Chapter. The feasibility of polysaccharide biomass conversion is firstly validated in **Chapter 4&5** with the emphasis of significant factors including temperature, solvent and catalyst in determining catalytic conversion of actual biomass to value-added chemicals with the methods summarized in **Chapter 3**. Economic solid catalyst derived from spent coffee ground is synthesized and applied in selective glucose isomerization to fructose (**Chapter 6**), which is identified as the rate-limiting step in starchy biomass conversion to platform chemicals such as HMF and LA. **Chapter 7** further investigates the relationship between catalyst nature/ local chemical environment and glucose activity, aiming to shed light on the design of selective catalysts for glucose isomerization via base catalysis. The findings of this thesis provides incentives to enhance food waste and other biomass waste recycling, offers a feasible technology for waste valorization, and elucidates the mechanisms involved in the catalytic pathways.

Chapter 3 - Materials and Methods

Abstract

The polysaccharide substrates, chemicals, catalytic conditions, analytical and characterization methods adopted in this study have been documented in this Chapter.

3.1 Polysaccharide waste

Pre-consumer vegetable food waste and bread waste adopted in this study were recycled from the local wet markets and the Hong Kong International Airport, respectively (**Figure 3.1a&b**). It was reported that approximately 38.7% of all lettuce and 22.4% of all bread were thrown away in the UK (The guardian, 2015). In view of the abundance of lettuce and bread in the local context as well as the worldwide dietary, they were selected as the representative cellulosic and starchy food waste, respectively. The food waste samples were freeze-dried as received, and then were ground/blended, sieved through a 0.2-mm-mesh, and stored in air-tight containers at 4 ^{o}C in the dark for the subsequent characterization and conversion experiments.

Paper towels comprised of 7% of total waste disposed in Hong Kong, where the daily disposal was 720 tonnes equivalent to 40 double-decker buses (South China Morning Post, 2018). Two types of paper towel waste, namely virgin pulp and recycle pulp, generated from the Terminal Hall of Hong Kong International Airport were adopted as the other common cellulosic waste in the metropolises to validate the technology flexibility and to evaluate the effect of composition variation and different acidic catalysts (*i.e.,* homogeneous and heterogeneous Brønsted acids) on the catalytic conversion (**Figure 3.1c&d**). The paper towel waste was oven-dried at 105 ^{o}C for 48 h for disinfection followed by blending (German Pool, Pro-6), and then stored in desiccators for further experiments.

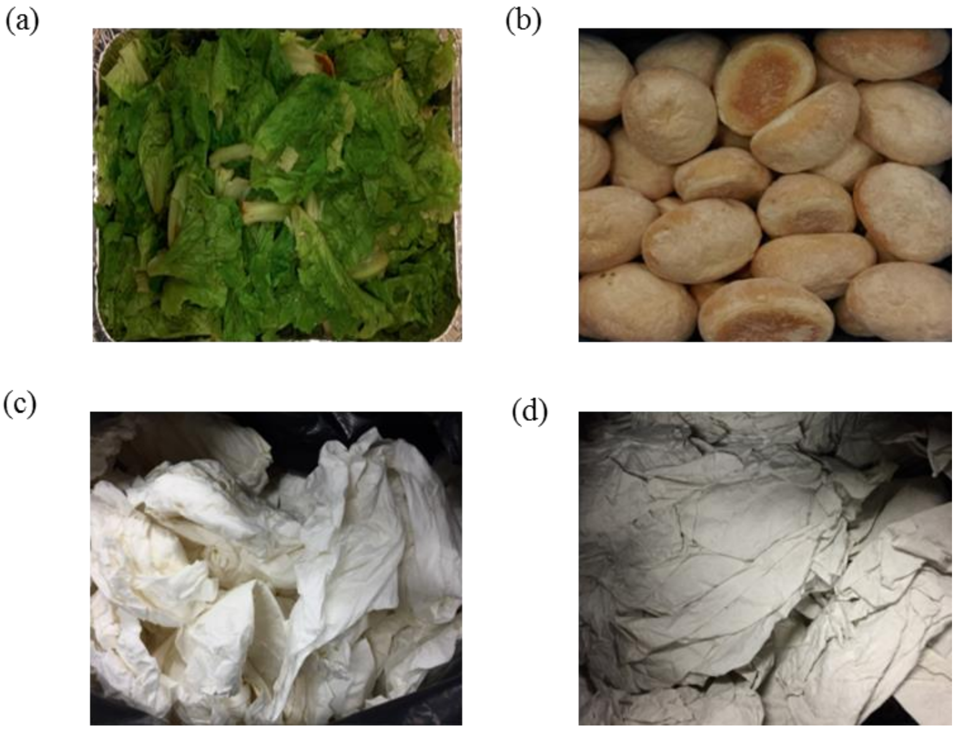

Figure 3.1 Polysaccharide waste used in this study: (a) Mixed vegetable waste; (b) bread waste (c) virgin pulp paper towel waste; and (d) recycle pulp paper towel waste.

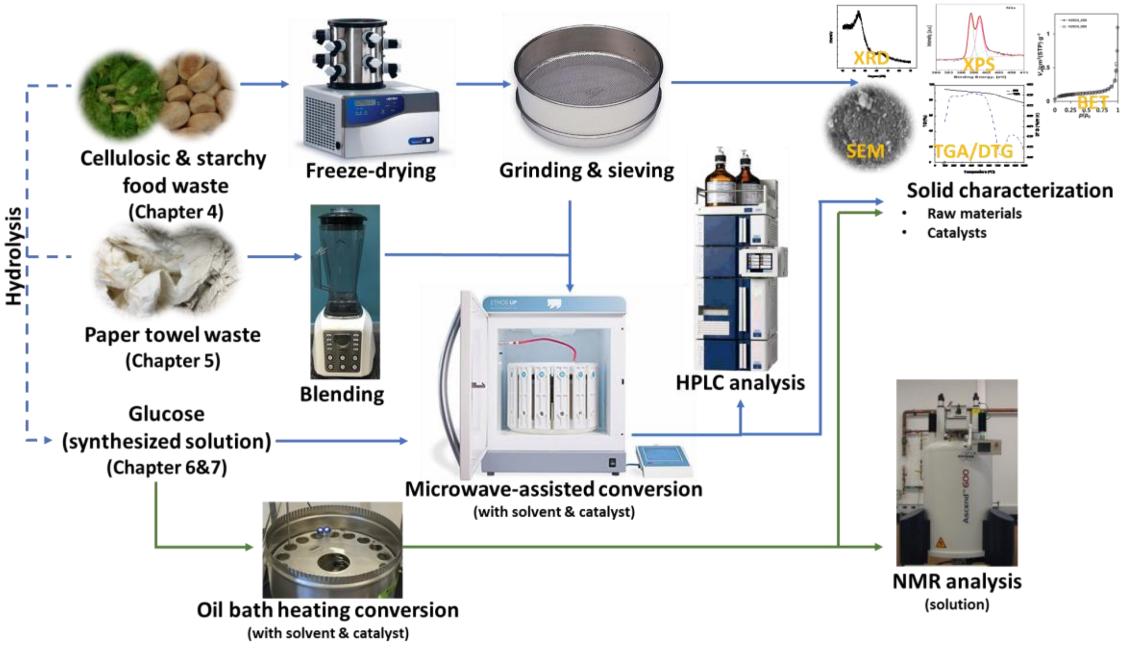

Figure 3.2 Experimental procedure at a glance.

The food waste characterization was conducted to analyze the contents of dietary fibre (including cellulose, hemicellulose, lignin, and pectin; AOAC 985.29), protein (N x 6.25, Kjeldahl Nitrogen Method, AOAC 928.08), total fat (acid hydrolysis and gravimetric method, AOAC 922.06), and ash (AOAC 923.03). Available carbohydrate was derived on the basis of a mass balance according to (HK FEHD (2008):

$$\text{Available carbohydrate} = 100 - \frac{(\text{Dietary fibre} + \text{Protein} + \text{Fat} + \text{Ash} + \text{Alcohol})\ \text{g}}{100\ \text{g Dried substrate}}, \qquad (1)$$

where alcohol content was negligible as indicated by the USDA National Nutrient Database. Free sugars were quantified as the total contents of disaccharides, glucose, and fructose dissolved in water analyzed by high-performance liquid chromatography (HPLC). Water content was determined based on the mass difference between as-received and dried samples. The total organic carbon (TOC) content was measured using the TOC analyser (Shimadzu SSM-5000A). The characterization of food waste sample is shown in **Table 3.1**.

The contents of structural carbohydrates (*i.e.,* cellulose and hemicellulose) and lignin in the raw paper towels (**Table 3.2**) were determined according to the National Renewable Energy Laboratory protocol by using a two-step acid hydrolysis (Sluiter et al., 2008).

Table 3.1 Characterization of vegetable waste used in this study.

	TC[a] (wt% dry basis)	Composition (wt% dry basis)							Water (wt%)
		Total dietary fibre[b]	Available carbohydrates[c]	Starch[d]	Free sugars	Protein	Total fat	Ash	
Mixed vegetables[g]	53.1	46.3	1.2	-	-	26	5.5	21	96.5

Bread waste	41.5	4.2	72.6	67.6	5	14.8	6.1	2.3	28.1

[a] Total carbon (TC);
[b] including cellulose, hemicellulose, lignin, and pectin;
[c] available carbohydrates were calculated according to HK FEHD (2008): 100 – [dietary fibre + protein + fat + water + ash + alcohol(ethanol)] g / 100 g substrate; alcohol was omitted in view of negligible concentration shown in the USDA National Nutrient Database;
[d] starch content was estimated by subtracting the content of available carbohydrates by free sugars (HK FEHD, 2008);

Table 3.2 Chemical compositions of the paper towel waste.

Type of Paper Towel Waste	**Chemical Compositions**		
	Cellulose	Hemicellulose	Lignin
Virgin pulps[*]	78.1% (13.03)[#]	20.6% (3.44)[#]	1.3%
Recycled pulps[*]	67.4% (11.23)[#]	20.8% (3.45)[#]	11.8%

[*] virgin pulp and recycled pulp paper towel wastes were produced from different origins/sources;
[#] number in the bracket represented the mole number of carbons in the corresponding portion for each experimental entry (0.5 g).

3.2 Chemicals

3.2.1 Model compounds

Standard compounds were used in the supplementary tests to enhance the understanding of cellulosic waste conversion chemistry (**Chapter 4&5**); as substrates to elucidate fundamental roles and interactions in substrate-catalyst-solvent system in the course of glucose isomerization to fructose (**Chapter 6&7**); and as standards in the calibration for sample analysis. Standard glucose (99%), cellobiose (≥ 98%), levulinic acid (98%) and formic acid (98%) from Alfa Aesar; fructose (≥ 99%) and maltose monohydrate (≥ 98%) from Wako; cellulose, microcrystalline cellulose (powder) and hydroxymethylfurfural (HMF) (≥ 99%) from Sigma Aldrich; and levoglucosan from Fluorochem, were used as receive. The molecular structures of major carbohydrates were provided in **Figure 3.3**

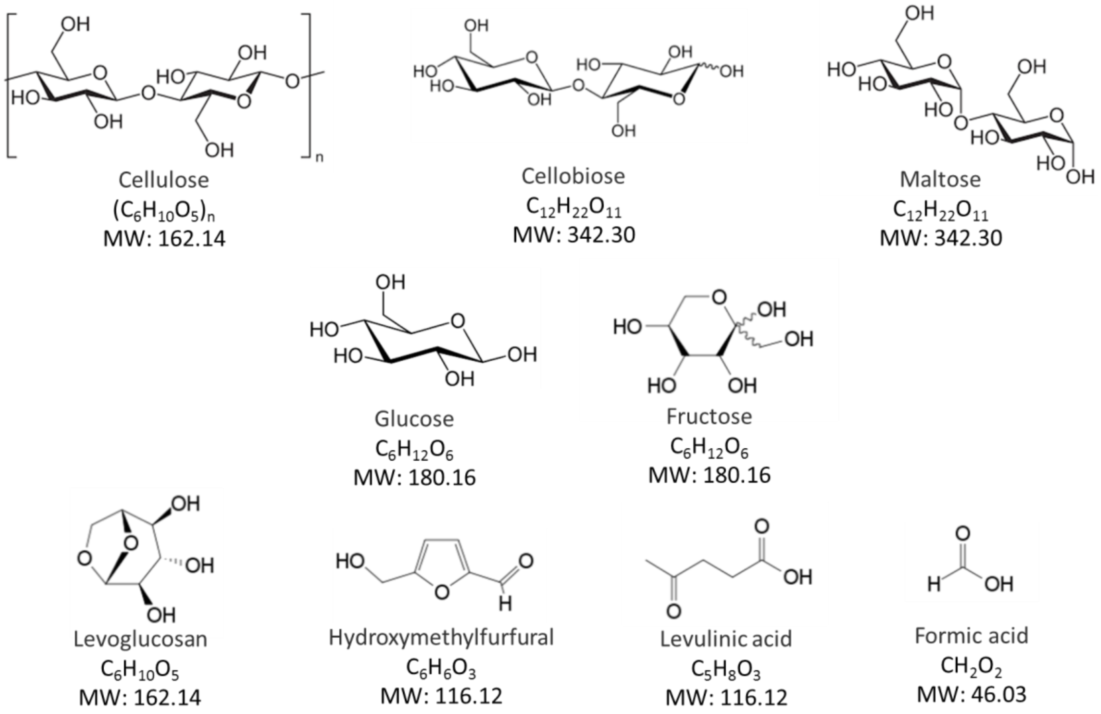

Cellulose
$(C_6H_{10}O_5)_n$
MW: 162.14

Cellobiose
$C_{12}H_{22}O_{11}$
MW: 342.30

Maltose
$C_{12}H_{22}O_{11}$
MW: 342.30

Glucose
$C_6H_{12}O_6$
MW: 180.16

Fructose
$C_6H_{12}O_6$
MW: 180.16

Levoglucosan
$C_6H_{10}O_5$
MW: 162.14

Hydroxymethylfurfural
$C_6H_6O_3$
MW: 116.12

Levulinic acid
$C_5H_8O_3$
MW: 116.12

Formic acid
CH_2O_2
MW: 46.03

Figure 3.3. Molecular structure, molecular formula, and molar weight (g mol^{-1}) of major carbohydrates in this study.

3.2.2 Catalysts

3.2.2.1 Catalysts for cellulosic waste conversion

In view of the strong acidity provided by the cation-exchange resins (**Chapter 2**), Amberlyst 36 (polystyrene-*co*-divinylbenzene sulfonic acid resin, Sigma Aldrich) was used as the heterogeneous Brønsted acid in the catalytic conversions for cellulosic waste (**Chapter 4&5**), while Amberlyst 15 (Sigma Aldrich) was also adopted in the supplementary reactions for comparing the effects of physiochemical properties of solid catalysts on the catalytic performance of vegetable waste conversion (**Chapter 4**). In addition, sulphuric acid (H_2SO_4, 98%, Sigma-Aldrich) were employed as homogeneous Brønsted acid (**Chapter 5**) to reveal potential mechanisms difference than heterogeneous Brønsted acid and highlight the economic and environmental implications.

3.2.2.2 Catalysts for glucose isomerization

3.2.2.2.1 Nitrogen-doped solid base catalyst

Low cost and environmental-friendly nitrogen-doped solid base catalyst was synthesized to demonstrate the feasibility in glucose isomerization to fructose (**Chapter 6**) in view of environmental drawbacks of some Lewis acid catalysts (e.g., heavy metal pollution or use of toxic ingredients in the synthesis), while Brønsted base catalysis offers an alternative for selective glucose conversion (**Chapter 2**).

Spent coffee grounds obtained from a local coffee shop and melamine (99%, Sigma Aldrich, USA) were used as carbon source and nitrogen sources, respectively. The spent coffee grounds were oven-dried (90 °C) until the moisture content was less than 1% based on mass balance. In the catalyst synthesis procedure, 5 g of melamine and 40 g of the prepared spent coffee grounds were mixed homogeneously in deionized water, and then the solution was evaporated at 80 °C to remove water from the mixture. Then the oven-dried composites were thermally treated by a two-step N_2-purged pyrolysis performed in a horizontal tubular furnace (AsOne TMF-300N, Japan). The composites were first heated up from 200 to 700 °C for 50 min, and then held at 700 °C for 2 h. The reactor conditions were referred to Kwon et al. [28] (e.g., stainless Ultra-Torr vacuum fitting, quartz tubing, and stainless tubing). The flow rate of nitrogen feed gas was set as 500 mL min^{-1}, and the temperature inside the furnace was measured using a S-type thermocouple (Omega, USA). The intent of the 2-step process was to remove any residual water that could cause gasification at 700 °C during the first step and to carbonize the sample by pyrolysis under water- and oxygen-free conditions in the second step. The resulting biochar catalysts were ground and sieved to 2 mm and stored in a desiccator at room temperature for further use.

3.2.2.2.2 Alkaline solutions and organic amines

The tested alkaline solutions included sodium hydroxide (>99.8%), calcium hydroxide (>98%) and barium hydroxide (>98.1%) from Fisher Scientific, and magnesium hydroxide (95%) from Sigma Aldrich. The hydroxides were dissolved in glucose solution to obtain a desirable concentration, and then the divalent hydroxide mixtures were filtered through a 0.22-μm syringe nylon filter (Celltreat®) to ensure homogeneous reaction.

The organic amines employed as homogeneous catalysts in were all from Sigma Aldrich. For example, compounds containing primary amines were L-arginine (≥98%, Sigma Aldrich), branched polyethylenimine (PEI) (Mw ~ 25,000), ethoxylated PEI (80% ethoxylated, 35~40 wt% in H2O), guanidine carbonate salt (99%), tris(2-aminoethyl)amine (96%), and N,N-dimethylethylenediamine (95%); compounds containing secondary amines were morpholine (≥99%), meglumine (99%), piperazine (99%), 1-methylpiperazine (99%), and piperidine (≥99.5%). Triethylamine ((≥99%) and 1,4-dimethylpiperazine (98%) were investigated as homogeneous tertiary amine.

Various styrene-divinylbenzene based commercial anion exchange resins were used as heterogeneous catalysts such as AMBERLYSTTM A21 and AMBERLITETM IRA96 with tertiary amines, and AMBERLYSTTM A26 OH and AMBERLITETM IRA900RF Cl with quaternary amines (DOW Chemical). The anion exchange resins were first regenerated in 1 M NaOH for 1 h at a 1:3 resin-to-solution volume ratio. (3-aminoproply)triethoxysilane (99%, Sigma Aldrich), (N,N-diethyl-3-aminopropyl)trimethoxysilane (>95%, Gelest), and 2-Chloro-N,N-dimethylethylamine hydrochloride (99%, Sigma Aldrich) were used to synthesize microcrystalline cellulose-based (powder, Sigma Aldrich) solid catalysts with primary amines and tertiary amines, respectively (**Appendix A**). Polyethylenimine on silica gel (20-60 mesh, Sigma Aldrich) was also tested as immobilized PEI compared to homogeneous PEI. The alkaline solutions and organic amines listed above were used in **Chapter 7** to examine the relationship between catalyst types/ structures and glucose isomerization performance.

3.2.3 Solvents

Deionized water is the major reaction media adopted in this study in view of most biomass materials will contain a certain amount of water. Polar aprotic solvents including dimethyl sulfoxide (DMSO, ≥99.9%) from Sigma Aldrich and acetone (99.5%) from Duksan Pure Chemicals were used as co-solvent to improve product selectivity and catalytic performance, which were commonly reported in recent literature (Yu and Tsang, 2017). According to the CHEM21 selection guide of solvents (Prat et al., 2016), the DMSO solvent is safe for field-scale operations in view of occupational safety and health, while the overall environmental implications of solvent use is investigated via a holistic life cycle analysis in our ongoing studies. Deuterium oxide (D_2O, ≥99.5%, Sigma Aldrich) was used as the reaction medium where *N,N*-dimethylformamide (≥99.8 %, Fisher Scientific) or dimethyl sulfone (98%, Sigma Aldrich) were used as internal standards for the experiments analyzed by ^1H NMR. All the solvents were used as received.

3.3 Catalytic conversion

3.3.1 Microwave-assisted heating

Cellulosic waste conversion (**Chapter 4&5**) and glucose isomerization via nitrogen-doped biochar catalyst (**Chapter 6**) were conducted in a 100 mL Ethos Up Microwave Reactor (Milestone, maximum power 1900 W) with continuous magnetic stirring in view of its virtue of fast kinetics at moderate temperatures and promoting product yields in significantly shorter reaction time on the scale of minutes (Francavilla et al., 2016; Chen et al., 2017). The reaction temperature was directly monitored by an in-situ temperature sensor in a reference vessel, and a contact-less pressure sensor was used to prevent leakage or venting. After the reaction, the vessels were cooled for 40 min by continuous mechanical/forced ventilation in the reactor. The parameters were adopted and modified according the reported literature and our preliminary studies (**Chapter 2**) to validate the feasibility and improve the cellulosic waste conversion. All experiments were conducted in duplicate or triplicate where necessary, and the control experiments were conducted at selected conditions without the addition of catalysts or without the addition of substrates where appropriate.

In **Chapter 4**, the vegetable waste was added at 5 wt/v% into the reaction medium (deionized water and DMSO-water (1:1 v/v) mixture, respectively), with the solid catalyst at a weight ratio of 1:1. The use of DMSO-water at this ratio corresponded to the scenario of using wet, as-received feedstock in pure DMSO solvent at a substrate-to-solvent weight ratio about 0.1, as there is approximately 90% water content in vegetable. The catalytic conversions of vegetable waste were conducted at three different reaction temperatures: 120, 135 and 150 °C. The lower and upper bound temperatures were determined by the highest operating limits for

Amberlyst 15 (*i.e.,* 120 °C) and Amberlyst 36 (*i.e.,* 150 °C), respectively. The reaction time varied from 0 to 120 min with a 5-min ramping, which has been widely adopted to capture the product profiles in the microwave-assisted conversion.

In **Chapter 5**, the blended paper towel was added into the microwave reactor at a weight-to-solvent-volume percentage of 5 wt/v%. Amberlyst 36 was added at an equivalent weight to the paper towel (0.5 g), and 10 mL deionized water was used as the reaction medium. The H_2SO_4 was used at 0.135 M as a homogeneous Brønsted acid catalyst with H^+ exchange capacity equivalent to Amberlyst 36. These conversions were conducted at 150 °C, which was the highest operating limit for Amberlyst 36. A higher concentration of 1 M H_2SO_4 was used at 150 and 200 °C to examine the effect of acidity and temperature on the catalytic conversion. The reaction time varied from 0 to 60 min with a 5-min ramping, which has been shown sufficient to capture the product profiles in our previous study.

In **Chapter 6**, stock glucose solution was prepared at 10 wt/wt%. In each catalytic reaction, 5 mL of stock glucose solution and 5 mL of deionized water or acetone together with 1 wt/wt% of catalyst relative to solution (equivalent to 15.4 N mol% relative to glucose) were added into the microwave reactor vessel. The reaction was subject to a 1-min ramping time to reach 100, 120 or 160 °C for desired reaction time (from 1 to 60 min) under continuous magnetic stirring.

After the catalytic reaction, the liquid and solid phases of the reacted mixture were separated by centrifugation. The liquid sample was filtered through a 0.22-μm pore-size membrane filter (ProMax$^{\text{TM}}$, DiKMA) before product analysis, while the solid residues were washed with deionized water three times to remove the remaining solvent and soluble products followed by centrifugation and decantation. The washed solid was then freeze-dried for microscopic and spectroscopic characterizations.

3.3.2 Oil bath heating

The microwave heating should be applied to the same reaction media in the same batch in view of the variation of microwave absorbing properties of each catalytic medium. Therefore, oil bath heating was adopted for batch experiments of glucose isomerization by various homogeneous and heterogeneous catalysts in **Chapter 7**. The 10 wt% glucose solution (≥99.5%, Sigma Aldrich) was prepared in deuterium oxide (99.9 atom% D, Sigma Aldrich), and the dosage of the catalysts was controlled at 12 mol% of N content relative to glucose, which was based on our previous study. The glucose isomerization experiment was conducted in 5-mL thick-walled glass reactors (Chemglass Life Sciences) containing a V-shaped stir bar, which was then placed in the preheated oil bath (digital stirring hot place IKA RCT equipped with PT100 thermocouple) at 100 °C for 30 min, and quenched in an ice bath after reaction. Both the glucose solution and the reactors were degassed by Ar gas to get rid of carbonic acid and CO_2 prior to the reaction. The pH values before and after the reaction were measured by a pH meter at room temperature (Metter Toledo).

3.4 Result analysis

3.4.1 Product analysis

High-performance liquid chromatography (HPLC) was one of the major equipment to quantify the products from the reaction, comprising Chromaster (Hitachi) 5110 pump, 5210 autosampler, 5310 column oven, and 5450 refractive index (RI) detector. The HPLC system was equipped with an Aminex HPX-87H column (Biorad), using 0.01 M H_2SO_4 as the mobile phase at a flow rate of 0.5 ml min^{-1} at a column temperature of 50 ^oC (Ohara et al., 2010). Blank (*i.e.,* water) and spiked samples with known model compounds were injected before every series of sample analysis for quality assurance and quality control.

When using raw cellulosic waste as substrate (*i.e.*, vegetable waste and paper towel), the product yield was calculated on the basis of carbon content as below.

$$Product\ yield\ (mol\%) = \frac{Conc_p(mg\ ml^{-1}) \times Vol(ml)/MW_P \times C_P}{C_S\ (mol)} \times 100, \tag{2}$$

where $Conc_P$ referred to the concentration of HPLC detectable products, *i.e.,* disaccharides, fructose, glucose, HMF, levoglucosan, LA, formic acid, and furfural; MW_P and C_P represented the molecular mass and the mole number of carbon in the corresponding product, respectively; C_S was the mole of carbon in the vegetable waste (15.6 mmol at each entry, accounting for 37.3 ± 0.2% of total weight of the substrate), the paper towel waste (13.03 mmol from cellulose and 3.44 mmol from hemicellulose for virgin pulp fibres, and 11.23 mmol from cellulose and 3.45 mmol from hemicellulose for recycled pulp fibres at each entry) or in bread waste (12.2 mmol at each entry, accounting for 29.2± 0.2% of total weight of the substrate).

As for glucose isomerization, the conversion, yield and selectivity of chemical products were presented on a mole basis as follows.

$$Glucose\ conversion\ (\%) = \frac{n_{Glu}(initial) - n_{Glu}(final)}{n_{Glu}(initial)} \times 100, \tag{3}$$

$$Product\ yield\ (\%) = \frac{Conc_P\ (mg\ ml^{-1}) \times Vol\ (ml)/\ MW_P}{n_{Glu}(initial)} \times 100, \tag{4}$$

$$Product\ selectivity\ (\%) = \frac{Product\ yield\ (\%)}{Glucose\ conversion\ (\%)} \times 100, \tag{5}$$

where $Conc_P$ represented the product concentration such as fructose, furfural, HMF, and levulinic acid detected by HPLC; MW_P referred to the molecular mass in the corresponding products; $n_{GLU(initial)}$ represented the initial moles of glucose in each reaction. Total product yield was calculated as a summary of entire soluble products detectable by HPLC including glucose.

For the glucose isomerization to fructose conducted in oil bath, the glucose conversion, fructose yield and selectivity were determined from ^{1}H NMR spectra (AVIII600, Bruker 600 MHz NMR) at room temperature acquisition.

3.4.2 Statistical analysis

Exploratory data analysis and unsupervised pattern recognition were employed in **Chapter 7** to gain better knowledge of the data sets. To eliminate redundancy and noise, the specific signals retaining meaningful information from the fingerprinting data of ^{1}H NMR spectra (*i.e.,* conversion, yield, selectivity derived from normalized peak intensities and pH change indicated by a characteristic peak shift) were used in the data processing (Berrueta et al., 2007). The relationship between the variables was investigated by a correlation matrix on a scatterplot, and principal component analysis (PCA) was performed to reduce variables to a smaller number of components and to understand the catalytic patterns (*i.e.,* conversion, selectivity, yield, and pH change) among groups (OriginPro 2017).

3.4.3 Characterization

Microscopic and spectroscopic characterizations were applied to the solid residues. The morphologies of the selected solid residues under different reaction conditions were investigated by using scanning electron microscope (SEM, JEOL Model JSM-6490) at an accelerating 20 kV voltages and 70-78 µA current. The change of crystalline structure of vegetable waste, paper towel waste, and nitrogen-doped catalyst under different reaction conditions were evaluated by a high resolution powdered X-ray diffraction (XRD, Rigaku SmartLab) analysis using Cu Kα radiation. The scanning degree ranged from 10 to 50° with a rate of 3° min^{-1} at 45 kV and 200 mA. The crystalline index (*CrI*) for the cellulosic structure was calculated by the signal for the crystalline portion ($I_{200} - I_{AM}$) over the total intensity of the crystalline peak portion (I_{200}, where $2\theta = 22.5°$ for vegetable waste and 18.5° for paper towel waste), where I_{AM} was the amorphous cellulose fraction at $2\theta = 18.5°$ (Luterbacher et al., 2014). The morphologies and crystalline structures of untreated cellulosic waste were also examined by using SEM and XRD, respectively. The thermal behavior of the cellulosic waste samples was examined by thermogravimetric analyzer (TGA, Rigaku Thermo plus EVO2) and differential thermal analysis (DTA) at a ramp rate of 10 ºC min^{-1} to 550 ºC. As for nitrogen-doped biochar catalyst, the test was conducted from 100 to 1000 ºC at a heating rate of 10 °C min^{-1} to determine thermal stability of the biochar catalyst and any adsorbed species on the catalyst after catalytic reaction. The organic carbon contents of the substrates were measured by using total organic carbon analyzer (TOC, Shimadzu SSM-5000A). The pH of the solutions was measured by a pH meter before and after reaction, which qualitatively descripted the Brønsted acidity among the samples with the same solvent media due to calibration of solvent acidity was not available for the organic solvent-water media in this study to our best knowledge.

The nitrogen-doped biochar catalyst was additionally characterized by the following techniques. Approximately 0.93 g of the catalyst was degassed in vacuum at 150 °C for 12 h, followed by N_2 adsorption-desorption isotherms at -196 °C. The specific surface area and pore volume of the catalyst were analyzed using Brunauer-Emmett-Teller (BET) surface analyzer (Belsorp-mini II, USA), while the pore size distributions were derived from Barrett-Joyner-Halenda (BJH) analysis. X-ray photoelectron spectroscopy (K-ALPHA+XPS System, Thermo Fisher Scientific) was performed with monochromated Al Kα radiation (1486.6 eV) system to examine the surface chemistry of the biochar catalyst. Survey scans from 0 to 1200 eV were obtained at 1 eV step^{-1}, and narrow scan was set at 0.1 eV step^{-1}. The core level spectra of C 1s (280-294 eV), N 1s (390-411 eV) and O 1s (524-542 eV) were recorded and fitted with Gaussian functions. The shift of binding energy due to the relative surface charge was corrected by the C1s level at 284.5 eV as an internal standard.

The acid-base properties of the catalyst were thoroughly characterized. The basic sites were measured by back titration (pH meter, Mettler Toledo). Approximately 0.4 g of solid was added into 40 mL of 0.05 M HCl and shaken for 24 h. A blank titration (only HCl, no catalyst) was also conducted. The mixture was then centrifuged at 5000 rpm for 15 min, and filtered by a 0.22 μm syringe filter. The filtrate was divided into two aliquots, of which the mass was also recorded. The aliquots were purged with N_2 gas for 2 h before starting titration with 0.05 M NaOH, and N_2 flow was continued during the titration process (Oickle et al., 2010). The acid sites were measured in a similar way. Microwave-heated (without substrate) catalyst was recycled, water-washed, oven-dried and ground before elemental analysis (Flash2000, Thermo Scientific) to investigate stability of the catalyst under hydrothermal conditions. Fresh catalyst was also examined as control.

Chapter 4 - Valorization of Cellulosic Food Waste

Abstract

This chapter presents the catalytic valorization of vegetable waste into levulinic acid (LA) over a solid Brønsted acid, Amberlyst 36, in aqueous solution with/without polar aprotic solvent (dimethyl sulfoxide, DMSO). With the aid of microwave heating, the cellulosic structure in the vegetable started hydrolysis at 120 °C. Increasing temperature to 135-150 °C accelerated the yield of LA to 13-17 C mol% in 5 min in aqueous solution due to the reduction of mass transfer limitations. At the same time, the generation of insoluble humins became more rapid and significant, leading to lesser amount of total soluble products. In comparison, in the DMSO-water mixture, the early-stage reaction produced up to 17 C mol% of hydroxymethylfurfural (HMF), which was gradually rehydrated to LA with increasing reaction time. This probably illustrated the effects of DMSO, *i.e.,* increased accessibility of glucose to protons for rapid HMF formation and preferential solvation of HMF to dampen further rehydration. The maximum yield of soluble products in DMSO-water mixture at 120-150 °C was higher than that in aqueous solution, which was attributed to the enhanced dissolution of cellulose in DMSO as supported by the SEM images. The XRD patterns of the reacted solids demonstrated more intensive peaks at the early stage of the reaction followed by broadening peaks at the later stage, indicating the hydrolysis of amorphous cellulose and formation of insoluble solids on the surface. Therefore, water serves as a green solvent for LA production while DMSO-water mixture is needed for HMF production from vegetable waste.

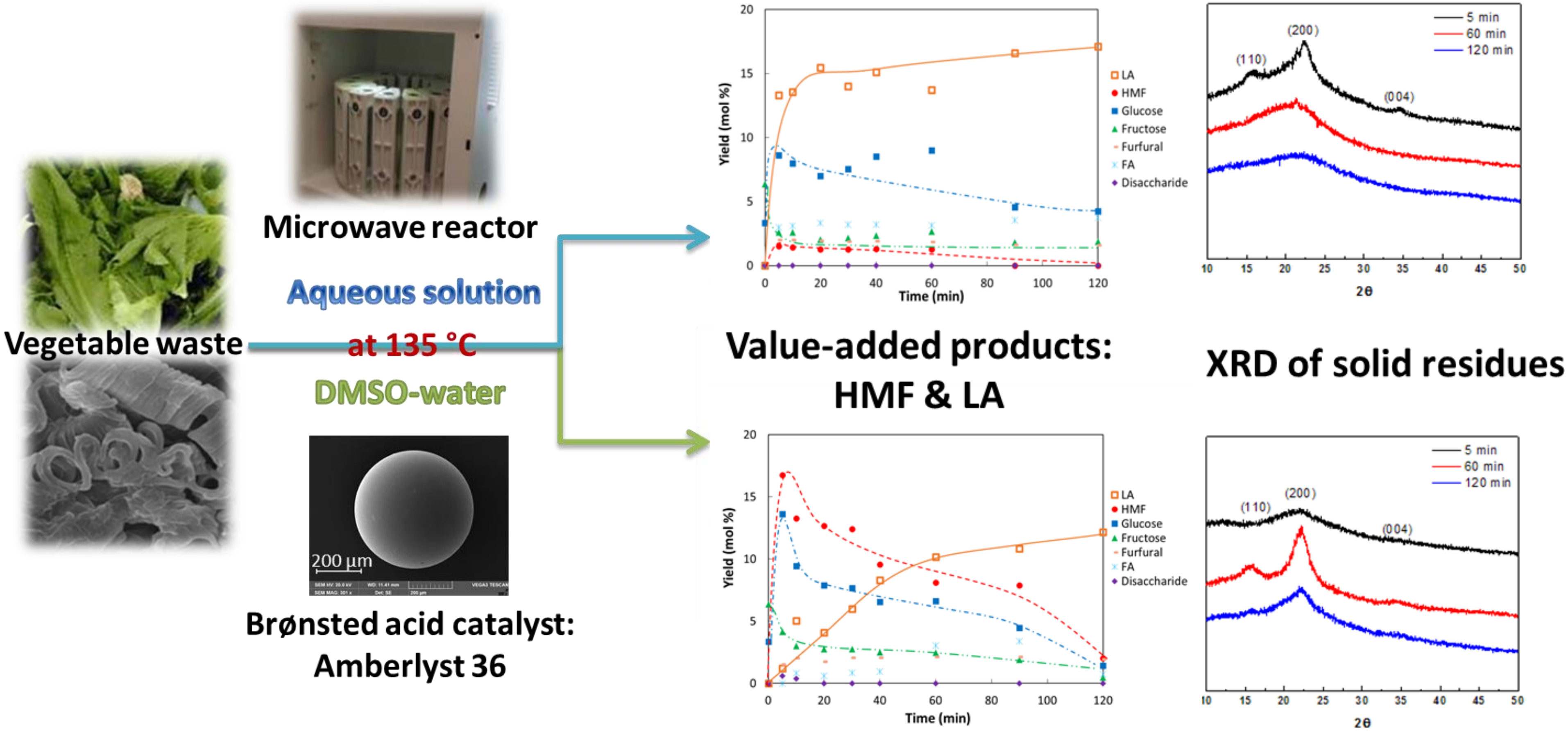

Figure 4.1. Graphical abstract of **Chapter 4**.

4.1 Research questions

As introduced in **Chapter 2**, valorization of actual biomass encounters the difficulties in view of its complex and recalcitrant nature. Vegetable waste is primarily composed of cellulose, and recent study showed that only approximately 5 C mol% HMF at most were converted from vegetable waste at 140 ^{o}C for 20 min in the presence of Lewis acid catalysts due to limited hydrolysis of the cellulosic food waste (Yu et al., 2017c). Levulinic acid (LA) is the rehydration product of HMF, which is one of the twelve bio-based platform chemicals for the production of chemicals, polymers, and biofuels, which can be produced through acid hydrolysis of biomass (Werpy and Peterson, 2004; Flannelly et al., 2016). A high yield of LA could be achieved by employing mineral acids, such as H_2SO_4 and HCl, because the polysaccharides undergo hydrolysis effectively over these homogeneous Brønsted acid catalysts. For example, a maximum yield of 70% LA was reported by using sulphuric acid at 220 °C in an industrial biorefinery process (Ritter, 2006)). However, the major hurdles of using homogeneous Brønsted acids have been highlighted in recent reviews (Morone et al., 2015; Mukherjee et al., 2015), including corrosion of the reactors, difficulty to separate the products, and energy-intensive processes to recycle the catalysts. Therefore, heterogeneous, solid catalysts are actively investigated nowadays (Alonso et al., 2013; Gallo et al., 2016).

Amberlyst, a sulphonated ion-exchange resin, has demonstrated successful hydrolysis of cellulose into glucose in aqueous solution (Onda et al., 2009); owing to its strong Brønsted acidity that is equivalent to 35% sulphuric acid according to the Hammett acidity function (Rys and Steinegger, 1979). The macroporous structure of the resin may facilitate substrate accessibility to the active sites. Although a high reaction temperature (> 190 °C) can improve dissolution of cellulose, it also causes leaching of sulphonic groups from the catalysts, resulting in catalyst deactivation (Carà, 2013). In addition, carbohydrate conversion at elevated reaction temperatures in water may generate a large portion of undesirable by-products due to condensation and polymerization of reactants (Ferreira et al., 2013; Shuai and Luterbacher, 2016). Given that water is an environmentally friendly and green solvent, it is the most practical and preferred choice of solvent for biomass conversion at an industrial scale (Morone et al., 2015; Li et al., 2017). Therefore, understanding the reaction kinetics in aqueous medium is crucial for optimizing the productivity of our proposed vegetable waste valorization.

The use of appropriate solvents can enhance cellulose solubility, which increases mass transfer rates between the biomass and the catalysts and consequently enhances the apparent reaction rates and conversion. In addition, the application of polar aprotic co-solvent such as dimethyl sulfoxide (DMSO) and γ-valerolactone (GVL) shows beneficial effects on the destabilization of acidic proton and suppression of glucose degradation (Mellmer et al., 2014; Li et al., 2017; Zhang et al., 2017). Organic solvents can increase the product selectivity with lower energy input by reducing the activation energy through its influence on the thermodynamics or reactivity of the reactants (Shuai and Luterbacher, 2016). For example, a yield of 69% LA was recorded with 90 wt% GVL and 10 wt% water at 160 °C with 2 wt% cellulose (Alonso et al., 2013).

Moreover, microwave-assisted heating in catalytic conversion has gained more attention due to its advantages of fast kinetics at moderate temperatures and increasing product yields in much shorter reaction time on the order of minutes (Liu et al., 2013; Sun et al., 2015; Francavilla et al., 2016). The tangent value of DMSO (0.825) is larger than that of water (0.123), representing its ability of converting more electromagnetic energy into heat at the same microwave frequency and temperature (Dallinger and Kappe, 2007). Thus, microwave heating can reduce the process cost via energy savings and improved product yields (De et al., 2011; Morone et al., 2015).

In this Chapter, we investigated the synergies of applying organic solvent and microwave-assisted heating on cellulosic waste valorization, where obtaining kinetic information of the conversion over heterogeneous Brønsted acids is essential for reactor designs, especially when solid Brønsted acids are responsible for the cellulose hydrolysis step. Therefore, this chapter aims to (i) investigate the feasibility of valorizing vegetable waste into LA and its intermediates/by-products; (ii) examine the reaction kinetics over promising heterogeneous Brønsted catalysts (Amberlyst) assisted with microwave heating at a moderate temperature range of 120-150 °C; (iii) understand the hydrolysis of cellulose in an aqueous medium and polar aprotic co-solvent with the aid of microscopic and spectroscopic analysis.

4.2 Results and discussion

4.2.1 Hydrolysis of cellulose to glucose by microwave heating in aqueous medium

In addition to cellulose, there were free sugars present in the vegetable waste (about 3 C mol% glucose and 6 C mol% fructose) as shown at 0 min in **Figure 4.2**. The yield of glucose rapidly increased in the first 5 min of the reaction (**Figure 4.2a**), which suggested the hydrolysis of cellulose from vegetable waste could initiate at a relatively mild temperature (120 °C) under microwave heating. It was reported that the hydrolysis of cellulose and the release of glucose monomers via the breakdown of hydrogen-bonded structure by water occurs at nearly 150 °C and above (Savage et al., 2010). Sakaki et al. (Sakaki et al., 2002) reported that cellulose starts to degrade into hexose and oligosaccharides at above 230 °C, and the decomposition of cellulose is almost complete at 295 °C in hot-compressed water. The rapid hydrolysis of a portion of cellulose in vegetable waste shown in **Figure 4.2a** is attributed to the efficient internal heating in water given by microwave irradiation, which corroborates the latest findings in a recent study (Francavilla et al., 2016).

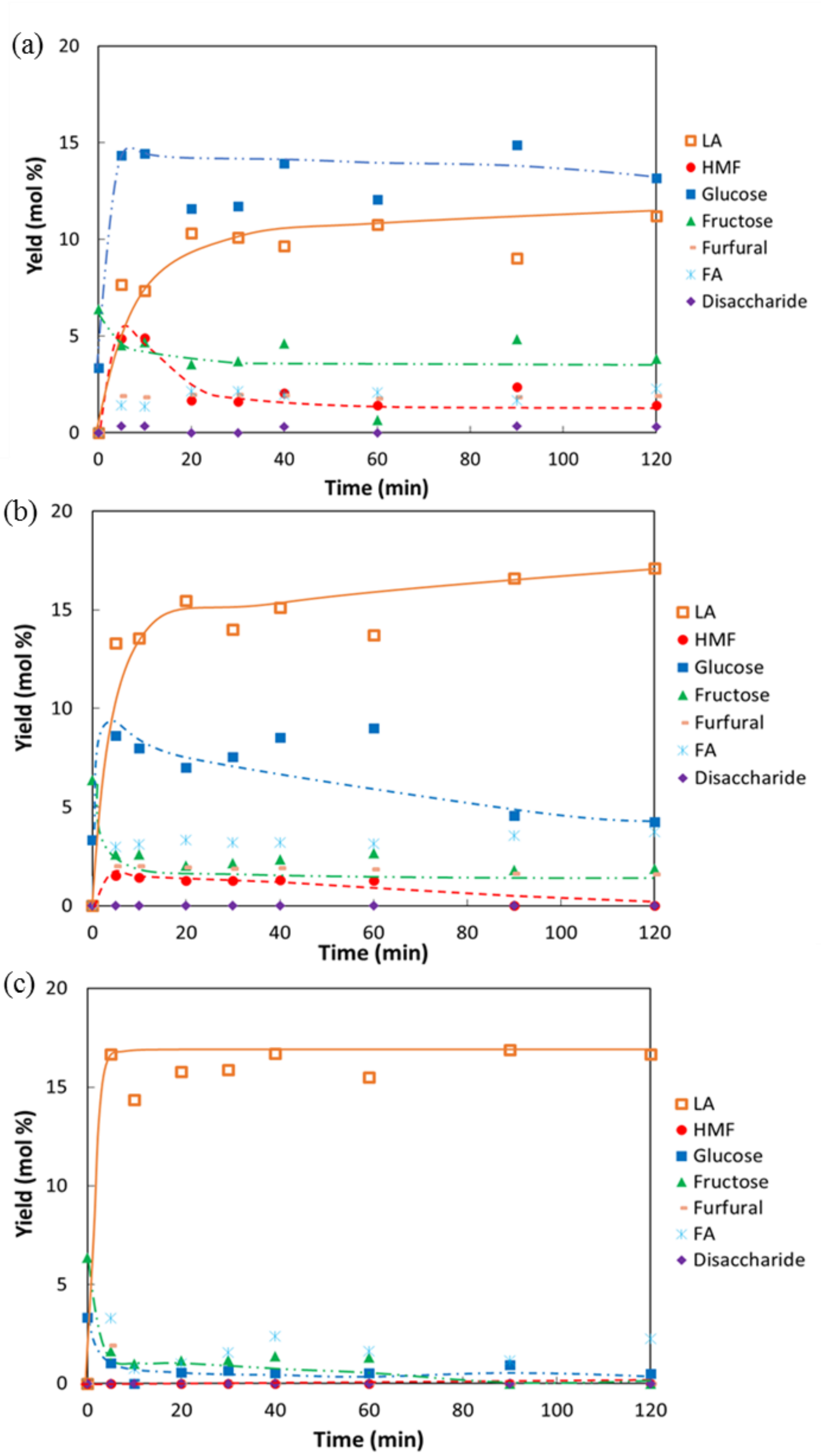

Figure 4.2 Product yields versus time under Amberlyst 36 catalyzed conversion of vegetable waste in water at (a) 120°C, (b) 135°C, and (c) 150°C (conditions: 5 wt/v% substrate and catalyst-to-substrate mass ratio = 1:1; yield = productCmol/substrateCmol × 100%).

A maximum total soluble product yield of 36 C mol% was achieved in the conversion of cellulose at 120 °C, possibly due to the strong interaction between the solid acid catalyst and β-1,4-glycosidic bonds in cellulose at lower temperatures (Huang and Fu, 2013). Amberlyst 15 and Amberlyst 36 showed comparable acid sites (ratio of 1.1) (**Table B1**), and no apparent difference was observed in their catalytic performance (**Figure B1**). These results inferred that surface area and pore volume of the catalysts were less influential (**Table B1**) compared to Brønsted acidity and the quantity of the acid sites in this situation. As the initial free sugars contributed to around 10 C mol%, the net hydrolysis from cellulose was approximately 26 C mol% (**Figure 4.3**). Higher temperatures at 135 and 150 °C did not apparently increase the glucose yield than 120 °C, probably because all the tested temperatures were below the temperature of cellulose depolymerization at 220 °C (Fan et al., 2013). The relatively high conversion of cellulose (26%) at 120 °C in **Figure 4.2a** suggested higher amorphous cellulose content in vegetable waste compared to commercially available cellulose (13%, (Fan et al., 2013)), Our findings demonstrate that vegetable waste is a favourable alternative for biomass valorization. The change of microscopic structures of the vegetable waste will be discussed in *Section 4.2.5*.

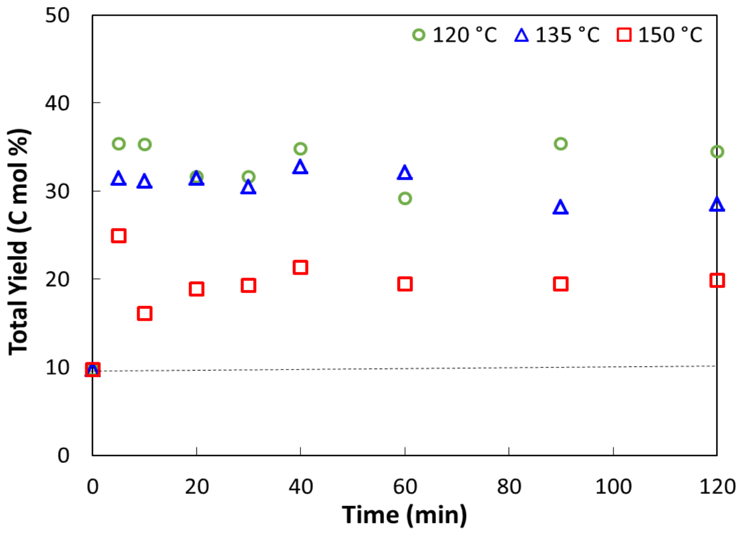

Figure 4.3 Total product yields versus time under Amberlyst 36 catalyzed conversion of vegetable waste in water at the three temperatures (conditions: 5 wt/v% substrate and catalyst-to-substrate mass ratio = 1:1; yield = productCmol/substrateCmol × 100%).

4.2.2 Brønsted acid-catalyzed glucose dehydration and HMF rehydration in aqueous medium

The catalytic conversion of vegetable waste showed relatively slow kinetics at 120 °C. **Figure 4.2a** showed a modest and gradual increase in the yield of LA from 20 to 120 min of reaction. Meanwhile, a significant amount of glucose (13 C mol%) and some fructose and HMF remained unreacted at the end of the reaction. As an intermediate of LA prior to its rehydration, HMF is one of the building block chemicals identified by the US Department of Energy (Werpy and Petersen, 2004). The slow conversion rates were first speculated to result from the catalyst deactivation due to transformation of solid surface or dissolution of sulphonic acid groups in view of previous studies (Alonso et al., 2013; Carà et al., 2013; Gallo et al., 2016).

Nevertheless, supplementary experiments with H_2O_2-washed catalysts (**Appendix B**) confirmed that the slow kinetics was a result of pore blockage by deposition of large cellulose molecules especially at 120 °C, which was in line with the observation in a recent study (Su and Guo, 2014).

By increasing the temperatures to 135 and 150 °C, energy barriers of the system are easier to overcome, where Amberlyst 36 catalyzed both glucose dehydration and HMF rehydration (**Figure 4.2b&c**). Within 10 min, the yield of LA increased to 13 C mol% at 135 °C and 17 C mol% at 150 °C, coupled with concurrent decrease in HMF yield. Given that Brønsted acids have negligible effect on glucose-fructose isomerization (Yang et al., 2015), our results evidenced that HMF and LA could be formed via direct glucose dehydration without interim production of fructose. The pH in the reaction system was stable along with the reaction time (**Figure B2**), where the pH value slightly decreased from 1.5 to 1.3 on average with the temperature increase from 120 to 150 °C. The molar ratio of formic acid (FA) to LA remained close to 1 at 120 and 135 °C (**Figure B3**), while it decreased to less than 0.7 at 150 °C. As no decomposition FA was reported at this temperature (Flannelly et al., 2016), a portion of FA may be lost by vaporization during pressure release at the end of reaction.

4.2.3 Kinetics of Brønsted acid-catalyzed by-products formation in aqueous medium

Figure 4.2c shows that the yield of LA reached plateau in 5 min at 150 °C, which was much faster than that at 135 °C. It is noteworthy that the maximum yield of LA at 150 °C remained approximately the same as those at lower temperatures, while the total yield of soluble products was reduced by more than 10 C mol% compared to that at lower temperatures. These results suggested that higher temperatures at 135 and 150 °C accelerated the undesirable reactions (e.g., formation of humins) to a comparable extent as the desirable reactions (e.g., formation of HMF and LA). A previous computational study suggested that Brønsted acid-catalyzed formation of HMF is initiated by protonation of glucose at O5 position and becomes more significant at higher temperature (Yang et al., 2012). Yet, besides glucose polymerization into humins, HMF is also known to form humins under acid catalysis via aldol condensation with an intermediate of 2,5-dioxo-6-hydroxyhexanal (Patil et al., 2012; Tsilomelekis et al., 2016). In contrast, LA is less likely to be transformed to humins and remains steady with the reaction time during acid catalysis, as verified by a recent study using nuclear magnetic resonance (van Zandvoort et al., 2015). Therefore, higher temperature in this study accelerated the formation of LA but also resulted in the greater extent of glucose- and HMF-derived humins (as reflected by the lower yield of total products).

4.2.4 Effects of polar aprotic solvent on product profiles of vegetable waste conversion

Although the yield of glucose and the amount of total soluble products in DMSO-water mixture (**Figure 4.4a**) were close to that in water at 120 °C, the yield of glucose was significantly higher in the DMSO-water media (about 13 C mol% in 5 min) when the reaction temperature increased to 135 °C (**Figure 4.4b**). The total yield of soluble products approached 40 C mol% (**Figure 4.5**), which was the highest in this study. As cellulose has better solvation in DMSO than in water (Shuai and Luterbacher, 2016), an improved conversion of vegetable waste in DMSO-water mixture at higher temperature could be attributed to higher solubility of cellulose and faster mass transfer of the hydrolyzed glucose from vegetable waste to the solid catalysts.

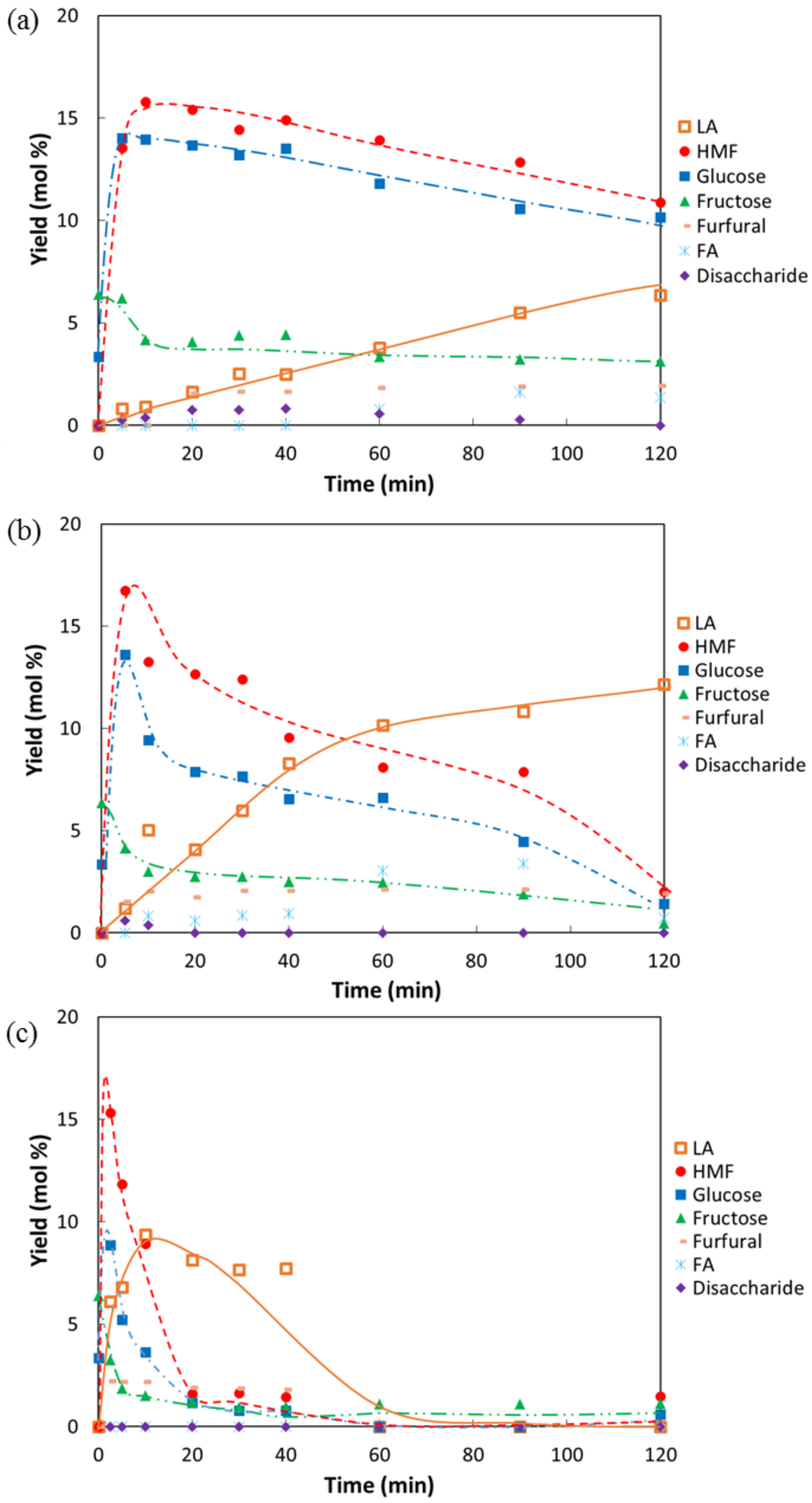

Figure 4.4 Product yields versus time under Amberlyst 36 catalyzed conversion of vegetable waste in DMSO-water (1:1 v/v) at (a) 120°C, (b) 135°C, and (c) 150°C; (conditions: 5 wt/v% substrate and catalyst-to-substrate mass ratio = 1:1; yield = $\text{product}_{\text{Cmol}}/\text{substrate}_{\text{Cmol}} \times 100\%$).

The yield of HMF was much higher (up to 17 C mol%) in DMSO-water mixture (**Figure 4.4a-c**) compared to that (only 5 C mol%) in aqueous medium at 120-150 °C, indicating greater dehydration of glucose to HMF and/or lesser rehydration of HMF to LA in DMSO-water mixture. The average pH values in the reaction system changed from 2.1 to 1.8 when the reaction temperature increased from 120 to 150 °C (**Figure B2**). The higher selectivity of HMF in DMSO-water mixture illustrates the solvent effect. In DMSO-water mixture, the hydrogen bonding between the Brønsted acid site on Amberlyst 36 and DMSO (polar aprotic solvent) is not as strong as that in aqueous medium. The competition for protons is weaker between glucose and DMSO than glucose and water. Hence, the presence of DMSO is more conducive to glucose protonation at C2-OH group by increasing the accessibility of its hydroxyl groups to more protons, which is known to be the rate-limiting step to form fructose and HMF (Qian, 2011; Qian and Liu, 2014). In addition, slower HMF rehydration to LA in DMSO-water mixture (**Figure 4.4**) is attributed to the preferential solvation of HMF by DMSO prior to water, which can minimize HMF degradation by suppressing nucleophilic attack at its carbonyl group (Tsilomelekis et al., 2016).

It is also noted that the maximum values of total soluble products from vegetable waste conversion at 120-150 °C were close to each other in DMSO-water mixture (**Figure 4.5**), which were in line with our previous findings of starch-rich food waste conversion using the same medium (Yu et al., 2017a). However, the total soluble products decreased rapidly with the reaction time at 150 °C (**Figure 4.5**), contrary to the stable yield in aqueous solution (**Figure 4.3**). Supplementary experiments (**Appendix B**) indicated that the single compounds of substrates and products remained stable for 2 h in DMSO-water mixture at 150 °C except for HMF. Qian and

Liu (Qian and Liu, 2014) argued that the solvent of DMSO lowers not only the activation energy for glucose dehydration via C2-OH protonation, but also the activation energy for humins formation via C1-OH protonation. Therefore, the formation of humins at higher temperature remains a major hurdle in DMSO-water mixture, which is more significant than that in aqueous medium. **Scheme 4.1** summarizes the major reaction pathways for valorization of vegetable waste by Amberlyst 36 under different reaction temperatures in water or water-DMSO mixture as reaction solvents.

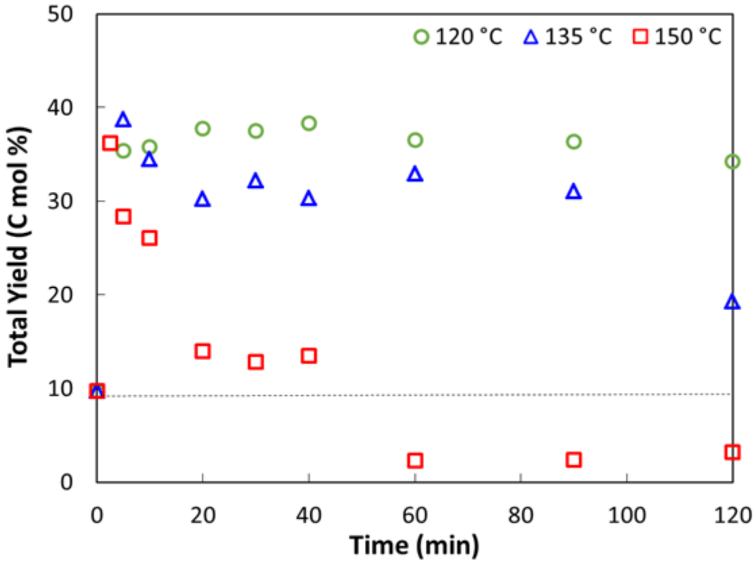

Figure 4.5 Total product yields versus time under Amberlyst 36 catalyzed conversion of vegetable waste in DMSO-water (1:1 v/v) at the three temperatures (conditions: 5 wt/v% substrate and catalyst-to-substrate mass ratio = 1:1; yield = $\text{product}_{\text{Cmol}}/\text{substrate}_{\text{Cmol}} \times 100\%$).

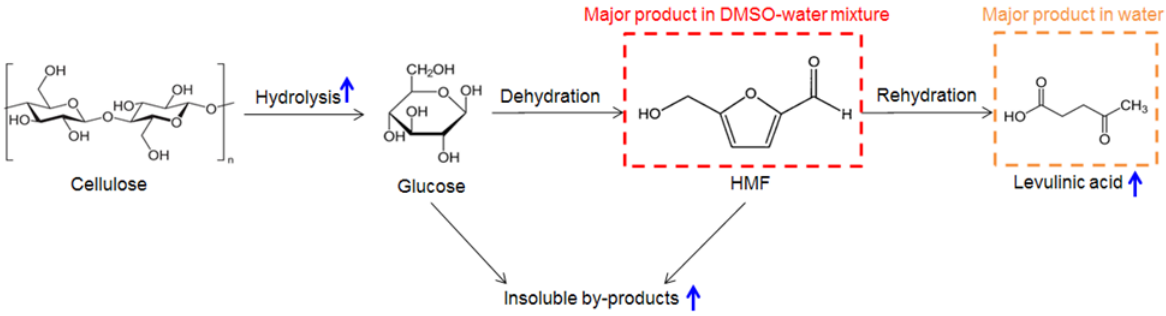

Scheme 4.1 Reaction pathways for valorization of vegetable waste by Amberlyst 36 under different conditions (blue arrows indicate the increase of products when the reaction temperature increases).

4.2.5 Microscopic and spectroscopic evidence of cellulose morphology and humins formation

The SEM images evidenced that the cellulose structure in untreated vegetable waste (**Figure B4**) was recalcitrant in water at 120-150 °C (**Figure 4.6a-c**), and undisrupted structure remained even after 120 min (**Figure B5a-c**). Although the cellulose structure became looser at 150 °C (**Figure 4.6c**, compared to **Figure B4**), it might be attributed to the decomposition of amorphous cellulose region (Fan et al., 2013). These observations reinforced the argument in Section 3.1 that the decomposition of cellulose was limited by its crystalline structure in aqueous solution at a relatively mild temperature in this study, compared to much higher temperatures (190-220 °C) used in previous studies (Chambon et al., 2011; Shuai and Pan, 2012). It should be noted that some spherical particles were observed after 5-min reaction in water at 150 °C (**Figure 4.6c**), and much more of these solids formed as the reaction time increased to 120 min (**Figure S5c**). Similar morphology has been reported as humins produced from C6 sugars (Zandvoort et al., 2013; Tsilomelekis et al., 2016). The formation of insoluble solids probably resulted from ill-defined by-products such as polymers and humins, which accounted for a lower total product yield at a higher temperature as discussed earlier.

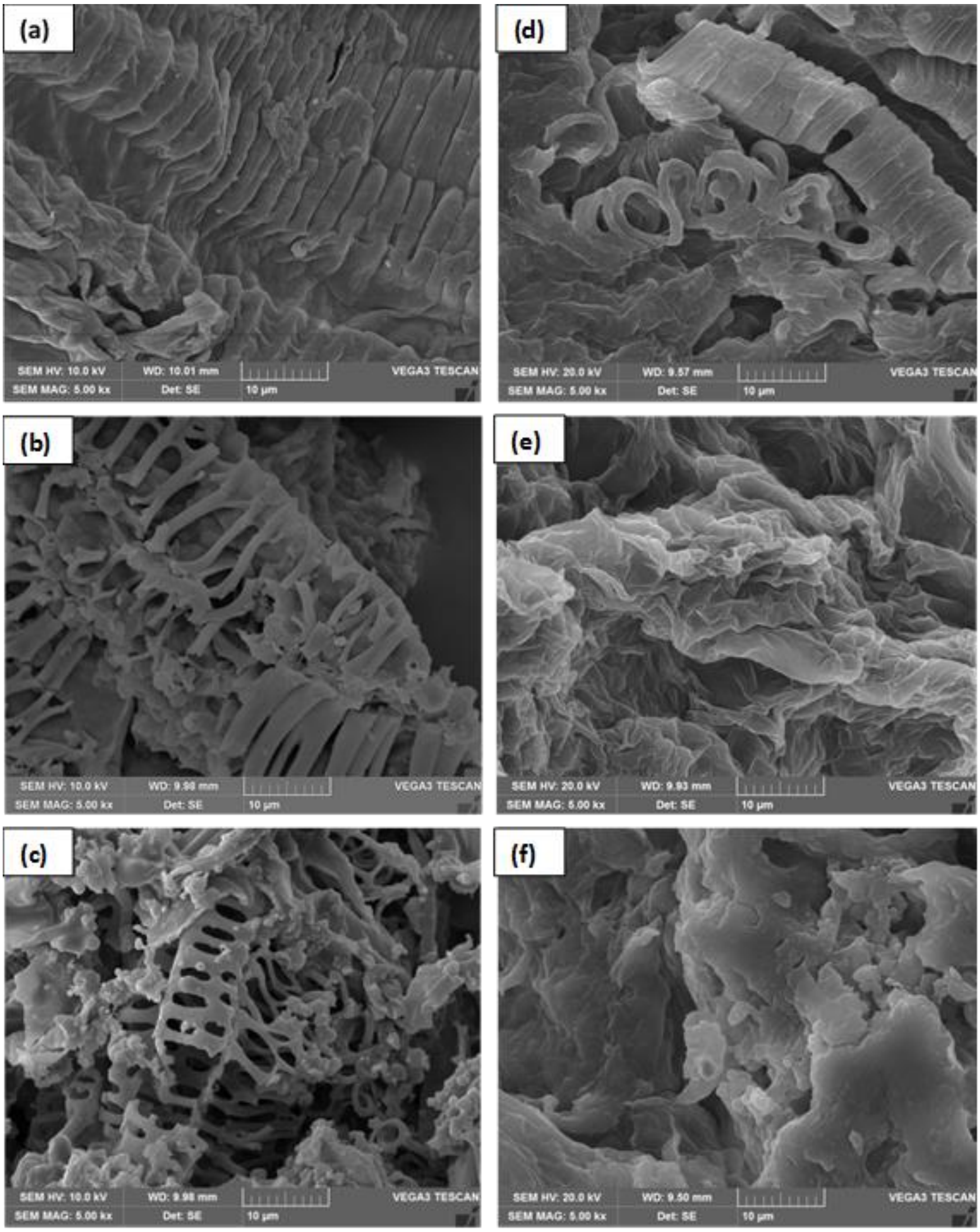

Figure 4.6 Scanning electron microscope (SEM) images of solid residues under Amberlyst 36 catalyzed conversion of vegetable waste in water (a-c) and DMSO-water (1:1 v/v) (d-f) at 120°C (a&d), 135°C (b&e), and 150°C (c&f) in 5 min.

In contrast, cellulose dissolution was significant in DMSO-water mixture, in which the compact structure underwent swelling at 120 °C (**Figure 4.6d**) and was completely disrupted after 120 min (**Figure B5d**). The cellulosic structure disappeared at a more rapid rate in 5 min at 135 and 150 °C (**Figure 4.6e&f**). The higher solubility of cellulose in DMSO-water mixture contributed to a higher and faster conversion rate, as shown in Figure 4.4. However, the SEM images clearly displayed the formation of insoluble solids in DMSO-water mixture after 120 min especially at 150 °C (**Figure B5f**), accounting for the sharp loss of total product yield in **Figure 4.5.**

The XRD spectra of the solid samples demonstrated similar diffraction peaks at 15.8°, 22.5° and 34.5° (**Figure 4.7**), corresponding to (110), (200) and (004) planes of Type-I crystalline cellulose (Nelson et al., 1964; Lu et al., 2015). In the aqueous medium, the peak intensity of the crystalline planes showed negligible change at 120 °C up to 120 min (**Figure 4.7a**). The calculated *CrI* also concluded insignificant change to the morphology and structure of cellulose (**Table B2**). The broadening peaks at higher temperature (**Figure 4.7b&c**) can be attributed to the amorphous cellulose, as suggested by a previous study (Morawski et al., 2013). However, the calculated *CrI* (9-38%) is believed to be too low at mild temperatures used in this study. It is probable that the disappearance of the peaks also results from the surface coverage by precipitation of insoluble solids on the solid samples, which agrees with the previous report (Wettstein et al., 2012).

Interestingly, while the SEM images illustrated better dissolution of cellulose in DMSO-water mixture, the XRD patterns revealed more intensive peaks at 120 and 135 °C after 60 min (**Figure 4.7d&e**). The corresponding *CrI* values also showed an increase compared to those at 5 min (**Table B4**). This may reflect the hydrolysis of amorphous cellulose in the course of the reaction (Luterbacher et al., 2014), which exposes or leaves behind the crystalline structure. However, the peaks of crystalline cellulose diminished after 120 min. Similarly, in DMSO-water mixture at 150 °C, a clear peak at 22.5° was observed after 5-min reaction and transformed into broad peak with increasing reaction time (**Figure 4.7f**). The peak transformation and disappearance reflect both facile cellulose hydrolysis and formation of by-products at higher temperatures. The changes of the XRD patterns provided spectroscopic evidence for the enhanced dissolution and hydrolysis of cellulose in DMSO-water mixture.

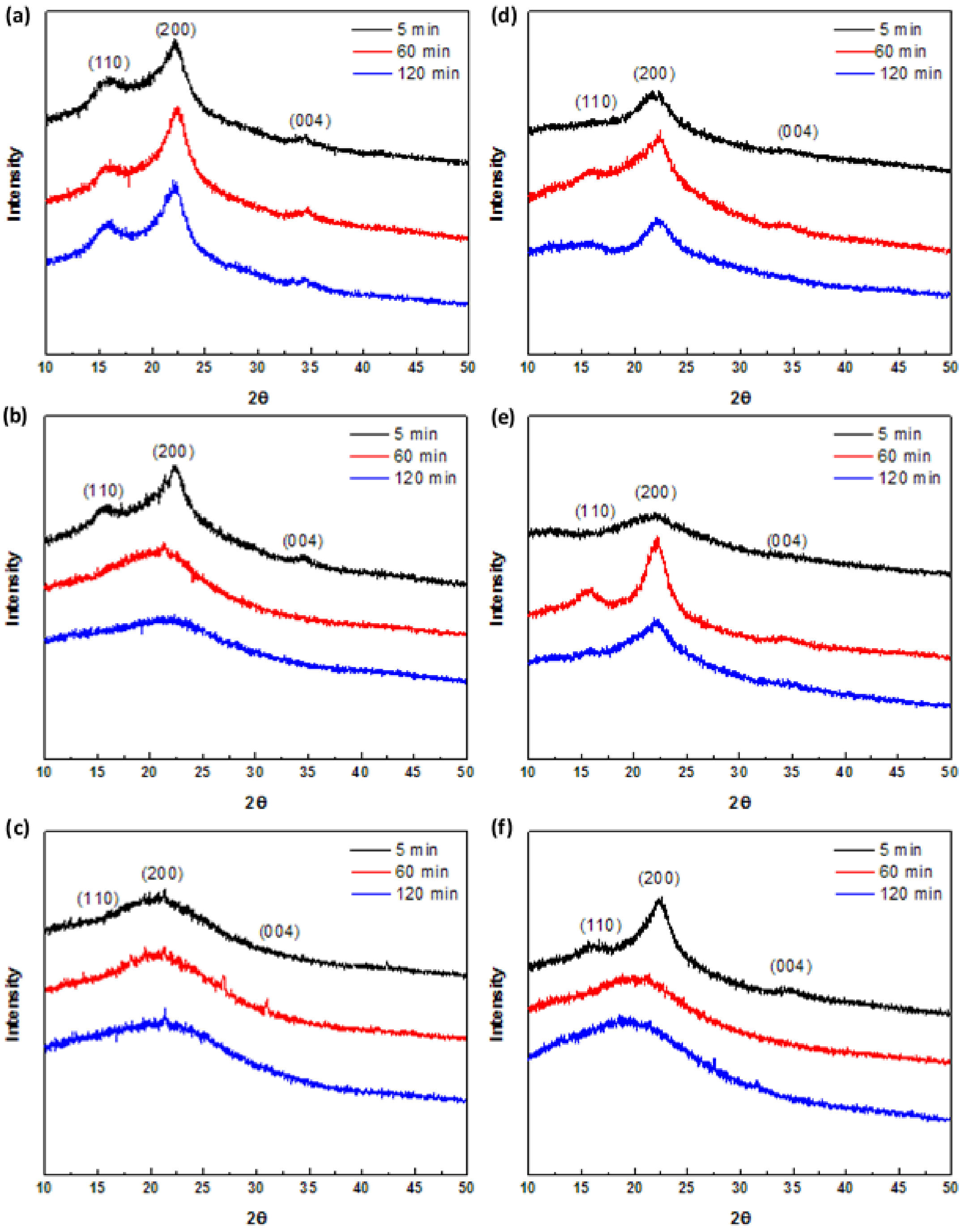

Figure 4.7 X-ray diffraction (XRD) patterns of solid residues under Amberlyst 36 catalyzed conversion of vegetable waste in water (a-c) and DMSO-water (1:1 v/v) (d-f) at 120°C (a&d), 135°C (b&e), and 150°C (c&f).

4.3 Summary

The hydrolysis of vegetable waste in aqueous solution started at a mild temperature of 120 °C in this study, which was attributed to efficient internal heating by microwave and high amorphous cellulose content in vegetable waste. The production of LA in aqueous solution rapidly increased to 17 C mol% in 5 min at 150 °C, while the formation of glucose- and HMF-derived humins also became significant as the temperature increased. In the DMSO-water mixture, the maximum soluble product achieved ~40 C mol% due to higher solubility of cellulose in DMSO that reduced the mass transfer limitation. The SEM images evidenced the enhanced dissolution of cellulose in DMSO-water mixture, contributing to higher conversion rate. At higher temperatures, the XRD patterns of the solid residues revealed more intensive peaks at first and broadening peaks along with increasing reaction time, which was the result of the exposure of crystalline structure upon the hydrolysis of amorphous cellulose and subsequent coverage by insoluble solids formation. This Chapter showcased an efficient valorization of vegetable waste into LA over solid Brønsted acid catalyst in aqueous solution and into HMF with co-solvent of DMSO, yet the formation of insoluble solids at high temperature was the major hurdle to high products yield that should be addressed in future investigations.

Chapter 5 - Roles of Solid and Aqueous Brønsted Acids in Cellulosic Fibres Conversion

Abstract

This chapter aims to produce levulinic acid (LA) from paper towel waste in environment-friendly and economically feasible conditions (based on preliminary cost-benefit analysis), and evaluate the difference using solid and aqueous Brønsted acids. Direct dehydration of glucose to LA required sufficiently strong Brønsted acidity, where Amberlyst 36 demonstrated rapid production of approximately 30 C mol% of LA in 20 min. However, the maximum yield of LA was limited by mass transfer. In contrast, the yield of LA gradually increased to over 40 C mol% in 1 M H_2SO_4 at 150 ºC in 60 min. The SEM images revealed the conversion in dilute acids under microwave at 150 ºC resulting in swelling structures of cellulose, which were similar to the pre-treatment process with concentrated acids. Further increase in reaction temperature to 200 ºC significantly shortened the reaction time from 60 to 2.5 min, which saved the energy cost as revealed in preliminary cost analysis.

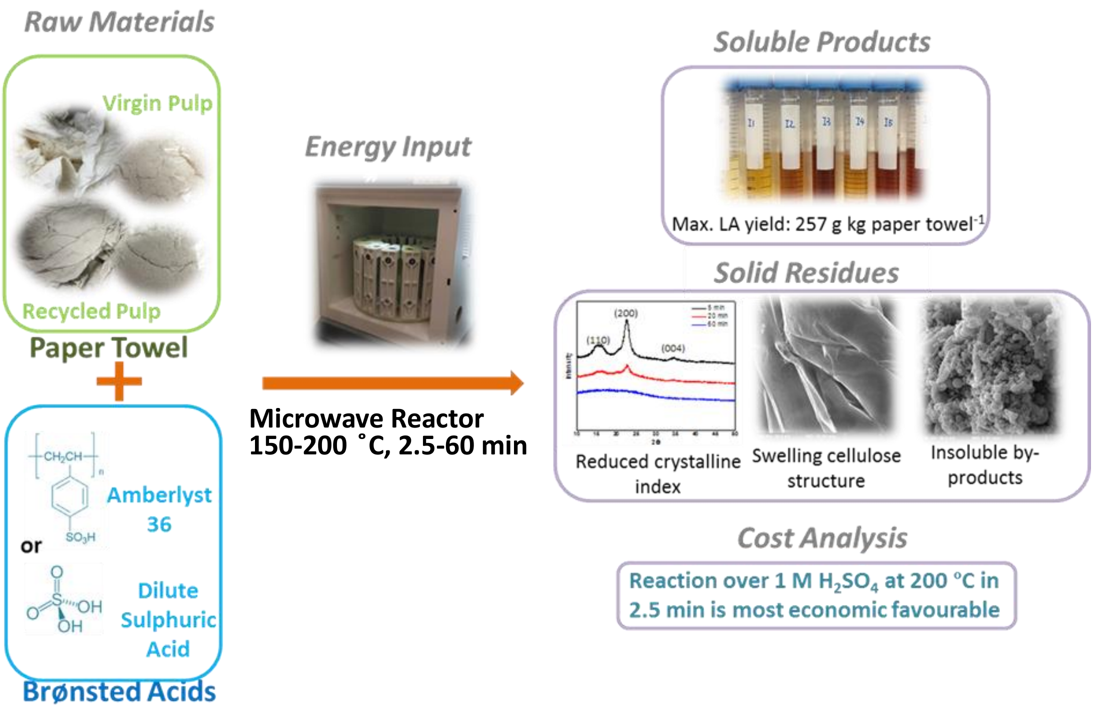

Figure 5.1 Graphical abstract of **Chapter 5**.

5.1 Research questions

As indicated in **Chapter 2**, complexity in actual biomass may result in varying results in the catalytic conversion. Therefore, in addition to polysaccharide-rich biomass waste (*i.e.,* vegetable waste) tested in **Chapter 4**, paper towel waste which is one of the most commonly used hygiene products containing primarily cellulosic fibres with a small amount of hemicellulosic fibres and lignin from wood pulps (Ruiken et al., 2013) is also tested the technology feasibility in view of composition variation.

A recent study showed that about two-thirds of the cellulosic fibres were not degraded under anaerobic digestion in the sewage plant (Ghasimi et al., 2016), whilst hygiene concerns make it unfeasible to recycle paper towels by the pulping industry.

Cellulose fibres have a limited recyclable life due to the reduction in length during the course of recycling process. However, the localized use of paper towels in most commercial buildings means that this waste is pre-sorted in nature, thus facilitating the logistics for possible valorization.

Amberlyst has shown a great potential in catalytic conversion of cellulosic waste to value-added chemicals with the aid of microwave heating in **Chapter 4**. It has been recently reported that the catalytic performance significantly varied between homogeneous and heterogeneous catalysts even at comparable levels of Brønsted acidity (Joo et al., 2017), while possible structural and morphological changes in the course of conversion remain unclear. A comparison and evaluation between the solid acid and homogeneous catalyst may offer new insight into the design of LA production. In addition to technology feasibility, the cost of the conversion is also an important factor to be considered. Therefore, robust comparison of the catalytic performance of aqueous and solid acids in terms of equivalent acid capacity is needed to reveal the potential difference in mechanisms and evaluate the economic and environmental implications.

In view of the inconsistent performance between homogeneous and heterogeneous catalysis and uncertain of substrate complexity on the conversion, this Chapter aims to (i) valorize paper towel waste into LA via catalytic conversion with the aid of microwave heating; (ii) evaluate the catalytic performance and preliminary cost-benefit analysis between solid Brønsted catalyst (Amberlyst) and dilute acids (< 1 M) at moderate temperatures; and (iii) understand the interaction between lignocellulosic fibres of paper towel waste and different types of acid via spectroscopic, microscopic, and thermal analyses.

5.2 Results and discussion

5.2.1 Conversion of paper towels by solid and aqueous acids at equivalent acid capacity

The catalytic reactions between virgin pulp and recycled pulp paper towel waste showed similar product profiles by using Amberlyst 36 **(Figure 5.2a&b)**. The hydrolysis of cellulose of paper towels at 150 ºC generated approximately 16-19 C mol% of glucose in 10 min, followed by a sharp increase of LA in 20 min to 34 C mol% and 30 C mol% in virgin and recycled pulp fibres, respectively. This result is promising and comparable to the conversion of the hydrothermally pre-treated standard cellulose at high temperature (190-270ºC) followed by acid catalysis at 160ºC, which produced 28% of LA in water (Weingarten et al., 2012a).

Reduction in total product yield was observed after 20 min using Amberlyst 36 but not sulphuric acid at 150 ºC (**Figure 5.3a&b**), which probably signified the blockage of active sites of the solid catalysts by large molecules, because the catalytic reactivity could be recovered by H_2O_2 washing (Chen et al., 2017a). Fructose and HMF was not observed during the conversion, while the molar ratio of FA to LA was significantly larger than one (1.1-1.6) in the first 20 min for virgin pulp and in the first 10 min for recycled pulp, respectively (**Figure 5.3c&d**). These results imply that a part of glucose may be dehydrated to LA and FA via the formation of furfuryl alcohol over strong Brønsted acid in the first stage (Yang et al., 2015; Chen et al., 2017a), as the HMF rehydration pathway will result in LA-to-FA molar ratio at one (Flannelly et al., 2016). The decrease in FA to LA ratio with a longer reaction time could reflect a smaller contribution of furfuryl alcohol pathway and/or possible loss of FA. The presence of xylose indicated simultaneous hydrolysis of hemicellulose of the paper towels (**Figure 5.2a&b**), which was gradually dehydrated to furfural. Choudhary et al. (2012) also reported direct dehydration of xylose to furfural under strong Brønsted acid. In view of the reactive nature of furan species, the observed decrease in furfural production was attributed to the condensation reaction between xylose intermediate and furfural (Agirrezabal-Telleria et al., 2011).

The conversion of paper towels over 0.135 M H_2SO_4 was distinct from those over Amberlyst 36 (**Figure 5.2c&d**), although the acid concentrations used in these two conditions were the same. The product profile was dominated by xylose as the hydrolysis product of hemicelluloses, reaching a maximum of around 60 C mol% in 20 min, indicating that the breakdown of hemicellulose fraction remained facile over the homogeneous catalyst. Meanwhile, the smaller amount of glucose produced by H_2SO_4-mediated conversion implied that the hydrolysis of cellulose was less efficient than that by using Amberlyst 36. There was no LA production probably because the actual proton availability was lower than the theoretical value of complete ionization. The second dissociation constant (pK_{a2}) of dilute sulphuric acid (< 1 M) increased from 1.99 to 3.53 when the temperature increased from 25 to 150 ºC (Marshall and Jones, 1966). Besides, H_2SO_4 may also be consumed by reaction with cellulosic fibres. This suggested an insufficient utilization of the H_2SO_4 acid capacity at elevated temperature.

Therefore, HCl (0.27 M) as a monoprotic acid with a lower pKa (-4.04 to -3.46 at 177ºC; McGrath et al., 2013) was adopted in the conversion of paper towels at 150 ºC to maximize proton release for a fair comparison between heterogeneous and homogeneous catalysts. Compared to 0.135 M H_2SO_4, the use of 0.27 M HCl (equivalent proton concentration) produced more glucose (approximately 20-27 C mol%) and furfural (up to 34 C mol%) (**Figure 5.2e&f**). The higher efficiency of cellulose hydrolysis into glucose and xylose conversion into furfural may suggest a higher acid capacity in HCl than that in H_2SO_4. However, the yield of LA was still limited ($\leq$ 10 C mol%) in comparison to that of Amberlyst 36 (30-34 C mol%). This variation may be ascribed to lower acid strength of the homogeneous acids compared to Amberlyst 36, of which the acidity is equal to 48% H_2SO_4 according to Hammett acidity function (Cadenas et al., 2011), in spite of the same amount of protons. In addition, the presence of lignin in the paper towel waste may consume a portion of the acid for depolymerization and cleavage of carbon-carbon bonds (Ahlkvist, 2014). Prolonging the reaction time only showed a marginal increase of LA yield in the HCl medium due to the side reactions such as humins and polymer formation among sugars and intermediates, as indicated by a slight loss of total products (**Figure 5.3a&b**). Reaction at 200 ^{o}C with 1 M H_2SO_4 was observed with drastic drop of total product yield due to formation of insoluble products, indicating severe polymerization elevated by high temperature and strong acidity in the system.

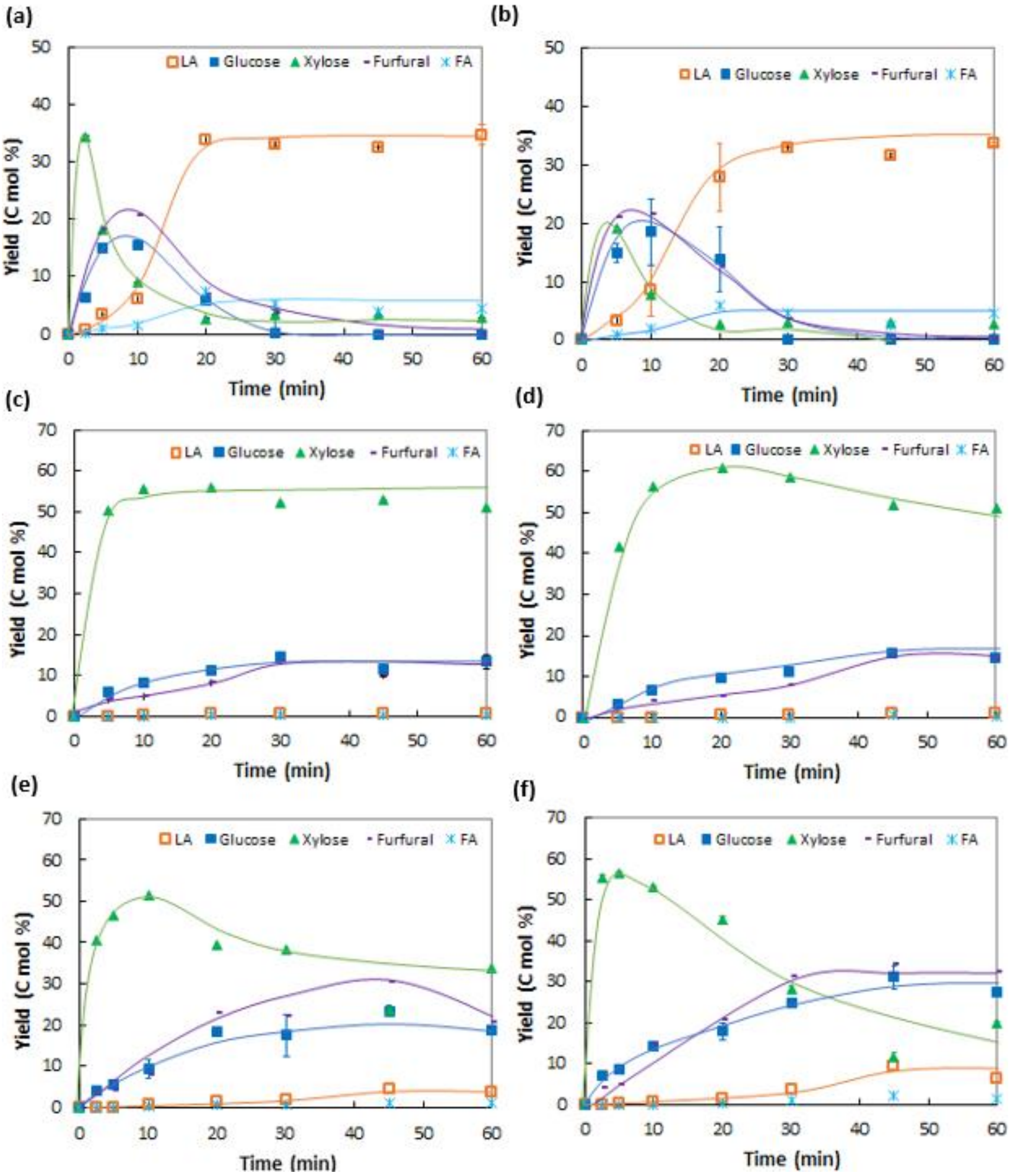

Figure 5.2 Product yields versus time under 0.5 g Amberlyst 36 (a&b), 0.135 M H_2SO_4 (c&d), and 0.27 M HCl (e&f) catalyzed conversion of 0.5 g virgin pulp (a&c&e) and 0.5 g recycled pulp (b&d&f) paper towel waste in 10 mL water.

(a)

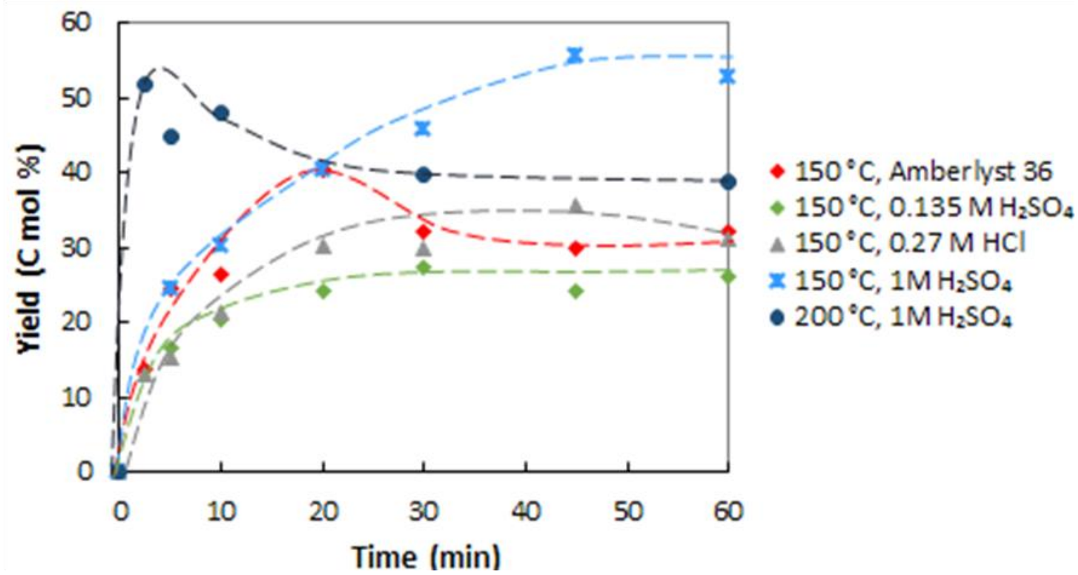
Yield (C mol %)
0
10
20
30
40
50
60
Time (min)
0
10
20
30
40
50
60
150 °C, Amberlyst 36
150 °C, 0.135 M H_2SO_4
150 °C, 0.27 M HCl
150 °C, 1M H_2SO_4
200 °C, 1M H_2SO_4

(b)

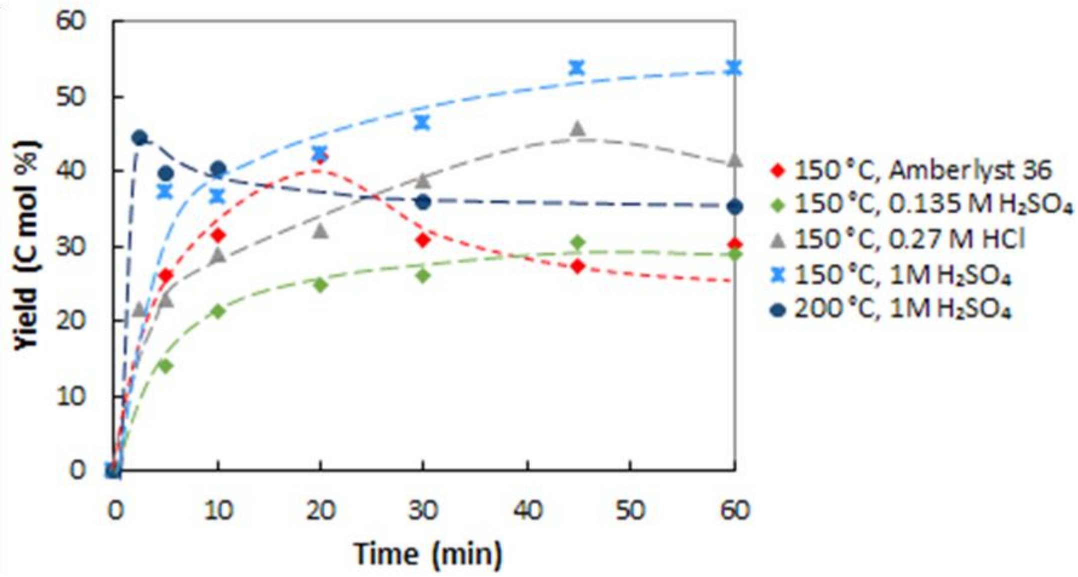
Yield (C mol %)
0
10
20
30
40
50
60
Time (min)
0
10
20
30
40
50
60
150 °C, Amberlyst 36
150 °C, 0.135 M H_2SO_4
150 °C, 0.27 M HCl
150 °C, 1M H_2SO_4
200 °C, 1M H_2SO_4

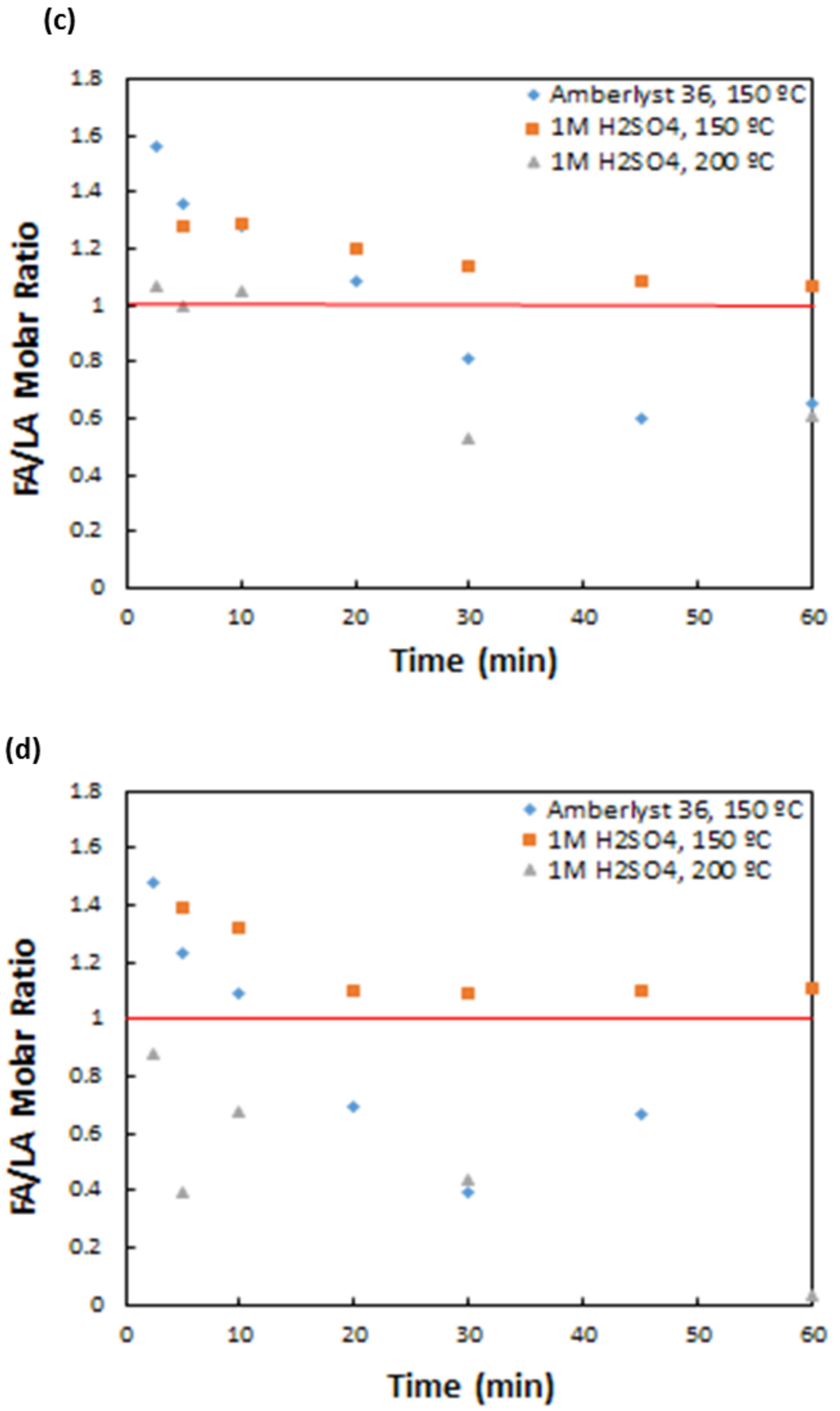

Figure 5.3 The yield of total products (a&b) and molar ratio of formic acid (FA) to levulinic acid (LA) (c&d) during the catalytic conversion of virgin pulp (a&c) and recycled pulp (b&d) paper towel waste at various conditions.

5.2.2 Improvement of LA production by employing higher acidity and higher temperature

Increasing the concentration of H_2SO_4 from 0.135 to 1 M showed a superior yield of LA over 40 C mol% in 60 min for both types of paper towel waste at 150 ºC (**Figure 5.4a&b**), showing that strong Brønsted acidity was necessary to trigger the dehydration of glucose to LA. The maximum yield of total hydrolysis products under 1 M H_2SO_4 conversion was twice as high as that using the 0.135 M H_2SO_4 at 150 ºC (**Figure 5.3a&b**). It was reported that the activation energy for cellulose hydrolysis was similar (170-180 kJ mol^{-1}, 150-200 ºC) regardless of the concentration of dilute sulphuric acid (0.05-1 M) (Girisuta et al., 2007). Therefore, the difference in maximum yields of total products may result from the effect of acid concentration on the crystalline structure of cellulose, which determined the amount of amorphous cellulose for glucose production (*Section 5.2.3 & 5.2.4)*.

The use of 1 M H_2SO_4 also performed better than Amberlyst 36 in terms of the maximum yields of LA, because of a greater extent of cellulose hydrolysis into glucose as the precursor of LA. Although the acidity strength of Amberlyst 36 (equivalent to 48% H_2SO_4) was much stronger than 1 M (~ 9%) H_2SO_4, there was limited mass transfer between paper towel waste and Amberlyst 36. The molar ratio of FA to LA decreased from 1.3 (virgin pulp) or 1.4 (recycled pulp) to 1.1 throughout the conversion in 1 M H_2SO_4 at 150 ºC (**Figure 5.3c&d**). At 200 ºC in 1 M H_2SO_4, the formation of LA swiftly reached a plateau of 46 C mol% within 2.5 min for both virgin pulp and recycled pulp (**Figure 5.4c&d**). These values were very close to those in 1 M H_2SO_4 at 150 ºC in 60 min, while extending the reaction time to 90 min at 150 ºC also increased the yield of LA to 46 C mol% (data not shown).

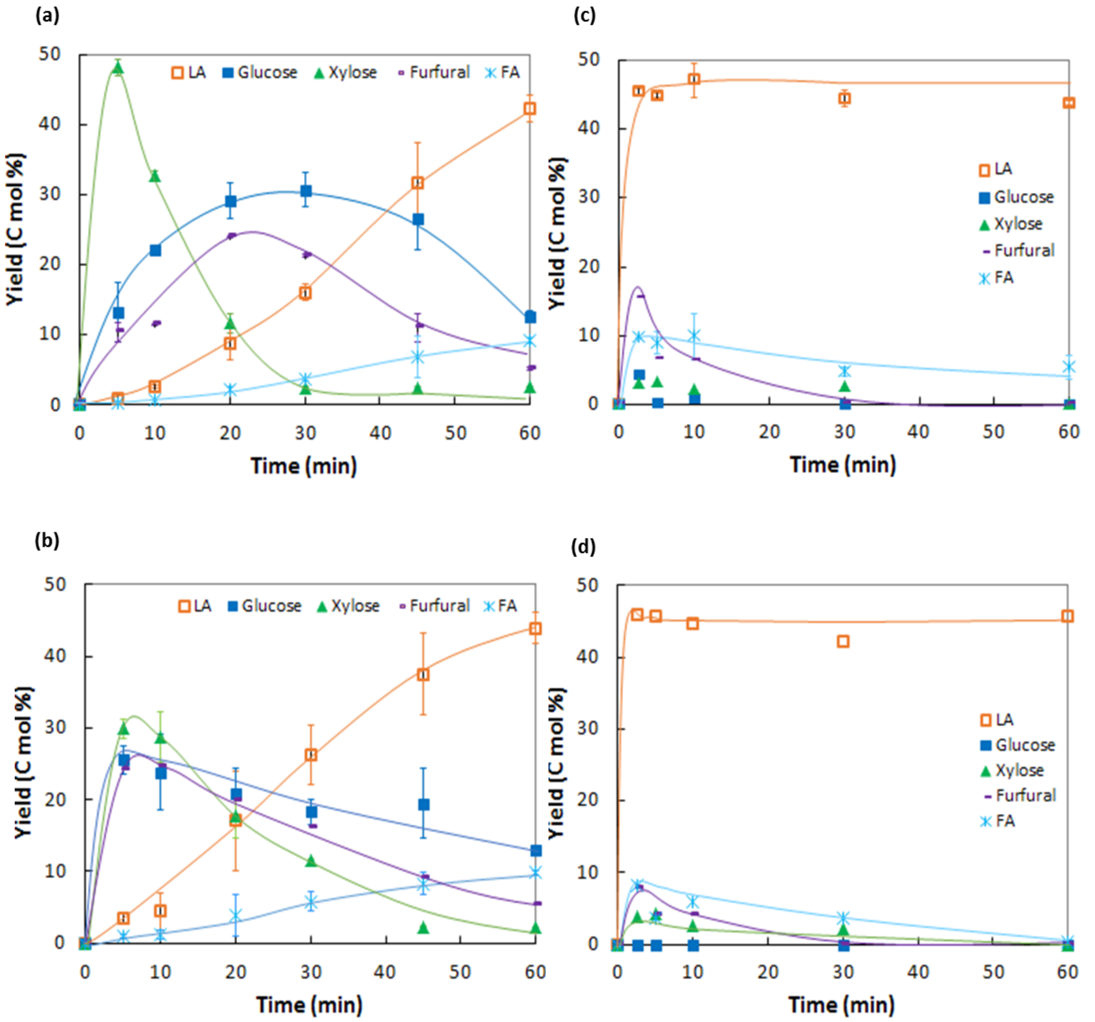

Figure 5.4 Product yields versus time under 1 M H_2SO_4 catalyzed conversion of virgin pulp (a&c) and recycled pulp (b&d) paper towel waste at 150 ºC (a&b), and 200 ºC (c&d) (condition: 5 wt/v% substrate; yield = product C_{mol}/substrate C_{mol} × 100%).

This revealed that the relative kinetics of favourable reactions to LA formation (*i.e.,* hydrolysis of cellulose and dehydration of glucose to LA) and undesirable reactions (*i.e.,* formation of humins and polymers) were comparable at 150 and 200 ºC in 1 M H_2SO_4. Similar observations have been reported in valorization of cellulose-rich vegetables over Amberlyst 36 and starch-rich bread waste over various metal catalysts (Chen et al., 2017a; Yu et al., 2017a). This highlights the need to balance the energy consumption at higher temperature versus longer reaction time for the synthesis of LA from paper towel waste. The ratio of FA to LA was smaller than one (**Figure 5.3c&d**) probably due to the volatilization of FA at 200 °C.

5.2.3 Microscopic and spectroscopic insights into conversion of paper towel pulps

The SEM images (**Figure C1**) showed highly ordered fibrous structure of untreated paper towels, primarily composed of microfibrils (Amiri and Karimi, 2013), whereas the recycled pulp showed more compact structure. As the length of fibre is reduced by recycling process, recycled pulp typically has shorter fibre length than virgin pulp (Ghasimi et al., 2016). The XRD spectra of untreated paper towel fibres revealed typical structure of cellulose I with main diffraction peaks at 16.3° and 22.7°, which were attributed to (110) plane and (200) plane, respectively (**Figure C2**) (Wada et al., 2014). The minor peak at 35° represented the one-fourth length of a cellobiose unit along the fibre direction (Ouyang et al., 2015). The virgin pulp and recycled pulp paper towel had similar *CrI* values of 67.1% and 65.5% (**Table 5.1**), which were slightly lower than the cellulose standard (75.1%).

Table 5.1 Crystallinity index (*CrI*) of paper towels at various reaction conditions.

Catalytic Conditions			**CrI of Paper Towels (%)**	
			Virgin Pulp	Recycled Pulp
Untreated			67.1	65.5
150 ºC	Amberlyst 36	5 min	76.9	74.1
		20 min	47.5	43.2
		60 min	22.6	13.0
	0.135 M H_2SO_4	5 min	76.9	71.1
		20 min	76.3	72.5
		60 min	75.1	70.9
	1 M H_2SO_4	5 min	41.7	19.7
		20 min	15.6	14.9
		60 min	19.1	18.7
200 ºC	1 M H_2SO_4	5 min	17.6	16.2
		60 min	20.5	20.1

Remark: there were no visible peaks in the XRD patterns in *CrI* values smaller than 30%

The conversion over Amberlyst 36 showed an increase of *CrI* values in the first 5 min as a result of the reaction of amorphous fraction (**Table 5.1**). However, the values decreased to 43-48% and 13-23% in 20 and 60 min, respectively. The SEM images revealed the formation and agglomeration of spherical particles on the surface of the fibres at 60 min (**Figure C3a&e**), which were possibly insoluble by-products such as humins and polymers (Hu et al., 2011) that may contribute to decreasing *CrI* values (Chen et al., 2017a). As shown in **Figure C4b&f**, the peaks representing (110) plane and (004) plane disappeared in 20 min, and then a plain line remained after the reaction at 60 min. However, a clear backbone structure of the cellulose fibres was still observed in the recycled pulps after 60-min reaction (**Figure C3e**), indicating marginal improvement of hydrolysis with a prolonged reaction time. As a result, 20-min conversion over Amberlyst produced the highest total product yield (**Figure 5.3a&b**).

Similarly, the early stage of conversion over 0.135 M H_2SO_4 (*i.e.,* 5 min) resulted in an increase of *CrI* in both pulps by 8.5-14.6% (**Table 5.1**) due to the decomposition of readily accessible amorphous portion of cellulose. The *CrI* values had little change along the reaction time, because dilute acid and moderate temperature were incapable of transforming crystalline cellulose to amorphous form (Chen et al., 2017a). The SEM images (**Figure C3b&f**) demonstrated the reduction of fibre sizes but there remained more intact structures than those catalyzed by Amberlyst. This reflected inefficient hydrolysis on cellulose chains over 0.135 M H_2SO_4 (Lacerda et al., 2013). Therefore, Amberlyst 36 generated a higher maximum yield of hydrolysis products than 0.135 M H_2SO_4 (**Figure 5.3a&b**).

The change of crystallinity was most significant in 1 M H_2SO_4 at 150 ^{o}C (**Table**

5.1), where the paper towels displayed gradual swelling to sponge-like structures with longer reaction time (**Figure C3c&g**). The morphological images were similar to those reported with 85% phosphoric acid pre-treatment at 50 °C for 60 min (Amiri and Karimi, 2013). This result suggested that the use of dilute acid under microwave heating could serve as an alternative to concentrated acid pre-treatment. The recycled pulp fibres were swollen to a smooth surface upon the 60-min reaction, while the virgin pulp fibres were covered by agglomerated products (**Figure C3c&g**), which may be hydrocellulose formed by partial hydrolysis with hot dilute acid (Xiang et al., 2003). The emergence of a subtle shoulder peak at 21.8° of the XRD spectra (**Figure C4e**) indicated the expansion of the cellulose lattice and removal of hemicellulose content (Singh et al., 2015). At 200 °C, the solid residues showed significant difference where the virgin pulps formed much larger spherical particles than recycled pulps (**Figure C3d&h**). Such distinctive characteristics might emerge from the variations in the compositions of paper towels (**Table 3.2**) due to different origins/sources.

5.2.4 Thermogravimetric analysis of solid residues

The thermal behaviour of untreated paper towels and standard cellulose showed nearly identical pattern (**Figures 5.5a & S5a**). The weight reduction of recycled pulp paper towel was less than virgin pulp and standard cellulose at the temperature range of 350-550 ºC, which was consistent with **Table 3.2** that recycled pulps contained higher lignin content (11.8%) than virgin pulp paper towel (1.3%) because of source/origin difference. A single peak was found from the DTG spectra of untreated fibres (**Figure 5.5a**), while the solid residues subject to acid hydrolysis showed dual degradation regions at approximately 200 and 350 °C (**Figure 5.5b&c**). The first degradation region was attributed to the release of water/H_2SO_4 from the cellulose (Huntley et al., 2015), which was in line with the swelling structure in the SEM images (**Figure C3**). The peak on the DTG spectra increased with a greater degree of swelling in the cellulose. The second degradation region was associated with the unreacted cellulose and polymeric by-products. It was noted that the solid residues displayed substantially less thermal decomposition than untreated fibres (**Figure C5b&c**), especially for those showing spherical particles resulting from the use of Amberlyst 36 at 150 °C (**Figure C3a&e**) and 1 M H_2SO_4 at 200 °C in 60 min (**Figure C3d&h**). This may provide circumstantial evidence of the formation of humins and polymers during the catalytic conversion.

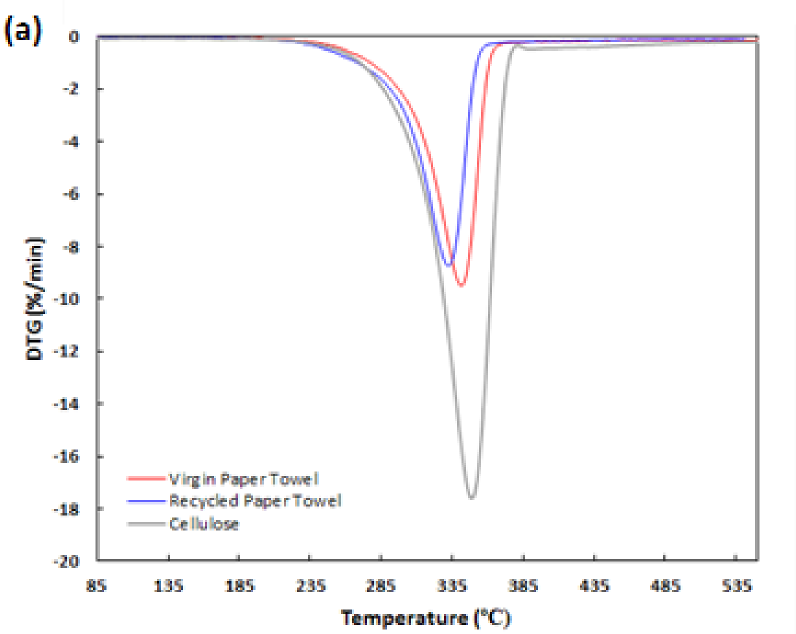

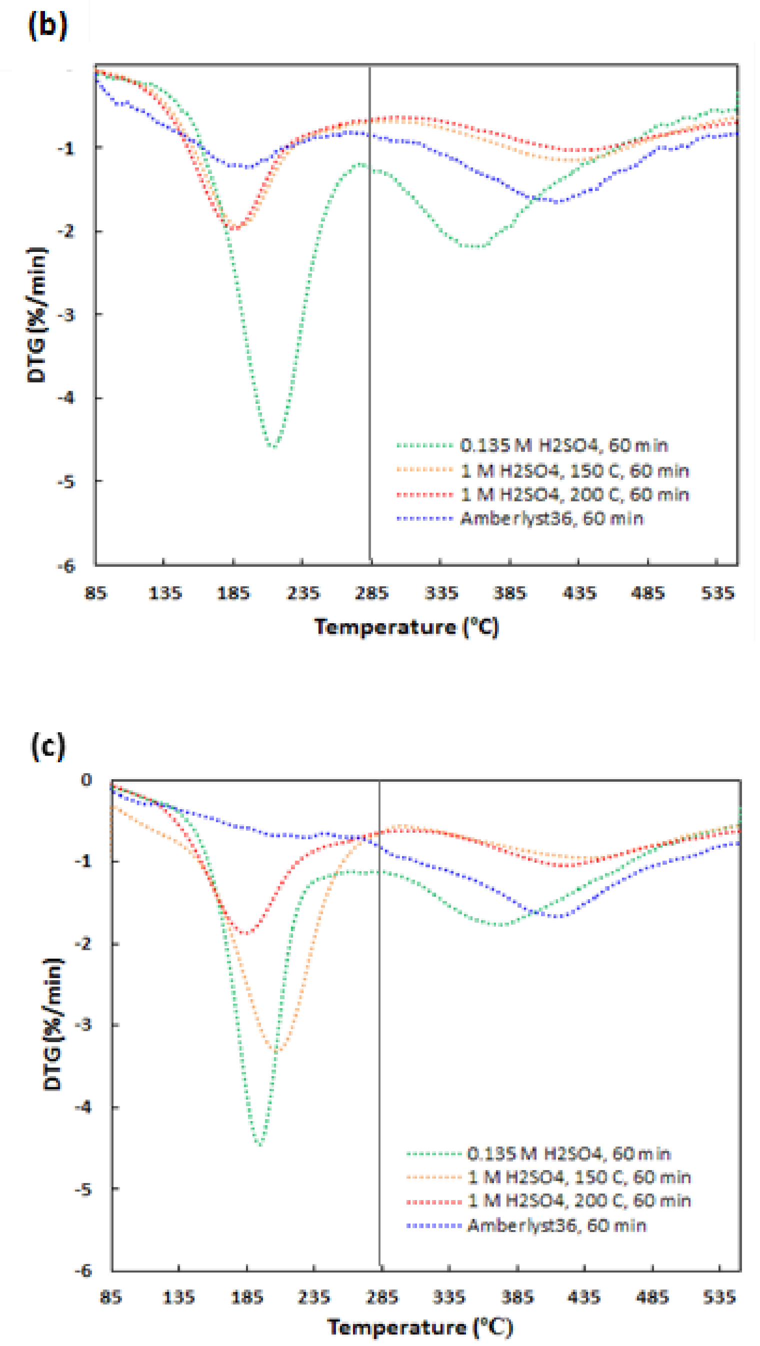

Figure 5.5 DTG of untreated paper towel waste and standard cellulose (a), treated virgin pulp (b) and treated recycled pulp (c) paper towel waste at selected conversion conditions.

5.2.5 Economic and environmental concerns of LA synthesis

Production of LA from paper towel waste not only reduced the use of valuable feedstocks but also avoided waste disposal fees. The cost of heterogeneous catalyst was a significant contribution to the overall costs followed by energy consumption (**Table C1**). In this study, solid catalysts demonstrated the advantage of recyclability and easy separation, where the yield of LA was maintained at 20-27 C mol% in five cycles of separation and reuse (**Figure C6**). However, product separation that generally contributes to a significant proportion to the total cost will require extensive analysis (e.g., Nhien et al., 2016) in future studies. Homogeneous catalyst in this study showed great advantage in the cost analysis due to the low price of sulphuric acid (**Table C1**), which made it favourable as an industrial method for LA production (Weingarten et al., 2012a). Nevertheless, simple neutralization with a base is not feasible for post-reaction separation of LA due to its acid functionality (Weingarten et al., 2012b). The environmental impact and carbon footprint associated with wastewater generation and the safety hazards in the working environment should be holistically assessed.

The output of LA was the largest (257.1 g kg^{-1} paper towel) when the conversion was carried out at 200 ºC, and the energy consumption was the lowest due to short reaction time, highlighting that the use of microwave was more energy efficient for short duration. Glasnov and Kappe (2011) illustrated the transformation of laboratory-scale microwave chemistry into scalable continuous-flow processes with comparable performance, which may further lower the production cost. Although high reaction temperature (200 ºC) and intensive microwave power generated the largest amount of insoluble humins in the biomass residues (Tsilomelekis et al., 2016), these by-products may be upcycled as potential feedstocks for the production of carbon foam, fibres, and resins (Alonso et al., 2017; Mija et al., 2017).

5.3 Summary

This Chapter demonstrates the valorization of paper towels into LA over Amberlyst or dilute H_2SO_4 catalysts at moderate temperatures, validated the catalytic conversion technology established in **Chapter 4** can also be applied in lignocellulosic waste. Similar to vegetable waste, production of LA from paper towel was rapid over Amberlyst 36, while the maximum yield was limited by mass transfer. The SEM images revealed swelling fibres with microwave heating over dilute H_2SO_4, despite under-utilization of its acid capacity at elevated temperature. The preliminary cost analysis showed the advantage of LA production at higher temperature and/or stronger acidity with shorter reaction time, while the environmental impacts of solid and aqueous acid catalysts should also be considered in future studies.

Chapter 6 - Glucose Isomerization to Fructose via Solid Base Catalyst

Abstract

In this Chapter, glucose isomerization to fructose was conducted via a solid base biochar catalyst derived from spent coffee grounds and melamine. The X-ray photoelectron spectroscopy (XPS) spectra identified the majority of pyridinic nitrogen on the biochar surface, which imparted the strong base character of the catalyst. Activity of the catalyst was evidenced by fast conversion of glucose (12%) and high selectivity to fructose (84%) in 20 min at a moderate temperature (120 °C) compared to recent reported immobilized tertiary amines at comparable N concentration (10-15 mol% relative to glucose). By increasing the reaction temperature to 160 °C, fructose yield achieved 14% in 5 min. The base biochar catalyst showed superior selectivity to commonly used homogeneous base catalysts such as aqueous hydroxides and amines (>80% vs. 50-80%) and comparable catalytic activity (~20 mol% conversion within 20 min). Moreover, co-solvent of acetone in the reaction system may increase the overall basicity by stabilizing protonated water clusters via hydrogen bonding, which led to faster conversion and higher fructose selectivity than those in water. Approximately 19% fructose was obtained at 160 °C, and the basic sites on the biochar catalyst were stable in hydrothermal environment as indicated by acid-base titration test. Therefore, nitrogen-doped engineered biochar can potentially serve as solid base catalyst for biorefinery processes.

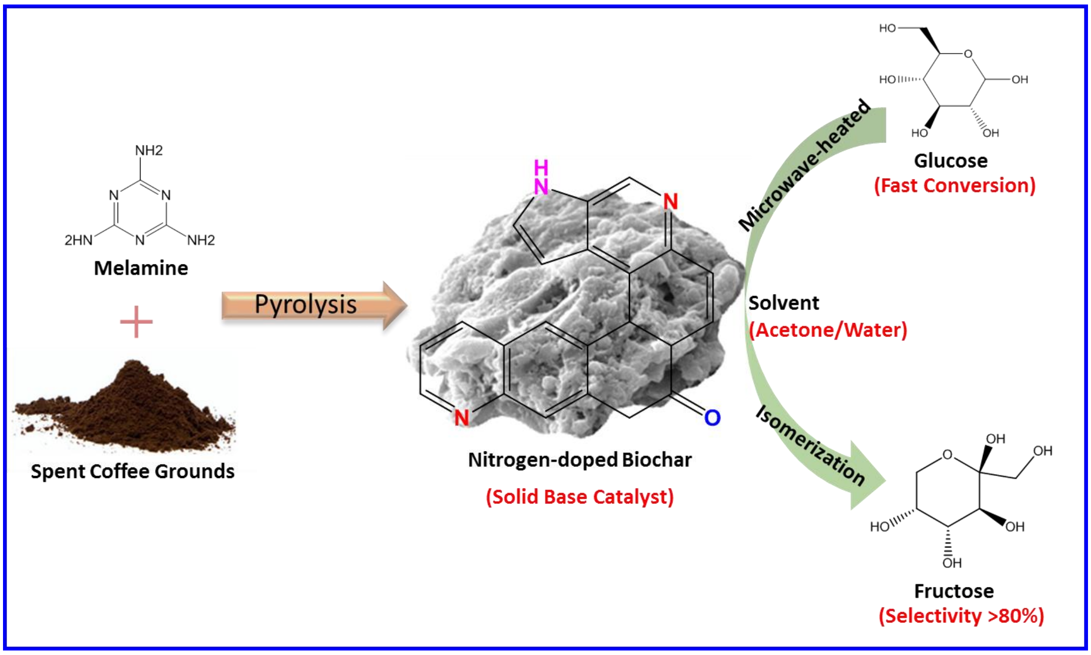

Figure 6.1 Graphical abstract of **Chapter 6**.

6.1 Research questions

Chapters 4 & 5 demonstrated effective catalytic conversion of cellulosic waste to value-added chemicals by Brønsted acid catalysts (*i.e.,* Amberlyst cation exchange resins and sulfuric acid). Similar conversion was performed to starchy-rich bread waste at varying substrate-to-catalyst mass ratio from 0.2 to 2 at different temperature in water (**Figure D1&2**). The results showed that the bread waste was selectively and rapidly converted to approximately 70 C mol% glucose at 120 °C regardless of the substrate loading (**Figure D1**). The yield of HMF, LA or the other products was negligible under this condition, implying the thermal dynamic hurdle for glucose dehydration at this temperature. At 135 °C, the maximum yield of glucose was also around 70 C mol%, which was further converted up to 25 C mol% LA along with the reaction (**Figure D2**). In addition, the higher substrate loading, the severer the side reactions resulting in a great loss of total product yield. Therefore, the conversion of bread waste was not satisfying in terms of carbon efficiency even though the yield of LA was comparable to that generated from vegetable waste.

Valorization of the bread waste was further examined in different reaction media at higher temperature (150 °C) (**Figure D3**). In the water medium, the elevation of temperature did not much enhance LA production but the side reaction since LA was the single product. The change to DMSO/H_2O mixture (1:1 v/v) retained partial HMF (~10 C mol%) from rehydration to LA, which was in line with the findings in **Chapter 4**, while the total product yield was similar to the one in water medium. On the contrary to **Chapter 5**, the use of 1 M H_2SO_4 as catalyst and solvent medium did not promote the conversion from glucose to LA, and glucose accounted for over 70 C mol% in the reaction system. These results indicated that solid Brønsted acid catalysts were effective in conversion starch waste to glucose at mild temperature (120 °C) in aqueous media. Increasing the reaction temperature resulted in great loss in product which was probably due to polymerization and other side reactions between the solid catalyst and the substrate while glucose yield remained unchanged under sulfuric acid catalysis.

Therefore, the solid Brønsted acid catalyst was considered unsuitable in this study. The accumulation of glucose during the conversion indicated glucose isomerization to fructose was the rate-limiting step. Lewis acid catalysts such as chromium and aluminum in homogeneous form (Choudhary et al., 2013; Swift et al., 2015) and tin-beta zeolites in heterogeneous form (Román-Leshkov et al., 2010; Bermejo-Deval et al., 2012) are effective catalysts for glucose isomerization. However, either the homogeneous catalyst itself or the synthesis materials of the heterogeneous catalyst contain hazardous materials, which pose environmental challenges in practical applications (**Chapter 2**). Recent studies have proven that Brønsted base can also catalyze glucose isomerization through a different mechanism involving hydrogen transfer [8] instead of hydride shift for Lewis acids (Román-Leshkov et al., 2010).

Fructose yields obtained from various homogeneous base catalysts such as triethylamine (Liu et al., 2014; Carraher et al., 2015), polyethylenimines (Yang and Runge, 2016), and basic amino acids (Yang et al., 2016) are comparable to those from Lewis acid catalysts (~30%). In particular, fructose selectivity catalyzed by Arginine (a type of amino acid) reached 78% compared to 54% by tin-beta zeolites (Román-Leshkov et al., 2010) at the same fructose yield. This suggests that base catalysis provides a promising alternative to Lewis acids for glucose isomerization. On the basis of these homogeneous catalytic results, Brunelli et al. (2017) synthesized heterogeneous base catalysts by immobilizing organosilanes with tertiary amine onto porous silica. The catalysts showed comparable fructose selectivity but lower catalytic activity than homogeneous amines. Hence, fabrication of environmentally friendly catalysts from renewable or waste biomass deserves more investigation. Biochar, an economically feasible and green material, has been extensively studied in environmental applications for pollution abatement and soil remediation in view of its versatile functional groups and favorable structure for modification (Rajapaksha et al., 2016; Song et al., 2017). It is noted that various functional groups on the surface of engineered biochar can be distinctive active sites for catalytic reactions (Xiong et al., 2017). The oxygen-containing functional groups such as carboxyl groups, phenolic groups and sulfonic groups generally contribute to weak/strong acidity of carbonaceous materials (Li et al., 2014; Ogino et al., 2015). For example, sulfonated biochar has been recently applied as Brønsted acid catalyst in bread waste or glucose conversion to HMF (Cao et al., 2018; Xiong et al., 2018).

The basicity of carbon surface is related to basic surface functional groups, mainly nitrogen-containing functional groups such as amine, pyrrole, and pyridine, or proton attraction by delocalized electrons of carbon aromatic rings (Shen and Fan, 2013). Therefore, nitrogen-enriched (N-enriched) biochar was hypothesized to be a potential catalyst for glucose isomerization if it presents intrinsic basicity and allows easy separation from the reaction stream. According to previous studies, spent coffee grounds are a nitrogen-rich biomass feedstock (30 wt% protein) (Cho et al., 2015), where the derived products can be a potential soil amendment with fertilizer or utilized in electrocatalytic applications and offer an option for waste valorization (Vardon et al., 2013; Ramasahayam et al., 2015). However, poor surface coverage by nitrogen could result from the thermal decomposition of nitrogen-containing functional groups in the structure of carbon during biomass pyrolysis at high temperatures above 700 °C (Chen et al., 2017e). Thus, melamine can serve as an additional nitrogen source for nitrogen doping on various carbon supports (e.g., graphene and carbon nanotubes/xerogels) to increase their nitrogen content (Gorgulho et al., 2009; Sheng et al., 2011; Hlekelele et al., 2016). In addition to the functional groups on the catalyst surface, solvents also affect chemical reactivity and selectivity of catalytic reactions (Bass et al., 2003; Cao et al., 2017). Our previous work showed that co-solvent of acetone or acetonitrile can enhance glucose isomerization under a Lewis acid catalyst (Yu et al., 2017c), however, it is unclear whether base-catalyzed glucose isomerization can also be promoted.

Therefore, the Chapter aims to: (i) synthesize N-enriched biochar catalyst for glucose isomerization to fructose; (ii) examine catalytic activity of resultant catalysts in relation to its physicochemical properties; (iii) assess the effect of co-solvent on base-catalyzed conversion; and (iv) evaluate the catalytic stability of the biochar catalyst in reuse.

6.2 Results and discussion

6.2.1 Physicochemical characteristics of the N-enriched biochar catalyst

The N-enriched biochar displayed Type II N_2 adsorption-desorption isotherm (**Figure D4a**), and the BJH plot (**Figure D4b**) also showed a much higher fraction of pore diameter ranging from 50 to 200 nm than that from 2-50 nm, indicating the characteristics of a macroporous material. In contrast to surface areas above 100 m^2 g^{-1} in other studies, the N-enriched biochar in this study showed a low specific surface area (S_{BET} = 0.35 m^2 g^{-1}) (**Table 6.1**), probably due to the aggregation of the biochar after the N-doping process (Cho et al., 2017). The SEM images revealed a layered morphology with irregular aggregates on the surface of the biochar catalyst (**Figure D5**), which may be responsible for its low surface area. The biochar catalyst showed characteristic diffraction peaks at $2\theta = 23.5°$ (002) and $2\theta = 43.6°$ (100) of carbon materials (Figure D6), though not as sharp crystalline peaks. The broadened (100) peak represents the disordering characteristic of non-graphitic carbons (Sharon et al., 2012), and the (002) reflection shows the stacking of aromatic carbon layers within the disordered crystallites (Sakintuna et al., 2004). Carbon (85.9 wt%) and oxygen (13.1 wt%) were the two main elements identified from the EDS analysis (**Figure D5**), while nitrogen was below the detection limit in this case.

Table 6.1 Surface characterization of the catalyst

BET Surface area (m^2 g^{-1}) [a]	0.35					
Composition (at. %) [b]	**C**		**N**		**O**	
	86.84		5.59		7.57	
Core level (%) [b]	**C 1s**		**N 1s**		**O 1s**	
	C-C	46.2	C-N=C	43.6	C-O	56.5
	C-O	34.2	N-H	37.3	C=O	43.5
	C=O	19.6	=N-O	19.1		
Basic /Acidic sites (mmol g^{-1})	**Basic**		**Acidic**			
	0.247		0			

[a] Data derived from N_2 adsorption-desorption isotherms

[b] Data obtained from XPS analysis.

The atomic ratios of carbon, nitrogen and oxygen determined by the XPS analysis, and the percentages of chemical species calculated by peak deconvolution were summarized in **Table 6.1.** In contrast to the EDS result, the XPS analysis indicated a nitrogen concentration of 5.59 wt%. This discrepancy is probably due to the scanning depth variation between the two methods (1-3 μm in EDS vs. 10 nm in XPS) (Igalavithana et al., 2017), where a deeper detection in EDS analysis might reduce the average concentration of nitrogen. In other words, this result might suggest that nitrogen element was doped on the external surface of the biochar, which implied favorable accessibility to the active sites. Deconvolution of the N 1s spectra (**Figure 6.2a**) distinguished three peaks at 398.2 eV, 400.3 eV, and 402.8 eV, which could be ascribed to pyridinic N (bound to two C atoms), pyrrolic N (bound to two C atoms and one H atom), and oxidized N, respectively (Matter et al., 2006; Arrigo et al., 2008). These identified nitrogen species were aligned with those of graphitic carbon nitride materials and nitrogen-doped carbon xerogels (Thomas et al., 2008; Gorgulho et al., 2009), while quaternary N was absent from the N-enriched biochar. Thus, the engineered biochar exhibited abundance of edge-terminating nitrogen species, *i.e.,* pyridinic N (43.6%) and pyrrolic N (37.3%) (**Table 6.1**). In general, pyridinic N can be more favorable to support glucose isomerization compared to pyrrolic N because the lone pair of pyridine is localized and free for donation whereas the pyrrole is completely delocalized over five atoms.

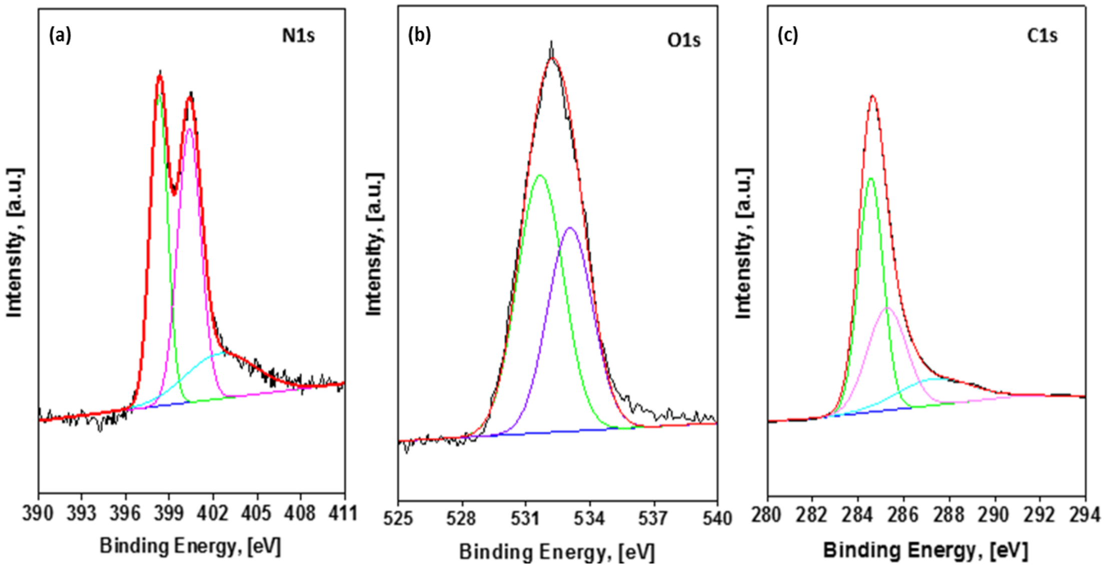

Figure 6.2 High-resolution XPS spectra of N 1s (a); O 1s (b); and C 1s (c) for N-doped biochar catalyst.

The titration results confirmed the biochar catalyst possessed basic sites (0.247 mmol g^{-1}) and free of acidic sites (**Table 6.1**). Given that the high ratio of pyridinic N would display a strong basic character (Faba et al., 2013), the results in this study revealed that N-doping onto biochar was successful for the fabrication of carbon-based base catalyst. In the O 1s spectra (**Figure 6.2b**), the peak at 531.6 eV and 533 eV represented carbonyl oxygen and ether-type oxygen (in esters and anhydrides) (Genovese et al., 2015). Oxygenated functional groups predominantly contributed to the acidity of carbon surface (Rajapaksha et al., 2016). The C 1s spectra exhibited two major peaks at 284.5 eV and 285.3 eV, which were assigned to C-C and C-O bond, respectively. A minor shoulder at 287.4 eV was associated with C=O bond.

The mass decay of the N-enriched biochar up to 1000 ° C heating in Ar gas was approximately 23% (**Figure 6.3**), which was consistent with the XPS analysis, and it was mainly attributed to the loss of heteroatom (*i.e.,* N) and O (16 wt% in total according to XPS results). A small reflection point at 250 °C in the DTG curve could result from the decomposition of insignificant amount of carboxyl-related groups, while rapid degradation rates that occurred from 560 to 740 °C were likely due to the decomposition of oxygen-containing groups such as ketones and lactones, and nitrogen-related species such as lactame- and pyrrole-like compounds, as suggested by a temperature-programmed desorption study equipped with mass spectrometer (Oickle et al., 2010). In addition, the mass decay evolving at the latter stage of >750 °C could be primarily associated with the decomposition of pyridinic N, which is more stable than pyrrolic N (Shi et al., 2016). The thermal degradation analysis was in line with the results of XPS analysis and showed high thermal stability of N-enriched biochar catalyst.

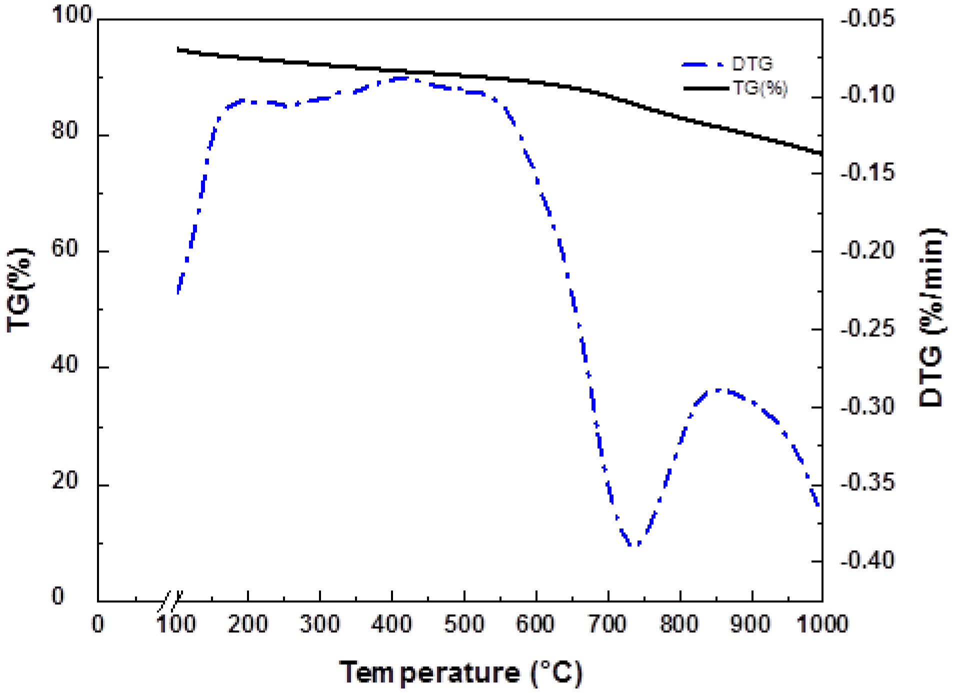

Figure 6.3 Thermogravimetric analysis of N-doped biochar catalyst at a heating rate of 10 °C min^{-1} under Argon gas.

6.2.2 Glucose isomerization catalyzed by N-enriched biochar in water medium

As shown in **Figure 6.4**, a rapid conversion of 11% glucose was achieved in 1 min with a selectivity close to 100% at 120 °C in water medium as a green solvent. The highest fructose yield was achieved in 20 min with a high selectivity of 84%. The N-enriched biochar catalyst demonstrated a catalytic activity for glucose isomerization to fructose that is comparable to homogeneous tertiary amines at similar N concentrations (Carraher et al., 2015), and a conversion higher than heterogeneous tertiary amines on porous materials (Deshpande et al., 2017). Extending the reaction time to 60 min, glucose conversion increased only slightly to 15%, which was still far from the equilibrium of glucose conversion (~ 60%) (Román-Leshkov et al., 2010; Bermejo-Deval et al., 2014; Carraher et al., 2015). Meanwhile, the selectivity to fructose decreased to 79%, which could be due to the formation of soluble intermediate products undetectable by HPLC along with the reaction at this temperature because insoluble humins were negligible over the course of reaction.

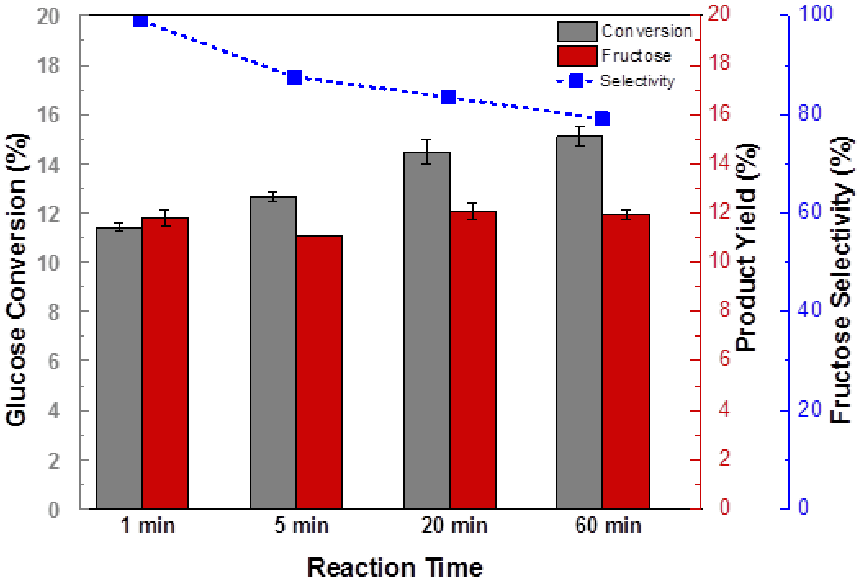

Figure 6.4 Activities of glucose isomerization in water at 120 °C with 1 wt % N-doped biochar catalyst (= 15.4 N mol% related to glucose) in a 5 wt% glucose solution.

Increasing the reaction temperature to 160 °C promoted glucose conversion to 19% in 20 min, while fructose yield merely increased to 13% (**Figure 6.5**). Selectivity to fructose decreased from 85 to 70% along with increasing reaction time, as a result of dehydration of fructose to HMF, which was a reaction favored at moderately high temperature and weakly acidic environment (solution pH was observed to decrease to 4.66 in 5 min) (Yu and Tsang, 2017). The catalytic activity of the N-enriched biochar catalysts for glucose isomerization was confirmed because only a small amount of glucose (~2%) was converted in the absence of the catalysts while HMF was the major product.

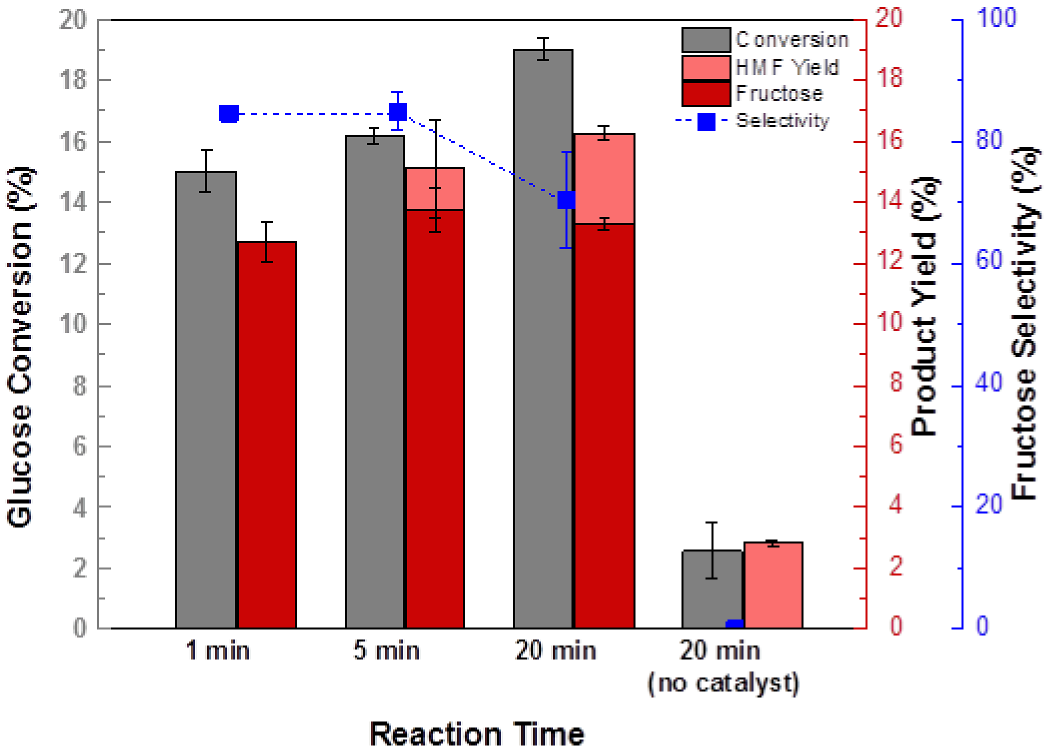

Figure 6.5 Activities of glucose isomerization in water at 160 °C with 1 wt % N-doped biochar catalyst (equals to 15.4 N mol% related to glucose) in a 5 wt% glucose solution.

It has been recognized that solution pH has a crucial effect on glucose isomerization, especially for base catalysis (Carraher et al., 2015). The pH value of the initial reaction solution (in the presence of catalysts) measured at room temperature was 7.24, which ruled out the possibility of catalysis via hydroxide ions in the bulk solution. Instead, this led to the presumption that the catalytic effect of N-enriched biochar may be largely induced from the lone pair of electrons in the nitrogen-terminated edge structures (Alatalo et al., 2016), which could attract hydrogen atoms in the vicinity of water molecules, and thus, increasing the basicity of the catalyst in the local environment. The majority of pyridinic N, as indicated by XPS analysis (**Figure 6.2** and **Table 6.1**), could facilitate the high conversion rate of glucose within a short reaction time due to its strong basicity. In addition, the carbonyl group on carbon materials has been known to impart certain basicity in surface chemistry, where the electron-withdrawing function forms hydrogen bonds with water molecules and thus induces partial negative charge of a hydroxyl group in water molecules.

The N-enriched biochar acting as a base catalyst for glucose isomerization in this study can explain stagnant production yield of fructose along with extending the reaction time (**Figures 6.6&7**), where the catalytic activity was inhibited due to the observed decrease of solution pH value. In this work, part of the pyridinic N species present on the catalyst could be protonated due to the decrease of pH from 7.24 to 6.58 in 20 min at 120 °C, thereby possibly decreasing their catalytic functions as the lone pair electrons on the N atom of pyridinic sites were donated to H^+ ions. It is noted that N-doped catalysts exhibit high sensitivity to acidic media due to the decrease in catalytic activity caused by protonation of pyridinic N to pyridinium cation ($pK_a = 5.7$) (Rauf et al., 2016). Consequently, the nitrogen-terminated edge species of the biochar catalyst may be protonated by the acidic compounds in the solution over an extended reaction time.

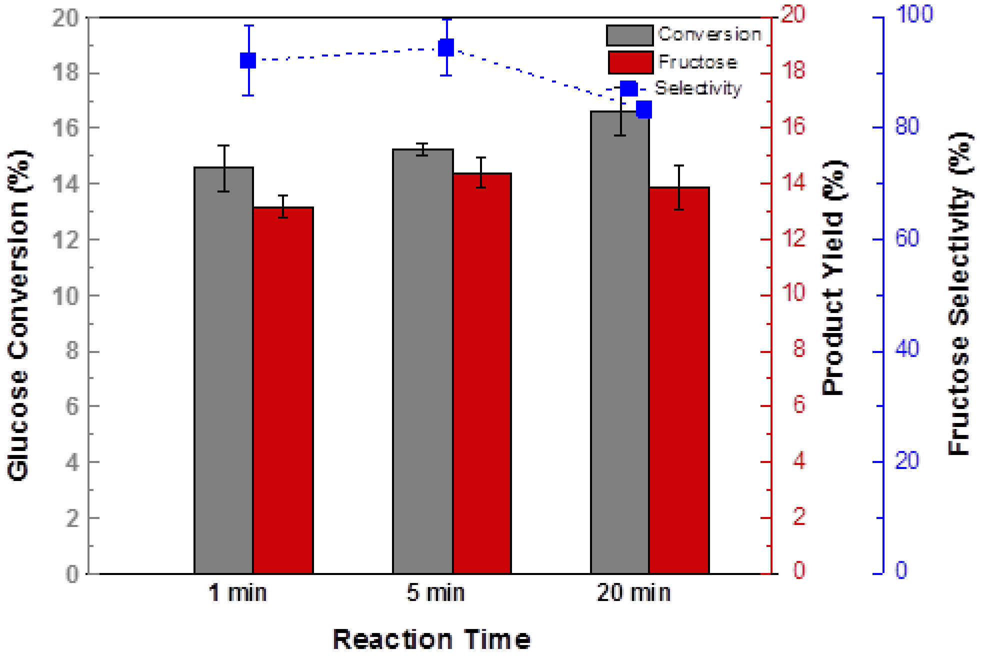

Figure 6.6 Activities of glucose isomerization in acetone/water (1:1 v/v) at 120 °C with 1 wt % N-doped biochar catalyst (equals to 15.4 N mol% related to glucose) in a 5 wt% glucose solution.

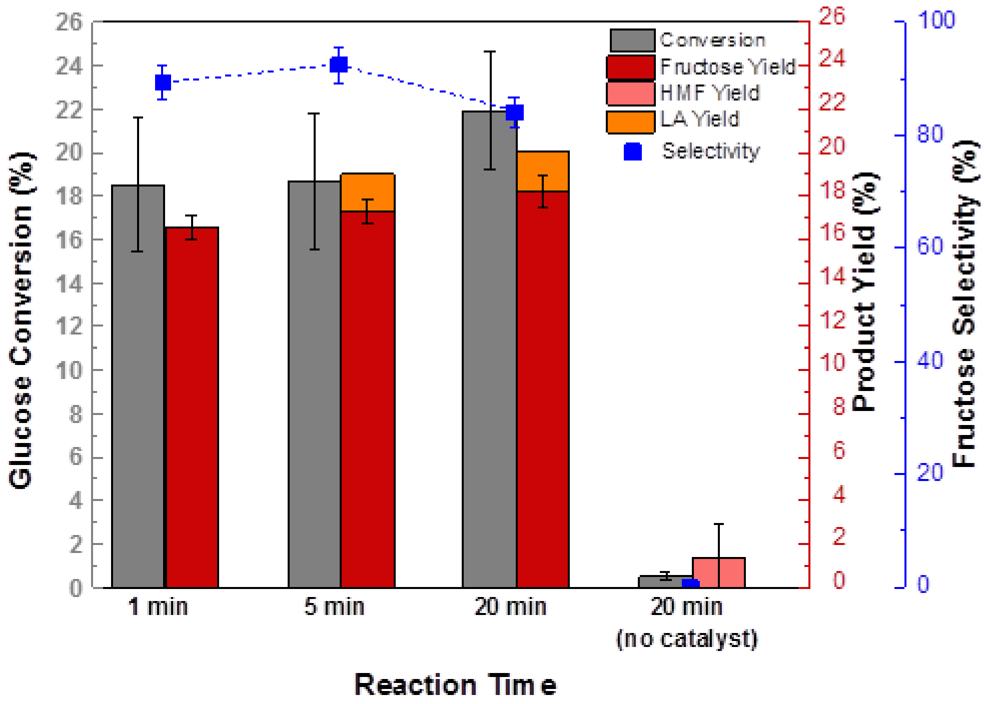

Figure 6.7 Activities of glucose isomerization in acetone/water (1:1 v/v) at 160 °C with 1 wt % N-doped biochar catalyst (equals to 15.4 N mol% related to glucose) in a 5 wt% glucose solution.

6.2.3 Enhanced glucose isomerization activity in acetone/H_2O mixture

The use of acetone as an environmentally-friendly co-solvent increased the glucose conversion rate compared to using water alone (**Figure 6.6**). The fructose yield rapidly attained 14% in 5 min at 120 °C, and the selectivity reached 95%. Similar to the reaction in water, increasing the reaction time to 20 min slightly increased the glucose conversion to 17%. However, the fructose yield did not increase accordingly as a result of decreased fructose selectivity to 83%, although it was still considered high. Increasing the reaction temperature to 160 °C led to 22% of glucose conversion and 18% of fructose yield in 20 min (**Figure 6.7**). Trivial amount of HMF (~ 1%) was found in 5 min, which was subsequently rehydrated into levulinic acid as can be seen in 20 min. The total carbon balance was between 96 and 102% in the presence of acetone, therefore, aldol reactions were supposed to be insignificant in this system. A recent study has shown that the presence of acid sites or nitro groups may be needed to activate aldol condensation (Collier et al., 2015).

On the contrary to water medium, the fructose selectivity in acetone/H_2O mixture was not compromised by high temperature (160 °C) in a short reaction period, which demonstrated an attractive benefit of the mixture system to enhance the glucose conversion while maintaining the high selectivity. Glucose conversion in acetone/H_2O mixture in the absence of N-enriched biochar catalyst was lower than that in aqueous solution (**Figures 6.6&7**). Therefore, the advantage of acetone as a co-solvent was partially attributed to interfacial interaction between the biochar catalyst and solvent, in addition to solution-phase interaction between glucose and solvent. The initial pH value of the reaction mixture was 8.24, however, one should be prudent in pH comparison as organic solvents may have different pH scales. According to a recent study, the addition of acetone may polarize in water and stabilize water hydration clusters via hydrogen bonding, rendering the acetone-water mixture more basic than water or acetone alone (Mellmer et al., 2018).

Apart from the effect of increased basicity in the solvent mixture, acetone as a co-solvent may demonstrate multiple advantages in glucose isomerization. The equilibrium proportion of fructose could increase in an exponential manner with increasing acetone (or ethanol) concentration in the solution, and the tautomer distribution of glucose was also observed with higher proportion of α-pyranose form (Vilonen et al., 2004). It has been revealed that pyranose glucose was the active species partitioning into tin-beta zeolites (Bermejo-Deval et al., 2012), yet the effect of a particular glucose structure for a heterogeneous base catalyst worth more understanding for rational design of superior solid catalyst. With the use of Lewis acid catalysts (Sn^{4+}), glucose isomerization rate could be faster in acetone (and acetonitrile) compared to other polar aprotic solvents such as tetrahydrofuran and dimethyl sulfoxide (Yu et al., 2017c). Due to negligible metal content in the biochar catalyst, Lewis acid site was less likely to contribute to glucose isomerization in this study. However, future computational simulation studies are recommended for elucidating how the mixture of acetone/H_2O enhances glucose isomerization in different isomerization pathways catalyzed by Lewis acid and Brønsted base, respectively.

6.2.4 Recyclability of the N-enriched biochar catalysts

The N-enriched biochar catalyst was microwave-heated in the aforementioned conditions without glucose, and then separated for elemental analysis for comparison with the unreacted catalyst. The results showed that the elemental composition (**Table 6.2**) had little change after microwave heating, indicating that the N-terminated edge species on the biochar catalysts were stable in the aqueous environment and resistant to thermal decomposition and water hydrolysis under the studied conversion conditions. In other words, the N-enriched biochar preserved activities under microwave heat and aqueous environment. However, no fructose was found in the recyclability tests in either water or acetone/water mixture at 120 °C for 1 min. The loss of activity was proposed to result from the neutralization of the basic sites by acidic compounds in the reaction in a recent study (Deshpande et al., 2017). To understand the deactivation mechanism in this study, the spent N-enriched biochar catalyst was rinsed by 0.01 M NaOH for 3 h and washed with deionized water until reaching neutral pH condition, according to a reported regeneration method (Qi et al., 2015). However, the catalytic activity could not be successfully restored in the subsequent recycling tests. The elemental analysis confirmed that the catalyst composition did not change after hydrothermal condition (**Table 6.2**), indicating the active N sites were free from leaching. In view of the high selectivity (>80%) of fructose and minimal formation of insoluble humins during the reactions with fresh catalysts, these results suggest that retention of carbonaceous materials on the catalyst surface may hinder regeneration by using dilute alkaline solution. Future work is required for understanding the significance of nitrogen/amine species on the catalyst and tailoring the synthesis design for higher reusability.

Table 6.2 Elemental analysis of the catalysts

Composition (wt %)	**N**	**C**	**H**	**O**	**Total**
Fresh Catalyst	10.42	77.47	2.39	7.29	97.57
Microwave-heated Catalyst [a]	11.13	74.91	2.08	7.30	95.42

[a] The N-doped biochar catalyst was microwave-heated in acetone/water mixture without substrate at 120 °C for 1 min

6.3 Summary

Waste-derived biochar from spend coffee grounds was doped with melamine as nitrogen source to produce N-enriched biochar catalyst under the optimized pyrolysis conditions. The XPS spectra showed the predominant formation of edge-terminating nitrogen functional groups (*i.e.,* pyridinic N) at a high ratio, which were largely responsible for the observed basicity in the acid-base titration test. The N-enriched biochar showed outstanding catalytic performance for glucose isomerization to fructose with high selectivity, and the reaction activity was comparable to that with homogeneous base. The use of acetone as a co-solvent increased the glucose isomerization rate and 14% of fructose was obtained with a selectivity of 95% at

120 °C in 5 min. The overall results of this study demonstrated that N-enriched biochar could serve as an efficient solid catalyst for glucose isomerization owing to the basicity of the functional groups. Further investigation efforts are deserved to distinguish the important roles of specific nitrogen groups and effects of physicochemical properties of the biochar on its catalytic efficiency, where ^{1}H and ^{13}C NMR can shed light on catalyst reaction/deactivation mechanisms. Tailored synthesis is recommended for advanced biochar catalyst in the future.

Chapter 7 – Roles of Chemical Environment in Glucose Isomerization to Fructose via Brønsted Bases

Abstract

Glucose isomerization to fructose via base catalysis has attracted growing interest in recent years. The work reported here stems from an interest to understand the key parameters governing glucose isomerization in addition to solution basicity, and to explore any catalytic patterns from the same group of catalysts. A wide range of homogeneous and heterogeneous bases were investigated at the same reaction conditions to enable cross comparison. The results showed that glucose conversion was positively correlated with the basicity in the solution, while exceptional cases were observed owing to the specific structure of that catalyst. Interaction between the cations in the catalysts and carbohydrates affected glucose activity in the presence of metal hydroxides, and intra- and intermolecular hydrogen bonding between the catalysts and glucose altered the molecular conformations in the solution. Principal component analysis illustrated that the catalytic patterns were dependent on the catalyst structure and nature. Overall, meglumine showed a superior catalytic performance than the other homogeneous bases with a yield of 35% fructose and approximately 80% selectivity. These results help to identify potentially effective catalyst structure for the development of heterogeneous catalyst.

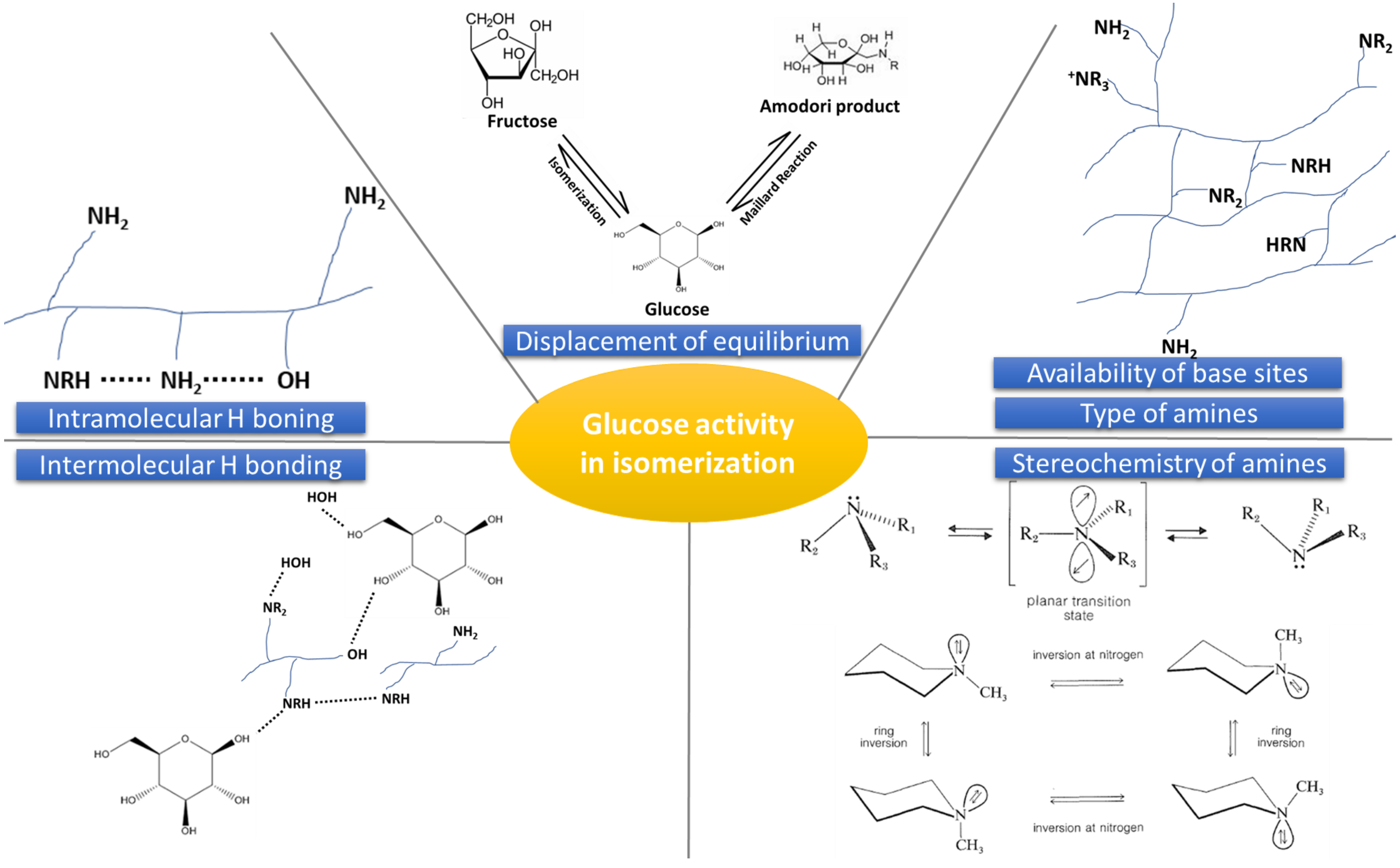

Figure 7.1 Graphical abstract of **Chapter 7.**

7.1 Research questions

Chapter 6 demonstrated the N-doped biochar catalyst is capable of selective glucose isomerization in aqueous and acetone-water mixture with the aid of microwave heating. Recent literature has reported effective fructose production with various base catalysts (**Chapter 2**). The hydroxide ions (OH^-) generated in situ through interaction between amine and water, rather than the amine itself, were the active species for the base catalysis. However, the initial pH in the reaction mixture often varied (or was not reported) among the previous studies, making it difficult to draw clear correlations between the catalyst properties and the catalytic performance.

To enhance engineering application, various heterogeneous bases have been examined. For example, organic bases with different types of nitrogen were introduced to polystyrene resins, (Yang et al., 2015; Yang et al., 2016a). However, inconsistent catalytic activity was observed between corresponding homogeneous and heterogeneous base catalysts, which was attributed to the steric hindrance and porous structure of the solid support, limiting the availability of immobilized amines (Yang et al., 2015). Amino-functionalized silane was incorporated onto mesoporous silica to improve accessibility to the catalytic sites (Deshpande et al., 2017). Although the uniform pores facilitated mass transfer, the catalyst activities were much lower than the homogeneous bases and required much longer hours to reach comparable glucose conversion with homogeneous catalysts. This result was likely associated with immobilization of the amine on the silica support, where the introduced surface silanols can also affect the reaction.

In addition, inorganic bases such as metal oxides (e.g., MgO, CaO, TiO_2, and ZrO_2), magnesium modified zeolites, and naturally occurring minerals (e.g., attapulgite and imogolite) have been examined as heterogeneous bases for glucose isomerization in recent years (Kitajima et al., 2016; Li et al., 2017; Graça et al., 2018; Olson et al., 2018). The tested catalysts rendered certain catalytic activity out of the basic nature, while they suffered from different extents of leaching and deactivation. Side reactions induced from sugar browning and degradation are associated with the production of acidic by-products, which lowered the pH of the reaction mixture and deactivated the catalysts. Rational design with lessons learned from the previous studies is important to devise effective heterogeneous base catalysts. However, cross comparison of previous studies for evaluating the catalyst effectiveness and relating the catalyst structure to glucose isomerization activity is rendered difficult owing to different protocols and incomplete information of operating systems.

Therefore, this study aims to (i) evaluate the catalytic performance of various groups of catalysts including anion exchange resins, cellulose-base heterogeneous bases, organic amines, and alkaline solutions at identical reaction conditions; (ii) reveal the critical parameters for base catalyzed glucose isomerization via correlation analysis; (iii) investigate the catalytic patterns in relation to catalyst structure and nature by principal component analysis (PCA); and (iv) identify potentially promising homogeneous bases for future design of heterogeneous catalysts.

7.2 Results and discussion

7.2.1 Relationships between variables in base catalyzed glucose conversion

Figure 7.2 showed the correlation matrix of reactivity-related variables in glucose isomerization. The histograms in diagonal cells displayed the frequency of the variables, and the red line and red circle in the scatter plot represented the linear fit and 95% confidence ellipse, respectively. In this study, glucose conversion ranged from 0 to 79% and the highest fructose yield was recorded at 38% with 54% glucose conversion. The fructose selectivity exhibited a bell-shaped distribution with the highest frequency between 50 and 70%. The pH value in the initial glucose solution ranged from 8.0 to 11.0, and approximately 70% of the compounds tested resulted in a solution pH higher than 9. After the reaction, the solution pH dropped due to the side reactions such as Millard reactions and caramelization which produced acidic byproducts and led to browning of sugar solutions (Simpson et al., 2012). The extent of decrease of pH value in the solution could be up to 3, and it was between 1 and 2 in the majority of tests.

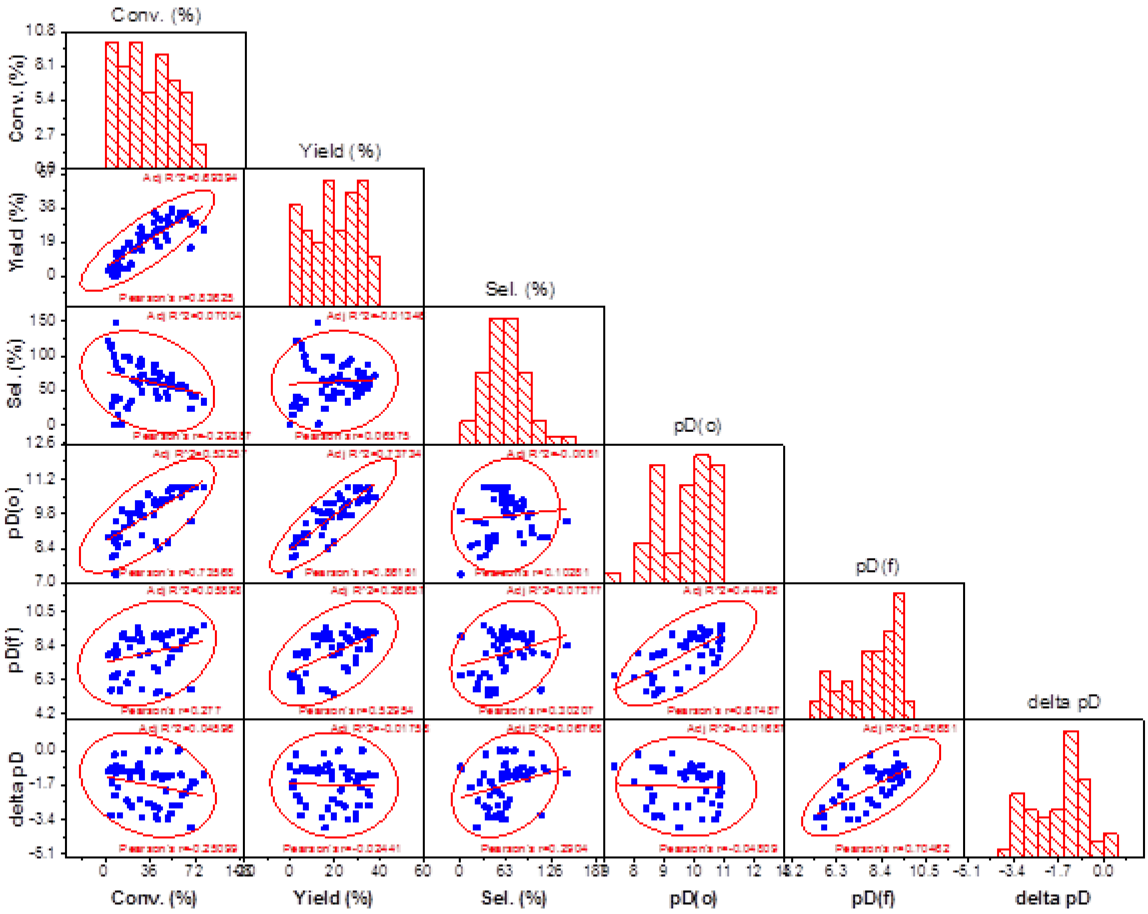

Figure 7.2 Correlation matrix of variables in glucose isomerization.

It can be seen from the correlation matrices that glucose conversion was strongly and positively correlated with fructose yield (r = 0.836) and initial pH value in the solution (pD_o) (r = 0.736), and the pD_o was also highly correlated with fructose yield (r = 0.862). These results reinforced the findings in our previous study that the hydroxide anion was the main drive that catalyzed glucose isomerization to fructose (Carraher et al., 2015). It was found that fructose selectivity was not significantly correlated with any variables, while it was generally true that the selectivity decreased with increasing glucose conversion. However, the selectivity was widely distributed at the two sides of the linear fitting when glucose conversion was less than 20%. This result implied that some catalysts may excel the others at the lower range of conversion, when the pD_o being close to 10 (for homogeneous catalysts) as shown in the conversion-pD_o matrix in **Figure 7.2**. Heterogeneous catalysts will be discussed in detail in the next section.

Since the pKa value of fructose was similar to that of glucose (~12), the pH value in the final solution (pD_f) could be an indication of the acidic compounds resulting from the side reactions. It was found that pD_f was poorly correlated with most variables ($r < 0.53$), except with the pD_o ($r = 0.675$) and the change of pH value before and after the reaction (ΔpD) ($r = 0.705$). As a matter of fact, pD_f was the only variable correlated with delta pD, which was fairly sensible because the solution pH decreased after the reaction and a high pD_f suggested a small pH drop during the reaction. The pD_f was sensitive to the pD_o. For instance, in a narrow pD_o range from 10.7 to 10.9, the pD_f varied from 7.3 to 9.7. Likewise, the pD_f ranged from 5.6 to 7.8 when the pD_o was between 8.4 and 8.6. It was more straightforward from the pD_o-delta pD matrix that regardless of the pD_o value, the pD_f value can decrease by 0.5 to 3. However, it should be highlighted that the large pD drop mostly happened in anion-exchange resins with quaternary amines. In addition to acidic byproducts, amine hydrolysis may also contribute to acidic environment in the final solution. It has been reported that Millard reactions and thermal-induced degradation of sugars were accelerated in basic condition (Simpson et al., 2012), while initial pH had little impact on the scale of pH drop. These results supported the hypothesis that some catalysts may inhibit or favor the side reactions (as indicated by pD_f value) regardless of the conversion extent as shown in the conversion versus pD_f /delta pD matrix. In other words, this analysis suggest that certain types of catalyst structures may outperform the others in glucose isomerization because of suppressed side reactions, which advocates further investigation or synthesis of more selective catalysts.

7.2.2 Glucose reaction sensitivity to catalyst structures

As informed by **Figure 7.2**, glucose conversion demonstrated a positive correlation with the pD_o in the solution. However, **Figure 7.3** illustrated that some catalysts displayed a large difference in conversion over a small pH range (Zone I in **Figure 7.3**), while the reaction activity could also vary little over a large pH range (Zone II in **Figure 7.3**). The representative zones were selected at moderate glucose conversion and pH values (which were mainly homogeneous catalysts) rather than at the lower ends in order to acquire higher precision in the analysis.

Table 7.1 shows the selected catalysts and their performance in Zone I. Under similar pD_o environment, the glucose conversion in the presence of L-arginine was 20% less than that in guanidine carbonate salt. It was also reflected from the pD_f that more acidic byproducts were generated in the presence of guanidine carbonate salt, which resulted in slightly lower fructose selectivity than that in L-arginine. Both guanidine carbonate salt and L-arginine possessed a guanidinium group, while it has been argued that the carboxyl group in L-arginine may act as a pH buffer resulting in lower pK_a than that in guanidine carbonate salt (12.48 vs. 13.6). This probably accounted for the lower glucose conversion in L-arginine, although the initial basicity in the solution was not given in the previous study (Yang et al., 2016b).

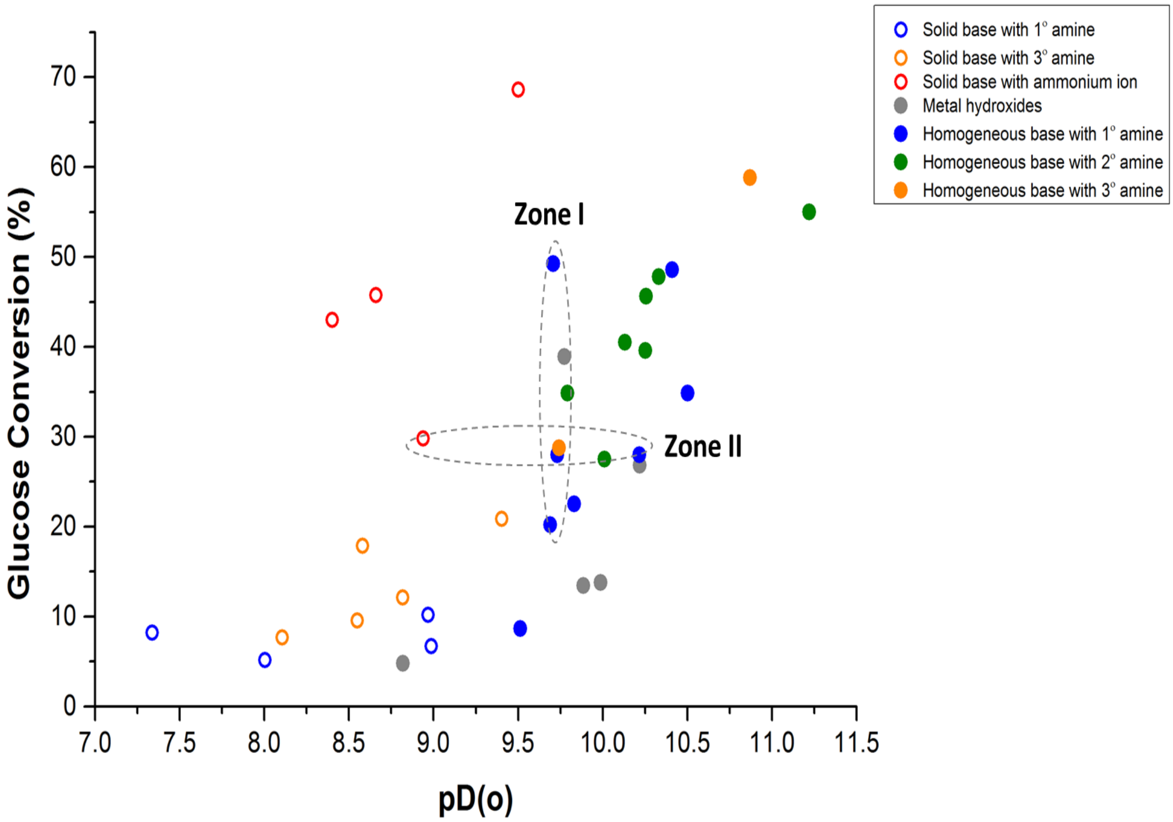

Figure 2. Glucose conversion as a function of pH in the solution (Zone I represented the catalysts giving similar basicity in the solution but resulting different conversion; Zone II represented varying catalyst basicity resulting in similar glucose conversion).

Table 7.1 Corresponding catalysts and catalytic performance in Zone I.

Catalyst	Basic Groups	pK_a	pD_o	pD_f	X (%)	S (%)
Guanidine carbonate salt	1° & 2° amines	13.6 [a]	9.71	7.02	49.3	59.9
NaOH	OH^-	13.46	9.77	7.04	38.9	62.8
Piperazine	2° amines	9.73 [b]	9.79	8.66	34.9	85.9
1,4-dimethylpiperazine	3° amines	8.38 [b]	9.74	8.70	28.8	94.3
L-arginine	1° amines	12.48 [a]	9.73	8.57	28.8	65.0
Branched PEI	1°, 2° & 3° amines	9.4-9.64 [c]	9.69	8.32	20.2	93.9

[a] Yang et al., 2016
[b] Khalili et al., 2009
[c] Yang and Runge, 2016

The substitution of two hydrogen of piperazine by two methyl groups resulted in lower pK_a in 1,4-dimethylpiperazine than that in piperazine (**Table 7.1**), due to the solvent effect in water aside from the polarization effect from alkyl group. In piperazine, the secondary ammonium ions were stabilized by hydrogen bonding to water more than those in 1,4-dimethylpiperazine. In other words, hydrogen bonding could increase the standard free-energy difference ΔG°_a between ammonium ions and its conjugate base amine, and therefore increased the amine basicity ($\Delta G^\circ_a = 2.3RT$ (pK_a)). Glucose conversion was in general agreement with the pK_a in the case of same pD$_o$ and similar catalyst structures – the stronger base of the catalyst, the higher the conversion. Branched PEI was less favorable for glucose conversion compared to the other catalysts in Zone I (**Table 7.1**). This could be attributed to the fact that the basic groups were less available for protonation in the polymeric structure of PEI, and there were less hydroxide ions generated *in situ* for glucose molecules.

Moreover, **Table 7.2** indicates that glucose conversion (X) via different groups of catalysts could reach the same level within a certain range of pH. The anion exchange resin (IRA900RF) showed the lowest pH value (8.94) in the initial glucose solution, yet the glucose conversion rate (29.8%) was as high as by the other catalysts. Glucose adsorption onto the macroporous resin may contribute to the observed higher conversion rate (Yang et al., 2015). Meanwhile, fructose selectivity was noticeably low ($S < 50\%$) using resin catalysts, which could also be related to its porous structure. Fructose generated from glucose isomerization may be re-adsorbed onto the pores, where more basic functional groups might be located, and the localized basicity could result in secondary reactions that consume the fructose (Pitochelli et al., 1975; Qi et al., 2008). It should be noted that the anion exchange resin functioned as immobilized base, and hence the pH in the bulk solution did not represent its true basicity, while the resin dosage was normalized to total nitrogen content.

Table 7.2 Corresponding catalysts and catalytic performance in Zone II.

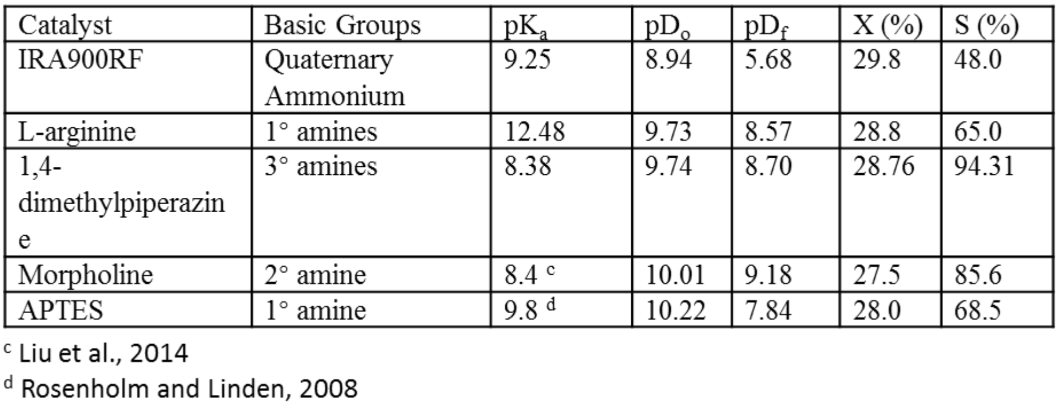

Catalyst	Basic Groups	pK_a	pD_o	pD_f	X (%)	S (%)
IRA900RF	Quaternary Ammonium	9.25	8.94	5.68	29.8	48.0
L-arginine	1° amines	12.48	9.73	8.57	28.8	65.0
1,4-dimethylpiperazine	3° amines	8.38	9.74	8.70	28.76	94.31
Morpholine	2° amine	8.4 [c]	10.01	9.18	27.5	85.6
APTES	1° amine	9.8 [d]	10.22	7.84	28.0	68.5

[c] Liu et al., 2014

[d] Rosenholm and Linden, 2008

As shown in **Figure 7.3** and **Table 7.2**, glucose conversion rate by morpholine and APTES fell behind the general trend in spite of their comparatively high initial solution pH values and pK_a values (Rosenholm and Linden, 2008). Amino-functionalized silane (APTES) can undergo hydrolysis and self-condensation under aqueous and heating environment (> 40 °C), which can form a polymeric structure and make the active sites less accessible (Castellano et al., 2004; Liu et al., 2013). A recent study also reported that amine-silanol or silanol-glucose interactions reduced the catalytic activity of glucose isomerization (Deshpande et al., 2017), while detailed explanation may need molecular level computational modeling in the future.

Although morpholine possessed secondary amine in the heterocyclic ring, fructose selectivity was not evidently affected by Maillard reactions, which is a typical non-enzymatic browning reaction between sugars and amino acids (*i.e.,* primary and secondary amines). Structures of amino acids have been demonstrated to play an important role on the capability of inducing Maillard reactions (Spark, 1969;

Ajandouz and Puigserver, 1999), indicating the structure of amines will also affect the extent of the Maillard reaction. However, it has also been reported that some amino acids present protective effect to lessen thermally induced glucose degradation (Ajandouz and Puigserver, 1999), which may be due to a displacement of the equilibrium in the formation of glycosylamine (*i.e.,* first step in the Maillard reaction) (Ge and Lee, 1997). This might be a reason for the lower glucose conversion by morpholine in **Table 7.2** in spite of its higher pH than other catalysts.

The reactions with divalent hydroxides were maintained in homogeneous conditions by syringe filtration in order to rule out mass transfer limitation. It was interesting that in spite of the higher basicity in $Mg(OH)_2$, $Ca(OH)_2$, and $Ba(OH)_2$ solution, glucose conversion was not necessarily higher than that in NaOH (**Table 7.3**). This indicated the impact of divalent metal ions on the base catalyzed glucose isomerization in addition to the hydroxide ions (Brønsted base). The effects of divalent metal ions could be attributed to their complexation with sugars or interference with sugar degradation (Angyal, 1989; Ajandouz and Puigserver, 1999). It has been known that $Ca(OH)_2$ favors retro-aldolization by-products via cation-ketose complexation (de Bruijn et al., 1986; Yang and Montgomery, 1996). Recent quantum mechanics studies showed that divalent ions bind more strongly and preferentially to α-glucose than monovalent ions (Mayes et al., 2014). The glucose anomeric distributions were identical between different alkaline solutions in this study (**Figure E1**), corroborating that the alkaline environment played a more dominant role than cations in anomeric distribution (Tajmir-Riahi, 1988). Nevertheless, varying binding strength between alkali/alkaline earth metals with sugars in various conformations probably determines the stability of sugars (Mayes et al., 2014), which may in turn influence the ring-opening and ring-closing rate (Goux, 1985). The above factors could account for the observed glucose reactivity that was not completely dependent on the pH in alkaline solutions.

Table 7.3 Glucose isomerization by metal hydroxides in homogeneous form.

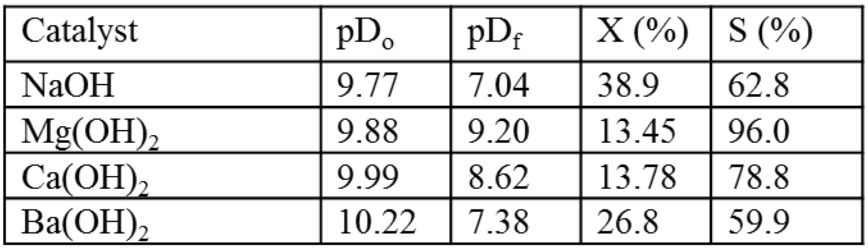

Catalyst	pD_o	pD_f	X (%)	S (%)
NaOH	9.77	7.04	38.9	62.8
$Mg(OH)_2$	9.88	9.20	13.45	96.0
$Ca(OH)_2$	9.99	8.62	13.78	78.8
$Ba(OH)_2$	10.22	7.38	26.8	59.9

Detailed analysis with the aid of computational modeling is needed to confirm the mechanism of each catalyst, while this study provided extensive experimental evidence that glucose isomerization can be mediated by the catalyst structures and microenvironment in different aspects apart from the Brønsted basicity in the solution.

7.2.3 Insights of base catalyst nature in glucose isomerization

The signal patterns obtained from normalized ^{1}H NMR spectra were analyzed by principal component analysis (PCA). The dataset used in PCA also included preliminary tests with various amounts of N mol% catalysts (2-75% relative to glucose) and recycled/regenerated solid catalysts to evaluate overall catalytic profiles of each catalyst. **Figure 7.4** illustrates that the patterns for heterogeneous catalysts and homogeneous catalysts were clearly different from each other, strongly suggesting the influence of the solid structures on the catalytic performance. The deviations displayed by the heterogeneous catalysts included: (1) localized basicity generated in the vicinity of nitrogen functional groups rather than in the bulk solution;

(2) polymeric structure, if any, hindered the accessibility of *in situ* generated OH^- for glucose isomerization; and (3) porous characteristics promoted sugar adsorption and/or secondary reactions resulting in low selectivity in general. Meanwhile, the solid bases with quaternary amines (anion exchange resins) clustered more in the profile than the other heterogeneous catalysts (**Figure 7.4**). This was possibly because the resins with quaternary amines contained exchangeable sites, where the hydroxide ions could detach from the resins via anion exchange. This would make the reaction more analogous to homogeneous condition. Hence, they exhibited higher conversion rates than the other resins with tertiary amines, which were known as weak base resins.

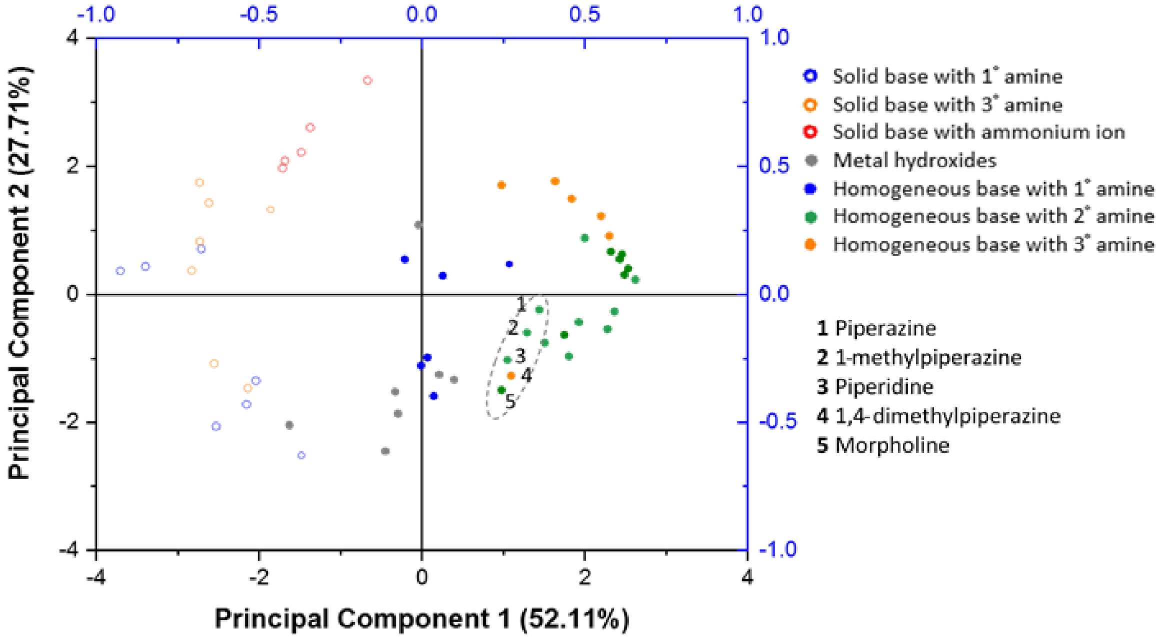

Figure 7.4 Principal component analysis of glucose isomerization via various catalysts (including experiments with various N amount).

The patterns of homogeneous catalysts with secondary amines and tertiary amines also formed certain level of clusters, respectively, implying that the catalytic activity was highly related to the characteristics of the type of catalysts (**Figure 7.4**). One of the homogeneous tertiary amines (no. 4 in **Figure 7.4**) fell into the territory of homogeneous secondary amines. The exceptional point represented 1,4-dimethylpiperazine, which was a heterocyclic amine. Interestingly, the PCA plots around 1,4-dimethylpiperazine were also heterocyclic amines. The acyclic amine has a pyramidal configuration at nitrogen that allows free inversion, of which the rate is markedly slower in heterocyclic amine. This inferred that the stereochemistry of amines governs glucose isomerization reaction in some way. In contrast, the patterns resulting from metal hydroxides were dispersed, which was consistent with previous analysis that each type of cations with the hydroxides interacted differently with glucose and its products. Therefore, different cations contributed to the overall reactivity and resulted in higher deviations in the PCA analysis.

As these results indicated that the catalytic results were affected by the nature and structure of the base catalysts, they can shed light on identifying the promising candidates from homogeneous catalysts for the rational design of heterogeneous catalysts. The desirable catalysts should attain satisfactory fructose yield, while the selectivity should not be much compromised in order to facilitate the downstream separation process. **Figure 7.5** illustrates that meglumine stood out from the other catalysts at an approximate yield of 35% and selectivity of 80%. In general, the fructose selectivity decreased with increasing solution pH value when comparing at similar fructose yield, which were in line with previous analysis. Meglumine is an amino sugar, which can be derived from glucose or sorbitol. The apparent activation energy of meglumine catalyzed glucose isomerization was 74 kJ mol^{-1} (**Figure E2&3**), which was close to that of triethylamine (61 kJ mol^{-1}) (Carraher et al., 2015), suggesting that the reaction mechanism of meglumine was likely to be similar to that of triethylamine.

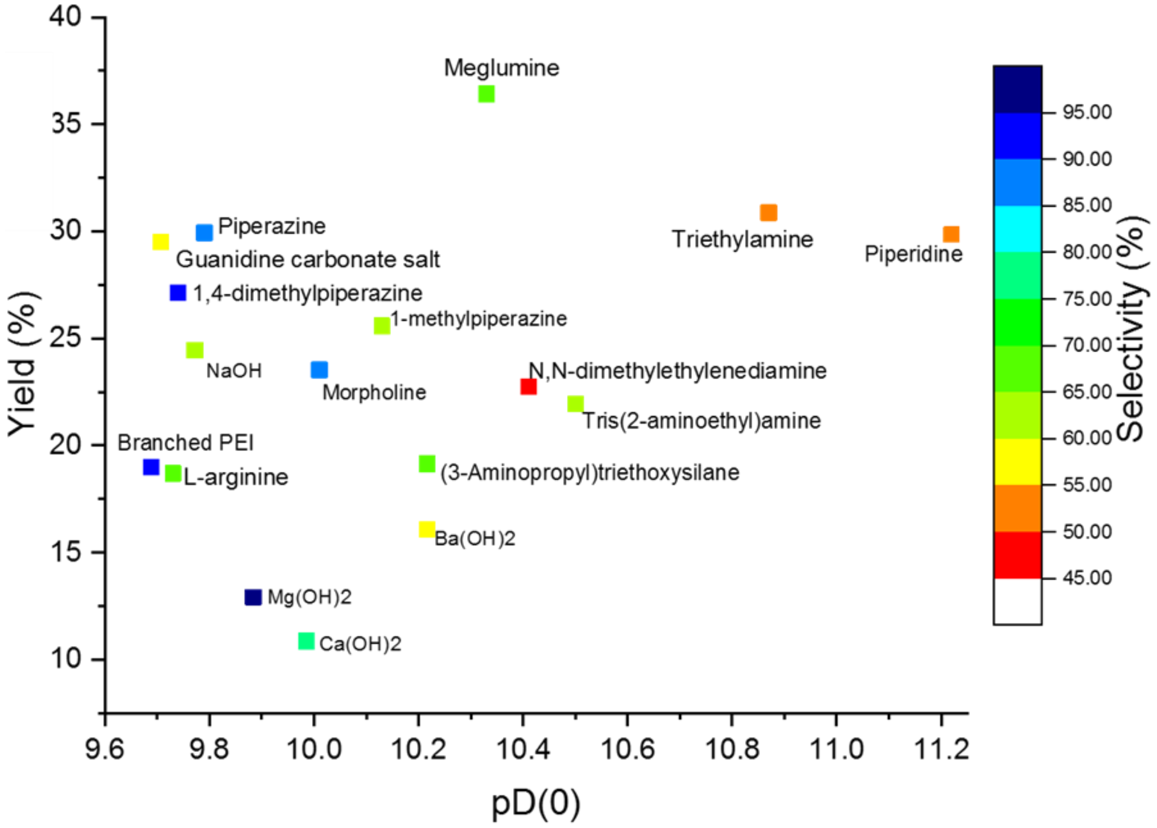

Figure 7.5 Fructose yield and selectivity as a function of pH in glucose isomerization (12 N mol% homogeneous catalysts relative to glucose at 100°C in 30 min).

Although it is unsure for now if the structure similarity between the catalyst and glucose is beneficial to the high selectivity or high yield of fructose, meglumine has been known to be adopted as an excipient to enhance substrate solubility and stability in pharmaceuticals (Bharate et al., 2010; Guo et al., 2013). The improvement of solubility may facilitate glucose conversion owing to a shift in glucose-fructose equilibrium. It was hypothesized that the intermolecular hydrogen bond networks between meglumine and sugars may stabilize the intermediates or enhance glucose adsorption to the active site (El Khadem et al., 1989; Yang et al., 2015). It was also hypothesized that the intramolecular hydrogen bond networks could alter the structure of surrounding water molecules, thus influencing the water molecular conformation around the sugars (Çarçabal et al., 2005; Dashnau et al., 2005). The mechanistic details should be further confirmed by computational modeling in future studies, while tailored synthesis of solid catalysts rendering similar structure with meglumine is also worth investigation

7.3 Summary

This study investigated a wide range of homogeneous and heterogeneous Brønsted bases for glucose isomerization to fructose at the same reaction conditions. The catalytic results reinforced the previous studies that the hydroxide ions were the active species to catalyze glucose conversion, where the conversion rate was positively correlated with the basicity in the solution. Due to the less available and accessible bases in the polymeric structures of heterogeneous catalysts, glucose conversion was lower than those of homogeneous catalysts. The porous structures might provide localized structures that induce secondary reactions and impair fructose selectivity. In addition to hydroxide ions, this study illustrated the metal cations also exhibit significant influence on glucose reactivities. The PCA results underlined that the nature and the structure of the catalysts had crucial impact on the overall catalytic profile, where the heterocyclic amines formed a cluster in the pattern. This result may indicate stereochemistry of amines may affect the interaction with glucose.

Meglumine outperformed the other homogeneous catalysts in view of its high fructose yield and selectivity at the same time, which may be related to its abundant hydroxyl groups in the structure. This study illustrated the effects of catalyst structure and characteristics on glucose isomerization in different aspects, and provided extensive experimental evidence for future computational study to reveal the detailed mechanisms. The new knowledge may also benefit ration design of the base catalyst for glucose isomerization.

Chapter 8 - Conclusions and Recommendations

8.1 Conclusions

This thesis investigates valorization of polysaccharide food waste such as vegetable waste and bread waste, representing cellulosic and starchy waste, respectively. In view of the knowledge gaps identified by the latest findings, this project highlights the following intellectual merits: (a) establish efficient catalytic reaction system for cellulosic and starchy waste conversion; (b) elucidate roles of catalysts (both homogenous and heterogeneous), temperatures, and solvents in the conversion; (c) identify the rate-limiting step in the valorization (*i.e.*, glucose isomerization) and synthesize cost-effective biochar catalyst for the production of fructose, the key intermediate of platform chemicals; and (d) articulate roles of catalyst nature and chemical environment on glucose isomerization.

From the environmental perspectives, adoption of new and appealing technology will promote waste recycling and reduce carbon footprint via diversion of organic waste from landfill disposal and production of petrochemical surrogates to combat global warming. Moreover, in terms of social aspects, development of a novel Hong Kong-based technique will facilitate knowledge transfer and incubate technology innovation to nourish the new establishment of local recycling industry. Demonstrated environmental and economic benefits of the high-value valorization technology will showcase international best practice in food waste recycling compared to traditional treatments. The waste valorization technology will boost circular bio-economy within the community to realize sustainable development in the long run. The key findings of this thesis are summarized below.

- **Chapter 4:** Valorization of vegetable waste to LA is highly efficient at moderate temperature (17 C mol% at 150 °C in 5 min) in aqueous environment owing to the strong Brønsted acidity of the heterogeneous catalyst (Amberlyst 36) and fast kinetics of microwave heating. In the DMSO/water media, the maximum yields of total product are higher than those in aqueous solution, and the major product is HMF.

- **Chapter 5:** Two types of paper towels demonstrate facile valorization into LA as lignocellulosic waste. The production of LA is about 30 C mol% over Amberlyst 36 at 150 ºC in 20 min. The use of dilute sulphuric acid at 150 ºC produces LA gradually to more than 40 C mol% in 60 min. In addition to formation of insoluble byproducts, swelling structure of fibres is also revealed under dilute-acid-mediated catalysis. Preliminary cost analysis suggested that heterogeneous catalyst accounted for significant portion in the expenditure, and microwave heating was more economically favourable for short duration.

- **Chapter 6:** Bread waste is converted to glucose with high selectivity (~80%) and high yield (~70%). However, production of HMF and LA is not as satisfying as that from vegetable waste by Brønsted acid catalysts regardless of temperature (120 - 150 ºC) and solvent environment (aqueous, DMSO or DMSO/water mixture) tested in the study. Glucose isomerization to fructose has been identified as the rate-limiting step in starchy food waste valorization. Nitrogen-doped biochar is adopted as the cost-effective solid base catalyst for glucose isomerization. The conversion of glucose was fast (12%) and selective to fructose

(84%) in 20 min at a moderate temperature (120 ºC). Fructose selectivity maintained high (over 80%) even the reaction temperature was increased to 160 ºC. Acetone demonstrated multiple advantages as a co-solvent in glucose isomerization. For example, it increased basicity and affected glucose tautomer distributions in the solvent mixture which may potentially increase active species for glucose isomerization.

- **Chapter 7:** Local chemical environment of the Brønsted base catalysts renders different effects on glucose isomerization. Intramolecular bonding of the catalyst or intermolecular bonding between the catalyst and water/glucose may alter glucose stability and reactivity. The presence of catalyst may also induce displacement of equilibrium between glucose isomerization to fructose and side reactions such as Maillard reaction. Stereochemistry of amines may be characteristic to be concerned in the reaction, where heterocyclic amines show cluster in the PCA result.

8.2 Recommendations and future work

Cellulosic food waste has demonstrated facile valorization to HMF or LA in the established reaction system. The production of HMF or LA is fast in DMSO/water or aqueous media, respectively, while dissolution of cellulose limits hydrolysis and the subsequent process that hinders higher yield of products. Therefore, chemical and mechanical pretreatment of vegetable waste can be applied in the future to further enhance product yield and value recovery. Understanding the structure and morphology change of cellulose subjected to various pretreatment process may inform scientific selection or combination of pretreatment methods for the following catalytic conversion.

In addition to value-added soluble products, acid-catalyzed conversion also generates significant amount of insoluble humins during dehydration of sugars. These solids are inseparable from the substrate and therefore are poorly characterized. Nevertheless, humin-based byproducts consist of carbon-rich agglomerate particles, which can be valorized by thermal and catalytic gasification to H_2 gas or bulk chemicals. Valorization of the byproducts can improve the economic viability of the proposed food waste conversion.

Starchy food waste valorization exhibits efficient and selective conversion to glucose (>70% glucose yield at 120 ºC in 60 min), while further conversion to HMF or LA is hindered by the rate-limiting step of glucose conversion to fructose. In view of humin formation in acid-catalyzed conversion, base-catalyzed glucose isomerization is adopted to enhance carbon efficiency. Nitrogen-doped biochar catalyst derived from spent coffee ground demonstrates catalytic capability of glucose isomerization and use of acetone as co-solvent enhances glucose activity. This study is a proof of concept of glucose isomerization via a cost-economic nitrogen base catalyst. However, base catalysts are usually deactivated by the acidic byproducts in the solution, which requires regeneration with alkaline solution. The exact reaction and deactivation reaction will be further studied with the aid of solid and solution NMR. Kinetic modeling of glucose isomerization and the competing side reactions will shed light on the design of a flow bed reactor which minimizes acidic species accumulation in the reaction system.

Roles of catalyst nature and chemical environment are examined in order to understand the key parameters governing glucose isomerization in base catalysis. The current study identifies meglumine as a superior homogeneous base catalyst with a yield of 35% fructose and approximately 80% selectivity. Efforts will be devoted to understanding how the structure and chemistry of meglumine favors glucose isomerization than the other homogeneous catalysts. Solid catalysts of immobilized meglumine or sharing structure similarity with meglumine will also be synthesized to examine activity for glucose isomerization.

In the future work, the one-step conversion for cellulosic waste or two-step conversion for starchy waste (*i.e.*, hydrolysis of starch to glucose, and isomerization of glucose to fructose) should be validated in a pilot-scale study. From the environmental perspectives, holistic life-cycle assessment should be conducted to evaluate the proposed technology for food waste valorization.

Appendix A

Synthesis of heterogeneous Brønsted base catalysts for glucose isomerization

Method 1: synthesis of mesoporous carbon nitride (mpg-C_3N_4)

Ammonium chloride and melamine was homogeneously mixed by using mortar and pestle at a mass ratio of 1:1. The mixture was then transferred to an alumina crucible boat with a lid, and heated to 550, 600 or 650°C for 2 h in air at a ramping rate of 2°C per min denoted as pristine mpg-C_3N_4 (Iqbal et al., 2017). One gram of the pristine mpg-C_3N_4 was then grounded and stirred in 10 mL of various concentrations of sodium hydroxide solution for overnight (Su et al., 2012). The solid was recovered by vacuum filtration, washed until pH steady, and then dried at 80°C oven. The modified mpg-C_3N_4 was stored in the desiccator for the use in glucose isomerization.

Method 2: synthesis of organic amine modified mpg-C_3N_4

2-chloro-N,N-dimethylethylamine hydrochloride (10 mmol), sodium bicarbonate (10 mmol) and mpg-C_3N_4 (~3 mmol NH) was successively added into a round-bottomed flask with 50 mL dimethylformamide. The mixture was reacted at 80°C for 48 h, and then collected by filtration, rinsing with deionized water and oven-dried (Yang et al., 2015).

Method 3: synthesis of organosilane modified cellulose (N-cellulose)

(3-aminoproply)triethoxysilane and (N,N-diethyl-3-aminopropyl)trimethoxysilane was first hydrolysed in water at room temperature for 1 h, respectively. A certain amount of microcrystalline cellulose was added to the hydrolyzed mixture under stirring for another 30 min. The mixture was transferred to a hot plate and heated at 110°C for a time period varying from 30 min to 48 h (Mekki Abdelmouleh, 2002; Deshpande et al., 2017). The resultant solids were denoted as N-cellulose, which was recovered by centrifugation, rinsing with deionized water and oven-dried.

Appendix B

Supplementary Experiments

In order to examine whether the catalysts were permanently deactivated due to leaching of sulphonic group or pore blockage at 120°C in 20 min. We prepared six samples that underwent the catalytic reactions at 120°C in 20 min in aqueous solution. For two of the samples (Sample A, Sample B), the catalysts and the reactants were separated by centrifugation, and the catalysts were recycled and washed overnight by using a H_2O_2 aqueous solution (28.5 wt%) at room temperature. It has been showed that the catalytic activity of the catalysts could be recovered by this method if the deactivation is due to coke deposition (Alonso et al., 2013). For the other two of the samples (Sample C, Sample D), the catalysts and the reactants were separated by centrifugation, and the used catalysts were replaced by the fresh catalysts. The last two samples (Sample E, Sample F) the catalysts were separated and reused. Samples were stored in -20°C fridge when the conversion was not performed. After the treatment, all the samples underwent another 20 min microwave heating at 120°C in aqueous solution again. The HPLC results are as follows.

Sample	Disaccharide	Glucose	Fructose	Levoglucosan	Formic acid	LA	HMF	Furfural
	Unit: mg mL^{-1}; reaction condition: 120°C, water							
Blank*	0.00	2.70	0.82	0.09	0.77	1.86	0.27	0.29
A	0.03	3.58	1.29	0.07	0.56	1.68	0.53	0.16
B	0.12	3.62	1.55	0.07	0.53	1.64	0.52	0.14
C	0.10	3.81	1.37	0.06	0.57	1.70	0.55	0.55
D	0.10	3.61	1.32	0.06	0.54	1.59	0.55	0.14
E	0.07	3.25	1.07	0.09	0.71	1.70	0.33	0.29
F	0.07	3.27	1.09	0.07	0.70	1.74	0.33	0.26

* Blank represented the sample determined after a reaction of 20 min at 120°C in water by HPLC.

Sample	Disaccharide	Glucose	Fructose	Levoglucosan	Formic acid	LA	HMF	Furfural
	Unit: mg mL-1; reaction condition: 150°C, water							
Blank*	0.00	0.13	0.27	0.09	0.36	2.84	0.00	0.00
A	0.00	0.14	0.30	0.07	0.83	3.08	0.00	0.00
B	0.00	0.10	0.29	0.07	0.85	3.03	0.00	0.00

C	0.00	0.10	0.33	0.07	0.87	3.06	0.00	0.00
D	0.00	0.11	0.31	0.08	0.84	3.00	0.00	0.00
E	0.00	0.12	0.32	0.08	0.85	3.01	0.00	0.00
F	0.00	0.10	0.30	0.08	0.81	3.05	0.00	0.00

* Blank represented the sample determined after a reaction of 20 min at 150 °C in water by HPLC.

Effect of water ionization

Conversion of glucose or fructose in the absence of Amberlyst 36 in water

Medium	Substrate	Temperature (°C)	Time (min)	HMF (mg mL^{-1})	LA (mg mL^{-1})
Water	Glucose	Room temperature	0	0	0
		120	120	0.10	0
		135	120	0.10	0
		150	120	0.12	0
	Fructose	Room temperature	0	0	0
		120	120	0.13	0
		135	120	0.10	0
		150	120	0.13	0

The initial concentration of the substrate is 50 mg mL^{-1}.

Stability of single compound in DMSO-water at 150°C for 2 h

Initial concentrations of the substrate were spiked to the solvent based on the concentration measured after 120-min reaction in the DMSO-water mixture at 150°C.

Substrate	Initial conc. (mg mL^{-1})	Final conc. (mg mL^{-1})
Glucose	0.17	0.17
Fructose	0.30	0.30
Levoglucosan	0.23	0.24
LA	1.53	1.55
HMF	0.20	0.00
Furfural	0.28	0.28

Table B1. Characteristics of Amberlyst catalysts.

Catalysts	Cation exchange capacity[a] (mmol g^{-1})	Surface area[b] (m^2 g^{-1})	Pore volume[c] (cm^3 g^{-1})	Average pore size (nm)
Amberlyst 15	4.7	37.3	0.203	24.0
Amberlyst 36	5.4	10.4	0.060	27.6

[a] Manufacturer data
[b] BET adsorption isotherm using N_2
[c] Total volume of pores with diameters 1.7-300 nm (BJH)
[*] Adapted from Siril et al. (2008)

Table B2. Crystallinity index of reacted solid residues.

[*] Crystallinity Index, which was calculated from XRD patterns (Luterbacher et al., 2014)

Medium	**Reaction Temperature (°C)**	**Reaction Time (min)**	***CrI* (%)** [*]
H_2O	120	5	60
		60	73
		120	69
	135	5	77
		60	23
		120	38
	150	5	17
		60	9
		120	11
DMSO/Water	120	5	74
		60	88
		120	71
	135	5	69
		60	81
		120	69
	150	5	74
		60	13
		120	27

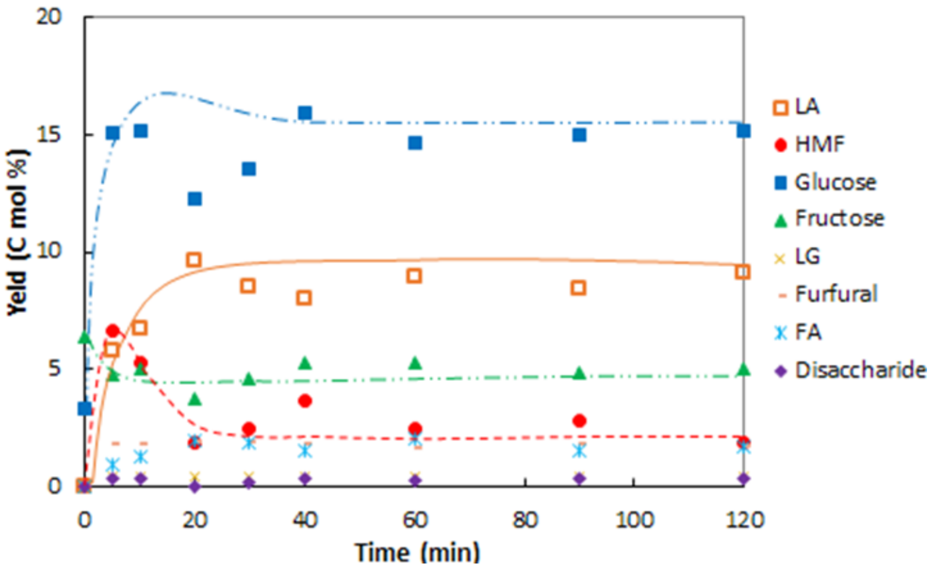

Figure B1. Product yields versus time under Amberlyst-15 catalyzed conversion of vegetable waste in water at 120°C (conditions: 5 wt/v% substrate and catalyst-to-substrate mass ratio = 1:1; yield = product C_{mol} / substrate C_{mol} × 100%).

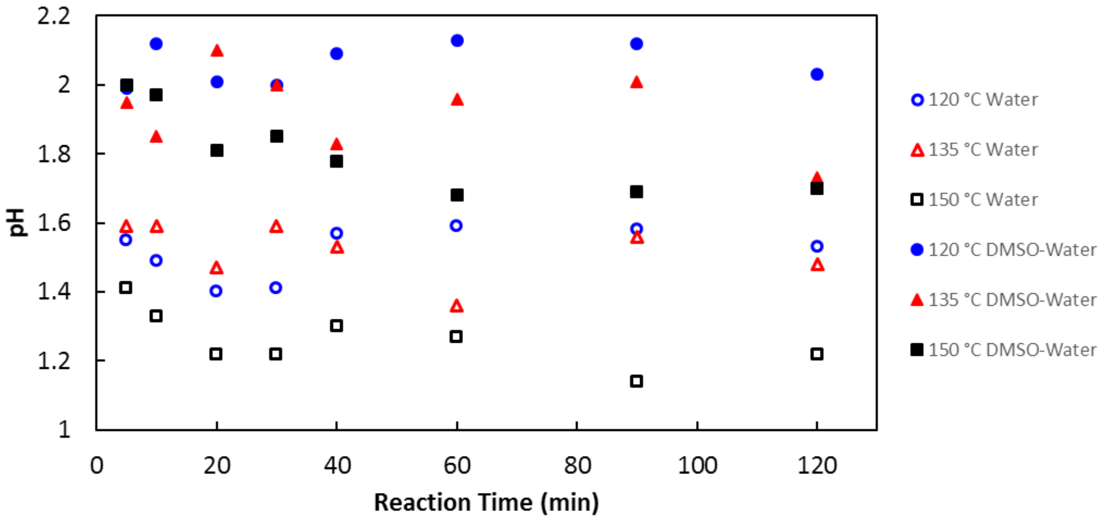

Figure B2. The pH values along with the reaction time at different reaction conditions (initial pH value was 4.4 and 6.2 in water and DMSO-water, respectively).

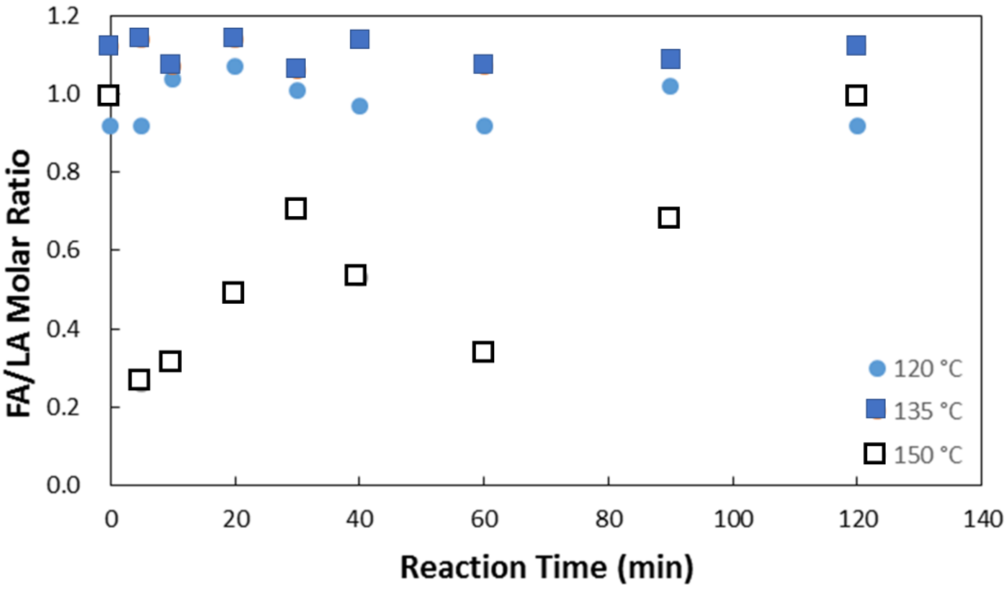

Figure B3. Molar ratios of formic acid (FA) to levulinic acid (LA) at different temperatures in water.

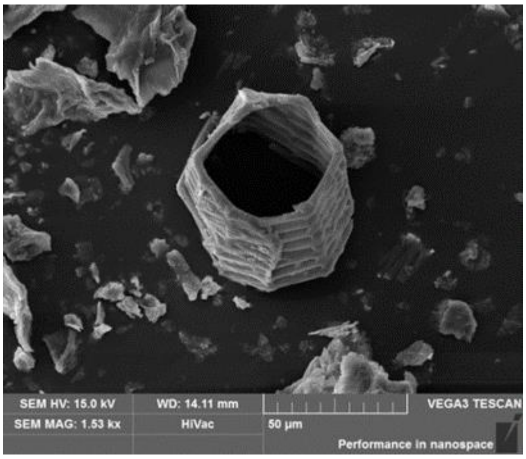

Figure B4. Scanning electron microscope (SEM) image of vegetable waste before treatment.

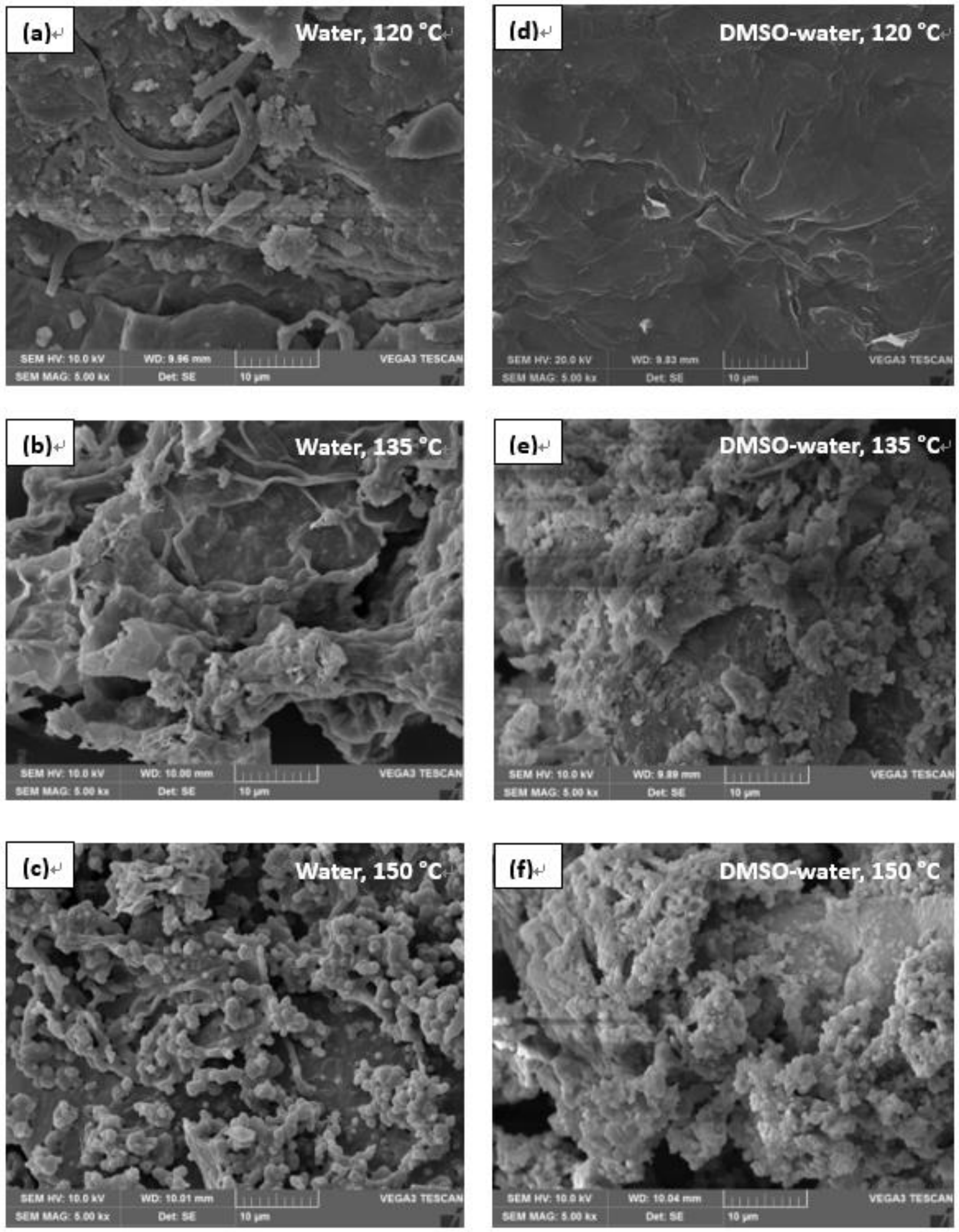

Figure B5. Scanning electron microscope (SEM) images of solid residues under Amberlyst 36 catalyzed conversion of vegetable waste in water (a-c) and DMSO-water (1:1 v/v) (d-f) at 120°C (a&d), 135°C (b&e), and 150°C (c&f) in 120 min.

References:

Luterbacher, J.S., Rand, J.M., Alonso, D.M., Han, J., Youngquist, J.T., Maravelias, C.T., Pfleger, B.F., Dumesic, J.A., 2014. Nonenzymatic sugar production from biomass using biomass-derived γ-valerolactone. Science 343, 277-280.

Siril, P.F., Cross, H.E., Brown, D.R., 2008. New polystyrene sulfonic acid resin catalysts with enhanced acidic and catalytic properties. J. Mol. Catal. A: Chem. 279, 63-68.

Appendix C

Table C1 Preliminary cost analysis of valorization of paper towel waste into value added chemicals at various scenarios.

Valorization of 1 kg paper towel waste *	**Items** (Unit price)	**Reaction Conditions**					
		Amberlyst 36 at 150 ºC (20 min)		1M H$_2$SO$_4$ at 150 ºC (60 min)		1M H$_2$SO$_4$ at 200 ºC (2.5 min)	
		Amount	Total (USD)	Amount	Total (USD)	Amount	Total (USD)
Input	Electricity (0.13 USD kWh^{-1})	316.67 kWh	41.17	358.33 kWh	46.58	83.33 kWh	10.83
	Water (0.0006 USD L^{-1})	20 L	0.012	20 L	0.012	20 L	0.012
	H$_2$SO$_4$ (98 wt.%) (0.1 USD kg^{-1})	/	/	1.96 kg	0.196	1.96 kg	0.196
	Amberlyst 36 (1.14 USD g^{-1})	200 g #	228	/	/	/	/
Output	Glucose (0.5 USD kg^{-1})	46.5 g	0.02	48.8 g	0.02	16.8 g	0.008
	Xylose (1 USD kg^{-1})	5.8 g	0.006	2.6 g	0.003	7.1 g	0.007
	Levulinic acid (70 USD kg^{-1})	177.7 g	12.43	244.2 g	17.06	257.1 g	18.03
	Formic acid (0.5 USD kg^{-1})	58.6 g	0.03	99.3 g	0.05	100.0 g	0.05
	Furfural (2 USD kg^{-1})	8.24 g	0.016	3.3 g	0.007	15.3 g	0.03
	Insoluble products (potential value)	308.2 g	/	371.5 g	/	601.9 g	/
Avoided cost	Municipal waste (0.047 USD kg^{-1})	1 kg	0.047 USD	1 kg	0.047 USD	1 kg	0.047 USD

* assuming the paper towel is homogeneously mixed with virgin and recycled pulps

assuming 5 times of recycling

The price of LA is based on Sigma-Aldrich, whereas the prices of glucose, xylose, formic acid, and furfural are based on Alibaba.com

The charge is applicable to those who hire private rubbish collectors to dispose of waste directly at landfills or refuse transfer stations

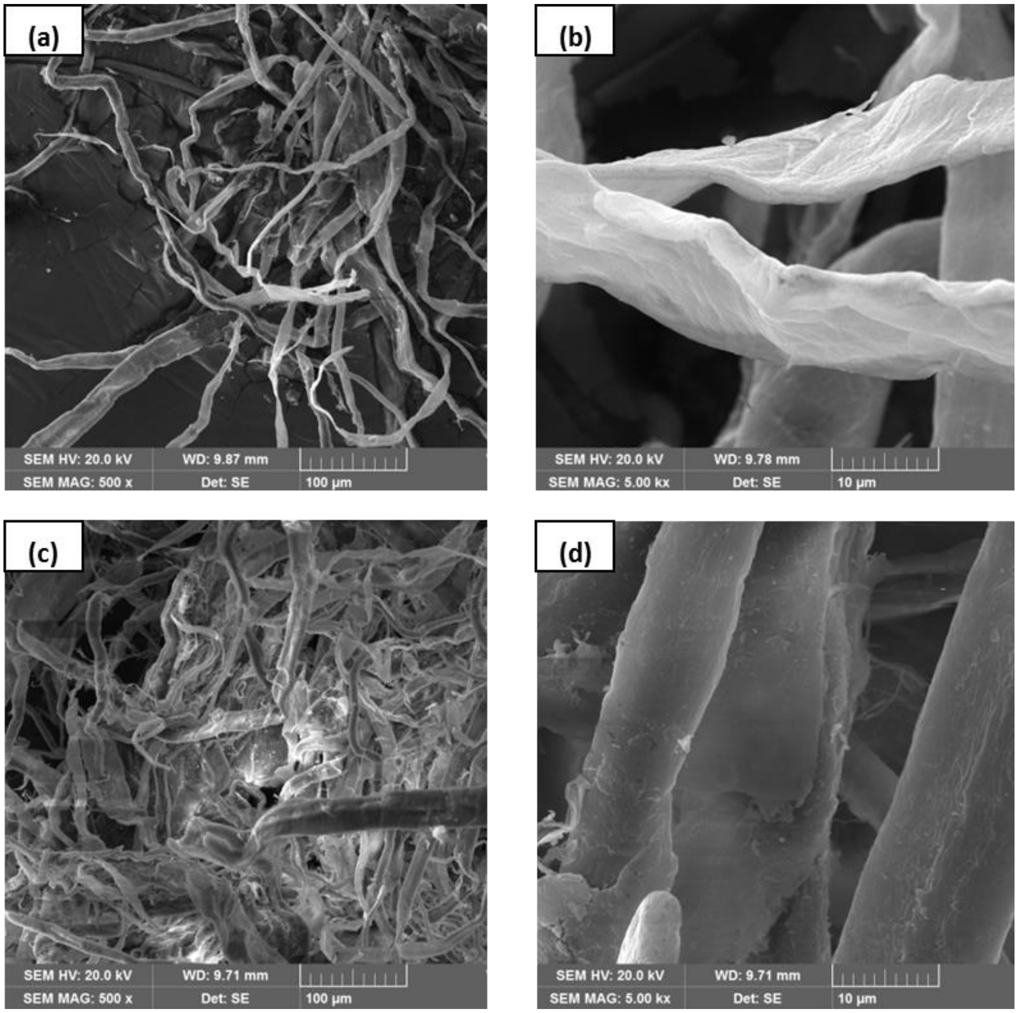

Figure C1 Scanning electron microscope (SEM) images of untreated virgin pulp (a&b) and recycled pulp (c&d) paper towels at 500x (a&c) and 5000x (b&d) magnification.

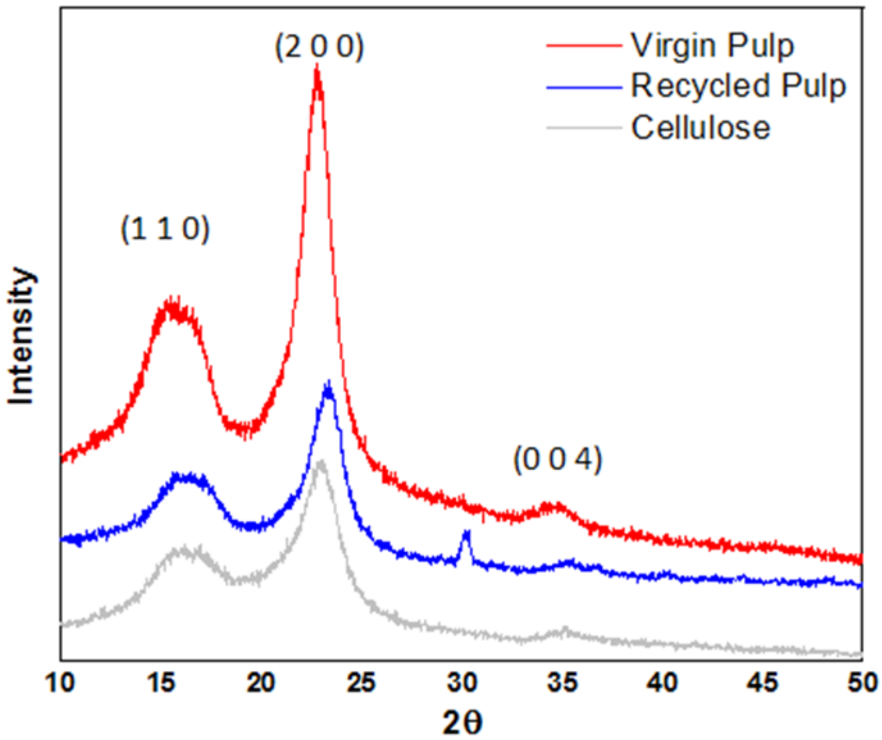

Figure C2 X-ray diffraction (XRD) patterns of untreated paper towel pulps and standard cellulose.

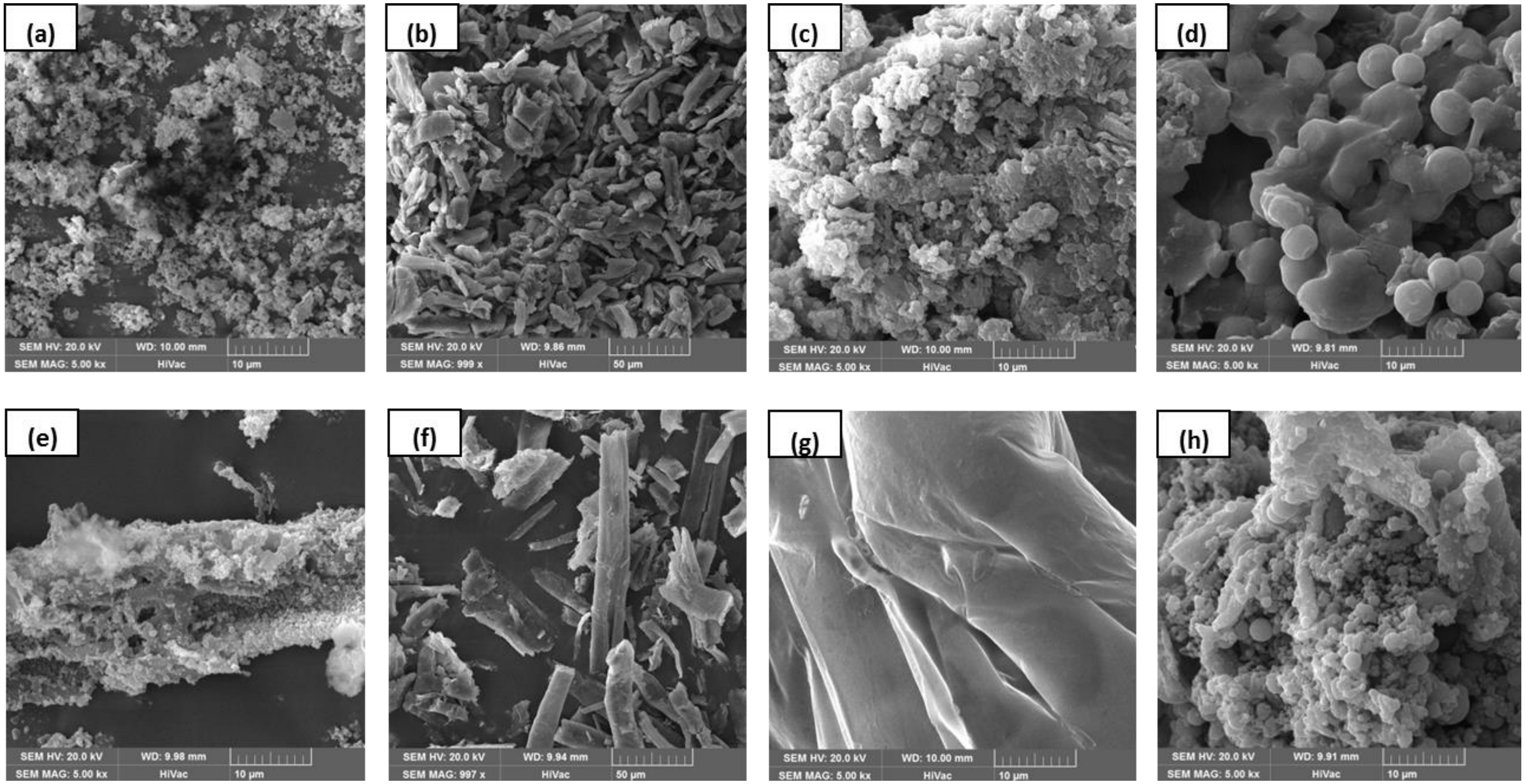

Figure C3 Scanning electron microscope (SEM) images of reacted virgin pulp (a-d), and recycled pulp (e-h) paper towels at selected conditions in 60 min (a&e: Amberlyst 36, x5k; b&f: 0.135 M H_2SO_4 , x1k; c&g: 1 M H_2SO_4 at 150 °C, x5k; d&h: 1 M H_2SO_4 at 200 °C, x5k)

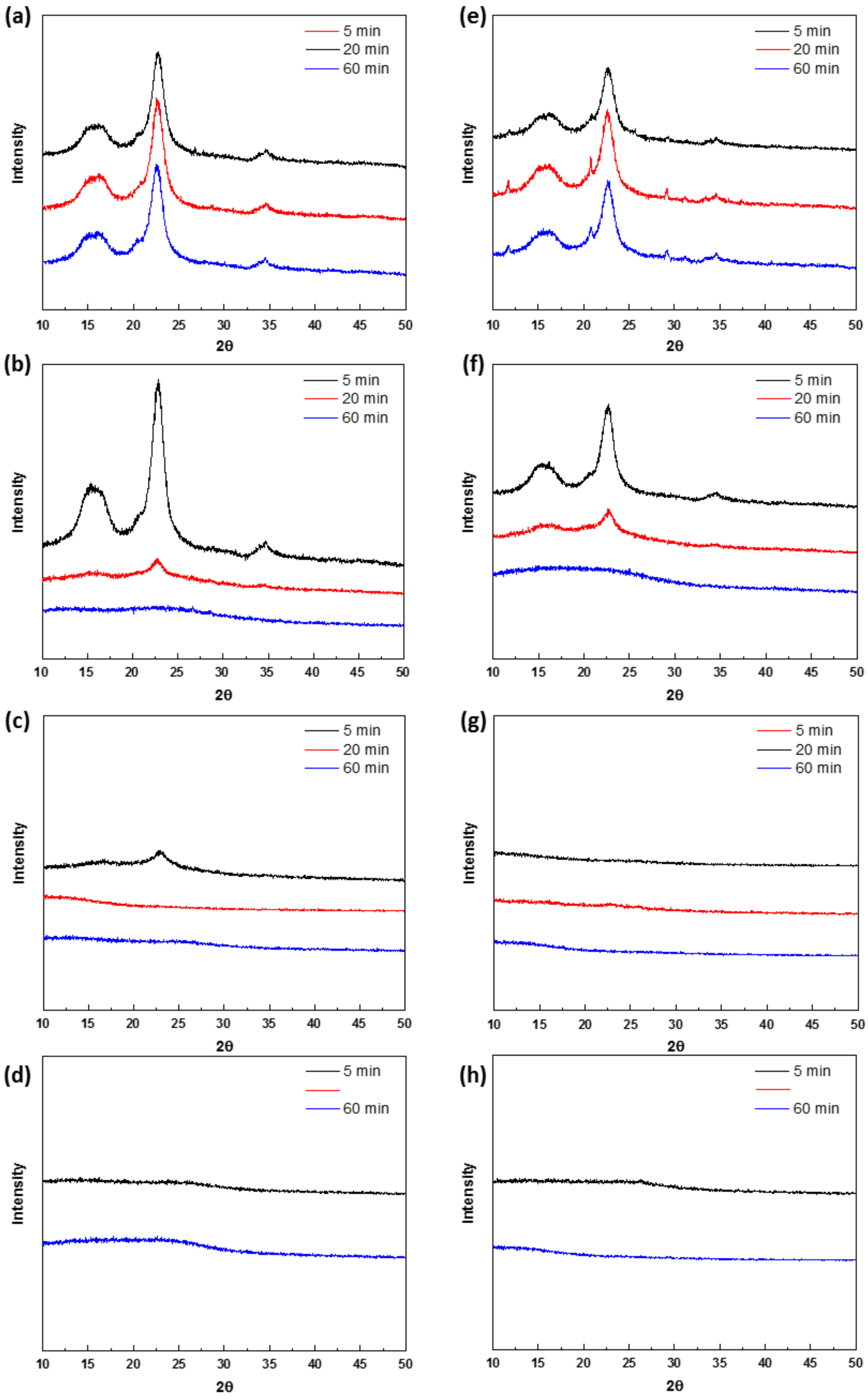

Figure C4 XRD of virgin pulp (a-d) and recycled pulp (e-h) paper towels in 0.135 M H_2SO_4 (a&e), Amberlyst 36 (b&f), 1 M H_2SO_4 (c&g) at 150 ºC, and 1 M H_2SO_4 (d&h) at 200 ºC.

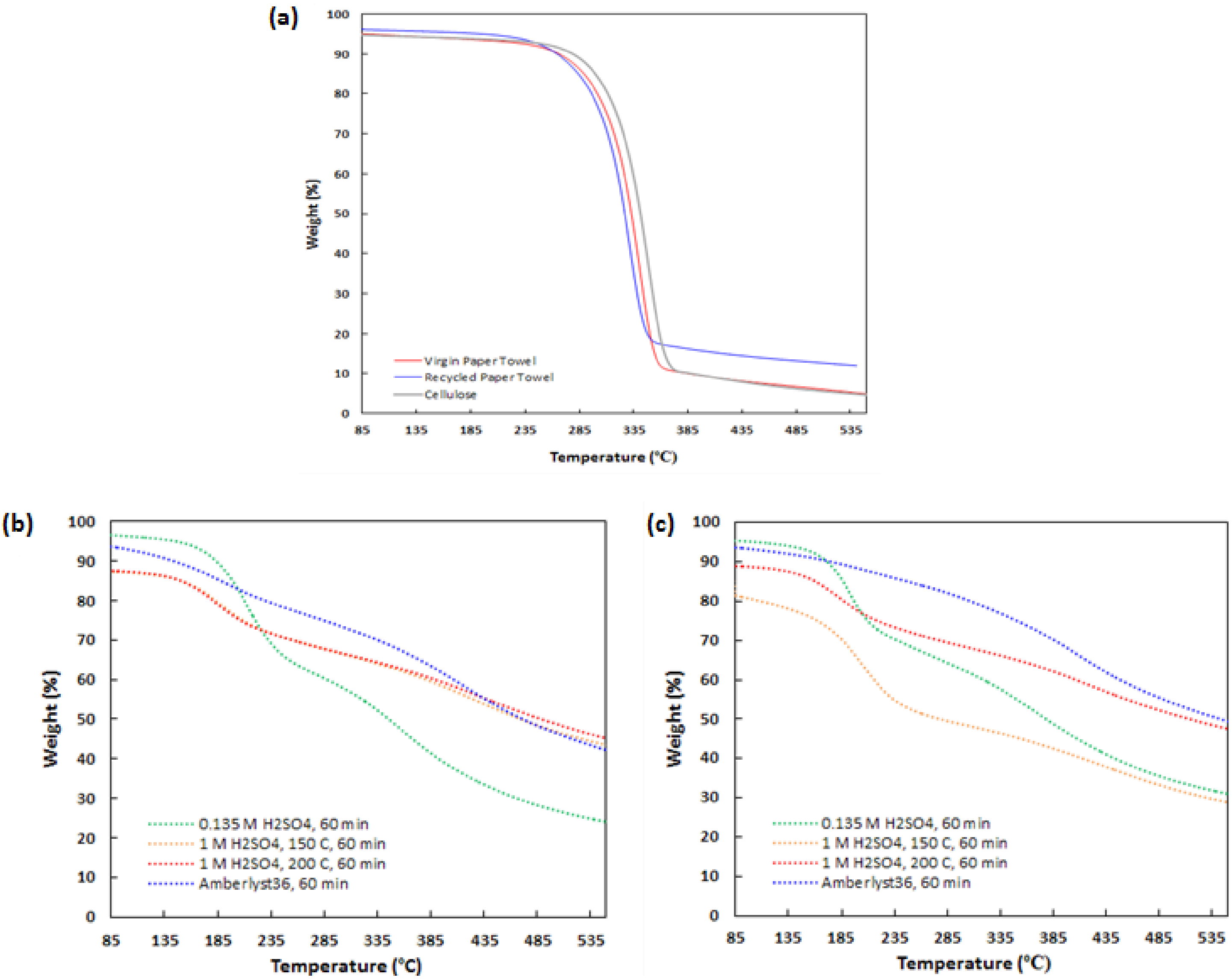

Figure C5 TGA of (a) untreated paper towels and cellulose, (b) treated virgin pulp paper towel, and (c) treated recycled pulp paper towel at selected conversion conditions.

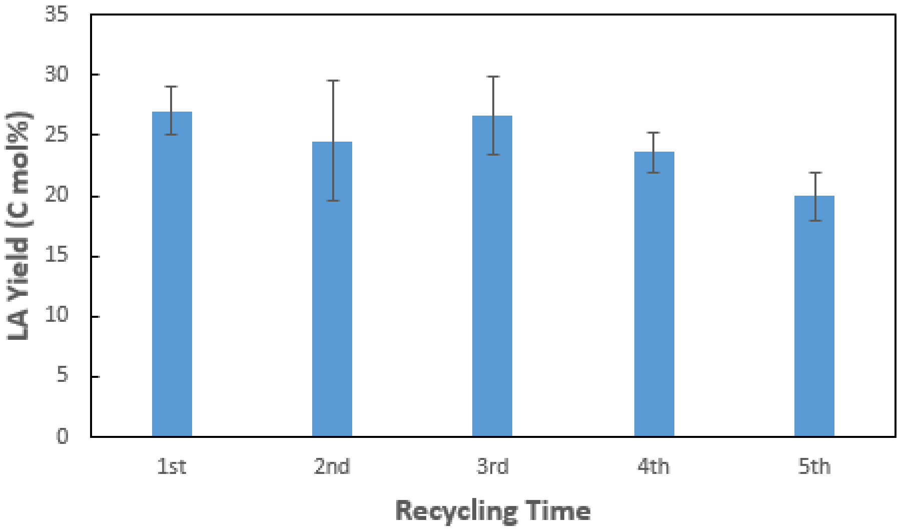

Figure C6 Recyclability test of Amberlyst 36 for LA synthesis from recycled pulp paper towel waste at 150 ˚C for 20 min in water

Appendix D

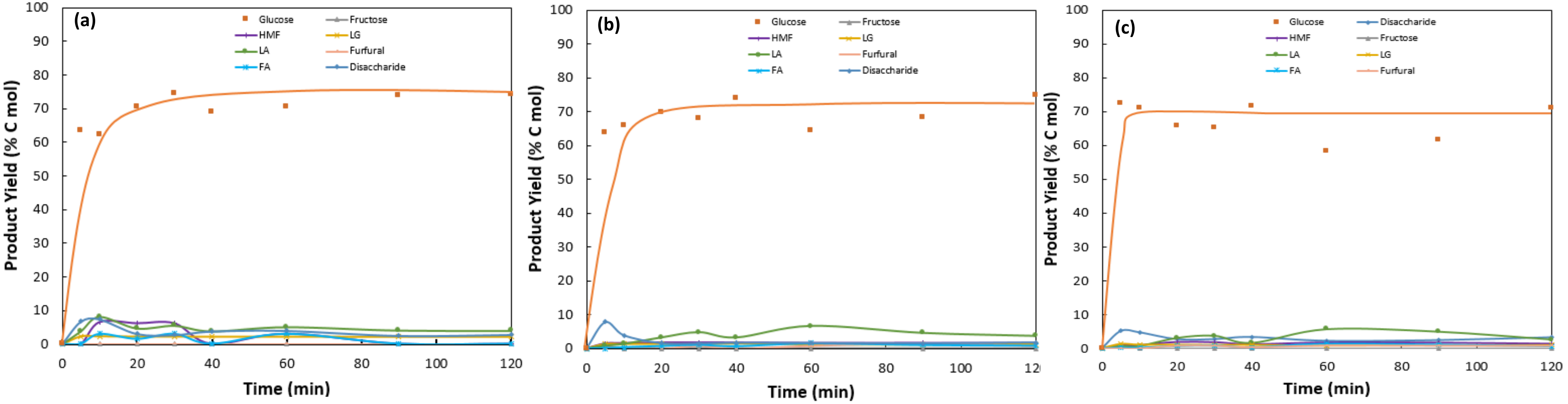

Figure D1 Product yields versus time under Amberlyst-36 catalyzed conversion of bread waste in water at catalyst-to-substrate mass ratio equals to: (a) 5; (b) 1; and (c) 0.5 at 120°C (conditions: 5 wt/v% substrate; yield = product C_{mol} / substrate C_{mol} × 100%).

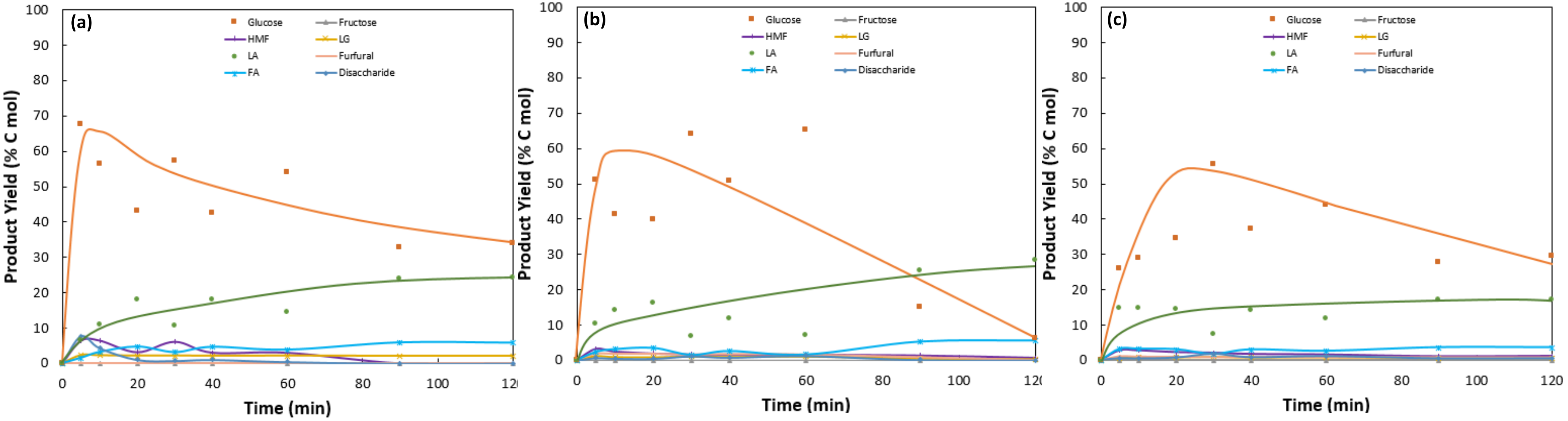

Figure D2 Product yields versus time under Amberlyst-36 catalyzed conversion of bread waste in water at catalyst-to-substrate mass ratio equals to: (a) 5; (b) 1; and (c) 0.5 at 135°C (conditions: 5 wt/v% substrate; yield = product C_{mol} / substrate C_{mol} × 100%).

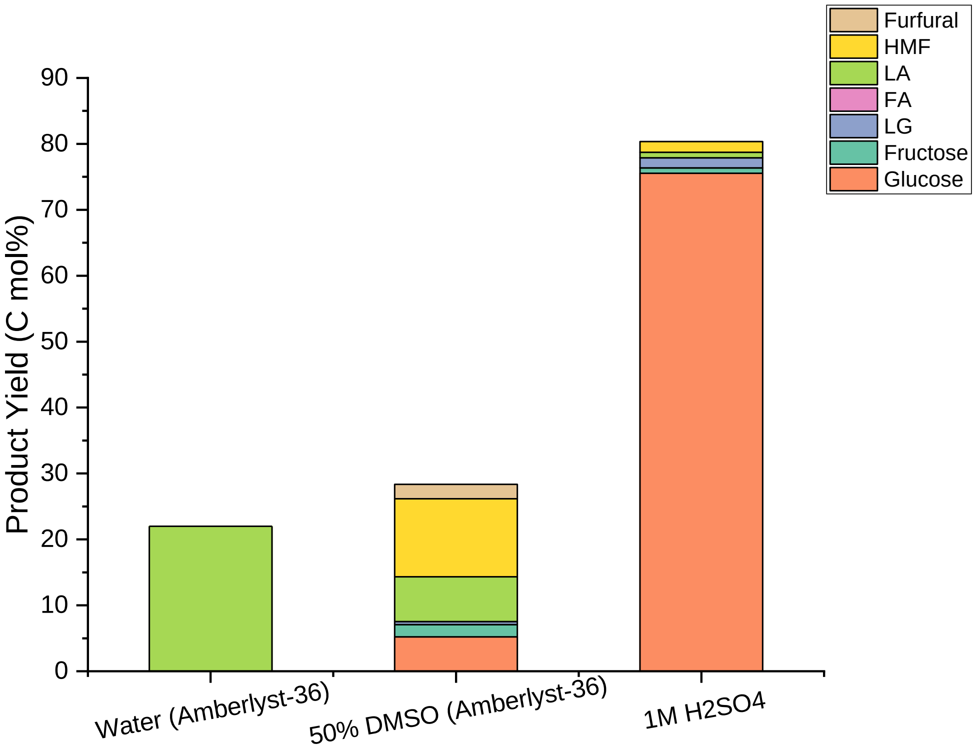

Figure D3 Product yields versus time under Brønsted acids catalyzed conversion of bread waste at different condition (conditions: 5 wt/v% substrate; catalyst-to-substrate mass ratio = 1 for heterogeneous catalysis; solvent volume = 10 mL; yield = product C_{mol} / substrate C_{mol} × 100%).

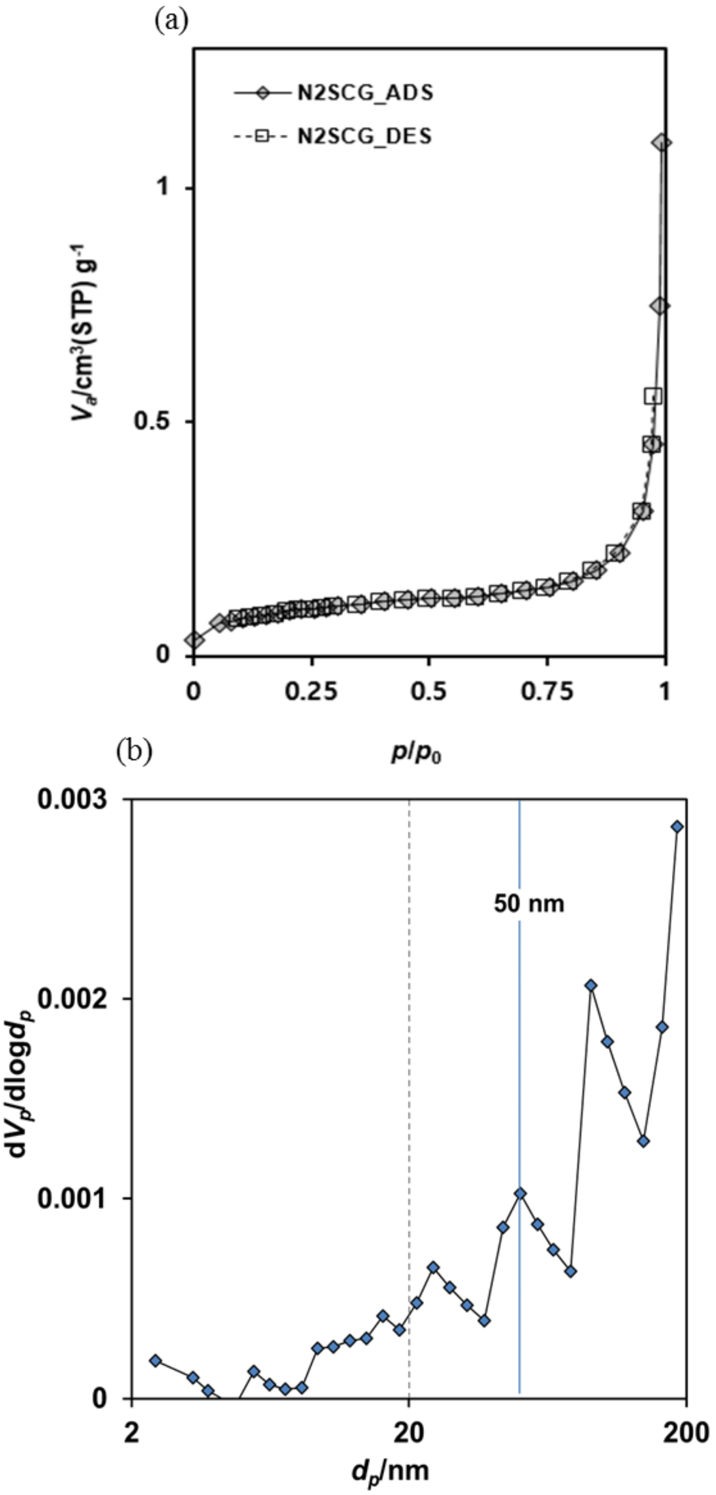

Figure D4 (a) Nitrogen adsorption (ADS)-desorption (DES) isotherms of N-doped biochar catalyst; (b) BJH plot of N-doped biochar catalyst (pore diameter d_p = 2-200 nm).

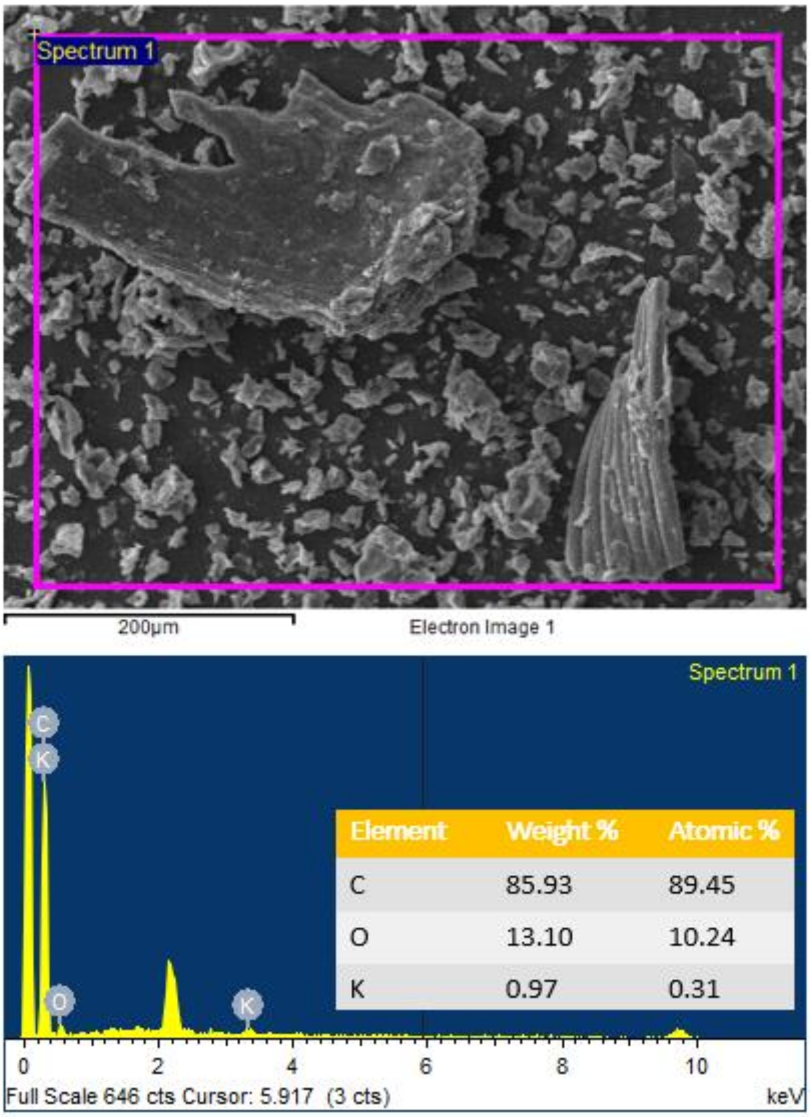

Element	Weight %	Atomic %
C	85.93	89.45
O	13.10	10.24
K	0.97	0.31

Figure D5 SEM-EDX images of N-doped biochar catalyst before catalytic reaction.

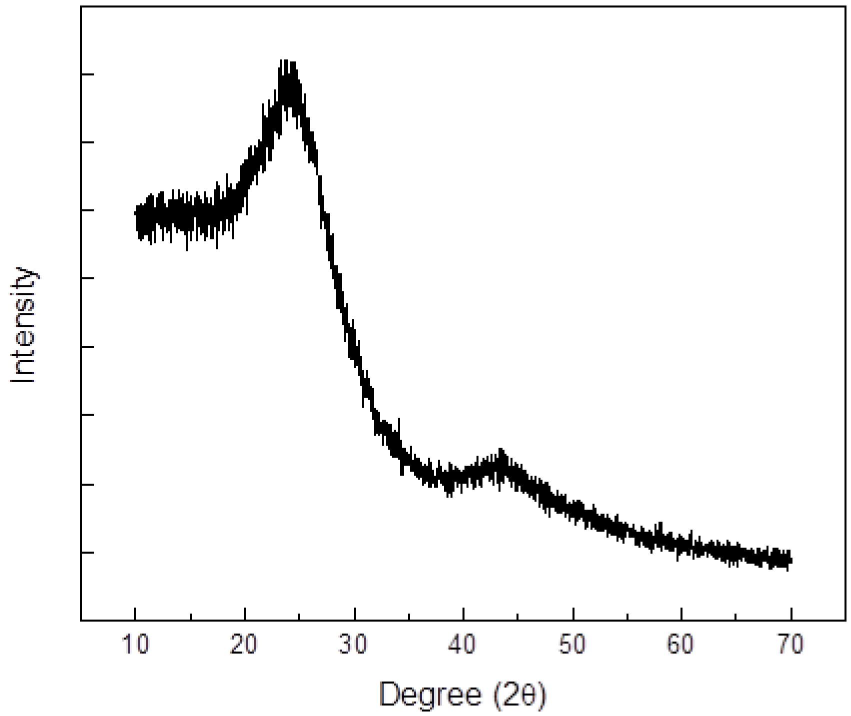

Figure D6 XRD image of N-doped biochar catalyst before catalytic reaction.

Appendix E

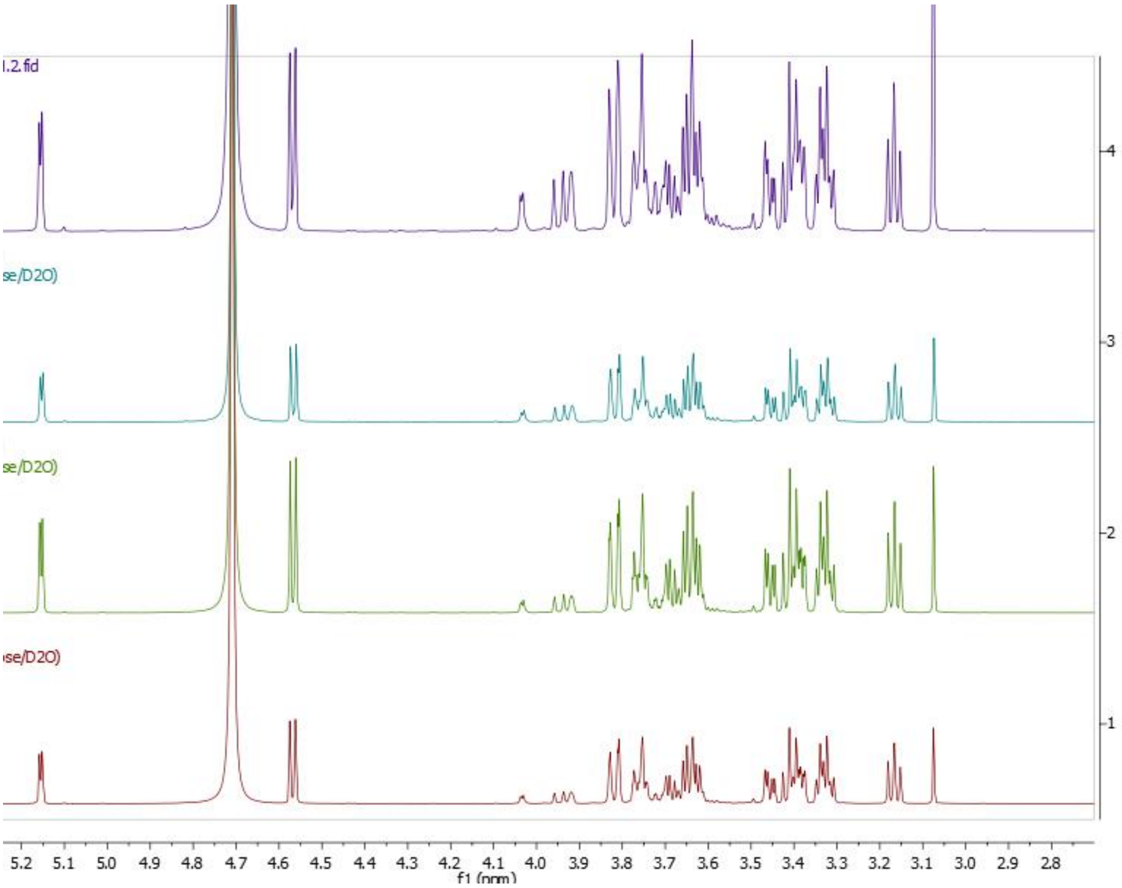

Figure E1 ^{1}H NMR spectra of different hydroxides catalyzed glucose isomerization: (1) $Mg(OH)_2$; (2) $Ca(OH)_2$; (3) Ba(OH$_2$; and (4) NaOH.

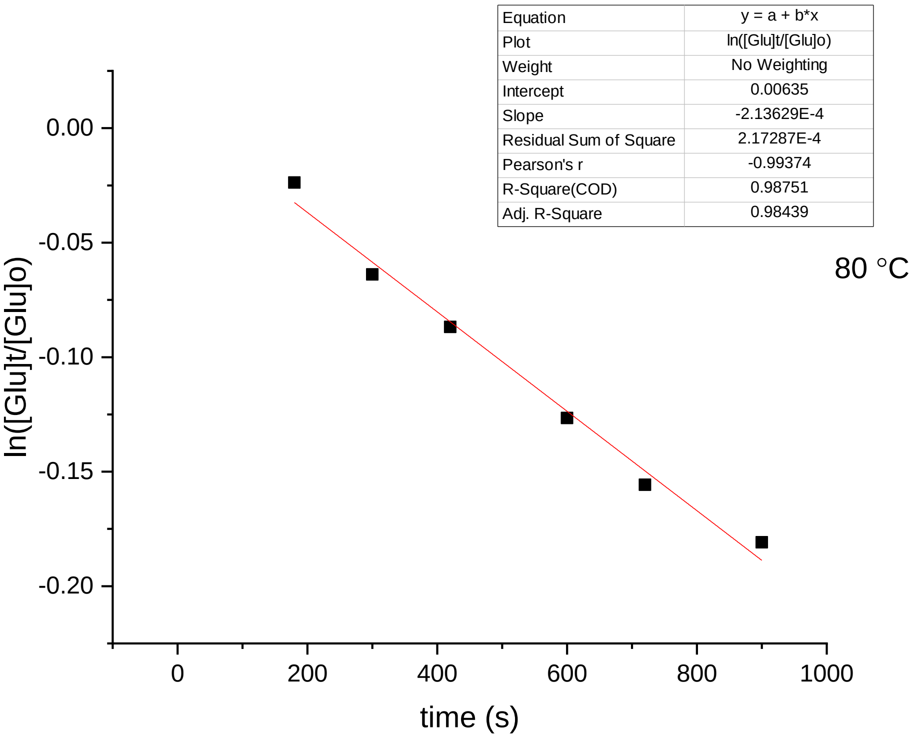

Equation	y = a + b*x
Plot	ln([Glu]t/[Glu]o)
Weight	No Weighting
Intercept	0.00635
Slope	-2.13629E-4
Residual Sum of Square	2.17287E-4
Pearson's r	-0.99374
R-Square(COD)	0.98751
Adj. R-Square	0.98439

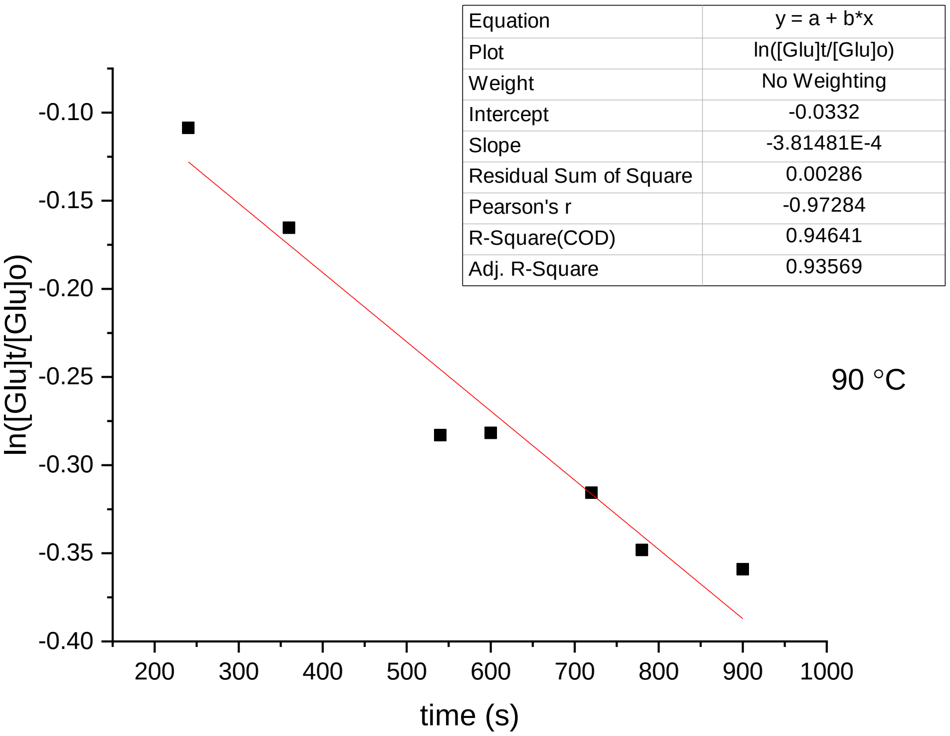

Equation	y = a + b*x
Plot	ln([Glu]t/[Glu]o)
Weight	No Weighting
Intercept	-0.0332
Slope	-3.81481E-4
Residual Sum of Square	0.00286
Pearson's r	-0.97284
R-Square(COD)	0.94641
Adj. R-Square	0.93569

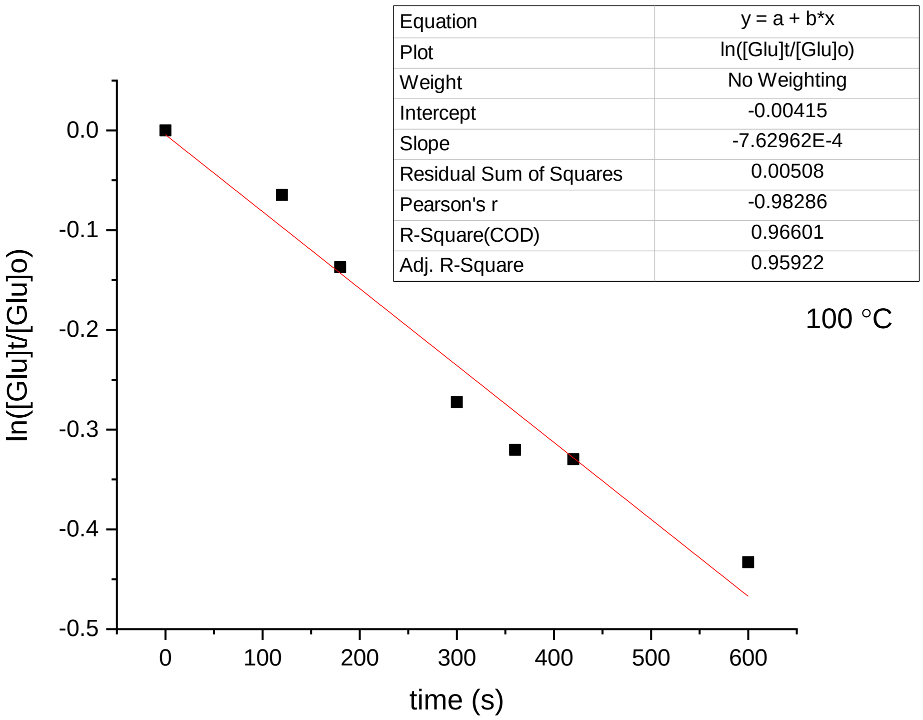

Equation	y = a + b*x
Plot	ln([Glu]t/[Glu]o)
Weight	No Weighting
Intercept	-0.00415
Slope	-7.62962E-4
Residual Sum of Squares	0.00508
Pearson's r	-0.98286
R-Square(COD)	0.96601
Adj. R-Square	0.95922

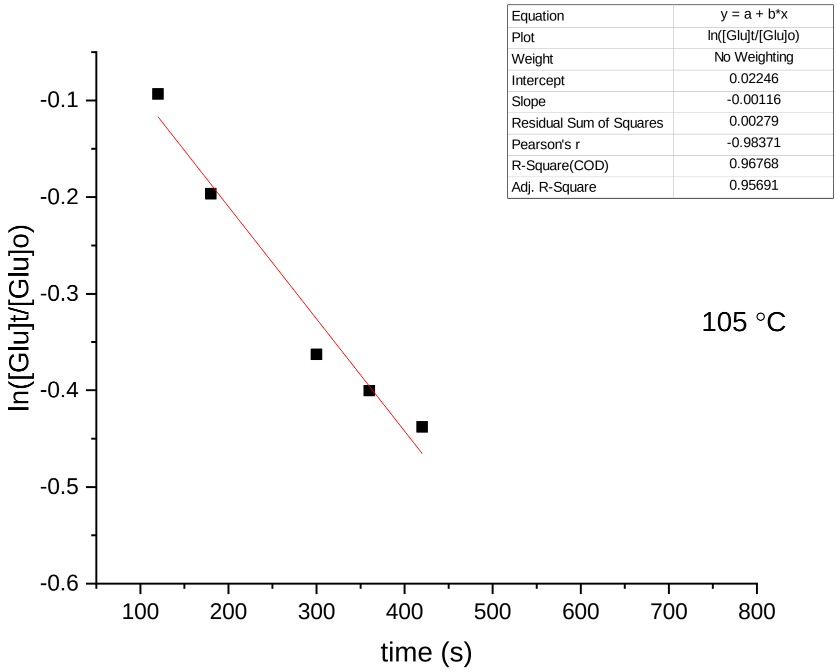

Equation	y = a + b*x
Plot	ln([Glu]t/[Glu]o)
Weight	No Weighting
Intercept	0.02246
Slope	-0.00116
Residual Sum of Squares	0.00279
Pearson's r	-0.98371
R-Square(COD)	0.96768
Adj. R-Square	0.95691

Figure E2 Kinetic tests of glucose isomerization by 12 mol N% meglumine (relative to glucose) at 80, 90, 100 and 105 °C, respectively.

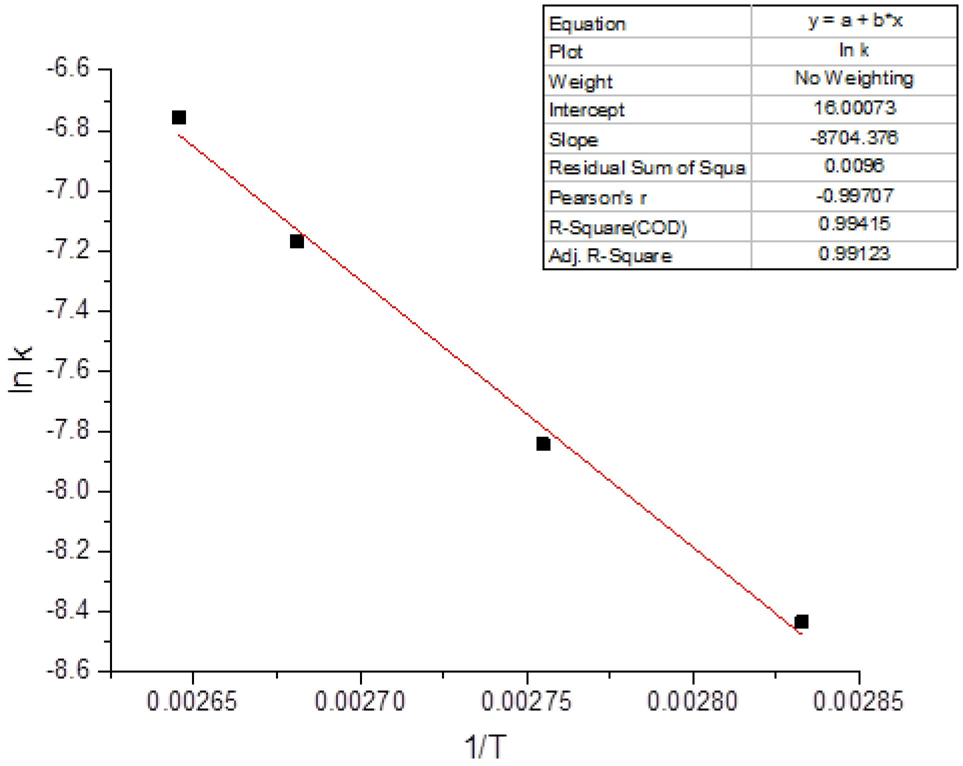

Figure E3 Apparent activation energy of meglumine catalyzed glucose isomerization calculated based on the kinetic results obtained from **Figure S2**.

References

Abdel-Rahman, M.A., Tashiro, Y., Sonomoto, K., 2013. Recent advances in lactic acid production by microbial fermentation processes. Biotechnology Advances 31, 877-902.

Agirrezabal-Telleria, I., Larreategui, A., Requies, J., Güemez, M.B., Arias, P.L., 2011. Furfural production from xylose using sulfonic ion-exchange resins (Amberlyst) and simultaneous stripping with nitrogen. Bioresource Technology 102, 7478-7485.

Ahlkvist, J., 2014. Formic and levilinic acid from cellulose via heterogeneous catalysis. Doctoral Dissertation.

Ajandouz, E.H., Puigserver, A., 1999. Nonenzymatic Browning Reaction of Essential Amino Acids: Effect of pH on Caramelization and Maillard Reaction Kinetics. Journal of Agricultural and Food Chemistry 47, 1786-1793.

Alatalo, S.M., Qiu, K.P., Preuss, K., Marinovic, A., Sevilla, M., Sillanpaa, M., Guo, X., Titirici, M.M. 2016. Soy protein directed hydrothermal synthesis of porous carbon aerogels for electrocatalytic oxygen reduction. Carbon 96, 622-630.

Alonso, D.M., Bond, J.Q., Dumesic, J.A., 2010. Catalytic conversion of biomass to biofuels. Green Chemistry 12, 1493-1513.

Alonso, D.M., Gallo, J.M.R., Mellmer, M.A., Wettstein, S.G., Dumesic, J.A., 2013. Direct conversion of cellulose to levulinic acid and gamma-valerolactone using solid acid catalysts. Catalysis Science and Technology 3, 927-931.

Alonso, D.M., Hakim, S.H., Zhou, S., Won, W., Hosseinaei, O., Tao, J., Garcia-Negron, V., Motagamwala, A.H., Mellmer, M.A., Huang, K., Houtman, C.J., Labbé, N., Harper, D.P., Maravelias, C.T., Runge, T., Dumesic, J.A., 2017. Increasing the revenue from lignocellulosic biomass: Maximizing feedstock utilization. Science Advances 3.

Alonso, D.M., Wettstein, S.G., Dumesic, J.A., 2012. Bimetallic catalysts for upgrading of biomass to fuels and chemicals. Chemical Society Reviews 41, 8075-8098.

Amiri, H., Karimi, K., 2013. Efficient dilute-acid hydrolysis of cellulose using solvent pretreatment. Industrial and Engineering Chemistry Research 52, 11494-11501.

Angyal, S.J., 1989. Complexes of Metal Cations with Carbohydrates in Solution. in: Tipson, R.S., Horton, D. (Eds.). Advances in Carbohydrate Chemistry and

Biochemistry. Academic Press, pp. 1-43.

Antonetti, C., Licursi, D., Fulignati, S., Valentini, G., Galletti, A.M.R., 2016. New frontiers in the catalytic synthesis of levulinic acid: From sugars to raw and waste biomass as starting feedstock. Catalysts 6.

Arrigo, R., Hävecker, M., Schlögl, R., Su, D.S., 2008. Dynamic surface rearrangement and thermal stability of nitrogen functional groups on carbon nanotubes. Chemistry Communications 4891-4893.

Asghari, F.S., Yoshida, H., 2006. Dehydration of fructose to 5-hydroxymethylfurfural in sub-critical water over heterogeneous zirconium phosphate catalysts. Carbohydrate Research 341, 2379-2387.

Bass, J.D., Anderson, S.L., Katz, A., 2003. The effect of outer-sphere acidity on chemical reactivity in a synthetic heterogeneous base catalyst. Angewandte Chemie International Edition 42, 5219-5222.

Bennett, J.A., Wilson, K., Lee, A.F., 2016. Catalytic applications of waste derived materials. Journal of Materials Chemistry A 4, 3617-3637.

Bermejo-Deval, R., Assary, R.S., Nikolla, E., Moliner, M., Román-Leshkov, Y., Hwang, S.J., Palsdottir, A., Silverman, D., Lobo, R.F., Curtiss, L.A., Davis, M.E., 2012. Metalloenzyme-like catalyzed isomerizations of sugars by Lewis acid zeolites. Proceedings of the National Academy of Sciences of the United States of America 109, 9727-9732.

Bermejo-Deval, R., Assary, R.S., Nikolla, E., Moliner, M., Román-Leshkov, Y., Hwang, S.J., Palsdottir, A., Silverman, D., Lobo, R.F., Curtiss, L.A., Davis, M.E., 2012. Metalloenzyme-like catalyzed isomerizations of sugars by Lewis acid zeolites. Proceedings of the National Academy of Sciences 109, 9727-9732.

Bermejo-Deval, R., Orazov, M., Gounder, R., Hwang, S.J., Davis, M.E., 2014. Active sites in Sn-beta for glucose isomerization to fructose and epimerization to mannose. ACS Catalysis 4, 2288-2297.

Berrueta, L.A., Alonso-Salces, R.M., Heberger, K., 2007. Supervised pattern recognition in food analysis. J Chromatogr A 1158, 196-214.

Besson, M., Gallezot, P., Pinel, C., 2014. Conversion of biomass into chemicals over metal catalysts. Chemical Reviews 114, 1827-1870.

Bharate, S.S., Bharate, S.B., Bajaj, A.N., 2010. Incompatibilities of Pharmaceutical Excipients with Active Pharmaceutical Ingredients: A Comprehensive Review. Journal of Excipients and Food Chemicals; Vol 1 No 3 (2010).

Bhosale, S.H., Rao, M.B., Deshpande, V.V., 1996. Molecular and industrial aspects of glucose isomerase. Microbiological Reviews 60, 280-300.

Bhosale, S.H., Rao, M.B., Desphande, V.V., 1996. Molecular and industrial aspects of glucose isomerase. Microbiological Reviews 60, 280-300.

Bond, J.Q., Upadhye, A.A., Olcay, H., Tompsett, G.A., Jae, J., Xing, R., Alonso, D.M., Wang, D., Zhang, T., Kumar, R., Foster, A., Sen, S.M., Maravelias, C.T., Malina, R., Barrett, S.R.H., Lobo, R., Wyman, C.E., Dumesic, J.A., Huber, G.W., 2014. Production of renewable jet fuel range alkanes and commodity chemicals from integrated catalytic processing of biomass. Energy and Environmental Science 7, 1500-1523.

Brand, S.K., Labinger, J.A., Davis, M.E., 2016. Tin Silsesquioxanes as Models for the "open" Site in Tin-Containing Zeolite Beta. ChemCatChem 8, 121-124.

Bridgwater, A.V., 2003. Renewable fuels and chemicals by thermal processing of biomass. Chemical Engineering Journal 91, 87-102.

Brown, R.C., Brown, T.R., 2014. Biorenewable Resources: Engineering New Products from Agriculture: Second Edition.

Brown, T.R., Zhang, Y., Hu, G., Brown, R.C., 2012. Techno-economic analysis of biobased chemicals production via integrated catalytic processing. Biofuels, Bioproducts and Biorefining 6, 73-87.

Buchholz, K., Seibel, J., 2008. Industrial carbohydrate biotransformations. Carbohydrate Research 343, 1966−1979.

Cadenas, M., Bringué, R., Fité, C., Ramírez, E., Cunill, F., 2011. Liquid-phase oligomerization of 1-hexene catalyzed by macroporous ion-exchange resins. Topics in Catalysis 54, 998-1008.

Cao, L., Yu, I.K.M., Chen, S.S., Tsang, D.C.W., Wang, L., Xiong, X., Zhang, S., Ok, Y.S., Kwon, E.E., Hocheol, S., Poon, C.S., 2018. Production of 5-hydroxymethylfurfural from starch-rich food waste catalyzed by sulfonated biochar. Bioresource Technology 252, 76-82.

Cao, Y., Yu, H., Wang, H., Peng, F., 2017. Solvent effect on the allylic oxidation of cyclohexene catalyzed by nitrogen doped carbon nanotubes. Solvent effect on the allylic oxidation of cyclohexene catalyzed by nitrogen doped carbon nanotubes. Catalysis Communications 88, 99-103.

Carà, P.D., Pagliaro, M., Elmekawy, A., Brown, D.R., Verschuren, P., Shiju, N.R., Rothenberg, G., 2013. Hemicellulose hydrolysis catalysed by solid acids. Catalysis Science and Technology 3, 2057-2061.

Çarçabal, P., Jockusch, R.A., Hünig, I., Snoek, L.C., Kroemer, R.T., Davis, B.G., Gamblin, D.P., Compagnon, I., Oomens, J., Simons, J.P., 2005. Hydrogen Bonding and Cooperativity in Isolated and Hydrated Sugars: Mannose, Galactose, Glucose, and Lactose. Journal of the American Chemical Society 127, 11414-11425.

Carraher, J.M., Fleitman, C.N., Tesonnier, J.-P., 2015. Kinetic and mechanistic study of glucose isomerization using homogeneous organic Brønsted base catalysts in water. ACS Catalysis 5, 3162-3173.

Castellano, M., Gandini, A., Fabbri, P., Belgacem, M.N., 2004. Modification of cellulose fibres with organosilanes: Under what conditions does coupling occur? J Colloid Interface Sci 273, 505-511.

Castro, C.S., Cardoso, D., Nascente, P.A.P., Assaf, J.M., 2011. MgAlLi mixed oxides derived from hydrotalcite for catalytic transesterification. Catalysis Letters 141, 1316-1323.

Cavani, F., Trifirò, F., Vaccari, A., 1991. Hydrotalcite-type anionic clays: Preparation, properties and applications. Catalysis Today 11, 173-301.

Chai, S.H., Yan, B., Tao, L.Z., Liang, Y., Xu, B.Q., 2014. Sustainable production of acrolein: Catalytic gas-phase dehydration of glycerol over dispersed tungsten oxides on alumina, zirconia and silica. Catalysis Today 234, 215-222.

Chambon, F., Rataboul, F., Pinel, C., Cabiac, A., Guillon, E., Essayem, N., 2011. Cellulose hydrothermal conversion promoted by heterogeneous Brønsted and Lewis acids: Remarkable efficiency of solid Lewis acids to produce lactic acid. Applied Catalysis B: Environmental 105, 171-181.

Chandra, D., Mukherjee, N., Mondal, A., Bhaumik, A., 2008. Design and synthesis of nanostructured porous SnO2with high surface areas and their optical and dielectric properties. Journal of Physical Chemistry C 112, 8668-8674.

Chen, L., Ji, T., Yuan, R., Mu, L., Brisbin, L., Zhu, J., 2015. Unveiling Mesopore Evolution in Carbonized Wood: Interfacial Separation, Migration, and Degradation of Lignin Phase. ACS Sustainable Chemistry and Engineering 3, 2489-2495.

Chen, S.S., Maneerung, T., Tsang, D.C.W., Ok, Y.S., Wang, C.H., 2017a. Valorization of biomass to hydroxymethylfurfural, levulinic acid, and fatty acid methyl ester by heterogeneous catalysts. Chemical Engineering Journal 328, 246-273.

Chen, S.S., Wang, L., Yu, I.K.M., Tsang, D.C.W., Hunt, A.J., Jérôme, F., Zhang, S., Ok, Y.S., Poon, C.S., 2017c. Valorization of lignocellulosic fibres of paper waste into levulinic acid using solid and aqueous brønsted acid. Bioresource Technology 247, 387-394.

Chen, S.S., Yu, I.K.M., Tsang, D.C.W., Yip, A.C.K., Khan, E., Wang, L., Ok, Y.S., Poon, C.S., 2017b. Valorization of cellulosic food waste into levulinic acid catalyzed by heterogeneous BrØnsted acids: Temperature and solvent effects. Chemical Engineering Journal 327, 328-335.

Chen, W., Yang, H., Chen, Y., Xia, M., Chen, X., Chen, H., 2017b. Transformation of nitrogen and evolution of N-containing species during algae pyrolysis. Environmental Science & Technology 51, 6570-6579.

Chen, W.H., Ye, S.C., Sheen, H.K., 2012. Hydrolysis characteristics of sugarcane bagasse pretreated by dilute acid solution in a microwave irradiation environment. Applied Energy 93, 237-244.

Chien, S.H., 1997. Hydrothermal synthesis and characterization of the vanadium-containing zeolite beta. Zeolites 18, 176-181.

Chinn, D., King, C.J., 1999. Adsorption of glycols, sugars, and related multiple -OH compounds onto activated carbons. 1. Adsorption mechanisms. Industrial and Engineering Chemistry Research 38, 3738-3745.

Cho, D.W., Cho, S.H., Song, H., Kwon, E.E., 2015. Carbon dioxide assisted sustainability enhancement of pyrolysis of waste biomass: A case study with spent coffee ground. Bioresource Technology 189, 1-6.

Cho, D.W., Kim, S., Tsang, Y.F., Song, H., 2017. Preparation of nitrogen-doped Cu-biochar and its application into catalytic reduction of p-nitrophenol. Environmental GeoChemistry and Health 1-9.

Cho, H.J., Dornath, P., Fan, W., 2014. Synthesis of hierarchical Sn-MFi as lewis acid catalysts for isomerization of cellulosic sugars. ACS Catalysis 4, 2029-2037.

Choudhary, V., Mushrif, S.H., Ho, C., Anderko, A., Nikolakis, V., Marinkovic, N.S., Frenkel, A.I., Sandler, S.I., Vlachos, D.G., 2013a. Insights into the interplay of lewis and Brønsted acid catalysts in glucose and fructose conversion to 5-(hydroxymethyl)furfural and levulinic acid in aqueous media. Journal of the American Chemical Society 135, 3997-4006.

Choudhary, V., Mushrif, S.H., Ho, C., Anderko, A., Nikolakis, V., Marinkovic, N,S., Frenkel, A.I., Sandler, S.I., Vlachos, D.G., 2013. Insights into the interplay of Lewis and Bronsted acid catalysts in glucose and fructose conversion to 5-(hydroxymethyl)furfural and levulinic acid in aqueous media. Journal of the American Chemical Society 135, 3997-4006.

Choudhary, V., Pinar, A.B., Lobo, R.F., Vlachos, D.G., Sandler, S.I., 2013b. Comparison of homogeneous and heterogeneous catalysts for glucose-to-fructose isomerization in aqueous media. ChemSusChem 6, 2369-2376.

Choudhary, V., Sandler, S.I., Vlachos, D.G., 2012. Conversion of xylose to furfural using Lewis and Brønsted acid catalysts in aqueous media. ACS Catalysis 2, 2022-2028.

Chung, P.W., Charmot, A., Olatunji-Ojo, O.A., Durkin, K.A., Katz, A., 2014. Hydrolysis catalysis of Miscanthus xylan to xylose using weak-acid surface sites. ACS Catalysis 4, 302-310.

Climent, M.J., Corma, A., Iborra, S., 2014. Conversion of biomass platform molecules into fuel additives and liquid hydrocarbon fuels. Green Chemistry 16, 516-547.

Corma, A., Iborra, S., Velty, A., 2007. Chemical Routes for the Transformation of Biomass into Chemicals. Chemical Reviews 107, 2411-2502.

Corma, A., Llabrés I Xamena, F.X., Prestipino, C., Renz, M., Valencia, S., 2009. Water resistant, catalytically active Nb and Ta isolated Lewis acid sites, homogeneously distributed by direct synthesis in a Beta zeolite. Journal of Physical Chemistry C 113, 11306-11315.

Correia, L.M., Saboya, R.M.A., de Sousa Campelo, N., Cecilia, J.A., Rodríguez-Castellón, E., Cavalcante, C.L., Vieira, R.S., 2014. Characterization of calcium oxide catalysts from natural sources and their application in the transesterification of sunflower oil. Bioresource Technology 151, 207-213.

da Silva Lacerda, V., López-Sotelo, J.B., Correa-Guimarães, A., Hernández-Navarro, S., Sánchez-Bascones, M., Navas-Gracia, L.M., Martín-Ramos, P., Pérez-Lebeña, E., Martín-Gil, J., 2015. A kinetic study on microwave-assisted conversion of cellulose and lignocellulosic waste into hydroxymethylfurfural/furfural. Bioresource Technology 180, 88-96.

Daengprasert, W., Boonnoun, P., Laosiripojana, N., Goto, M., Shotipruk, A., 2011. Application of sulfonated carbon-based catalyst for solvothermal conversion of cassava waste to hydroxymethylfurfural and furfural. Industrial and Engineering Chemistry Research 50, 7903-7910.

Dallinger, D., Kappe, C.O., 2007. Microwave-assisted synthesis in water as solvent. Chemical Reviews 107, 2563-2591.

Dapsens, P.Y., Mondelli, C., Jagielski, J., Hauert, R., Pérez-Ramírez, J., 2014. Hierarchical Sn-MFI zeolites prepared by facile top-down methods for sugar isomerisation. Catalysis Science and Technology 4, 2302-2311.

Dashnau, J.L., Sharp, K.A., Vanderkooi, J.M., 2005. Carbohydrate intramolecular hydrogen bonding cooperativity and its effect on water structure. J. Phys. Chem. B 109, 24152-24159.

Davis, M.E., 2015. Heterogeneous Catalysis for the Conversion of Sugars into Polymers. Topics in Catalysis 58, 405-409.

de Bruijn, J.M., Kieboom, A.P.G., van Bekkum, H., 1986. Alkaline degradation of monosaccharides III. Influence of reaction parameters upon the final product composition. Recueil des Travaux Chimiques des Pays-Bas 105, 176-183.

De Wit, G., Kieboom, A.P.G., van Bekkum, H., 1979. Enolisation and isomerisation of monosaccharides in aqueous, alkaline solution. Carbohydrate Research 74, 157-175.

De, S., Dutta, S., Patra, A.K., Rana, B.S., Sinha, A.K., Saha, B., Bhaumik, A., 2012. Biopolymer templated porous TiO2: An efficient catalyst for the conversion of unutilized sugars derived from hemicellulose. Applied Catalysis A: General 435-436, 197-203.

De, S., Dutta, S., Saha, B., 2011. Microwave assisted conversion of carbohydrates and biopolymers to 5-hydroxymethylfurfural with aluminium chloride catalyst in water. Green Chemistry 13, 2859-2868.

De, S., Dutta, S., Saha, B., 2016. Critical design of heterogeneous catalysts for biomass valorization: Current thrust and emerging prospects. Catalysis Science and Technology 6, 7364-7385.

Decolatti, H.P., Dalla Costa, B.O., Querini, C.A., 2015. Dehydration of glycerol to acrolein using H-ZSM5 zeolite modified by alkali treatment with NaOH. Microporous and Mesoporous Materials 204, 180-189.

Delidovich, I., Leonhard, K., Palkovits, R., 2014. Cellulose and hemicellulose valorisation: An integrated challenge of catalysis and reaction engineering. Energy and Environmental Science 7, 2803-2830.

Delidovich, I., Palkovits, R., 2015. Structure-performance correlations of Mg-Al hydrotalcite catalysts for the isomerization of glucose into fructose. Journal of Catalysis 327, 1-9.

Delidovich, I., Palkovits, R., 2016. Catalytic Isomerization of Biomass-Derived Aldoses: A Review. ChemSusChem 9, 547-561.

Deshpande, N., Pattanaik, L., Whitaker, M.R., Yang, C.-T., Lin, L.-C., Brunelli, N.A., 2017. Selectively converting glucose to fructose using immobilized tertiary amines. Journal of Catalysis 353, 205-210.

Díaz, J.F., Balkus Jr, K.J., 1996. Enzyme immobilization in MCM-41 molecular sieve. Journal of Molecular Catalysis B: Enzymatic 2, 115-126.

Dijkmans, J., Dusselier, M., Janssens, W., Trekels, M., Vantomme, A., Breynaert, E., Kirschhock, C., Sels, B.F., 2016. An Inner-/Outer-Sphere Stabilized Sn Active Site in β-Zeolite: Spectroscopic Evidence and Kinetic Consequences. ACS Catalysis 6, 31-46.

Dos Reis, S.C.M., Lachter, E.R., Nascimento, R.S.V., Rodrigues Jr, J.A., Reid, M.G., 2005. Transesterification of Brazilian vegetable oils with methanol over ion-exchange resins. JAOCS, Journal of the American Oil Chemists' Society 82, 661-665.

Dzwigaj, S., Millot, Y., Méthivier, C., Che, M., 2010. Incorporation of Nb(V) into BEA zeolite investigated by XRD, NMR, IR, DR UV-vis, and XPS. Microporous and Mesoporous Materials 130, 162-166.

El Khadem, H.S., Ennifar, S., Isbell, H.S., 1989. Evidence of stable hydrogen-bonded ions during isomerization of hexoses in alkali. Carbohydrate Research 185, 51-59.

Elliott, D.C., Biller, P., Ross, A.B., Schmidt, A.J., Jones, S.B., 2015. Hydrothermal liquefaction of biomass: Developments from batch to continuous process. Bioresource Technology 178, 147-156.

Elumalai, S., Agarwal, B., Sangwan, R.S., 2016. Thermo-chemical pretreatment of rice straw for further processing for levulinic acid production. Bioresource Technology 218, 232-246.

Ennaert, T., Geboers, J., Gobechiya, E., Courtin, C.M., Kurttepeli, M., Houthoofd, K., Kirschhock, C.E.A., Magusin, P.C.M.M., Bals, S., Jacobs, P.A., Sels, B.F., 2015. Conceptual frame rationalizing the self-stabilization of H-USY zeolites in hot liquid water. ACS Catalysis 5, 754-768.

Ennaert, T., Op De Beeck, B., Vanneste, J., Smit, A.T., Huijgen, W.J.J., Vanhulsel, A., Jacobs, P.A., Sels, B.F., 2016a. The importance of pretreatment and feedstock purity in the reductive splitting of (ligno)cellulose by metal supported USY zeolite. Green Chemistry 18, 2095-2105.

Ennaert, T., Van Aelst, J., Dijkmans, J., De Clercq, R., Schutyser, W., Dusselier, M., Verboekend, D., Sels, B.F., 2016b. Potential and challenges of zeolite chemistry in the catalytic conversion of biomass. Chemical Society Reviews 45, 584-611.

Estevez, R., Lopez-Pedrajas, S., Blanco-Bonilla, F., Luna, D., Bautista, F.M., 2015. Production of acrolein from glycerol in liquid phase on heterogeneous catalysts. Chemical Engineering Journal 282, 179-186.

Ezzah-Mahmudah, S., Lokman, I.M., Saiman, M.I., Taufiq-Yap, Y.H., 2016. Synthesis and characterization of Fe2O3/CaO derived from Anadara Granosa for methyl ester production. Energy Conversion and Management 126, 124-131.

Faba, L., Criado, Y.A., Gallegos-Suarez, E., Perez-Cadenas, M., Diaz, E., Rodriguez-

Ramos, I., Guerrero-Ruiz, A., Ordonez, S. 2013. Preparation of nitrogen-containing carbon nanotubes and study of their performance as basic catalysts. Applied Catalysis A: General 458, 155-161.

Fadhil, A.B., Aziz, A.M., Altamer, M.H., 2016. Potassium acetate supported on activated carbon for transesterification of new non-edible oil, bitter almond oil. Fuel 170, 130-140.

Fan, J., De Bruyn, M., Budarin, V.L., Gronnow, M.J., Shuttleworth, P.S., Breeden, S., Macquarrie, D.J., Clark, J.H., 2013a. Direct microwave-assisted hydrothermal depolymerization of cellulose. Journal of the American Chemical Society 135, 12728-12731.

Fan, J., De bruyn, M., Zhu, Z., Budarin, V., Gronnow, M., Gomez, L.D., Macquarrie, D., Clark, J., 2013b. Microwave-enhanced formation of glucose from cellulosic waste. Chemical Engineering and Processing: Process Intensification 71, 37-42.

Fang, Z., Zhang, F., Zeng, H.Y., Guo, F., 2011. Production of glucose by hydrolysis of cellulose at 423K in the presence of activated hydrotalcite nanoparticles. Bioresource Technology 102, 8017-8021.

Fenn, T.D., Ringe, D., Petsko, G.A., 2004. Xylose isomerase in substrate and inhibitor michaelis states: Atomic resolution studies of a metal-mediated hydride shift. Biochemistry 43, 6464-6474.

Ferreira, L.R., Lima, S., Neves, P., Antunes, M.M., Rocha, S.M., Pillinger, M., Portugal, I., Valente, A.A., 2013. Aqueous phase reactions of pentoses in the presence of nanocrystalline zeolite beta: Identification of by-products and kinetic modelling. Chemical Engineering Journal 215-216, 772-783.

Filiciotto, L., Balu, A.M., Van der Waal, J.C., Luque, R., 2018. Catalytic insights into the production of biomass-derived side products methyl levulinate, furfural and humins. Catalysis Today 302, 2-15.

Flannelly, T., Lopes, M., Kupiainen, L., Dooley, S., Leahy, J.J., 2016. Non-stoichiometric formation of formic and levulinic acids from the hydrolysis of biomass derived hexose carbohydrates. RSC Advances 6, 5797-5804.

Foo, G.S., Van Pelt, A.H., Krötschel, D., Sauk, B.F., Rogers, A.K., Jolly, C.R., Yung, M.M., Sievers, C., 2015. Hydrolysis of Cellobiose over Selective and Stable Sulfonated Activated Carbon Catalysts. ACS Sustainable Chemistry and Engineering 3, 1934-1942.

Foston, M., Ragauskas, A.J., 2010. Changes in lignocellulosic supramolecular and ultrastructure during dilute acid pretreatment of Populus and switchgrass. Biomass and Bioenergy 34, 1885-1895.

Francavilla, M., Intini, S., Luchetti, L., Luque, R., 2017. Tunable microwave-assisted aqueous conversion of seaweed-derived agarose for the selective production of 5-hydroxymethyl furfural/levulinic acid. Green Chemistry 18, 5971-5977.

Gade, S.M., Munshi, M.K., Chherawalla, B.M., Rane, V.H., Kelkar, A.A., 2012. Synthesis of glycidol from glycerol and dimethyl carbonate using ionic liquid as a catalyst. Catalysis Communications 27, 184-188.

Gallo, J.M.R., Alamillo, R., Dumesic, J.A., 2016. Acid-functionalized mesoporous carbons for the continuous production of 5-hydroxymethylfurfural. Journal of Molecular Catalysis A: Chemical 422, 13-17.

Gallo, J.M.R., Alonso, D.M., Mellmer, M.A., Dumesic, J.A., 2013. Production and upgrading of 5-hydroxymethylfurfural using heterogeneous catalysts and biomass-derived solvents. Green Chemistry 15, 85-90.

Gardner, D.W., Huo, J., Hoff, T.C., Johnson, R.L., Shanks, B.H., Tessonnier, J.P., 2015. Insights into the Hydrothermal Stability of ZSM-5 under Relevant Biomass Conversion Reaction Conditions. ACS Catalysis 5, 4418-4422.

Geng, L., Wang, Y., Yu, G., Zhu, Y., 2011. Efficient carbon-based solid acid catalysts for the esterification of oleic acid. Catalysis Communications 13, 26-30.

Genovese, M., Jiang, J., Lian, K., Holm, N., 2015. High capacitive performance of exfoliated biochar nanosheets from biomass waste corn cob. Journal of Materials Chemistry A 3, 2903-2913.

Geun Goo, B., Baek, G., Jin Choi, D., Il Park, Y., Synytsya, A., Bleha, R., Ho Seong, D., Lee, C.G., Kweon Park, J., 2013. Characterization of a renewable extracellular polysaccharide from defatted microalgae Dunaliella tertiolecta. Bioresource Technology 129, 343-350.

Ghasimi, D.S.M., Zandvoort, M.H., Adriaanse, M., van Lier, J.B., de Kreuk, M., 2016. Comparative analysis of the digestibility of sewage fine sieved fraction and hygiene paper produced from virgin fibers and recycled fibers. Waste Management 53, 156-164.

Giang, C.H., Osatiashtiani, A., dos Santos, V.C., Lee, A.F., Wilson, D.R., Waldron, K.W., Wilson, K., 2014. Valorisation of vietnamese rice straw waste: Catalytic aqueous phase reforming of hydrolysate from steam explosion to platform chemicals. Catalysts 4, 414-426.

Girisuta, B., Janssen, L.P.B.M., Heeres, H.J., 2007. Kinetic study on the acid-catalyzed hydrolysis of cellulose to levulinic acid. Industrial and Engineering Chemistry Research 46, 1696-1708.

Glasnov, T.N., Kappe, C.O., 2011. The microwave-to-flow paradigm: Translating high-temperature batch microwave chemistry to scalable continuous-flow processes. Chemistry - A European Journal 17, 11956-11968.

Gorgulho, H.F., Gonçalves, F., Pereira, M.F.R., Figueiredo, J.L., 2009. Synthesis and characterization of nitrogen-doped carbon xerogels. Carbon 47, 2032-2039.

Goux, W.J., 1985. Complex isomerization of ketoses_a carbon-13 NMR study of the base-catalyzed ring-opening and ring-closing rates of D-fructose isomers in aqueous solution. J. Am. Chem. Soc. 107, 4320-4327.

Graça, I., Bacariza, M.C., Fernandes, A., Chadwick, D., 2018. Desilicated NaY zeolites impregnated with magnesium as catalysts for glucose isomerisation into fructose. Applied Catalysis B: Environmental 224, 660-670.

Guo, H., Lian, Y., Yan, L., Qi, X., Smith, R.L., 2013. Cellulose-derived superparamagnetic carbonaceous solid acid catalyst for cellulose hydrolysis in an ionic liquid or aqueous reaction system. Green Chemistry 15, 2167-2174.

Guo, R.-Y., An, Z.-M., Mo, L.-P., Yang, S.-T., Liu, H.-X., Wang, S.-X., Zhang, Z.-H., 2013. Meglumine promoted one-pot, four-component synthesis of pyranopyrazole derivatives. Tetrahedron 69, 9931-9938.

Gürbüz, E.I., Alonso, D.M., Bond, J.Q., Dumesic, J.A., 2011. Reactive extraction of levulinate esters and conversion to γ-Valerolactone for production of liquid fuels. ChemSusChem 4, 357-361.

Gürbüz, E.I., Gallo, J.M.R., Alonso, D.M., Wettstein, S.G., Lim, W.Y., Dumesic, J.A., 2013. Conversion of hemicellulose into furfural using solid acid catalysts in γ-valerolactone. Angewandte Chemie - International Edition 52, 1270-1274.

Gurgel, L.V.A., Marabezi, K., Zanbom, M.D., Curvelo, A.A.D.S., 2012. Dilute acid hydrolysis of sugar cane bagasse at high temperatures: A Kinetic study of cellulose saccharification and glucose decomposition. Part I: Sulfuric acid as the catalyst. Industrial and Engineering Chemistry Research 51, 1173-1185.

Halim, S.F.A., Harun Kamaruddin, A., 2008. Catalytic studies of lipase on FAME production from waste cooking palm oil in a tert-butanol system. Process Biochemistry 43, 1436-1439.

Hara, M., 2010. Biomass conversion by a solid acid catalyst. Energy and Environmental Science 3, 601-607.

He, J., Xu, Y., Ma, H., Zhang, Q., Evans, D.G., Duan, X., 2006. Effect of surface hydrophobicity/hydrophilicity of mesoporous supports on the activity of immobilized lipase. Journal of Colloid and Interface Science 298, 780-786.

He, Y., Hoff, T.C., Emdadi, L., Wu, Y., Bouraima, J., Liu, D., 2014. Catalytic consequences of micropore topology, mesoporosity, and acidity on the hydrolysis of sucrose over zeolite catalysts. Catalysis Science and Technology 4, 3064-3073.

He, Y., Pang, Y., Liu, Y., Li, X., Wang, K., 2008. Physicochemical characterization of rice straw pretreated with sodium hydroxide in the solid state for enhancing biogas production. Energy and Fuels 22, 2775-2781.

Helms, B., Guillaudeu, S.J., Xie, Y., McMurdo, M., Hawker, C.J., Fréchet, J.M.J., 2005. One-pot reaction cascades using star polymers with core-confined catalysts. Angew. Chem. 117, 6542-6545.

Hill, C.L., 2007. Progress and challenges in polyoxometalate-based catalysis and catalytic materials chemistry. Journal of Molecular Catalysis A: Chemical 262, 2-6.

Hk, E.P.D., 2015. Monitoring of Solid Waste in Hong Kong: Waste Statistics for 2011. Monitoring of Solid Waste in Hong Kong - Waste Statistics for 2013.

Hlekelele, L., Franklyn, P.J., Tripathi, P.K., Durbach, S.H., 2016. Morphological and crystallinity differences in nitrogen-doped carbon nanotubes grown by chemical vapour deposition decomposition of melamine over coal fly ash. RCS Advances 6, 76773-76779.

Hsu, A.F., Jones, K., Marmer, W.N., Foglia, T.A., 2001. Production of alkyl esters from tallow and grease using lipase immobilized in a phyllosilicate sol-gel. JAOCS, Journal of the American Oil Chemists' Society 78, 585-588.

Hu, K., Wang, H., Liu, Y., Yang, C., 2015a. KNO<inf>3</inf>/CaO as cost-effective heterogeneous catalyst for the synthesis of glycerol carbonate from glycerol and dimethyl carbonate. Journal of Industrial and Engineering Chemistry 28, 334-343.

Hu, L., Li, Z., Wu, Z., Lin, L., Zhou, S., 2016. Catalytic hydrolysis of microcrystalline and rice straw-derived cellulose over a chlorine-doped magnetic carbonaceous solid acid. Industrial Crops and Products 84, 408-417.

Hu, L., Lin, L., Wu, Z., Zhou, S., Liu, S., 2015b. Chemocatalytic hydrolysis of cellulose into glucose over solid acid catalysts. Applied Catalysis B: Environmental 174-175, 225-243.

Hu, S., Smith, T.J., Lou, W., Zong, M., 2014. Efficient hydrolysis of cellulose over a novel sucralose-derived solid acid with cellulose-binding and catalytic sites. Journal of Agricultural and Food Chemistry 62, 1905-1911.

Hu, X., Lievens, C., Larcher, A., Li, C.Z., 2011. Reaction pathways of glucose during esterification: Effects of reaction parameters on the formation of humin type polymers.

Bioresource Technology 102, 10104-10113.

Huang, Y.B., Fu, Y., 2013. Hydrolysis of cellulose to glucose by solid acid catalysts. Green Chemistry 15, 1095-1111.

Huang, Z., Cui, F., Kang, H., Chen, J., Zhang, X., Xia, C., 2008. Highly dispersed silica-supported copper nanoparticles prepared by precipitation-gel method: A simple but efficient and stable catalyst for glycerol hydrogenolysis. Chemistry of Materials 20, 5090-5099.

Huber, G.W., Iborra, S., Corma, A., 2006. Synthesis of Transportation Fuels from Biomass: Chemistry, Catalysts, and Engineering. Chemical Reviews 106, 4044-4098.

Huntley, C.J., Crews, K.D., Abdalla, M.A., Russell, A.E., Curry, M.L., 2015. Influence of strong acid hydrolysis processing on the thermal stability and crystallinity of cellulose isolated from wheat straw. International Journal of Chemical Engineering 2015.

Igalavithana, A.D., Mandal, S., Niazi, N.K., Vithanage, M., Parikh, S.J., Mukome, F.N.D., Rizwan, M., Oleszczuk, P., Al-Wabel, M., Bolan, N.S., Tsang, D.C.W., Kim, K.H., Ok, Y.S. Advances and future directions of biochar characterization methods and applications. Crit. Rev. Environmental Science & Technology 2017, 23, 2275-2230.

Imteyaz Alam, M., De, S., Dutta, S., Saha, B., 2012. Solid-acid and ionic-liquid catalyzed one-pot transformation of biorenewable substrates into a platform chemical and a promising biofuel. RSC Advances 2, 6890-6896.

Ishida, K., Matsuda, S., Watanabe, M., Kitajima, H., Kato, A., Iguchi, M., Aida, T.M., Smith, R.L., Qi, X., Tago, T., Masuda, T., 2014. Hydrolysis of cellulose to produce glucose with solid acid catalysts in 1-butyl-3-methyl-imidazolium chloride ([bmIm][Cl]) with sequential water addition. Biomass Conversion and Biorefinery 4, 323-331.

Jacobs, P.A., Dusselier, M., Sels, B.F., 2014. Will zeolite-based catalysis be as relevant in future biorefineries as in crude oil refineries? Angewandte Chemie - International Edition 53, 8621-8626.

Jae, J., Tompsett, G.A., Foster, A.J., Hammond, K.D., Auerbach, S.M., Lobo, R.F., Huber, G.W., 2011. Investigation into the shape selectivity of zeolite catalysts for biomass conversion. Journal of Catalysis 279, 257-268.

Jagtap, S., Yenkie, M.K.N., Labhsetwar, N., Rayalu, S., 2011. Defluoridation of drinking water using chitosan based mesoporous alumina. Microporous and Mesoporous Materials 142, 454-463.

Jeong, J., Antonyraj, C.A., Shin, S., Kim, S., Kim, B., Lee, K.Y., Cho, J.K., 2013. Commercially attractive process for production of 5-hydroxymethyl-2-furfural from high fructose corn syrup. Journal of Industrial and Engineering Chemistry 19, 1106-1111.

Jeong, K.H., Choi, D.H., Lee, D.J., Kim, J.K., Kim, H., Ok, Y.S., Kwon, E.E., 2018. CO2-looping in pyrolysis of horse manure using CaCO3, Journal Cleaner Production 174, 616-624.

Jiang, Y., Li, X., Wang, X., Meng, L., Wang, H., Peng, G., Wang, X., Mu, X., 2012. Effective saccharification of lignocellulosic biomass over hydrolysis residue derived solid acid under microwave irradiation. Green Chemistry 14, 2162-2167.

Jiménez-Morales, I., Moreno-Recio, M., Santamaría-González, J., Maireles-Torres, P., Jiménez-López, A., 2014a. Mesoporous tantalum oxide as catalyst for dehydration of glucose to 5-hydroxymethylfurfural. Applied Catalysis B: Environmental 154-155, 190-196.

Jiménez-Morales, I., Santamaría-González, J., Maireles-Torres, P., Jiménez-López, A., 2011. Calcined zirconium sulfate supported on MCM-41 silica as acid catalyst for ethanolysis of sunflower oil. Applied Catalysis B: Environmental 103, 91-98.

Jiménez-Morales, I., Teckchandani-Ortiz, A., Santamaría-González, J., Maireles-Torres, P., Jiménez-López, A., 2014b. Selective dehydration of glucose to 5-hydroxymethylfurfural on acidic mesoporous tantalum phosphate. Applied Catalysis B: Environmental 144, 22-28.

Joo, H.W., Kim, Y.J., Park, J., Chang, Y.K., 2017. Hydrolysis of Golenkinia sp. biomass using Amberlyst 36 and nitric acid as catalysts. Algal Research 25, 32-38.

Käldström, M., Kumar, N., Tenho, M., Mokeev, M.V., Moskalenko, Y.E., Murzin, D.Y., 2012. Catalytic transformations of birch kraft pulp. ACS Catalysis 2, 1381-1393.

Karimi, B., Vafaeezadeh, M., 2012. SBA-15-functionalized sulfonic acid confined acidic ionic liquid: A powerful and water-tolerant catalyst for solvent-free esterifications. Chemical Communications 48, 3327-3329.

Kazi, F.K., Patel, A.D., Serrano-Ruiz, J.C., Dumesic, J.A., Anex, R.P., 2011. Techno-economic analysis of dimethylfuran (DMF) and hydroxymethylfurfural (HMF) production from pure fructose in catalytic processes. Chemical Engineering Journal 169, 329-338.

Kim, B., Antonyraj, C.A., Kim, Y.J., Kim, B., Shin, S., Kim, S., Lee, K.Y., Cho, J.K., 2014. Facile production of 5-hydroxymethyl-2-furfural from industrially supplied fructose syrup using a wood powder-derived carbon catalyst in an ethylene glycol-based solvent. Industrial and Engineering Chemistry Research 53, 4633-4641.

Kim, S.J., Dwiatmoko, A.A., Choi, J.W., Suh, Y.W., Suh, D.J., Oh, M., 2010. Cellulose pretreatment with 1-n-butyl-3-methylimidazolium chloride for solid acid-catalyzed hydrolysis. Bioresource Technology 101, 8273-8279.

Kitajima, H., Higashino, Y., Matsuda, S., Zhong, H., Watanabe, M., Aida, T.M., Smith, R.L., 2016. Isomerization of glucose at hydrothermal condition with TiO2, ZrO2, CaO-doped ZrO2or TiO2-doped ZrO2. Catalysis Today 274, 67-72.

Kitano, M., Yamaguchi, D., Suganuma, S., Nakajima, K., Kato, H., Hayashi, S., Hara, M., 2009. Adsorption-enhanced hydrolysis of /?-1,4-glucan on graphene-based amorphous carbon bearing so3H, COOH, and OH groups. Langmuir 25, 5068-5075.

Kobayashi, H., Komanoya, T., Hara, K., Fukuoka, A., 2010. Water-tolerant mesoporous-carbon-supported ruthenium catalysts for the hydrolysis of cellulose to glucose. ChemSusChem 3, 440-443.

Kozhevnikov, I.V., 2009. Heterogeneous acid catalysis by heteropoly acids: Approaches to catalyst deactivation. Journal of Molecular Catalysis A: Chemical 305, 104-111.

Kreissl, H.T., Nakagawa, K., Peng, Y.K., Koito, Y., Zheng, J., Tsang, S.C.E., 2016. Niobium oxides: Correlation of acidity with structure and catalytic performance in sucrose conversion to 5-hydroxymethylfurfural. Journal of Catalysis 338, 329-339.

Kruger, J.S., Nikolakis, V., Vlachos, D.G., 2012. Carbohydrate dehydration using porous catalysts. Current Opinion in Chemical Engineering 1, 312-320.

Kubička, D., Kikhtyanin, O., 2015. Opportunities for zeolites in biomass upgrading-Lessons from the refining and petrochemical industry. Catalysis Today 243, 10-22.

Kumar, V.B., Pulidindi, I.N., Mishra, R.K., Gedanken, A., 2016. Development of Ga Salt of Molybdophosphoric Acid for Biomass Conversion to Levulinic Acid. Energy and Fuels 30, 10583-10591.

Kuster, B.F.M., 1990. 5 - Hydroxymethylfurfural (HMF). A Review Focussing on its Manufacture. Starch - Stärke 42, 314-321.

Lacerda, T.M., Zambon, M.D., Frollini, E., 2013. Effect of acid concentration and pulp properties on hydrolysis reactions of mercerized sisal. Carbohydrate Polymers 93, 347-356.

Lai, D.M., Deng, L., Guo, Q.X., Fu, Y., 2011. Hydrolysis of biomass by magnetic solid acid. Energy and Environmental Science 4, 3552-3557.

Langlois, D.P., Larson, R.F., Patent, U.S., 1956. 2746889.

Lanzafame, P., Temi, D.M., Perathoner, S., Spadaro, A.N., Centi, G., 2012. Direct conversion of cellulose to glucose and valuable intermediates in mild reaction conditions over solid acid catalysts. Catalysis Today 179, 178-184.

Lee, H.I., Lee, Y.Y., Kang, D.U., Lee, K., Kwon, Y.U., Kim, J.M., 2016. Self-arrangement of nanoparticles toward crystalline metal oxides with high surface areas and tunable 3D mesopores. Scientific Reports 6.

Lee, J.W., Jeffries, T.W., 2011. Efficiencies of acid catalysts in the hydrolysis of lignocellulosic biomass over a range of combined severity factors. Bioresource Technology 5884-5890.

Lew, C.M., Rajabbeigi, N., Tsapatsis, M., 2012. Tin-containing zeolite for the isomerization of cellulosic sugars. Microporous and Mesoporous Materials 153, 55-58.

Lewis, J.D., Van De Vyver, S., Crisci, A.J., Gunther, W.R., Michaelis, V.K., Griffin, R.G., Román-Leshkov, Y., 2014. A continuous flow strategy for the coupled transfer hydrogenation and etherification of 5-(hydroxymethyl)furfural using lewis acid zeolites. ChemSusChem 7, 2255-2265.

Li, B., Li, L., Zhang, Q., Weng, W., Wan, H., 2017. Attapulgite as natural catalyst for glucose isomerization to fructose in water. Catalysis Communications 99, 20-24.

Li, G., Pidko, E.A., Hensen, E.J.M., 2016a. A Periodic DFT Study of Glucose to Fructose Isomerization on Tungstite (WO3·H2O): Influence of Group IV-VI Dopants and Cooperativity with Hydroxyl Groups. ACS Catalysis 6, 4162-4169.

Li, H., Yang, S., Riisager, A., Pandey, A., Sangwan, R.S., Saravanamurugan, S., Luque, R., 2016. Zeolite and zeotype-catalysed transformations of biofuranic compounds. Green Chemistry 18, 5701-5735.

Li, H., Yang, S., Saravanamurugan, S., Riisager, A., 2017a. Glucose Isomerization by Enzymes and Chemo-catalysts: Status and Current Advances. ACS Catalysis 7, 3010-3029.

Li, M., Liu, Q., Lou, Z., Wang, Y., Zhang, Y., Qian, G., 2014. Method to characterize acid-base behavior of biochar: Site modeling and theoretical simulation. ACS Sustainable Chemistry Engineering 2, 2501-2509.

Li, S., Qian, E.W., Shibata, T., Hosomi, M., 2012a. Catalytic hydrothermal saccharification of rice straw using mesoporous silica-based solid acid catalysts. Journal of the Japan Petroleum Institute 55, 250-260.

Li, S.X., Li, M.F., Yu, P., Fan, Y.M., Shou, J.N., Sun, R.C., 2017b. Valorization of bamboo by Γ-valerolactone/acid/water to produce digestible cellulose, degraded sugars and lignin. Bioresource Technology 230, 90-96.

Li, X., Jiang, Y., Wang, L., Meng, L., Wang, W., Mu, X., 2012b. Effective low-temperature hydrolysis of cellulose catalyzed by concentrated H3PW12O40under microwave irradiation. RSC Advances 2, 6921-6925.

Li, X., Luque-Moreno, L.C., Oudenhoven, S.R.G., Rehmann, L., Kersten, S.R.A., Schuur, B., 2016b. Aromatics extraction from pyrolytic sugars using ionic liquid to enhance sugar fermentability. Bioresource Technology 216, 12-18.

Li, X., Peng, K., Xia, Q., Liu, X., Wang, Y., 2018. Efficient conversion of cellulose into 5-hydroxymethylfurfural over niobia/carbon composites. Chemistry Engineering Journal 332, 528-536.

Lim, L.H., Saville, B.A., 2007. Thermoinactivation mechanism of glucose isomerase. Appl. BioChemistry BioTechnology 137, 115-130.

Lima, S., Dias, A.S., Lin, Z., Brandão, P., Ferreira, P., Pillinger, M., Rocha, J., Calvino-Casilda, V., Valente, A.A., 2008. Isomerization of d-glucose to d-fructose over metallosilicate solid bases. Applied Catalysis A: General 339, 21-27.

Lin, C.S.K., Pfaltzgraff, L.A., Herrero-Davila, L., Mubofu, E.B., Abderrahim, S., Clark, J.H., Koutinas, A.A., Kopsahelis, N., Stamatelatou, K., Dickson, F., Thankappan, S., Mohamed, Z., Brocklesby, R., Luque, R., 2013. Food waste as a valuable resource for the production of chemicals, materials and fuels. Current situation and global perspective. Energy and Environmental Science 6, 426-464.

Liu, B., Zhang, Z., Zhao, Z.K., 2013. Microwave-assisted catalytic conversion of cellulose into 5-hydroxymethylfurfural in ionic liquids. Chemical Engineering Journal 215-216, 517-521.

Liu, C., Carraher, J.M., Swedberg, J.L., Herndon, C.R., Fleitman, C.N., Tessonnier, J.-P., 2014. Selective Base-Catalyzed Isomerization of Glucose to Fructose. ACS Catalysis 4, 4295-4298.

Liu, F., Wang, L., Sun, Q., Zhu, L., Meng, X., Xiao, F.S., 2012. Transesterification catalyzed by ionic liquids on superhydrophobic mesoporous polymers: Heterogeneous catalysts that are faster than homogeneous catalysts. Journal of the American Chemical Society 134, 16948-16950.

Liu, Q., Wang, B., Wang, C., Tian, Z., Qu, W., Ma, H., Xu, R., 2014b. Basicities and transesterification activities of Zn-Al hydrotalcites- derived solid bases. Green Chemistry 16, 2604-2613.

Liu, Y., Li, Y., Li, X.M., He, T., 2013. Kinetics of (3-aminopropyl)triethoxylsilane (APTES) silanization of superparamagnetic iron oxide nanoparticles. Langmuir 29, 15275-15282.

Liu, Z., Wang, J., Kang, M., Yin, N., Wang, X., Tan, Y., Zhu, Y., 2015. Structure-activity correlations of LiNO3 Mg4AlO5.5 catalysts for glycerol carbonate synthesis from glycerol and dimethyl carbonate. Journal of Industrial and Engineering Chemistry 21, 394-399.

Loerbroks, C., Rinaldi, R., Thiel, W., 2013. The electronic nature of the 1,4-β-glycosidic bond and its chemical environment: DFT insights into cellulose chemistry. Chemistry - A European Journal 19, 16282-16294.

López, D.E., Goodwin Jr, J.G., Bruce, D.A., Furuta, S., 2008. Esterification and transesterification using modified-zirconia catalysts. Applied Catalysis A: General 339, 76-83.

Lu, Q.L., Li, X.Y., Tang, L.R., Lu, B.L., Huang, B., 2015. One-pot tandem reactions for the preparation of esterified cellulose nanocrystals with 4-dimethylaminopyridine as a catalyst. RSC Advances 5, 56198-56204.

Lucas-Torres, C., Lorente, A., Cabañas, B., Moreno, A., 2016. Microwave heating for the catalytic conversion of melon rind waste into biofuel precursors. Journal of Cleaner Production 138, 59-69.

Luo, H.Y., Lewis, J.D., Román-Leshkov, Y., 2016. Lewis Acid Zeolites for Biomass Conversion: Perspectives and Challenges on Reactivity, Synthesis, and Stability. Annual Review of Chemical and Biomolecular Engineering 7, 663-692.

Luterbacher, J.S., Rand, J.M., Alonso, D.M., Han, J., Youngquist, J.T., Maravelias, C.T., Pfleger, B.F., Dumesic, J.A., 2014. Nonenzymatic sugar production from biomass using biomass-derived γ-valerolactone. Science 343, 277-280.

Ma, Y., Wang, Q., Zheng, L., Gao, Z., Wang, Q., Ma, Y., 2016. Mixed methanol/ethanol on transesterification of waste cooking oil using Mg/Al hydrotalcite catalyst. Energy 107, 523-531.

Macht, J., Janik, M.J., Neurock, M., Iglesia, E., 2007. Catalytic consequences of composition in polyoxometalate clusters with keggin structure. Angewandte Chemie - International Edition 46, 7864-7868.

Mäki-Arvela, P., Simakova, I.L., Salmi, T., Murzin, D.Y., 2014. Production of Lactic Acid/Lactates from Biomass and Their Catalytic Transformations to Commodities. Chemical Reviews 114, 1909-1971.

Mal, N.K., Ramaswamy, A.V., 1997. Synthesis and catalytic properties of large-pore Sn-β and Al-free Sn-β molecular sieves. Chemical Communications, 425-426.

Mal, N.K., Ramaswamy, V., Ganapathy, S., Ramaswamy, A.V., 1994. Synthesis and characterization of crystalline, tin-silicate molecular sieves with MFI structure.

Journal of the Chemical Society, Chemical Communications, 1933-1934.

Maleki, E., Aroua, M.K., Sulaiman, N.M.N., 2013. Castor oil - A more suitable feedstock for enzymatic production of methyl esters. Fuel Processing Technology 112, 129-132.

Malihan, L.B., Nisola, G.M., Mittal, N., Lee, S.P., Seo, J.G., Kim, H., Chung, W.J., 2016. SBA-15 supported ionic liquid phase (SILP) with H2PW12O40 for the hydrolytic catalysis of red macroalgal biomass to sugars. RSC Advances 6, 33901-33909.

Malyaadri, M., Jagadeeswaraiah, K., Sai Prasad, P.S., Lingaiah, N., 2011. Synthesis of glycerol carbonate by transesterification of glycerol with dimethyl carbonate over Mg/Al/Zr catalysts. Applied Catalysis A: General 401, 153-157.

Marianou, A.A., Michailof, C.M., Pineda, A., Iliopoulou, E.F., Triantafyllidis, K.S., Lappas, A.A., 2016. Glucose to Fructose Isomerization in Aqueous Media over Homogeneous and Heterogeneous Catalysts. ChemCatChem 8, 1100-1110.

Maris, E.P., Ketchie, W.C., Murayama, M., Davis, R.J., 2007. Glycerol hydrogenolysis on carbon-supported PtRu and AuRu bimetallic catalysts. Journal of Catalysis 251, 281-294.

Marshall, W.L., Jones, E.V., 1966. Second dissociation constant of sulfuric acid from 25 to 350° evaluated from solubilities of calcium sulfate in sulfuric acid solutions. Journal of Physical Chemistry 70, 4028-4040.

Matter, P.H., Zhang, L., Ozkan, U.S., 2006. The role of nanostructure in nitrogen-containing carbon catalysts for the oxygen reduction reaction. Journal of Catalysis 239, 83-96.

Mayes, H.B., Tian, J., Nolte, M.W., Shanks, B.H., Beckham, G.T., Gnanakaran, S., Broadbelt, L.J., 2014. Sodium ion interactions with aqueous glucose: insights from quantum mechanics, molecular dynamics, and experiment. J Phys Chem B 118, 1990-2000.

McCusker, L.B., Olson, D.H., Baerlocher, C., 2007. Atlas of Zeolite Framework Types.

McGrath, M.J., Kuo, I.F.W., Ngouana W, B.F., Ghogomu, J.N., Mundy, C.J., Marenich, A.V., Cramer, C.J., Truhlar, D.G., Siepmann, J.I., 2013. Calculation of the Gibbs free energy of solvation and dissociation of HCl in water via Monte Carlo simulations and continuum solvation models. Physical Chemistry Chemical Physics 15, 13578-13585.

Mellmer, M.A., Sanpitakseree, C., Demir, B., Bai, P., Ma, K., Neurock, M., Dumesic, J.A., 2018. Solvent-enabled control of reactivity for liquid-phase reactions of biomass-derived compounds. Nature Catalysis 1, 199-207.

Mellmer, M.A., Sener, C., Gallo, J.M.R., Luterbacher, J.S., Alonso, D.M., Dumesic, J.A., 2014. Solvent effects in acid-catalyzed biomass conversion reactions. Angewandte Chemie - International Edition 53, 11872-11875.

Mija, A., van der Waal, J.C., Pin, J.M., Guigo, N., de Jong, E., 2017. Humins as promising material for producing sustainable carbohydrate-derived building materials. Construction and Building Materials 139, 594-601.

Mirabella, N., Castellani, V., Sala, S., 2014. Current options for the valorization of food manufacturing waste: A review. Journal of Cleaner Production 65, 28-41.

Mohd Kamal, N., Wan Abu Bakar, W.A., Ali, R., 2017. Catalytic optimization and physicochemical studies over Zn/Ca/Al2O3 catalyst for transesterification of low grade cooking oil. Energy Conversion and Management 137, 113-120.

Moliner, M., 2014. State of the art of Lewis acid-containing zeolites: Lessons from fine chemistry to new biomass transformation processes. Dalton Transactions 43, 4197-4208.

Moliner, M., Román-Leshkov, Y., Davis, M.E., 2010. Tin-containing zeolites are highly active catalysts for the isomerization of glucose in water. Proceedings of the National Academy of Sciences of the United States of America 107, 6164-6168.

Mondal, S., Mondal, J., Bhaumik, A., 2015. Sulfonated Porous Polymeric Nanofibers as an Efficient Solid Acid Catalyst for the Production of 5-Hydroxymethylfurfural from Biomass. ChemCatChem 7, 3570-3578.

Morales-delaRosa, S., Campos-Martin, J.M., Fierro, J.L.G., 2012. High glucose yields from the hydrolysis of cellulose dissolved in ionic liquids. Chemistry Engineering Journal 181-182, 538-541.

Morawski, A.W., Kusiak-Nejman, E., Przepiórski, J., Kordala, R., Pernak, J., 2013. Cellulose-TiO2 nanocomposite with enhanced UV-Vis light absorption. Cellulose 20, 1293-1300.

Morone, A., Apte, M., Pandey, R.A., 2015. Levulinic acid production from renewable waste resources: Bottlenecks, potential remedies, advancements and applications. Renewable and Sustainable Energy Reviews 51, 548-565.

Mukherjee, A., Dumont, M.J., 2016. Levulinic Acid Production from Starch Using Microwave and Oil Bath Heating: A Kinetic Modeling Approach. Industrial and Engineering Chemistry Research 55, 8941-8949.

Mukherjee, A., Dumont, M.J., Raghavan, V., 2015. Review: Sustainable production of hydroxymethylfurfural and levulinic acid: Challenges and opportunities. Biomass and Bioenergy 72, 143-183.

Nakajima, K., Baba, Y., Noma, R., Kitano, M., N. Kondo, J., Hayashi, S., Hara, M., 2011. Nb2O5•nH2O as a heterogeneous catalyst with water-tolerant lewis acid sites. Journal of the American Chemical Society 133, 4224-4227.

Nakajima, K., Hara, M., 2012. Amorphous carbon with SO3H groups as a solid brønsted acid catalyst. ACS Catalysis 2, 1296-1304.

Nakatani, N., Takamori, H., Takeda, K., Sakugawa, H., 2009. Transesterification of soybean oil using combusted oyster shell waste as a catalyst. Bioresource Technology 100, 1510-1513.

Nanda, S., Dalai, A.K., Kozinski, J.A., 2014. Butanol and ethanol production from lignocellulosic feedstock: Biomass pretreatment and bioconversion. Energy Science and Engineering 2, 138-148.

Nandiwale, K.Y., Galande, N.D., Thakur, P., Sawant, S.D., Zambre, V.P., Bokade, V.V., 2014. One-pot synthesis of 5-hydroxymethylfurfural by cellulose hydrolysis over highly active bimodal micro/mesoporous H-ZSM-5 catalyst. ACS Sustainable Chemistry and Engineering 2, 1928-1932.

Natake, M., 1968. Studies on Glucose Isomerizing Enzyme of Bacteria. Agricultural and Biological Chemistry 32, 303-313.

Nawirska, A., Kwaśniewska, M., 2005. Dietary fibre fractions from fruit and vegetable processing waste. Food Chemistry 91, 221-225.

Nelson, M.L., O'Connor, R.T., 1964. Relation of certain infrared bands to cellulose crystallinity and crystal latticed type. Part I. Spectra of lattice types I, II, III and of amorphous cellulose. Journal of Applied Polymer Science 8, 1311-1324.

Ngee, E.L.S., Gao, Y., Chen, X., Lee, T.M., Hu, Z., Zhao, D., Yan, N., 2014. Sulfated Mesoporous Niobium Oxide Catalyzed 5-Hydroxymethylfurfural formation from sugars. Industrial and Engineering Chemistry Research 53, 14225-14233.

Nhien, L.C., Long, N.V.D., Lee, M., 2016. Design and optimization of the levulinic acid recovery process from lignocellulosic biomass. Chemical Engineering Research and Design 107, 126-136.

Nikolla, E., Román-Leshkov, Y., Moliner, M., Davis, M.E., 2011. "One-pot" synthesis of 5-(hydroxymethyl)furfural from carbohydrates using tin-beta zeolite. ACS Catalysis 1, 408-410.

Noma, R., Nakajima, K., Kamata, K., Kitano, M., Hayashi, S., Hara, M., 2015. Formation of 5-(Hydroxymethyl)furfural by stepwise dehydration over TiO_2 with water-tolerant Lewis acid sites. Journal of Physical Chemistry C 119, 17117-17125.

Ogino, I., Suzuki, Y., Mukai, S.R., 2015. Tuning the pore structure and surface properties of carbon-based acid catalysts for liquid-phase reactions. ACS Catalysis 4951-4958.

Oh, S.J., Park, J., Na, J.G., Oh, Y.K., Chang, Y.K., 2015. Production of 5-hydroxymethylfurfural from agarose by using a solid acid catalyst in dimethyl sulfoxide. RSC Advances 5, 47983-47989.

Oh, W.-D., Lisak, G., Webster, R.D., Insights into the thermolytic transformation of lignocellulosic biomass waste to redox-active carbocatalyst: Durability of surface active sites, Applied Catalysis B: Environment 233, 120-129.

Ohara, M., Takagaki, A., Nishimura, S., Ebitani, K., 2010. Syntheses of 5-hydroxymethylfurfural and levoglucosan by selective dehydration of glucose using solid acid and base catalysts. Applied Catalysis A: General 383, 149-155.

Oickle, A.M., Goertzen, S.L., Hopper, K.R., Abdalla, Y.O., Andreas, H.A., 2010. Standardization of the Boehm titration: Part II. Method of agitation, effect of filtering and dilute titrant. Carbon 48, 3313-3322.

Okuhara, T., Nishimura, T., Watanabe, H., Misono, M., 1992. Insoluble heteropoly compounds as highly active catalysts for liquid-phase reactions. Journal of Molecular Catalysis 74, 247-256.

Olson, N., Deshpande, N., Gunduz, S., Ozkan, U.S., Brunelli, N.A., 2018. Utilizing imogolite nanotubes as a tunable catalytic material for the selective isomerization of glucose to fructose. Catalysis Today.

Onda, A., Ochi, T., Yanagisawa, K., 2008. Selective hydrolysis of cellulose into glucose over solid acid catalysts. Green Chemistry 10, 1033-1037.

Onda, A., Ochi, T., Yanagisawa, K., 2009. Hydrolysis of cellulose selectively into glucose over sulfonated activated-carbon catalyst under hydrothermal conditions. Topics in Catalysis 52, 801-807.

O'Neil, R., Ahmad, M.N., Vanoye, L., Aiouache, F., 2009. Kinetics of aqueous phase dehydration of xylose into furfural catalyzed by ZSM-5 zeolite. Industrial and Engineering Chemistry Research 48, 4300-4306.

Orazov, M., Davis, M.E., 2015. Tandem catalysis for the production of alkyl lactates from ketohexoses at moderate temperatures. Proceedings of the National Academy of Sciences of the United States of America 112, 11777-11782.

Ordomsky, V.V., Schouten, J.C., van der Schaaf, J., Nijhuis, T.A., 2012. Foam supported sulfonated polystyrene as a new acidic material for catalytic reactions.

Chemical Engineering Journal 207-208, 218-225.

Orozco, A.M., Al-Muhtaseb, A.H., Albadarin, A.B., Rooney, D., Walker, G.M., Ahmad, M.N.M., 2011. Acid-catalyzed hydrolysis of cellulose and cellulosic waste using a microwave reactor system. RSC Advances 1, 839-846.

Ortega, K.F., Arrigo, R., Frank, B., Schlögl, R., Trunschke, A., 2016. Acid-base properties of N-doped carbon nanotubes: A combined temperature-programmed desorption, X-ray photoelectron spectroscopy, and 2-propanol reaction investigation. Chemistry of Materials 28, 6826-6839.

Osatiashtiani, A., Lee, A.F., Brown, D.R., Melero, J.A., Morales, G., Wilson, K., 2014. Bifunctional SO4ZrO2; catalysts for 5-hydroxymethylfufural (5-HMF) production from glucose. Catalysis Science and Technology 4, 333-342.

Osatiashtiani, A., Lee, A.F., Granollers, M., Brown, D.R., Olivi, L., Morales, G., Melero, J.A., Wilson, K., 2015. Hydrothermally Stable, Conformal, Sulfated Zirconia Monolayer Catalysts for Glucose Conversion to 5-HMF. ACS Catalysis 5, 4345-4352.

Otomo, R., Yokoi, T., Kondo, J.N., Tatsumi, T., 2014. Dealuminated Beta zeolite as effective bifunctional catalyst for direct transformation of glucose to 5-hydroxymethylfurfural. Applied Catalysis A: General 470, 318-326.

Ouyang, X., Wang, W., Yuan, Q., Li, S., Zhang, Q., Zhao, P., 2015. Improvement of lignin yield and purity from corncob in the presence of steam explosion and liquid hot pressured alcohol. RSC Advances 5, 61650-61656.

Padovan, D., Parsons, C., Simplicio Grasina, M., Hammond, C., 2016. Intensification and deactivation of Sn-beta investigated in the continuous regime. Green Chemistry 18, 5041-5049.

Pang, Q., Wang, L., Yang, H., Jia, L., Pan, X., Qiu, C., 2014. Cellulose-derived carbon bearing -Cl and -SO3H groups as a highly selective catalyst for the hydrolysis of cellulose to glucose. RSC Advances 40, 41212-41218.

Panwar, N.L., Shrirame, H.Y., Rathore, N.S., Jindal, S., Kurchania, A.K., 2010. Performance evaluation of a diesel engine fueled with methyl ester of castor seed oil. Applied Thermal Engineering 30, 245-249.

Parida, K.M., Sahu, N., Mohapatra, P., Scurrell, M.S., 2010. Low temperature CO oxidation over gold supported mesoporous Fe-TiO2. Journal of Molecular Catalysis A: Chemical 319, 92-97.

Park, S., Baker, J.O., Himmel, M.E., Parilla, P.A., Johnson, D.K., 2010. Cellulose crystallinity index: Measurement techniques and their impact on interpreting cellulase performance. Biotechnology for Biofuels 3.

Parshetti, G.K., Suryadharma, M.S., Pham, T.P.T., Mahmood, R., Balasubramanian, R., 2015. Heterogeneous catalyst-assisted thermochemical conversion of food waste biomass into 5-hydroxymethylfurfural. Bioresource Technology 178, 19-27.

Patil, S.K.R., Heltzel, J., Lund, C.R.F., 2012. Comparison of structural features of humins formed catalytically from glucose, fructose, and 5-hydroxymethylfurfuraldehyde. Energy and Fuels 26, 5281-5293.

Pereira Ramos, L., 2003. The chemistry involved in the steam treatment of lignocellulosic materials. Quimica Nova 26, 863-871.

Pileidis, F.D., Titirici, M.M., 2016. Levulinic Acid Biorefineries: New Challenges for Efficient Utilization of Biomass. ChemSusChem 9, 562-582.

Pitochelli, A.R., Rohm, Company, H., 1975. Ion Exchange Catalysis and Matrix Effects. Rohm and Haas.

Pleissner, D., Qi, Q., Gao, C., Rivero, C.P., Webb, C., Lin, C.S.K., Venus, J., 2016. Valorization of organic residues for the production of added value chemicals: A contribution to the bio-based economy. Biochemical Engineering Journal 116, 3-16.

Pu, Y., Hu, F., Huang, F., Davison, B.H., Ragauskas, A.J., 2013. Assessing the molecular structure basis for biomass recalcitrance during dilute acid and hydrothermal pretreatments. Biotechnology for Biofuels 6.

Qi, P., Chen, S., Chen, J., Zheng, J., Zheng, X., Yuan, Y., 2015. Catalysis and reactivation of ordered mesoporous carbon-supported gold nanoparticles for the base-free oxidation of glucose to gluconic acid. ACS Catalysis 5, 2659-2670.

Qi, X., Watanabe, M., Aida, T.M., Smith, J.R.L., 2008. Catalytic dehydration of fructose into 5-hydroxymethylfurfural by ion-exchange resin in mixed-aqueous system by microwave heating. Green Chemistry 10.

Qian, E.W., Sukma, L.P.P., Li, S., Higashi, A., 2016. Saccharification of cellulosic biomass using sulfonated mesoporous carbon-based catalysts. Environmental Progress and Sustainable Energy 35, 574-581.

Qian, X., 2011. Mechanisms and energetics for acid catalyzed β-D-glucose conversion to 5-hydroxymethylfurfurl. Journal of Physical Chemistry A 115, 11740-11748.

Qian, X., Liu, D., 2014. Free energy landscape for glucose condensation and dehydration reactions in dimethyl sulfoxide and the effects of solvent. Carbohydrate Research 388, 50-60.

Qureshi, N., Saha, B.C., Dien, B., Hector, R.E., Cotta, M.A., 2010. Production of butanol (a biofuel) from agricultural residues: Part I - Use of barley straw hydrolysate.

Biomass and Bioenergy 34, 559-565.

Rackemann, D.W., Doherty, W.O., 2011. The conversion of lignocellulosics to levulinic acid. Biofuels, Bioproducts and Biorefining 5, 198-214.

Rajabbeigi, N., Torres, A.I., Lew, C.M., Elyassi, B., Ren, L., Wang, Z., Je Cho, H., Fan, W., Daoutidis, P., Tsapatsis, M., 2014. On the kinetics of the isomerization of glucose to fructose using Sn-Beta. Chemical Engineering Science 116, 235-242.

Rajapaksha, A.U., Chen, S.S., Tsang, D.C.W., Zhang, M., Vithanage, M., Mandal, S., Gao, B., Bolan, N.S., Ok, Y.S., 2016. Engineered/designer biochar for contaminant removal/immobilization from soil and water: Potential and implication of biochar modification. Chemosphere 148, 276-291.

Ramli, N.A.S., Amin, N.A.S., 2014. Catalytic hydrolysis of cellulose and oil palm biomass in ionic liquid to reducing sugar for levulinic acid production. Fuel Processing Technology 128, 490-498.

Ramli, N.A.S., Amin, N.A.S., 2015. Fe/HY zeolite as an effective catalyst for levulinic acid production from glucose: Characterization and catalytic performance. Applied Catalysis B: Environmental 163, 487-498.

Ramli, N.A.S., Amin, N.A.S., 2016. Kinetic study of glucose conversion to levulinic acid over Fe/HY zeolite catalyst. Chemical Engineering Journal 283, 150-159.

Raspolli Galletti, A.M., Antonetti, C., Ribechini, E., Colombini, M.P., Nassi o Di Nasso, N., Bonari, E., 2013. From giant reed to levulinic acid and gamma-valerolactone: A high yield catalytic route to valeric biofuels. Applied Energy 102, 157-162.

Rauf, M., Zhao, Y.-D., Wang, Y.-C., Zheng, Y.-P., Chen, C., Yang, X.-D., Zhou, Z.-Y., Sun, S.-G., 2016. Insight into the different ORR catalytic activity of Fe/N/C between acidic and alkaline media: Protonation of pyridinic nitrogen, Electrochemistry Communications 73, 71-74.

Ravindran, R., Jaiswal, A.K., 2016. A comprehensive review on pre-treatment strategy for lignocellulosic food industry waste: Challenges and opportunities. Bioresource Technology 199, 92-102.

Reche, M.T., Osatiashtiani, A., Durndell, L.J., Isaacs, M.A., Silva, Â., Lee, A.F., Wilson, K., 2016. Niobic acid nanoparticle catalysts for the aqueous phase transformation of glucose and fructose to 5-hydroxymethylfurfural. Catalysis Science and Technology 6, 7334-7341.

Ren, L., Guo, Q., Kumar, P., Orazov, M., Xu, D., Alhassan, S.M., Mkhoyan, K.A., Davis, M.E., Tsapatsis, M., 2015. Self-Pillared, Single-Unit-Cell Sn-MFI Zeolite

Nanosheets and Their Use for Glucose and Lactose Isomerization. Angewandte Chemie - International Edition 54, 10848-10851.

Rinaldi, R., Palkovits, R., Schüth, F., 2008. Depolymerization of cellulose using solid catalysts in ionic liquids. Angewandte Chemie - International Edition 47, 8047-8050.

Ritter, S., 2006. Biorefinery gets ready to deliver the goods. Chemical and Engineering News 84, 47.

Román-Leshkov, Y., Davis, M.E., 2011. Activation of carbonyl-containing molecules with solid lewis acids in aqueous media. ACS Catalysis 1, 1566-1580.

Román-Leshkov, Y., Dumesic, J.A., 2009. Solvent effects on fructose dehydration to 5-hydroxymethylfurfural in biphasic systems saturated with inorganic salts. Topics in Catalysis 52, 297-303.

Román-Leshkov, Y., Moliner, M., Labinger, J.A., Davis, M.E., 2010. Mechanism of glucose isomerization using a solid Lewis acid catalyst in water. Angewandte Chemie International Edition 49, 8954-8957.

Rosenholm, J.M., Linden, M., 2008. Towards establishing structure-activity relationships for mesoporous silica in drug delivery applications. J Control Release 128, 157-164.

Roy, D., Semsarilar, M., Guthrie, J.T., Perrier, S., 2009. Cellulose modification by polymer grafting: A review. Chemical Society Reviews 38, 2046-2064.

Ruiken, C.J., Breuer, G., Klaversma, E., Santiago, T., van Loosdrecht, M.C.M., 2013. Sieving wastewater - Cellulose recovery, economic and energy evaluation. Water Research 47, 43-48.

Runge, T., Zhang, C., 2012. Two-stage acid-catalyzed conversion of carbohydrates into levulinic acid. Industrial and Engineering Chemistry Research 51, 3265-3270.

Russbueldt, B.M.E., Hoelderich, W.F., 2009. New sulfonic acid ion-exchange resins for the

Rys, P., Steinegger, W.J., 1979. Acidity function of solid-bound acids1, 2. Journal of the American Chemical Society 101, 4801-4806.

Sádaba, I., López Granados, M., Riisager, A., Taarning, E., 2015. Deactivation of solid catalysts in liquid media: the case of leaching of active sites in biomass conversion reactions. Green Chemistry 17, 4133-4145.

Sakaki, T., Shibata, M., Sumi, T., Yasuda, S., 2002. Saccharification of cellulose using a hot-compressed water-flow reactor. Industrial and Engineering Chemistry Research 41, 661-665.

Sakintuna, B. and Yürüm, Y., 2004. Evolution of Carbon Microstructures during the Pyrolysis of Turkish Elbistan Lignite in the Temperature Range 700−1000 °C, Energ Fuel. 18, 883-888.

Saravanamurugan, S., Paniagua, M., Melero, J.A., Riisager, A., 2013. Efficient isomerization of glucose to fructose over zeolites in consecutive reactions in alcohol and aqueous media. Journal of the American Chemical Society 135, 5246-5249.

Savage, P.E., Levine, R.B., Huelsman, C.M., 2010. Hydrothermal processing of biomass. RSC Energy and Environment Series, pp. 192-221.

Schmidt, W., 2009. Solid catalysts on the nanoscale: Design of complex morphologies and pore structures. ChemCatChem 1, 53-67.

Schutyser, W., Renders, T., Van den Bosch, S., Koelewijn, S.F., Beckham, G.T., Sels, B.F., 2018. Chemicals from lignin: an interplay of lignocellulose fractionation, depolymerisation, and upgrading. Chem Soc Rev 47, 852-908.

Senthur Prabu, S., Asokan, M.A., Roy, R., Francis, S., Sreelekh, M.K., 2017. Performance, combustion and emission characteristics of diesel engine fuelled with waste cooking oil bio-diesel/diesel blends with additives. Energy 122, 638-648.

Serrano-Ruiz, J.C., Dumesic, J.A., 2011. Catalytic routes for the conversion of biomass into liquid hydrocarbon transportation fuels. Energy and Environmental Science 4, 83-99.

Shanks, B.H., 2007. Unleashing Biocatalysis/Chemical Catalysis Synergies for Efficient Biomass Conversion. ACS Chemical Biology 2, 533-535.

Sharon, M. and Sharon, M., 2012. Effect of Inherent Anatomy of Plant Fibers on the Morphology of Carbon Synthesized from Them and Their Hydrogen Absorption Capacity, Carbon Letter 13, 161-166.

Shen, J., Wyman, C.E., 2012. Hydrochloric acid-catalyzed levulinic acid formation from cellulose: Data and kinetic model to maximize yields. AIChE Journal 58, 236-246.

Shen, S., Cai, B., Wang, C., Li, H., Dai, G., Qin, H., 2014. Preparation of a novel carbon-based solid acid from cocarbonized starch and polyvinyl chloride for cellulose hydrolysis. Applied Catalysis A: General 473, 70-74.

Shen, W., Fan, W., 2013. Nitrogen-containing porous carbons: synthesis and application. J. Materials Chemistry A 1, 999-1013.

Sheng, Z.H., Shao, L., Chen, J.J., Bao, W.J., Wang, F.B., Xia, X.H., 2011. Catalyst-free synthesis of nitrogen-doped graphene via thermal annealing graphite oxide with melamine and its excellent electrocatalysis. ACS Nano 5, 4350-4358.

Shi, J.J., Guan, J.Y., Guo, D.W., Zhang, J.S., France, L.J., Wang, L.F., Li, X.H. 2016. Nitrogen Chemistry and Coke Transformation of FCC Coked Catalyst during the Regeneration Process. Scientific Reports 6.

Shimizu, K.I., Furukawa, H., Kobayashi, N., Itaya, Y., Satsuma, A., 2009. Effects of Brønsted and Lewis acidities on activity and selectivity of heteropolyacid-based catalysts for hydrolysis of cellobiose and cellulose. Green Chemistry 11, 1627-1632.

Shopsowitz, K.E., Hamad, W.Y., MacLachlan, M.J., 2011. Chiral nematic mesoporous carbon derived from nanocrystalline cellulose. Angewandte Chemie - International Edition 50, 10991-10995.

Shuai, L., Luterbacher, J., 2016. Organic Solvent Effects in Biomass Conversion Reactions. ChemSusChem 9, 133-155.

Shuai, L., Pan, X., 2012. Hydrolysis of cellulose by cellulase-mimetic solid catalyst. Energy and Environmental Science 5, 6889-6894.

Simpson, B.K., Nollet, L.M.L., T, F., Benjakul, S., Paliyath, G., Hui, Y.H. (Eds.), 2012. Food Biochemistry and Food Processing. John Wiley & Sons, Inc.

Singh, A.K., Xu, Q., 2013. Synergistic Catalysis over Bimetallic Alloy Nanoparticles. ChemCatChem 5, 652-676.

Singh, J., Suhag, M., Dhaka, A., 2015. Augmented digestion of lignocellulose by steam explosion, acid and alkaline pretreatment methods: A review. Carbohydrate Polymers 117, 624-631.

Singh, V., Sharma, Y.C., 2017. Low cost guinea fowl bone derived recyclable heterogeneous catalyst for microwave assisted transesterification of Annona squamosa L. seed oil. Energy Conversion and Management 138, 627-637.

Siril, P.F., Cross, H.E., Brown, D.R., 2008. New polystyrene sulfonic acid resin catalysts with enhanced acidic and catalytic properties. Journal of Molecular Catalysis A: Chemical 279, 63-68.

Sluiter, A., Hames, B., Ruiz, R., Scarlata, C., Sluiter, J., Templeton, D., 2004. Determination of structural carbohydrates and lignin in biomass. Determination of Structural Carbohydrates and Lignin in Biomass.

Smith, S.M., Oopathum, C., Weeramongkhonlert, V., Smith, C.B., Chaveanghong, S., Ketwong, P., Boonyuen, S., 2013. Transesterification of soybean oil using bovine bone waste as new catalyst. Bioresource Technology 143, 686-690.

Soltani, S., Rashid, U., Al-Resayes, S.I., Nehdi, I.A., 2017. Sulfonated mesoporous ZnO catalyst for methyl esters production. Journal of Cleaner Production 144, 482-491.

Song, X., Li, K., Wang, C., Sun, X., Ning, P., Tang, L., 2017. Regeneration performance and mechanism of modified walnut shell biochar catalyst for low temperature catalytic hydrolysis of organic sulfur. Chemistry Engineering Journal 330, 727-735.

Spark, A.A., 1969. Role of amino acids in non‐enzymic browning. J. Sci. Fd Agric. 20, 308-315.

Speck, J.C., 1958. The Lobry De Bruyn-Alberda Van Ekenstein Transformation. in: Wolfrom, M.L. (Ed.). Advances in Carbohydrate Chemistry. Academic Press, pp. 63-103.

Su, F., Guo, Y., 2014. Advancements in solid acid catalysts for biodiesel production. Green Chemistry 16, 2934-2957.

Sun, B., Duan, L., Peng, G., Li, X., Xu, A., 2015. Efficient production of glucose by microwave-assisted acid hydrolysis of cellulose hydrogel. Bioresource Technology 192, 253-256.

Swift, T.D., Nguyen, H., Anderko, A., Nikolakis, V., Vlachos, D.G., 2015. Tandem Lewis/Brønsted homogeneous acid catalysis: conversion of glucose to 5-hydoxymethylfurfural in an aqueous chromium(III) chloride and hydrochloric acid solution. Green Chemistry 17, 4725-4735.

Swift, T.D., Nguyen, H., Erdman, Z., Kruger, J.S., Nikolakis, V., Vlachos, D.G., 2016. Tandem Lewis acid/Brønsted acid-catalyzed conversion of carbohydrates to 5-hydroxymethylfurfural using zeolite beta. Journal of Catalysis 333, 149-161.

Szabolcs, Á., Molnár, M., Dibó, G., Mika, L.T., 2013. Microwave-assisted conversion of carbohydrates to levulinic acid: An essential step in biomass conversion. Green Chemistry 15, 439-445.

Taarning, E., Saravanamurugan, S., Holm, M.S., Xiong, J., West, R.M., Christensen, C.H., 2009. Zeolite-catalyzed isomerization of triose sugars. ChemSusChem 2, 625-627.

Tabasso, S., Carnaroglio, D., Calcio Gaudino, E., Cravotto, G., 2015. Microwave, ultrasound and ball mill procedures for bio-waste valorisation. Green Chemistry 17, 684-693.

Tabasso, S., Montoneri, E., Carnaroglio, D., Caporaso, M., Cravotto, G., 2014. Microwave-assisted flash conversion of non-edible polysaccharides and post-harvest tomato plant waste to levulinic acid. Green Chemistry 16, 73-76.

Tai, Z., Isaacs, M.A., Parlett, C.M.A., Lee, A.F., Wilson, K., 2017. High activity magnetic core-mesoporous shell sulfonic acid silica nanoparticles for carboxylic acid esterification. Catalysis Communications 92, 56-60.

Tajmir-Riahi, H.-A., 1988. Interaction of D-glucose with alkaline-earth metal ions. Synthesis, spectroscopic, and structural characterization of Mg(II)- AND Ca(Il)-D-glucose adducts and the effect of metal-ion binding on anomeric configuration of the sugar. Carbohydrute Research 183, 35-46.

Takagaki, A., Nishimura, M., Nishimura, S., Ebitani, K., 2011. Hydrolysis of sugars using magnetic silica nanoparticles with sulfonic acid groups. Chem. Lett. 40, 1195-1197.

Takagaki, A., Tagusagawa, C., Hayashi, S., Hara, M., Domen, K., 2010. Nanosheets as highly active solid acid catalysts for green chemical syntheses. Energy and Environmental Science 3, 82-93.

Takahashi, H., Li, B., Sasaki, T., Miyazaki, C., Kajino, T., Inagaki, S., 2001. Immobilized enzymes in ordered mesoporous silica materials and improvement of their stability and catalytic activity in an organic solvent. Microporous and Mesoporous Materials 44-45, 755-762.

Tan, M., Zhao, L., Zhang, Y., 2011. Production of 5-hydroxymethyl furfural from cellulose in CrCl2/Zeolite/BMIMCl system. Biomass and Bioenergy 35, 1367-1370.

Tang, J., Guo, X., Zhu, L., Hu, C., 2015. Mechanistic study of glucose-to-fructose isomerization in water catalyzed by [Al(OH)2(aq)]+. ACS Catalysis 5, 5097-5103.

Teong, S.P., Yi, G., Zhang, Y., 2014. Hydroxymethylfurfural production from bioresources: Past, present and future. Green Chemistry 16, 2015-2026.

Tewari, Y.B., Goldberg, R.N., 1985. Thermodynamics of the conversion of aqueous glucose to fructose. Appl. BioChemistry BioTechnology 11, 17-24.

Thomas, A., Fischer, A., Goettmann, F., Antonietti, M., Müller, J.-O., Schlögl, R., Carlsson, J.M., 2008. Graphitic carbon nitride materials: variation of structure and morphology and their use as metal-free catalysts. Journal of Materials Chemistry 18, 4893-4908.

Tian, J., Wang, J., Zhao, S., Jiang, C., Zhang, X., Wang, X., 2010. Hydrolysis of cellulose by the heteropoly acid H3PW12O40. Cellulose 17, 587-594.

Tsilomelekis, G., Orella, M.J., Lin, Z., Cheng, Z., Zheng, W., Nikolakis, V., Vlachos, D.G., 2016. Molecular structure, morphology and growth mechanisms and rates of 5-hydroxymethyl furfural (HMF) derived humins. Green Chemistry 18, 1983-1993.

Van De Vyver, S., Peng, L., Geboers, J., Schepers, H., De Clippel, F., Gommes, C.J., Goderis, B., Jacobs, P.A., Sels, B.F., 2010. Sulfonated silica/carbon nanocomposites as novel catalysts for hydrolysis of cellulose to glucose. Green Chemistry 12, 1560-

1563.

van Putten, R.-J., van der Waal, J.C., de Jong, E., Rasrendra, C.B., Heeres, H.J., de Vries, J.G., 2013. Hydroxymethylfurfural, a versatitle platform chemical made from renewable resources. Chemistry Reviews 113, 1499-1597.

van Zandvoort, I., Koers, E.J., Weingarth, M., Bruijnincx, P.C.A., Baldus, M., Weckhuysen, B.M., 2015. Structural characterization of 13C-enriched humins and alkali-treated 13C humins by 2D solid-state NMR. Green Chemistry 17, 4383-4392.

van Zandvoort, I., Wang, Y., Rasrendra, C.B., Van Eck, E.R.H., Bruijnincx, P.C.A., Heeres, H.J., Weckhuysen, B.M., 2013. Formation, molecular structure, and morphology of humins in biomass conversion: Influence of feedstock and processing conditions. ChemSusChem 6, 1745-1758.

Vardon, D.R., Moser, B.R., Zheng, W., Witkin, K., Evangelista, R.L., Strathmann, T.J., Rajagopalan, K., Sharma, B.K., 2013. Complete utilization of spent coffee grounds to produce biodiesel, bio-oil, and biochar. ACS Sustainable Chemistry Engineering 1, 1286−1294.

Verma, D., Tiwari, R., Sinha, A.K., 2013. Depolymerization of cellulosic feedstocks using magnetically separable functionalized graphene oxide. RSC Advances 3, 13265-13272.

Vilonen, K.M., Vuolanto, A., Jokela, J., Leisola, M.S.A., Krause, A.O.I., 2004. Enhanced glucose to fructose conversion in acetone with xylose isomerase stabilized by crystallization and cross-linking. BioTechnology Progress 20, 1555-1560.

Wada, M., Heux, L., Sugiyama, J., 2004. Polymorphism of cellulose I family: Reinvestigation of cellulose IVl. Biomacromolecules 5, 1385-1391.

Wang, K., Jiang, J., Xu, J., Feng, J., Wang, J., 2016. Effective saccharification of holocellulose over multifunctional sulfonated char with fused ring structures under microwave irradiation. RSC Advances 6, 14164-14170.

Wang, R., Xie, X., Liu, Y., Liu, Z., Xie, G., Ji, N., Ma, L., Tang, M., 2015. Facile and low-cost preparation of Nb/Al oxide catalyst with high performance for the conversion of kiwifruit waste residue to levulinic acid. Catalysts 5, 1636-1648.

Wang, T., Nolte, M.W., Shanks, B.H., 2014. Catalytic dehydration of C6 carbohydrates for the production of hydroxymethylfurfural (HMF) as a versatile platform chemical. Green Chemistry 16, 548-572.

Watanabe, M., Aizawa, Y., Iida, T., Nishimura, R., Inomata, H., 2005. Catalytic glucose and fructose conversions with TiO2 and ZrO2 in water at 473 K: Relationship between reactivity and acid-base property determined by TPD measurement. Applied

Catalysis A: General 295, 150-156.

Weingarten, R., Cho, J., Xing, R., Conner, W.C., Huber, G.W., 2012a. Kinetics and reaction engineering of levulinic acid production from aqueous glucose solutions. ChemSusChem 5, 1280-1290.

Weingarten, R., Conner, W.C., Huber, G.W., 2012b. Production of levulinic acid from cellulose by hydrothermal decomposition combined with aqueous phase dehydration with a solid acid catalyst. Energy and Environmental Science 5, 7559-7574.

Werpy, T., Petersen, G., 2004. Top value added chemicals from biomass. Top Value Added Chemicals from Biomass.

Wettstein, S.G., Alonso, D.M., Chong, Y., Dumesic, J.A., 2012a. Production of levulinic acid and gamma-valerolactone (GVL) from cellulose using GVL as a solvent in biphasic systems. Energy and Environmental Science 5, 8199-8203.

Wettstein, S.G., Martin Alonso, D., Gürbüz, E.I., Dumesic, J.A., 2012b. A roadmap for conversion of lignocellulosic biomass to chemicals and fuels. Current Opinion in Chemical Engineering 1, 218-224.

Wu, Q., Chen, H., Han, M., Wang, D., Wang, J., 2007. Transesterification of cottonseed oil catalyzed by brønsted acidic ionic liquids. Industrial and Engineering Chemistry Research 46, 7955-7960.

Wu, W.H., Foglia, T.A., Marmer, W.N., Phillips, J.G., 1999. Optimizing production of ethyl esters of grease using 95% ethanol by response surface methodology. JAOCS, Journal of the American Oil Chemists' Society 76, 517-521.

Xiang, Q., Kim, J.S., Lee, Y.Y., 2003. A comprehensive kinetic model for dilute-acid hydrolysis of cellulose. Applied Biochemistry and Biotechnology - Part A Enzyme Engineering and Biotechnology 106, 337-352.

Xiong, X., Yu, I.K.M., Cao, L., Tsang, D.C.W., Zhang, S., Ok, Y.S., 2017. A review of biochar-based catalysts for chemical synthesis, biofuel production, and pollution control. Bioresource Technology 246, 254-270.

Xiong, X., Yu, I.K.M., Chen, S.S., Tsang, D.C.W., Cao, L., Song, H., Kwon, E.E., Ok, Y.S., Zhang, S., Poon, C.S., 2018. Sulfonated biochar as acid catalyst for sugar hydrolysis and dehydration. Catalysis Today, 314, 52-61.

Xu, Z., Li, W., Du, Z., Wu, H., Jameel, H., Chang, H.M., Ma, L., 2015. Conversion of corn stalk into furfural using a novel heterogeneous strong acid catalyst in γ-valerolactone. Bioresource Technology 198, 764-771.

Ya'aini, N., Amin, N.A.S., Asmadi, M., 2012. Optimization of levulinic acid from lignocellulosic biomass using a new hybrid catalyst. Bioresource Technology 116, 58-

65.

Yabushita, M., Kobayashi, H., Fukuoka, A., 2014. Catalytic transformation of cellulose into platform chemicals. Applied Catalysis B: Environmental 145, 1-9.

Yadav, G.D., Chandan, P.A., 2014. A green process for glycerol valorization to glycerol carbonateover heterogeneous hydrotalcite catalyst. Catalysis Today 237, 47-53.

Yan, H., Yang, Y., Tong, D., Xiang, X., Hu, C., 2009. Catalytic conversion of glucose to 5-hydroxymethylfurfural over SO42-/ZrO2and SO42-/ZrO2-Al2O3solid acid catalysts. Catalysis Communications 10, 1558-1563.

Yan, L., Liu, N., Wang, Y., Machida, H., Qi, X., 2014. Production of 5-hydroxymethylfurfural from corn stalk catalyzed by corn stalk-derived carbonaceous solid acid catalyst. Bioresource Technology 173, 462-466.

Yang, B.Y., Montgomery, R., 1996. Alkaline degradation of glucose: effect of initial concentration of reactants. Carbohydrate Research 280, 27-45.

Yang, F., Li, Y., Zhang, Q., Sun, X., Fan, H., Xu, N., Li, G., 2015a. Selective conversion of cotton cellulose to glucose and 5-hydroxymethyl furfural with SO42-/MxOysolid superacid catalyst. Carbohydrate Polymers 131, 9-14.

Yang, F., Liu, Q., Bai, X., Du, Y., 2011a. Conversion of biomass into 5-hydroxymethylfurfural using solid acid catalyst. Bioresource Technology 102, 3424-3429.

Yang, F., Liu, Q., Yue, M., Bai, X., Du, Y., 2011b. Tantalum compounds as heterogeneous catalysts for saccharide dehydration to 5-hydroxymethylfurfural. Chemical Communications 47, 4469-4471.

Yang, G., Pidko, E.A., Hensen, E.J.M., 2012. Mechanism of Bronsted acid-catalyzed conversion of carbohydrates. Journal of Catalysis 295, 122-132.

Yang, G., Pidko, E.A., Hensen, E.J.M., 2013. Structure, stability, and lewis acidity of mono and double Ti, Zr, and Sn framework substitutions in BEA zeolites: A periodic density functional theory study. Journal of Physical Chemistry C 117, 3976-3986.

Yang, L., Tsilomelekis, G., Caratzoulas, S., Vlachos, D.G., 2015b. Mechanism of Brønsted Acid-Catalyzed Glucose Dehydration. ChemSusChem 8, 1334-1341.

Yang, Q., Lan, W., Runge, T., 2016a. Salt-Promoted Glucose Aqueous Isomerization Catalyzed by Heterogeneous Organic Base. ACS Sustainable Chemistry & Engineering 4, 4850-4858.

Yang, Q., Runge, T., 2016. Polyethylenimines as homogeneous and heterogeneous catalysts for glucose isomerization. ACS Sustainable Chemistry Engineering 4, 6951-6961.

Yang, Q., Sherbahn, M., Runge, T., 2016. Basic amino acids as green catalysts for isomerization of glucose to fructose in water. ACS Sustainable Chemistry & Engineering 4, 3526-3534.

Yang, Q., Zhou, S., Runge, T., 2015. Magnetically separable base catalysts for isomerization of glucose to fructose. Journal of Catalysis 330, 474-484.

You, S., Ok, Y.S., Chen, S.S., Tsang, D.C.W., Kwon, E.E., Lee, J., Wang, C.H., 2017. A critical review on sustainable biochar system through gasification: Energy and environmental applications. Bioresource Technology 246, 242-253.

Yu, I.K.M., Tsang, D.C.W., 2017. Conversion of biomass to hydroxymethylfurfural: A review of catalytic systems and underlying mechanisms. Bioresource Technology 238, 716-732.

Yu, I.K.M., Tsang, D.C.W., Chen, S.S., Wang, L., Hunt, A.J., Sherwood, J., De oliveira Vigier, K., Jérôme, F., Ok, Y.S., Poon, C.S., 2017c. Polar aprotic solvent-water mixture as the medium for catalytic production of hydroxymethylfurfural (HMF) from bread waste. Bioresource Technology 245, 456-462.

Yu, I.K.M., Tsang, D.C.W., Yip, A.C.K., Chen, S.S., Ok, Y.S., Poon, C.S., 2016. Valorization of food waste into hydroxymethylfurfural: Dual role of metal ions in successive conversion steps. Bioresource Technology 219, 338-347.

Yu, I.K.M., Tsang, D.C.W., Yip, A.C.K., Chen, S.S., Ok, Y.S., Poon, C.S., 2017a. Valorization of starchy, cellulosic, and sugary food waste into hydroxymethylfurfural by one-pot catalysis. Chemosphere 184, 1099-1107.

Yu, I.K.M., Tsang, D.C.W., Yip, A.C.K., Chen, S.S., Wang, L., Ok, Y.S., Poon, C.S., 2017b. Catalytic valorization of starch-rich food waste into hydroxymethylfurfural (HMF): Controlling relative kinetics for high productivity. Bioresource Technology 237, 222-230.

Yu, J.T., Dehkhoda, A.M., Ellis, N., 2011. Development of biochar-based catalyst for transesterification of canola oil. Energy and Fuels 25, 337-344.

Yu, S., Kim, E., Park, S., Song, I.K., Jung, J.C., 2012. Isomerization of glucose into fructose over Mg-Al hydrotalcite catalysts. Catalysis Communications 29, 63-67.

Yuan, Z., Wang, L., Wang, J., Xia, S., Chen, P., Hou, Z., Zheng, X., 2011. Hydrogenolysis of glycerol over homogenously dispersed copper on solid base catalysts. Applied Catalysis B: Environmental 101, 431-440.

Yue, C., Li, G., Pidko, E.A., Wiesfeld, J.J., Rigutto, M., Hensen, E.J.M., 2016.

Dehydration of Glucose to 5-Hydroxymethylfurfural Using Nb-doped Tungstite. ChemSusChem 9, 2421-2429.

Yue, C., Magusin, P.C.M.M., Mezari, B., Rigutto, M., Hensen, E.J.M., 2013. Hydrothermal synthesis and characterization of a layered zirconium silicate. Microporous and Mesoporous Materials 180, 48-55.

Yun, Y.S., Kim, T.Y., Yun, D., Lee, K.R., Han, J.W., Yi, J., 2017. Understanding the Reaction Mechanism of Glycerol Hydrogenolysis over a CuCr2O4Catalyst. ChemSusChem 10, 442-454.

Zeng, W., Cheng, D.G., Zhang, H., Chen, F., Zhan, X., 2010. Dehydration of glucose to levulinic acid over MFI-type zeolite in subcritical water at moderate conditions. Reaction Kinetics, Mechanisms and Catalysis 100, 377-384.

Zhang, F., Fang, Z., 2012. Hydrolysis of cellulose to glucose at the low temperature of 423K with CaFe2O4-based solid catalyst. Bioresource Technology 124, 440-445.

Zhang, L., Xi, G., Chen, Z., Jiang, D., Yu, H., Wang, X., 2017a. Highly selective conversion of glucose into furfural over modified zeolites. Chemical Engineering Journal 307, 868-876.

Zhang, L., Xi, G., Zhang, J., Yu, H., Wang, X., 2017b. Efficient catalytic system for the direct transformation of lignocellulosic biomass to furfural and 5-hydroxymethylfurfural. Bioresource Technology 224, 656-661.

Zhang, T., Li, W., Xu, Z., Liu, Q., Ma, Q., Jameel, H., Chang, H.M., Ma, L., 2016a. Catalytic conversion of xylose and corn stalk into furfural over carbon solid acid catalyst in γ-valerolactone. Bioresource Technology 209, 108-114.

Zhang, X., Wilson, K., Lee, A.F., 2016b. Heterogeneously Catalyzed Hydrothermal Processing of C5-C6 Sugars. Chemical Reviews 116, 12328-12368.

Zhang, X., Zhang, D., Sun, Z., Xue, L., Wang, X., Jiang, Z., 2016c. Highly efficient preparation of HMF from cellulose using temperature-responsive heteropolyacid catalysts in cascade reaction. Applied Catalysis B: Environmental 196, 50-56.

Zhang, Y., Wang, J., Li, X., Liu, X., Xia, Y., Hu, B., Lu, G., Wang, Y., 2015. Direct conversion of biomass-derived carbohydrates to 5-hydroxymethylfurural over water-tolerant niobium-based catalysts. Fuel 139, 301-307.

Zhao, Q., Sun, Z., Wang, S., Huang, G., Wang, X., Jiang, Z., 2014. Conversion of highly concentrated fructose into 5-hydroxymethylfurfural by acid-base bifunctional HPA nanocatalysts induced by choline chloride. RSC Advances 4, 63055-63061.

Zhao, Y., Zhou, X., Ye, L., Tsang, S.C.E., 2012. Nanostructured Nb2O5 catalysts. Nano Rev. 3.

Zheng, L., Li, X., Du, W., Shi, D., Ning, W., Lu, X., Hou, Z., 2017. Metal-organic framework derived Cu/ZnO catalysts for continuous hydrogenolysis of glycerol. Applied Catalysis B: Environmental 203, 146-153.

Zheng, Y., Lin, H.M., Tsao, G.T., 1998. Pretreatment for cellulose hydrolysis by carbon dioxide explosion. Biotechnology Progress 14, 890-896.

Zhou, L., Shi, M., Cai, Q., Wu, L., Hu, X., Yang, X., Chen, C., Xu, J., 2013. Hydrolysis of hemicellulose catalyzed by hierarchical H-USY zeolites – The role of acidity and pore structure. Microporous and Mesoporous Materials 169, 54-59.

Zhou, P., Zhang, Z., 2016. One-pot catalytic conversion of carbohydrates into furfural and 5-hydroxymethylfurfural. Catalysis Science and Technology 6, 3694-3712.